

# **GEOHYDROLOGICAL INVESTIGATION AND EVALUATION OF THE ZULULAND COASTAL AQUIFER**

**Report to the  
WATER RESEARCH COMMISSION**

by

**R Meyer<sup>1</sup>, A S Talma<sup>1</sup>, A W A Duvenhage<sup>1</sup>, B M Eglinton<sup>1</sup>,  
J Taljaard<sup>1</sup>, J F Botha<sup>2</sup>, J Verwey<sup>2</sup> and I van der Voort<sup>2</sup>**

<sup>1</sup>Environmentek, CSIR

<sup>2</sup>University of the Free State

## EXECUTIVE SUMMARY

### 1. INTRODUCTION

The Zululand coastal plain, with a surface area of approximately 7 000 km<sup>2</sup> in South Africa, is located on the north east coast of Kwazulu-Natal and extends from Mtunzini in the south to the Mocambique border in the north. This is a distance of about 250 km whereas the Coastal Plain stretches for another almost 1000 km in Mozambique. It constitutes the largest primary coastal aquifer in South Africa. From a ground water perspective this aquifer has until a few years ago received little attention. Several large lakes, some of which have a direct connection to the ocean while others are isolated from the ocean, occur along this stretch of land and form an integral part of this delicate ecosystem.

During the 1960's the town of Richards Bay was proclaimed a national growth point and has developed over the years into an industrial city along the coast. Developments such as this and the expansion of the agricultural, forestry and tourism industry, together with the development of large industrial factories is placing unprecedented demands on this environmentally sensitive area. The proposed mining of heavy minerals along the Eastern Shores of Lake St Lucia in the early 1990s, has again raised the sensitivity and complexity of the area in terms of the functioning of the environment in this region.

Large gaps in our knowledge base, and thus our understanding of the functioning of the system, has prompted this study. Despite several mostly unrelated studies of the ground water resources on the Zululand Coastal Plain have been done over the years. This project was initiated to address some of the many interesting geohydrological features of the coastal plain that are fundamental to our understanding of this aquifer and its associated environment and to integrate the knowledge that already exists for the area. Because of the extent of the large extent of the aquifer (250km north-south and 60km maximum east-west), the aim was not to understand the detailed geohydrology of this rather complex area, but to add to the already existing data base of knowledge of the aquifer in order to obtain a conceptual model of the aquifer system.

The report is divided into 6 chapters of which **Chapter 1** contains mainly background information to this study. This is followed by a chapter (**Chapter 2**) which describes the geology and the geophysical investigations that were conducted and the results of the geophysical surveys. In **Chapter 3** various aspects of the geohydrology, such as a description of the aquifer, ground water quality and isotope studies, thickness of the

aquifer succession, hydraulic characteristics of the aquifer, recharge and pollution vulnerability, are described. The development of a mathematical simulation model and the results from modelling various ground water utilization options for the Coastal Plain including the effect of afforestation on the aquifer, is described in **Chapter 4**. This is followed by **Chapter 5** which contains water balance calculations and a description of the utilization of the ground water resource. Conclusions and recommendations emanating from the project are contained in **Chapter 6**.

## **2. STUDY OBJECTIVES**

The objectives of the study as stated in the original project proposal were

- to determine the extent and geohydrological conditions of the aquifer associated with the Zululand coastal plain between Richards Bay and the Mocambique border by means of geophysical surveys and subsequent drilling and pump testing;
- to determine the regional ground water flow pattern;
- to determine the vulnerability to pollution of the aquifer and the associated effect it may have on pollution of the inland lake systems;
- to determine the amount of ground water recharge to the aquifer under current land-use practices and the role that the inland lake systems play in this regard;
- to evaluate the response of the aquifer to large scale abstraction of ground water as well as the interaction between ground water, forestry and the lake systems through a mathematical simulation;
- to determine what amounts of ground water can be abstracted from the aquifer without causing negative effects on the ground water system;
- to evaluate the possibility of sea water intrusion into the aquifer; and
- to determine a water balance for the Coastal Plain.

## **3. METHODOLOGY**

In the course of the study the Steering Committee decided that the application of stable isotopes determinations, in conjunction with the ground water chemistry to study the recharge to the coastal aquifer would add significantly to our understanding of the recharge pattern across the study area. The continuous monitoring of the isotopic and chemical character of the rainfall and water from the lakes over a three-year period was therefore initiated as a way to determine the recharge to the aquifer.

Due to the deterioration of the security situation on the coastal plain, both in the northern areas as well as the area around Kwambonambi, the drilling programme had

to be curtailed before all exploration boreholes could be completed. No production boreholes for pump testing were therefore drilled apart from a few around Lake Mzingazi drilled by the Department of Water Affairs and Forestry for assessing the flow conditions around this lake. The result was that all objectives (for example determining the sustainable yield of the aquifer) could not be fully achieved.

Crucial to the understanding of the geohydrology of the coastal plain, is a knowledge of the thickness of the alluvial succession defining the aquifer. The study area is underlain by alluvial deposits of Holocene age (<100 00 years), and rocks of Tertiary and Quaternary age (<65 million years). Geophysical techniques provide one way of determining the thickness of these successions. The application and success of the direct current resistivity and time domain electromagnetic exploration techniques to study the geological successions has already been proven on the Zululand coastal plain and were therefore further applied to map the geological succession overlying the Cretaceous floor rocks over the entire coastal plain. Initially an area on the coastal plain had been selected where the different aspects influencing the geohydrological conditions could be studied. These included the lake systems, dunes, plantations, geological succession, etc. The following step then was to extend the study to eventually cover the entire coastal plain. The thickness and lateral extent of the post-Cretaceous sedimentary succession was studied using geophysical techniques followed by the drilling of boreholes in selected localities for calibration purposes.

Water samples were collected from boreholes and other water sources for chemical and isotopic analyses to identify different ground water types and to contribute to our understanding of the recharge characteristics. The chemical and isotopic characteristics of rainfall and ground water were studied in depth to produce a recharge relationship for the coastal aquifer. Eventually all the collected information was integrated and a conceptual geohydrological model was formulated. This model was then developed further into a mathematical simulation model with which different geohydrological scenarios could be tested on a regional scale.

#### **4. SUMMARY OF MAJOR RESULTS AND CONCLUSIONS**

The objectives for the project as stated in the contract conditions, and listed in the introduction to this report, have been met, with the exception of all the exploration drilling and test pumping originally envisaged. This was due a deteriorating security situation which made the area unsafe for the drilling and test pumping crews. This had the effect that the sustainability of the aquifer in terms of abstraction could not be assessed over the entire coastal plain.



The earlier statement that the Zululand Coastal Plain Aquifer can be regarded as one of the largest alluvial aquifers in South Africa has been confirmed by the additional information collected during this investigation. Although the investigation has also led to a better understanding of the aquifer system, several aspects warrant more study. In this regard the interaction between vegetation, whether it be natural or commercial (forestry and agriculture for example), and the ground water regime needs to be assessed thoroughly before any large scale development of the ground water resource is envisaged.

There exists a fine balance between the ecology of the region and the ground water regime. Any future development plans for the region, whether development for tourism, rural settlements, agriculture, mining or afforestation have to take into account the delicate balance of the ecosystem. Ground water plays a crucial role in this ecosystem and any change in the ground water conditions may influence the ecosystem negatively.

Some specific conclusions emanating from this study are listed below:

- The thickness of the aquifers stratigraphically above the Cretaceous age sediments, was mapped over the entire coastal plain using geophysical techniques. Confidence in the thickness determinations was achieved by calibrating the interpreted thicknesses against known borehole information.
- The electrical resistivity sounding technique used to determine the depth to the top of the Cretaceous age formations is more appropriate than the electromagnetic techniques to determine the thickness of the different units in the geological succession.
- Interpretation of direct current (dc) soundings is complicated because of the continuous decrease of the resistivity with depth. Similarly depth penetration by Electromagnetic (EM) techniques was also found to be restricted due to the decrease in resistivity with depth of the different geological units and the very conductive nature of the sedimentary succession.
- Resolution of individual geological units with geophysical methods proved not always to be successful. The depth to the top of the Cretaceous formations can, however, be determined with a large degree of confidence.
- Borehole geophysical measurements also failed to clearly identify different geological horizons.
- Gravity surveys were not able to detect palaeo-channels subsequently filled with younger sediments.
- Two palaeo-channels were detected geophysically and by drilling, through which increased seepage towards the sea can and does occur. One of these is situated opposite Lake Sibayi and the other one is near Mission Rocks opposite Lake St Lucia.

- A water level contour map was constructed for the entire coastal plain using measured water levels and applying statistical techniques to infer elevations in areas where data points were sparse.
- A ground water divide, roughly parallel to the coastline, could clearly be identified from this map.
- From the available water level information, three different water level scenarios in the vicinity of the coastal dune cordon could be identified. These are at Lake Sibayi, Eastern Shores of Lake St Lucia, and at Richards Bay.
- A regional mathematical simulation model was designed to simulate steady state conditions. This model was used to determine ground water flow directions and velocities over the entire coastal plain.
- It was further used to simulate the effect of an afforested area around Lake Sibayi to determine the effect on lake and ground water levels. This model indicates that if evapotranspiration by the plantations exceeds 1 000 mm/ha/a, water levels in the lake may already be affected. A number of assumptions have, however, been made during this simulation. These figures should therefore be regarded as provisional.
- An important rainfall-recharge relationship was established which varies with distance from the coast. Recharge as a percentage of MAP varies from 18 % at the coast to 5 % at a distance of 50 km inland.
- The rainfall-recharge relationship was used as input to the mathematical simulation exercise.
- Ground water quality over the entire coastal plain is generally of good quality. There are, however, due to changing geological conditions, regional differences in the chemical character.
- A hydrochemical "fingerprinting" technique was developed and used successfully to correlate the water chemistry with the geological horizon from which it originates.
- Stable isotopes were used to great advantage to distinguish between seepage from lakes and ground water. Stable isotopes also confirmed a considerable residence time for water in the larger lakes like Sibayi and Bhangazi.
- No seasonal isotopic variation was recognized in rainwater. Isotope analyses could also not be used to trace the movement of ground water due to insignificant variations observed
- Carbon-14 analyses indicated that the ground water recharge is mostly post-1960. This is in accordance with the high through-flow of water through the aquifer deduced from recharge estimates and modelling.  
Isotope analyses confirmed that the fresh water occurrence along the coast opposite Lake Sibayi originates from the lake.
- Sea-water intrusion into the aquifer is unlikely to occur due to an effective above sea level piezometric head along the coastal dune cordon.
- The aquifer is highly vulnerable to surface sources of pollution.

In view of the ecologically sensitive nature of the area and the dominating role that ground water plays in maintaining the balance has again been reiterated by the results obtained during this investigation. Based on the result attained, a number of important recommendations for future studies and development initiatives on the Coastal Plain are made. These include that:

- A water level monitoring programme should be initiated and maintained to document the long term character of the regional water level and ground water quality.
- The interaction between the ground water and the vegetation in the area be investigated in detail and that a research program to address this aspect be compiled as soon as possible. This would assist to better understand the effect of large scale development projects (for example extensive commercial forestry) on the aquifer and the ecology of the region as a whole.
- This research program should include input from ecologists, the Department of Water Affairs and Forestry, the commercial forestry sector, nature conservation officials, tourism authorities and regional planners.
- Further work is required to quantify the effect of afforestation on the ground water conditions in more detail.
- The mathematical simulation model should be refined and updated once more data becomes available.
- The pollution vulnerability of the aquifer should be brought to the attention of the planners.

## ACKNOWLEDGMENTS

The research described in this report emanated from a project funded by the Water Research Commission and entitled:

### **“GEOHYDROLOGICAL INVESTIGATION AND EVALUATION OF THE ZULULAND COASTAL AQUIFER”**

Contributions throughout the duration of the project by members of the Steering Committee are gratefully acknowledged. The Steering Committee responsible for this project consisted of the following persons:

Mr A G Reynders	Water Research Commission (Chairman)
Mr H M du Plessis	Water Research Commission
Mr R Bush	Department of Water Affairs and Forestry
Dr J H de Beer	Environmentek, CSIR
Mr F Bosman	Richards Bay Municipality
Mr P Conant	Kwazulu Bureau of Natural Resources
Prof J F Botha	Institute for Ground-water Studies, University of the Orange Free State
Dr D B Bredenkamp	Department of Water Affairs and Forestry

The authors further wish to thank the many individuals, institutions and companies who contributed to the project, by supplying information, either in the form of fruitful discussions or from reports and publications. All this information in some way or another contributed to the success of the project.

We would like to acknowledge the contributions made by the following individuals or institutions:

Prof B Kelbe, University of Zululand  
Richards Bay Minerals  
Natal Parks Board  
Kwazulu Department of Natural Resources  
Department of Water Affairs and Forestry  
Council for Geoscience  
Industrial Development Corporation  
Forestry Industry  
Borough of Richards Bay  
Atomic Energy Corporation  
Davies, Lynn and Partners, Durban  
Mr M J McCarthy, Durban

## TABLE OF CONTENTS

Executive Summary .....	i
Acknowledgments .....	vii
Table of Contents .....	viii
List of Appendices .....	ix
List of Figures .....	x
List of Tables .....	xii

<b>CHAPTER 1: INTRODUCTION AND SUMMARY OF PREVIOUS GEOHYDROLOGICAL STUDIES OF THE COASTAL PLAIN .....</b>	<b>1</b>
<b>1.1 Introduction .....</b>	<b>1</b>
<b>1.2 Research objectives .....</b>	<b>2</b>
<b>1.3 Approach to study .....</b>	<b>2</b>
<b>1.4 Report layout .....</b>	<b>3</b>
<b>1.5 Summary of previous geohydrological studies on the Coastal Plain ..</b>	<b>3</b>
 <b>CHAPTER 2: GEOLOGY OF THE COASTAL PLAIN AND GEOPHYSICAL INVESTIGATIONS .....</b>	 <b>6</b>
<b>2.1 Information Sources .....</b>	<b>6</b>
<b>2.2 Geological Succession .....</b>	<b>8</b>
2.2.1 <i>Basement rocks (Cretaceous age)</i> .....	8
2.2.2 <i>Tertiary age sediments</i> .....	8
2.2.3 <i>Pleistocene deposits</i> .....	9
2.2.4 <i>Younger unconsolidated deposits</i> .....	9
<b>2.3 Geophysical Investigation and Techniques used .....</b>	<b>10</b>
<b>2.4 Electrical Methods .....</b>	<b>10</b>
2.4.1 <i>Direct Current Resistivity Technique (Schlumberger Array)</i> .....	10
2.4.2 <i>Types of sounding curves</i> .....	11
2.4.3 <i>Geoelectric layer resistivities</i> .....	11
2.4.4 <i>Calibration soundings</i> .....	11
<b>2.5 Electromagnetic Soundings .....</b>	<b>13</b>
2.5.1 <i>General</i> .....	13
2.5.2 <i>Calibration soundings</i> .....	13
<b>2.6 Gravity Survey .....</b>	<b>14</b>
<b>2.7 Results of Geophysical Investigation .....</b>	<b>14</b>
2.7.1 <i>Geoelectrical Techniques</i> .....	14
2.7.2 <i>Geophysical Borehole Logging</i> .....	15

<b>CHAPTER 3: GEOHYDROLOGY OF THE ZULULAND COASTAL PLAIN</b>	<b>17</b>
3.1 Aquifer description	17
3.2 Hydrochemisry and Isotope Studies	18
3.2.1 Ground Water Chemistry	18
3.2.2 Isotopes in Water	19
Stable isotopes	19
Radiocarbon	20
3.3 Ground Water Leakage to the Sea	20
3.4 Rain Water Chemistry	23
3.4.1 Sampling	23
3.4.2 Rain water chemistry	24
3.4.3 Isotopes in rainfall	26
3.5 Ground Water Recharge Estimates	27
3.6 Potential for Ground Water Pollution	29
<b>CHAPTER 4: MATHEMATICAL MODELLING OF THE COASTAL PLAIN AQUIFER</b>	<b>32</b>
4.1 General	32
4.2 Geohydrology	32
4.3 The Finite Element Model	33
4.4 Results from the Finite Element Model	33
4.5 The Impact of Afforestation on the Aquifer: A Hypothetical Case Study	34
4.6 Conclusions	36
<b>CHAPTER 5: WATER BALANCE CALCULATIONS</b>	<b>37</b>
5.1 Recharge Driven Water Balance	37
5.2 Flow Equation Derived Water Balance	37
5.3 Preferential Flow Paths to the Sea	38
5.4 Utilization of Ground Water Resource	39
<b>CHAPTER 6: CONCLUSIONS AND RECOMMENDATIONS</b>	<b>40</b>
6.1 Conclusions	40
6.2 Recommendations	42
<b>LIST OF REFERENCES</b>	<b>43</b>

## LIST OF APPENDICES

**APPENDIX A: Geochemical classification of ground water on the Zululand Coastal Plain**

**APPENDIX B: Ground water recharge calculations**

## LIST OF FIGURES

- Figure 1:** Geological map of the Zululand Coastal area.
- Figure 2:** Resistivity sounding locations.
- Figure 3:** A typical direct current (DC) resistivity sounding curve and interpretation.
- Figure 4:** Sounding curve and model for resistivity sounding ES 85.
- Figure 5:** DC sounding curve and interpretations for ES 235 (Lebombo Group) and ES 224 (Makatini Formation).
- Figure 6:** DC sounding curve and interpretations for ES 180 (Mzineni Formation) and ES 155 (St Lucia Formation).
- Figure 7:** DC sounding curve and interpretations for ES 188 (Uloa Formation) and ES 105 (Port Durnford Formation).
- Figure 8:** DC sounding curve and interpretations for ES 42 (Berea-type Red Sand) and ES 168 (Holocene sands).
- Figure 9:** Histogram of surface measured formation resistivities based on calibration soundings (Worthington, 1979).
- Figure 10:** Sounding curves and models for ES 1, ES 2 and ES 4.
- Figure 11:** Electromagnetic sounding (EM-37) Sounding locations.
- Figure 12:** Comparison between the results of electromagnetic sounding interpretations and drilling results .
- Figure 13:** Transient electromagnetic sounding curves and models for soundings EM 21 and EM 36.
- Figure 14:** Borehole positions on the Zululand Coastal Plain.
- Figure 15:** Boreholes where Cretaceous age rocks were intersected.
- Figure 16:** Positions of modeled depths to Cretaceous.
- Figure 17:** Post Cretaceous sediment thickness north of Lake St Lucia.
- Figure 18:** Post-Cretaceous sediment thickness on the Zululand Coastal Plain south of Lake St Lucia.
- Figure 19:** Boreholes sampled for water chemistry.
- Figure 20a:** Results of chemical analyses of all water samples entered into the Hydrocom database. Data are represented as Piper and Durov diagrams.
- Figure 20b:** Results of chemical analyses of all water samples entered into the Hydrocom database. Data are represented as a Schoeller diagram.
- Figure 21:** Ground water sampling positions for isotope analyses.
- Figure 22:** Distribution of  $\delta^{18}\text{O}$  levels on ground water and surface water in the study area. Surface waters show the effect of isotope enrichment due to evaporation.
- Figure 23:** Relation between  $^{18}\text{O}$  and deuterium in ground water and surface water. Ground water falls on the Meteoric Water Line (MWL) following a general pattern. Deviations from the MWL by surface water are due to evaporation enrichment.
- Figure 24:** Time series of chloride (Cl) and  $^{18}\text{O}$  in Lake Sibayi. The overall constancy of both parameters indicates that the annual (rain/ground) water inflow is small compared with the lake volume.

- Figure 25:**  $^{18}\text{O}$  and chloride relation for the Gobey's Point seepage and the waters likely to be its sources.
- Figure 26:** Schematic cross-section through the coastal dune between Lake Sibayi and the sea.
- Figure 27:**  $^{18}\text{O}$  and deuterium relation for Gobey's Point seepage and its likely sources. The seepage is also located directly on the mixing line between lake and sea water and distinctly different from the MWL representing rain and ground water.
- Figure 28:**  $^{18}\text{O}$  and chloride time series of Lake Bhangazi and the Cape Vidal seepage water. The average  $^{18}\text{O}$  content of ground water is shown for comparison.
- Figure 29:** Comparison of  $^{18}\text{O}$  and Cl in the Cape Vidal/Bhangazi system. Average values for ground water in the area are taken from Bredenkamp (1993). Cape Vidal seepage can be seen to be a mixture between Lake Bhangazi water and ground water with occasional sea water contributions. Note the logarithmic scale.
- Figure 30:**  $^{18}\text{O}$  and deuterium relation for water in the Cape Vidal/Lake Bhangazi system. The interpretation of Cape Vidal seepage as mixing between Lake Bhangazi water and local ground water is evident.
- Figure 31:** Rainfall monitoring stations used for this study.
- Figure 32:** Results of principle component analysis of the rainfall chemistry data. The weights of the various ions contributing to the first two principle components are shown.
- Figure 33:** Annual calcium deposition rates for the three sampling years.
- Figure 34:** Annual chloride deposition rates for the three sampling years. The coastal stations (SOD, MBA, MAN) show more annual variations than do the inland stations.
- Figure 35:** Relation between annual chloride deposition (for each of the three years) and the rainfall of that year.
- Figure 36:** Average (three years) chloride and calcium deposition with distance inland.
- Figure 37:** Seasonal pattern of rainfall and its  $^{18}\text{O}$  content for the six rainfall stations.
- Figure 38:**  $^{18}\text{O}$  deuterium relation for rainfall. Most are located on the MWL ( $\delta\text{D} = 8\delta^{18}\text{O} + 10$ ) which holds worldwide (Gat and Giorntini, 1981).
- Figure 39:** Relation between weighted annual  $^{18}\text{O}$  content in rain and the total rainfall for that year. Note the large difference (especially for the coastal stations SOD, MAN, MBA) and the driest year (1991/92).
- Figure 40:** Pollution vulnerability map for the fresh waters of the inner catchment of Lake Mzingazi (Worthington, 1978).
- Figure 41:** The borders of the Zululand aquifer, as well as the positions of the lakes and boreholes used in this study, are shown. The hypothetical afforestation around Lake Sibayi is also shown.
- Figure 42:** The ground water velocities in the Zululand aquifer, as computed from the 140 boreholes.
- Figure 43:** The finite element grid drawn over the Zululand aquifer. The grid excludes the three lakes, Lake St Lucia, Lake Sibayi and Lake Kosi.
- Figure 44:** The piezometric heads from the 140 boreholes were interpreted to all the nodes of the finite element grid, resulting in head contours as shown.



- Figure 45:** Contours from the simulated piezometric heads for the Zululand aquifer after a simulation period of one year.
- Figure 46:** A comparison of the initial (solid lines) and simulated (dots) piezometric heads of the numerical model, taken at a few sections parallel to the x-axis. The line numbers are according to the finite element model of Figure 47, counted from the bottom of the grid.
- Figure 47:** Contours of the water levels, simulated for one year, with hypothetical; recharge and evaporation figures of 150 mm/year and 2000 mm/year respectively
- Figure 48:** Section AA' through Lake Sibayi, perpendicular to the coast, showing the effect of a variation in evapotranspiration values. The evapotranspiration specified for the cases was 0, 200, 1 000, 2 000 and 4 000 mm per annum, per unit area.
- Figure 49:** Section BB' through Lake Sibayi, parallel to the coast, showing the effect of a variation in evapotranspiration values. The evapotranspiration specified for the cases was 0, 200, 1 000, 2 000 and 4 000 mm per annum, per unit area.
- Figure 50:** The direction of flow of ground water around Lake Sibayi and through the simulation area under normal conditions of 150 mm recharge per year.
- Figure 51:** The direction of flow of ground water around Lake Sibayi and through the simulation area under extreme conditions of an effective discharge of 2 500 mm per year.
- Figure 52:** Map indicating the aquifer potential in different parts of the Zululand Coastal Plain.

## LIST OF TABLES

- Table 1:** Simplified geological sequence: Zululand Coastal Plain
- Table 2:** Correlation of the biostratigraphic, lithostratigraphic and geoelectrical subdivisions of the Cenozoic and late Mesozoic succession on the Zululand Coastal Plain (Adapted and extended from Worthington, 1978).
- Table 3:** Porosity determinations using "Archie's Law" where  $F = \rho_r / \rho_w = a^{-m}$  (with  $a=1$  and  $m=1.5$ ).
- Table 4:** Porosity values for different geological sequences as derived from geophysical borehole logging and other techniques
- Table 5:** Radiocarbon content of ground and surface water samples.
- Table 6:** Details of rainfall stations.
- Table 7:** Correlation matrix of major constituents of rain water (based on 157 analyses).
- Table 8:** Chloride deposition at rainfall stations (annual rainfall in millimetres in brackets).
- Table 9:** Three year  $^{18}\text{O}$  average weighted by annual rainfall less a cut-off value.
- Table 10:** Three year average ground water recharge data.
- Table 11:** Classification of proposed development zones within the Mzingazi catchment (Worthington, 1978)
- Table 12:** The movement of the piezometric level as observed at a few boreholes compared to the simulated values in a one year period.

## CHAPTER 1

### INTRODUCTION AND SUMMARY OF PREVIOUS GEOHYDROLOGICAL STUDIES OF THE COASTAL PLAIN

---

#### 1.1 Introduction

The Zululand coastal plain is an environmentally sensitive region located on the coast of northern Natal. The Zululand coastal plain, with a surface area of approximately 7 000 km<sup>2</sup> in South Africa, extends from Mtunzini in the south to the Mocambique border in the north and forms the largest primary coastal aquifer in South Africa. Despite several isolated studies of the aquifer, the vast ground water resources are, however, only exploited on a very limited scale for urban water supply and intermittently as an additional source of water for the coastal mining operations. Several large lakes, some of which have a direct connection to the ocean while others are isolated from the ocean, occur along this stretch of land and form an integral part of this delicate ecosystem. The inland lakes are in direct hydraulic contact with the ground water system.

During the 1960's the town of Richards Bay was proclaimed a national growth point and has developed over the years into an industrial city along the coast. Developments such as this and the expansion of the agricultural and forestry industry, together with the development of large industrial factories is placing unprecedented demands on this environmentally sensitive area. The proposed mining of heavy minerals along the Eastern Shores of Lake St Lucia and along the coast south of Richards Bay, as well as the proclamation of the Greater St Lucia Wetland Park, has again increased the awareness of the sensitivity and complexity of the area in terms of the functioning of this ecosystem.

Large gaps in our knowledge base, and thus our understanding of the functioning of the system, has prompted this study. The CSIR has been involved in several investigations and research projects along the coastal plain for many years ( Van Zijl, 1971; Vogel and Van Urk, 1975; Worthington, 1978; Meyer *et al*, 1982; Kruger and Meyer, 1986; Meyer *et al*, 1989; Meyer *et al*, 1993). The most extensive contributions to our understanding of the geohydrology of the coastal plain, was the work done by Australian Groundwater Consultants (1975) and Worthington (1978), and more recently by Kelbe and Rawlins (1992). Extensive studies have also been conducted around Lake Sibayi, the largest South African inland fresh water lake, by Pitman and Hutchinson (1975).

This project was initiated to address some of the many interesting geohydrological features of the coastal plain that are fundamental to our understanding of this aquifer and its associated environment and to integrate the knowledge that already exists for the area.

## **1.2 Research objectives**

The objectives of the study as stated in the original project proposal were

- to determine the extent and geohydrological conditions of the aquifer associated with the Zululand coastal plain between Richards Bay and the Mocambique border by means of geophysical surveys and subsequent drilling and pump testing;
- to determine the regional ground water flow pattern;
- to determine the vulnerability to pollution of the aquifer and the associated effect it may have on pollution of the inland lake systems;
- to determine the amount of ground water recharge to the aquifer under current land-use practices and the role that the inland lake systems play in this regard;
- to evaluate the response of the aquifer to large scale abstraction of ground water as well as the interaction between ground water, forestry and the lake systems through a mathematical simulation;
- to determine what amounts of ground water can be abstracted from the aquifer without causing negative effects on the ground water system;
- to evaluate the possibility of sea water intrusion into the aquifer; and
- to determine a water balance for the Coastal Plain.

In the course of the study the Steering Committee decided that the application of stable isotopes determinations, in conjunction with the ground water chemistry to study the recharge to the coastal aquifer would add significantly to our understanding of the recharge pattern across the study area. The continuous monitoring of the isotopic and chemical character of the rainfall and water from the lakes over a three-year period was therefore initiated as a way to determine the recharge to the aquifer.

Due to the deterioration of the security situation on the coastal plain, both in the northern areas as well as the area around Kwambonambi, the drilling programme had to be curtailed before all exploration boreholes could be completed. No production boreholes for pump testing were therefore drilled apart from a few around Lake Mzingazi drilled by the Department of Water Affairs and Forestry for assessing the flow conditions around this lake. The result was that all objectives (for example determining the sustainable yield of the aquifer) could not be fully achieved. This prompted the collation of all existing geological and borehole information available on the coastal plain. Although many boreholes were located, well documented information on these hardly existed.

## **1.3 Approach to study**

Crucial to the understanding of the geohydrology of the coastal plain, is a knowledge of the thickness of the alluvial succession defining the aquifer. The study area is underlain by alluvial deposits of Holocene age (<100 00 years), and rocks of Tertiary and

Quaternary age (<65 million years). Geophysical techniques provide one way of determining the thickness of these successions. The application and success of the direct current resistivity and time domain electromagnetic exploration techniques to study the geological successions has already been proven on the Zululand coastal plain and were therefore further applied to map the geological succession overlying the Cretaceous floor rocks over the entire coastal plain (Worthington, 1978; Meyer and Kruger, 1987; Meyer *et al.*, 1982; 1987; 1989). Initially an area on the coastal plain had been selected where the different aspects influencing the geohydrological conditions could be studied. These included the lake systems, dunes, plantations, geological succession, etc. The following step then was to extend the study to eventually cover the entire coastal plain. The thickness and lateral extent of the post-Cretaceous sedimentary succession was studied using geophysical techniques followed by the drilling of boreholes in selected localities for calibration purposes.

Water samples were collected from boreholes and other water sources for chemical and isotopic analyses to identify different ground water types and to contribute to our understanding of the recharge characteristics. The chemical and isotopic characteristics of rainfall and ground water were studied in depth to produce a recharge relationship for the coastal aquifer. Eventually all the collected information was integrated and a conceptual geohydrological model was formulated. This model was then developed further into a mathematical simulation model with which different geohydrological scenarios could be tested on a regional scale.

#### **1.4 Report layout**

The report is divided into 6 chapters of which **Chapter 1** contains mainly background information to this study. This is followed by a chapter (**Chapter 2**) which describes the geology and the geophysical investigations that were conducted and the results of the geophysical surveys. In **Chapter 3** various aspects of the geohydrology, such as a description of the aquifer, ground water quality and isotope studies, thickness of the aquifer succession, hydraulic characteristics of the aquifer, recharge and pollution vulnerability, are described. The development of a mathematical simulation model and the results from modelling various ground water utilization options for the Coastal Plain including the effect of afforestation on the aquifer, is described in **Chapter 4**. This is followed by **Chapter 5** which contains water balance calculations and a description of the utilization of the ground water resource. Conclusions and recommendations emanating from the project are contained in **Chapter 6**. A comprehensive list of references follows after Chapter 6.

#### **1.5 Summary of previous geohydrological studies on the Coastal Plain**

Over the years, several geohydrological investigations of different scales have been conducted on parts of the Zululand coastal plain. Some of the more important investigations were those by Van Wyk (1963), Australian Groundwater Consultants

(1975), Worthington (1978), Meyer *et al.* (1982), Kruger (1986), Kelbe and Rawlins (1992), and some more recent detailed investigations of well field developments east of Kwambonambi (Johnson, personal communication). In addition, a number of hydrological studies were also done on the lake systems so frequently found on the coastal plain. These were mainly done by the Hydrological Research Unit of the University of the Witwatersrand, and concentrated on Lakes St Lucia and Sibayi (Hutchinson and Pitman, 1973; Pitman and Hutchinson, 1975).

The reports by Van Wyk (1963), Worthington (1978), Australian Groundwater Consultants (1975) and Kruger (1986) were perhaps the most extensive studies over this period. Van Wyk's and Kruger's studies concentrated on the northern part of the coastal plain, whereas those by the Australian Groundwater Consultants and Worthington concentrated on the area around Richards Bay, Lake Mzingazi and Lake Nhlabane.

Worthington's approach was that of an integrated geophysical and geohydrological investigation directed at a detailed evaluation of the hydrological conditions around Richards Bay and Lake Mzingazi. Worthington (1978) used the results of some 900 direct current Schlumberger resistivity soundings to establish the geological succession above the extensive and impermeable siltstone of Cretaceous and Palaeocene age. He concluded that the compacted coquina and calcarenite of Miocene age overlying the siltstones in places, constitutes the major aquifer and attains thicknesses in excess of 20m in places. This view was also shared by Australian Groundwater Consultants (1975). The younger Pleistocene succession of fine-grained sands, clays and lignites generally give rise to leaky confined aquifer conditions in the Richards Bay area.

The interpretation of the geoelectric data, supported by calibration soundings and lithostratigraphic records from borehole logs, provided an adequate definition of the mode of occurrence of the Miocene aquifer which is present discontinuously and irregularly within the southern part of the Zululand coastal plain. The average hydraulic conductivity and storage coefficient of the Miocene Formation was established through pumping tests to be 4,5m/d and  $2 \times 10^{-4}$  respectively.

Within the area surveyed by Worthington, the potentiometric levels show a striking correlation with topography, a feature he interpreted as a direct consequence of the relatively low permeability of the Pleistocene succession, and which, through the presence of the coastal dune barrier complex, affords strong protection against saline water intrusion. This conclusion was also reached by Simmonds (1990) and Botha *et al.* (1989). Recent intensive studies around the Eastern Shores and dune cordon east of Lake St Lucia as part of the Environmental Impact Report for the proposed heavy mineral mining at Eastern Shores, Lake St Lucia, provided detailed information on the geohydrology associated with the dune cordon (Davies, Lynn and Partners, 1992; Kelbe and Rawlins, 1992; Meyer *et al.*, 1993). An intensive drilling programme across the dune cordon revealed that the dunes, which reach an elevation of up to 130m amsl at Mt Tabor, are virtually dry, and do not contain any perched water tables (Meyer *et al.*, 1993). In addition, and contrary to expectations and general belief (Van Zijl, 1971;

Pitman and Hutchison, 1975), the dunes do not support a ground water mound. The phreatic surface has nowhere been found to be in excess of 10m amsl and the ground water divide is situated to the west of the dune cordon between the dunes and the eastern shore of Lake St Lucia.

The distribution of aquifer transmissivity has been used by Worthington (1978) in conjunction with the map of potentiometric levels to estimate the subsurface seepage into Lake Mzingazi. His calculations indicated that ground water seepage accounts for over 30% of the total replenishment of Lake Mzingazi. The base flow was calculated to be about 80 000m<sup>3</sup>/day. He also predicted that the base flow would be severely affected, if significant ground water abstraction takes place in the Mzingazi catchment. Worthington also studied the pollution vulnerability of the aquifer and based on hydraulic properties of the aquifer, thickness of aquifer units, and depth to water table, subdivided the area into six zones; from a "green-light" area (favorable for urban development) to a "red-light" area where urban development is not recommended. He further warned that, because of the effectively steady-state conditions in the area, any serious change to the water balance by excessive surface and ground water abstraction, will cause a significant interaction between the different fresh water regimes which might, in turn, have undesirable consequences from the point of view of pollution vulnerability. A steady-state finite element ground water simulation model indicated that the two lakes, Nhlabane and Mzingazi, are hydrologically independent.

The procedure of combining geophysical and geohydrological information adopted in the study by Worthington was suggested as a future strategy for optimum ground water exploration in similar coastal regions. One reason why this approach was successful, was the high density of geoelectrical sounding positions.

Lindley and Scott (1987), Rawlins and Kelbe (1990) and Rawlins (1991) conducted investigations into the geohydrology of the area between the coastal dune cordon and the Eastern Shores of Lake St Lucia. As this area is covered by extensive timber plantations, the prime objectives of these investigations were to determine the influence of the plantations on the ground water regime. A comprehensive network of shallow boreholes, meteorological stations with continuous rainfall monitoring and stream gauging was installed and operated for a period of three years. Lindley and Scott (1987) concluded that pine plantations, and in particular *Pinus elliottii*, are responsible for an additional annual evapotranspiration loss of approximately 2 100 m<sup>3</sup>/ha. Rawlins (1991) arrived at an evapotranspiration loss figure for pine plantations ranging between 1 500m<sup>3</sup>/ha/yr and 1 750m<sup>3</sup>/ha/yr. He calculated that the commercial plantations at Eastern Shores account for an estimated total annual inflow reduction of water to Lake St Lucia of between 37 x 10<sup>6</sup>m<sup>3</sup> and 43 x 10<sup>6</sup>m<sup>3</sup> or 10% to 12% of the fresh water inflow to the Lake. This would affect the water balance to the Lake seriously and with reduced fresh water inflow into the Lake, the salinity balance of the Lake will be changed. This in turn, will have a direct impact on the flora and fauna of the Lake and its environments.

## CHAPTER 2

### GEOLOGY OF THE COASTAL PLAIN AND GEOPHYSICAL INVESTIGATIONS

#### 2.1 Information sources

The study area is covered by two 1:250 000 scale geological maps 2632 Kosi Bay and 27½32 St Lucia. In general, Quaternary geology has been neglected in South African geology, with the main emphasis being placed on the older economically more interesting geology. The Zululand coastal plain, being one of the main areas of Quaternary geology, has also suffered from the lack of attention. Over the last decade or two, a considerable amount of geological research has been done on the southern part of the coastal plain, south of Lake St Lucia. As a result of the heavy mineral mining activities north of Richards Bay and the proposed mining along the dune cordon east of Lake St Lucia, a substantial amount of new information has been accumulated for the coastal dune cordon and in its immediate vicinity (Fockema, 1986). In addition, the development of the town of Richards Bay and all the infrastructure associated with this development in the late 1960's and early 1970's, has provided a wealth of information on engineering geological aspects.

The northern half of the coastal plain, north of Lake St Lucia, and which includes the largest part of the coastal plain, has not been so fortunate in terms of new geological information. The information on post-Cretaceous geology is almost exclusively restricted to the records of a few deep oil exploration boreholes (Wolmarans and Du Preez, 1986; Du Preez and Wolmarans, 1986) and boreholes drilled for a geohydrological study of a small portion in the Muzi swamp area north of Lake Sibayi (Kruger and Meyer, 1988).

Some of the more important sources of information on the geology of the Zululand coastal plain, apart from the ones mentioned above, are by the following authors: Frankel (1960), Maud (1961), Van Wyk (1963), Frankel (1966), Orme (1973), Hobday and Orme (1974), Maud and Orr (1975), Stapleton (1977), Worthington (1978), Hobday and Jackson (1979), Dingle *et al* (1983), Tinley (1985), Fockema (1986), Kruger and Meyer (1988), McCarthy (1988) and Davies *et al* (1992). Reference is also made to unpublished reports made available by the Department of Water Affairs and Forestry, the Geological Survey of South Africa and numerous internal reports of consultants. A geological map, compiled from the 1:250 000 map sheets, is shown in **Figure 1**. A description of the geological succession is listed in **Table 1**.

**Table 1:** Simplified geological sequence for the Zululand Coastal Plain

Age (ma)	System/Period	Series/Epoch	Etage	Group	Formation	Lithology
0.1	Quaternary	Holocene (Recent)				Alluvium, dune, aeolian and beach sands
<1.6		Pleistocene	Upper Pleistocene		Berea	Sand, red clay rich sand
			Middle Upper Pleistocene		Bluff	Calcareous sandstone
			Lower Pleistocene		Upper Port Durnford	Sand and sandstone
						Lignite
					Lower Port Durnford	Clay rich sandstone
1.6 - 65		Tertiary	Late Miocene to Pleistocene		Uloa	Calcareous sandstone and coquina
	Palaeocene		Thanetian - Danian	St Lucia	Siltstone and sandstone	
65 - 146	Cretaceous	Late Cretaceous	Albian - Cenomanian	Zululand	Mzinene	Glauconitic siltstone
		Early Cretaceous	Upper Barremian - Upper Aptian		Makatini	Conglomerate, sandstone and siltstone
146 - 208	Jurassic			Lebombo	Mpilo/Movene	Amygdaloidal trachybasalt
					Jozini	Riodacite and rhyolite
					Letaba	Basalt and rhyolitic lava



## 2.2 Geological succession

### 2.2.1 *Basement rocks (Cretaceous age)*

For the purpose of this study, the rocks of Cretaceous and Palaeocene age can be regarded as the "basement rocks". This succession of mainly siltstones, conglomerates and sandstones is collectively known as the Zululand Group and comprises three formations; the St Lucia, Mzinene and Makatini Formations. The fine siltstones are virtually uniform with occasional thin bands of hard sandy limestone. Apart from having a very low permeability, the quality and quantity of ground water encountered in these formations is extremely poor (TDS >8 000 mg/l), and therefore are regarded as the "basement" rocks for this study. The siltstones range in age from late Cretaceous to early Palaeocene (Orr and Chapman, 1974). Kennedy and Klinger (1975) introduced the name St Lucia Formation for all the Cretaceous bedrock in the Zululand coastal plain. Since the lower Palaeocene strata possess an identical lithology, and there is no evidence of a pronounced unconformity at the Cretaceous/Palaeocene interface, the Palaeocene, for practical purposes may be regarded as part of the St Lucia Formation. On the geological map 27½32 St Lucia, the term Richards Bay Formation has been introduced to describe these Palaeocene age siltstones. According to Stapleton (1975), the Palaeocene deposits are thought to have originated during times of climatic changes. Although these siltstones are lithologically very similar, it does appear that a geoelectrical distinction can be made based on the interpretations of geoelectrical sounding data (see Section 6). The strike direction of the Cretaceous formations is roughly parallel to the coast and dipping towards the coast at an angle of 3-5°.

### 2.2.2 *Tertiary age sediments*

The Cretaceous age sediments are overlain by a sequence of mainly calcarenites in turn overlying basal boulder beds. These relatively thin Miocene age sediments are geohydrologically very important as they can be regarded as one of the main aquifers in the succession (Worthington, 1978). The best outcrops of these rocks occur at Uloa, Sapolwana (Umfolozzi plain) and Lake View along the Pongola River. Maud and Orr (1975) have described the Miocene strata as comprising a lower coquina and an upper calcarenite. Because of the outcrops at Uloa, this sequence was given the name Uloa Formation. The coquina rests unconformably on the siltstones, is hard and coarse and contains abundant fossils. The upper surface of the coquina has apparently been subject to karst solution weathering prior to the deposition of the overlying calcarenite. Cooper and McCarthy (1988) are of the opinion that the Uloa Formation, which grades up into the overlying aeolianites is the result of marine regression. The age of the Uloa Formation is currently disputed. Most authors are of the opinion that the Uloa is of Miocene age (~20 Ma), although a much younger middle Pleistocene age is attributed to this formation by McMillan (1987, 1993). Following an intensive geohydrological investigation in the Richards Bay region, Worthington (1978) was of the opinion that the Uloa Formation occurs in lower lying areas or valleys eroded into Cretaceous age rocks.

### 2.2.3 Pleistocene deposits

The Miocene sediments are extensively overlain by a thick succession of loosely consolidated sands, silts, clays and lignite. The lower late Middle Pleistocene age sediments are known as the Port Durnford Formation and are described in detail by Hobday and Orme (1974). The Port Durnford Formation has been described in the Richards Bay area as comprising of a lower, more argillaceous layer, separated from an upper arenaceous layer by a persistent but discontinuous lignite band. This lignite band was formed over larger areas and was observed in a borehole near Kosi Bay by Kruger and Meyer (1988). The Port Durnford Formation is found in boreholes along the entire coastal dune cordon. The upper surface varies between about 40m amsl near Richards Bay to about 50m amsl near Mbazwana (Fockema, 1986; Kruger and Meyer, 1988; Davies *et al*, 1992). The total thickness of the Port Durnford has been recorded as 25-30m by Worthington (1978) in the Richards Bay area. However, Davies *et al* (1992) reported thicknesses of up to 70m in boreholes north of St Lucia.

### 2.2.4 Younger unconsolidated deposits

The Port Durnford Formation is overlain by fluvial and aeolian sands of Middle to Upper Pleistocene and Holocene age. These sands are predominantly fine grained, contain an average of about 5 % silt and clay (Davies *et al*, 1992; Meyer *et al*, 1993) and are largely unconsolidated. Extensive exposures of clayey red sand, especially more inland, has been termed the Berea-type clayey red sand (McCarthy, 1992). These red sands are the result of intense weathering of dune rock. Although it has mainly formed from late Tertiary aeolianites, it is also known to have formed from younger aeolianites. Weathering and oxidation of minor iron-bearing silicate minerals in the sand form clay and hematite, the latter producing the deep red pigmentation of the weathered mantle.

The Zululand coastal plain is known for its numerous palaeo-dune cordons. In the northern part of the coastal plain six dune cordons can be distinguished progressively increasing in age away from the coast. The most pronounced and youngest of these is the coastal dune cordon stretching all the way from Port Durnford in the south up to the Mocambique border in the north. These dunes are up to 60m amsl. An extensive description of these dunes is given by Davies *et al*, (1992) and Meyer *et al*, (1993). Davies *et al*, (1992) described the typical dune succession at Eastern Shores as follows: "*Deposited onto the Port Durnford Formation are interlayered calcareous sandstones and uncemented sands which are up to 40m thick in places. These are followed by what is termed 'Older aeolian sands' which in turn is overlain by 'Coversands'*". The coversands are mined for their heavy mineral content and contain occasional calcrete nodules. No layering of any form has been observed during an extensive drilling program at Eastern Shores (Davies *et al*, 1992; Meyer *et al*, 1993). These coversands are most probably of Holocene age and extend to depths exceeding 70m. The "older aeolian sands" possess a marginally higher fraction of silt and clay particles and are considered to be of Late Pleistocene age (Davies *et al*, 1992).

## 2.3 Geophysical investigation and techniques used

Previous experience on the Zululand coastal plain and in other similar situations, has indicated that because of the contrast in resistivity and low contact resistance, depth penetration capabilities and the speed of operation, electrical techniques are the most suitable and cost effective geophysical techniques to apply in the circumstances (Van Zijl, 1971; Australian Groundwater Consultants, 1975; Worthington, 1978; Meyer and De Beer, 1981; Meyer *et al* 1982; Meyer *et al*, 1983; Meyer *et al*, 1987; Coetsee, 1991). Therefore the emphasis was placed on the direct current and electromagnetic sounding techniques. The Directorate Geohydrology of the Department of Water Affairs and Forestry suggested that the gravity method also be applied to detect some palaeo-erosion features. In the Environmental Impact Report (EIA) regarding the proposed mining along the Eastern Shores of Lake St Lucia, it is mentioned that the Ground Penetrating Radar technique has been tried without success to determine the internal dune structure of the coastal dunes (Coastal and Environmental Services, 1992).

## 2.4 Electrical methods

### 2.4.1 Direct current resistivity technique (Schlumberger array)

The method of Schlumberger electrical sounding essentially involves the passage of an applied current  $I$  into the ground through two current electrodes and the measurement of the resulting potential difference  $\nabla V$  between a second electrode pair. From a knowledge of the geometry of the electrode arrangement it is possible to calculate the apparent resistivity of the subsurface as viewed by the configuration. By expanding the electrode configuration about a fixed reference point, a sequence of apparent resistivity values can be obtained which relate to progressively greater, and therefore deeper, volumes of earth. These data are plotted as a sounding curve which depicts the variation of apparent resistivity with current-electrode spacing, the latter serving as a pseudo-depth. The object is to obtain, by graphic or analytical interpretation of the sounding curve, the vertical distribution of electrical resistivity beneath the reference point in the form of a horizontal layering of discrete intrinsic resistivities.

The sounding data compiled for this report consist of 408 sounding curves (**Figure 2**). The majority of these soundings were done during the first phases of this project but work done previously in the area was also used extensively (Van Zijl, 1971; Australian Groundwater Consultants, 1975; Worthington, 1978; Meyer *et al*, 1987; Meyer *et al*, 1989a; 1989b). Most of the electrical soundings were expanded to maximum current electrode (AB) spacings of 1km, but several, especially those used for calibration purposes at boreholes had longer AB spacings, with AB = 6 km being the maximum used.

#### 2.4.2 *Types of sounding curves*

Sounding curves are predominantly of the descending type (or Q, QQ and QQQ type) which indicates a decrease in resistivity with the depth. **Figure 3** shows a typical example. At short current electrode spacings, corresponding to a small depth of investigation, the apparent resistivity is high ( $>4\,000\text{ ohm.m}$ ) indicating the dry surface sand (Holocene age). Following this, the resistivity decreases with depth with indications of a thick layer with a resistivity below  $100\text{ ohm.m}$  (the Upper Pleistocene?) and finally the sounding curve flattens out at large current electrode spacings to approach a value of around  $4\text{ ohm.m}$ . This layer indicates the Cretaceous/Palaeocene siltstone unit.

In some of the longer soundings, the presence of the resistive basement could be observed at the longest AB spacings. The sounding curve at ES 85, where the maximum current electrode spacing (AB) was 6 km, is a good example (**Figure 4**). The minimum value the curve attains is  $5.5\text{ ohm.m}$  which means that the true resistivity must be somewhat lower. This conductive layer represents the Cretaceous/Palaeocene siltstone unit. The final segment of the curve, however, rises again and is the manifestation of the more resistive rocks of the Lebombo Group which are expected to underlie the siltstones in this region.

Representative sounding curves measured on outcrops of the different geological formations or sequences are given in **Figures 5 to 8** (Lebombo, Makatini, Mzinene, St Lucia, Uloa, Port Durnford, Berea formations and Holocene sediments).

#### 2.4.3 *Goelectric layer resistivities*

Using all the goelectric data available Worthington (1978) compiled a histogram of surface-measured formation resistivities and divided the geological succession into four goelectric units. These are shown in **Figure 9**. With additional data collected after Worthington's survey, it became apparent that the Middle-Palaeocene/Late Cretaceous siltstones (goelectric Unit 4), with a resistivity range of  $3\text{--}15\text{ ohm.m}$  can, however, often be divided into two units, an upper more resistive unit, and a lower, more conductive unit. Otherwise the classification scheme used by Worthington still holds. The extended biostratigraphic, lithostratigraphic and goelectric subdivision of the Cenozoic and Mesozoic succession is given in **Table 2**.

#### 2.4.4 *Calibration soundings*

Electrical resistivity soundings were done near all existing boreholes where reliable geological control was available in order to be able to calibrate the interpretations. The interpretations (layer resistivities and thicknesses) were adjusted to correspond to the geological borehole information until a good fit to the field data was obtained. In this way a narrow range of resistivity values were obtained for the different geological formations and these were then used to interpret the rest of the sounding curves.

**Table 2:** Correlation of the biostratigraphic, lithostratigraphic and geoelectrical subdivisions of the Cenozoic and late Mesozoic succession on the Zululand Coastal Plain (Adapted and extended from Worthington, 1978).

Biostratigraphic range	Lithostratigraphic range	Geoelectric Unit	Resistivity range (ohm.m)	Approximate position of geological formations
Holocene - latest Pleistocene	Dune and beach sand	Surficial Units 1(a) and 1(b)	250 - 7 500	_____ Berea Formation
Late Pleistocene	Fine-grained aeolian quartz sand	Upper Pleistocene Unit 2	90 - 350	Bluff Formation
Middle Pleistocene	very fine-grained quartz sand	Middle Pleistocene Unit 3(a)	24 - 75	Port Durnford and Uloa Formations
Middle Palaeocene	Calcarenite, coquina	Miocene Unit 3(b)		
Late Cretaceous	Glauconite	Palaeocene? Unit 4(a)	8 - 15	St Lucia Formation
	Siltstone	Late Cretaceous Unit 4(b)	3 - 8	Mzinene Formation?

Examples of interpreted calibration curves are given in **Figure 10**. All borehole information, together with the sounding results obtained from DC soundings done on outcrops of the various geological formations, were used to compile a list of the variation in the apparent resistivity of the different geological formations (**Table 2**).

## **2.5 Electromagnetic soundings**

### **2.5.1 General**

A total of 68 Transient Electromagnetic Soundings (TEM) were conducted in the northern part of the Zululand coastal area. A Geonics EM-37 instrument was used for this survey. The results of 23 additional TEM soundings done previously are also included in this report. The localities of TEM soundings are shown on **Figure 11**.

To evaluate the TEM sounding results with the direct current (DC) results, a number of the TEM soundings were done at the same location as the DC soundings. The interpretation of some of the TEM soundings proved to be of a complex nature, due to the fact that the depth of investigation attained with the TEM method was restricted by conductive, near surface layers. A factor that reduces the effective use of the TEM method in the Zululand coastal area is that the TEM method is very effective in recognizing conductive layers, whereas the DC method recognizes both conductive and resistive layers as long as they are well defined in terms of thicknesses. Furthermore, it is well known that the absolute interpreted conductivity value for a certain layer differs, depending on the geophysical method that is being used. This makes a direct correlation between the two methods difficult. The successful application for the TEM method in the Zululand coastal area was further restricted by the fact that the conductive lower Port Durnford Formation was absent in certain areas. The TEM method defines the depth to the first conductive layer with a high degree of confidence, but it was often uncertain whether this conductive layer represents the lower Port Durnford, the Muzi or the Cretaceous Formations.

### **2.5.2 Calibration soundings**

The results of TEM measurements near boreholes in the northern part of the investigation area is shown in **Figure 12**. It was possible to achieve an excellent correlation between the TEM results and the actual borehole results for the depth to the Cretaceous floor in two cases, namely at boreholes ZD 1/71 and ZG 1/72 (**Figure 13**). In all the other cases, the Cretaceous floor was more than 20 m deeper than the interpreted depth to the conductive layer from the TEM results (**Figure 12**).

In the early phase of this investigation, the Uloa Formation was regarded as having a conductive character and that the top of this formation could be used as a conductive marker when dealing with the TEM method. However, as the investigation was extended to cover the whole of the Zululand coastal area, it became evident from

borehole and DC results that the lower Port Durnford and the Cretaceous formations are much more conductive than the Uloa Formation. The resistivity of the Uloa Formation falls in a range of 40-100 ohm.m, i.e. within the range of geoelectric Unit 3 (**Table 2**).

## **2.6 Gravity survey**

The Directorate Geohydrology, Department of Water Affairs and Forestry conducted a short gravity survey in the vicinity of St Lucia. The objective was to establish whether the gravity method could be used successfully to locate the palaeo-channels eroded into the Cretaceous and which have subsequently been filled with younger sediments. The survey was, however, unsuccessful due to the steep gradient of the gravity field observed along large sections of the South African coastline. Unless the regional gravity field can be removed successfully from the survey data, small perturbations on the gravity field, as would be expected under the conditions in Zululand, cannot be recognized successfully. The survey was abandoned after two profiles did not reveal the presence of a palaeo-channel identified by the drilling results.

## **2.7 Results of geophysical investigation**

### **2.7.1 Geoelectrical techniques**

As was discussed in the previous chapter, the electrical techniques gave the best results in terms of the depth to the Cretaceous basement. Although both these techniques result in a geoelectrical layered interpretation of the geological succession, it was not possible to unambiguously relate the different geological formations/units to specific geoelectrical layers. This is also clearly illustrated in **Table 2** which indicates a large range in and a large degree of overlap of the resistivities allocated to different geoelectrical/geological units.

From a comparison between the results of the resistivity (DC) and the electromagnetic (TEM) surveys in determining the depth to Cretaceous, it appears that with the TEM technique the top of the Uloa Formation could be mapped, whereas at the same locality the DC technique indicated the depth to the top of the Cretaceous. By combining the interpretations of the two techniques, the thickness of the Uloa Formation could therefore theoretically be resolved.

Our knowledge of the extent and occurrence of the Uloa Formation is, however, not sufficient to collect an extensive set of correlation soundings to be able to use the two techniques in a complimentary way to resolve the presence and thickness of the Uloa Formation across the Zululand coastal plain. The application of the TEM technique was therefore only restricted to the northern part of the coastal plain.

In view of the uncertainties associated with the results of the TEM interpretations, these interpretations were not used in the compilation of an elevation map of the top of the Cretaceous. **Figure 14** shows all boreholes drilled on the Coastal Plain where geological information was available, whereas **Figure 15** indicates those boreholes that intersected Cretaceous sediments and which were used for calibrating the resistivity and EM sounding interpretations. **Figure 16** shows those localities where the depth to Cretaceous could be confidently interpreted from the sounding curves. By combining all DC sounding interpretations and borehole information, separate contour maps of the depth to Cretaceous were compiled for the northern and southern parts of the Coastal Plain (**Figures 17 and 18**). These maps must, however, be seen as first approximations of the post Cretaceous topography as there are still several unresolved issues with regard to the interpretation of the geophysical data.

One significant feature, not revealed by the contour map, is the presence of an extremely wide palaeo-channel eroded into the Cretaceous floor rocks and subsequently filled by younger deposits. This channel is situated between Lake Sibayi and the coast. Interpretations of the geoelectrical data indicates an erosional depth to approximately ~120 m below mean sea level. This channel is almost 20 km wide and occurs over the entire length of Lake Sibayi. The existence of this channel could not be proved by drilling due to access and drilling restrictions, but the geoelectrical character of the material deposited in this area, differs significantly from that found to the north and south of Lake Sibayi. The implications this channel has on the seepage of water from Lake Sibayi is discussed later (**Chapter 5.3**).

#### **2.7.2 Geophysical borehole logging**

Geophysical borehole logging was not able to resolve the interfaces between the different geological formations uniquely. This is due to a lack of sufficient contrast in physical properties of the different units in the succession. The electrical logs were, however, used to calculate porosity values for the geological units using Archie's Law. The results are presented in **Table 3**. As can be seen from this table, a wide variation in the values calculated for porosity were observed. Because of the many assumptions made when applying Archie's Law, the porosity values should only be used as an indication of the relative porosity of the different horizons.

The unrealistically high value for the Uloa Formation (**Table 3**) may in part be due to karstified conditions developed in the formation. In comparison, the values listed by Davies, Lynn and Partners (1992) for the Eastern Shores area of St Lucia are also listed in **Tables 3 and 4**.



**Table 3:** Porosity determinations using "Archie's Law" where  $F = \rho_r / \rho_w = a\phi^m$  (with  $a=1$  and  $m=1.5$ )

Borehole	Depth interval	$\rho_r$ (ohm.m)	$\rho_w$ (ohm.m)	$\phi$ (%) ( $m = 1.5$ )	Geology	$\phi$ (%) Average
P110/1	0-8	430	19	12.4	0-15m Holocene deposits 15-31m Upper Port Durnford Formation 31-47m Uloa Formation	21  55
	8-12	160	19	24		
	12-16	160-60	19	24-46		
	16-30	40	19	60.7		
	30-42	10	19	-		
	42-47	30	19	73.886		
P110/2	0-40	100	11	22.8	0-7m Holocene deposits 7-55m Upper Port Durnford Formation 55-84m Uloa Formation	23 29  49
	40-54	100-20	11	22.8-67		
	54-72	25	11	57.7		
	72-78	52	11	35.3		
	78-84	38	11	43.6		
P110/3	0-5	250	23	20.3	0-14m Holocene deposits 14-54m Upper Port Durnford Formation 89-98 Upper Cretaceous	27  37  69  -
	5-16	140	23	29.8		
	16-28	170	23	25.2		
	28-33	170-110	23	26.2-52.6		
	33-57	110-60	23	35-52.6		
	57-71	40	23	69		
	71-87	62	23	51.5		
	87-98	15	23	-		
P110/4	0-2.5	50	55	-	0-2.5m Holocene deposits 2.5-12m Upper Port Durnford Formation 12-17m Peat	31
	2.5-11	320	55	30.9		
	11-17	40	55	-		
P110/5	0-7	66	5	17.8	0-16 Holocene deposits 16-41m Upper Port Durnford Formation	16   16
	7-16	95	5	13.9		
	16-21	140	5	10.7		
	21-28	70	5	17.1		
	28-41	64	5	18.1		
P110/6	0-5	300	23	6917.9	Holocene deposits Upper Port Durnford Formation Uloa Formation	28  27.5  61
	5-12	110	23	35		
	12-30	220	23	22		
	30-56	130	23	31.3		
	56-68	55	23	55.8		
	68-75	40	23	69		

Average: Holocene ~23%; Port Durnford Formation ~31%; Uloa Formation > 50%(?)

**Table 4:** Porosity values for different geological sequences as derived from geophysical borehole logging and other techniques

Geological unit	Resistivity logging derived porosity	Porosity (as per Davies Lynn and Partners report (1992))
Holocene deposits	~23%	
"Cover sands" (Holocene)		38%
Older aeolian sands		36%
Port Durnford Formation	~31%	
Uloa Formation	~50%	42%

## CHAPTER 3

### GEOHYDROLOGY OF THE ZULULAND COASTAL PLAIN

---

#### 3.1 Aquifer description

Because all the formations above the Cretaceous floor rocks are composed of mainly quartzitic sands, many of which are unconsolidated to consolidated, they can all be treated as potential aquifer units. The report by Davies, Lynn and Partners (1992) indicated that the grain size distribution, as well as the porosity of the young Holocene age cover sands, the underlying more cemented aeolian sands and the Port Durnford Formation are virtually the same. The variation in permeability of these three units, listed by Davies, Lynn and Partners (1992) (from 0.8 m/d to 17 m/d) can in part be explained by the small variation (a few percent only) in the silt and clay content of the samples.

Borehole data, as well as hand dug wells and shallow augering have indicated that the arenaceous succession is generally fully saturated from the interface with the Cretaceous formations up to a frequently shallow water level. The data set of water levels collected during the study indicated a close relationship to the topography. This suggests that the near surface deposits possess a relatively low hydraulic permeability. This mimic of the topography by the water level, was used to interpolate water level information in areas where little or no data was available (see **Chapter 4**).

The many shallow wells (mainly hand dug) that exploit this shallow aquifer, have a low yield and are often equipped with hand pumps.

The next aquifer unit in the succession is the Upper Port Durnford Formation. This aquifer has not been exploited to any great extent, although north of Richards Bay new well fields have been developed recently in this formation with good success. Hydraulic permeability of the Port Durnford Formation has been determined for the Eastern Shores of Lake St Lucia and found to be around 4 - 5 m/d.

The study by Australian Groundwater Consultants (1975) and Worthington (1978) identified the Uloa Formation to be the most promising aquifers unit in the region. As described above, this formation consists of a coarse-grained shelly sandstone with calcarenite associated with it. The calcarenite has been observed in borehole core samples to contain some dissolution channels which increases its porosity significantly. This layer is however usually only a few metres thick and is not present everywhere. Thicknesses of up to 25 m have been reported. Worthington (1978) is of the opinion that the mode of distribution of this Miocene succession is determined to a large extent by the undulations in the erosion surface of the underlying Palaeocene siltstones.

Pumping tests results from this aquifer reported by Australian Groundwater Consultants (1975), Worthington (1978) and Simmonds (1990) indicated yields of up to 25 l/s in areas where this layer is more than 20m thick.

The permeabilities obtained from pumping tests are within the range of 0.5 - 23.6 m/d with an average of 4.5 m/d. Values for the storage coefficient range from  $1.9 \times 10^{-5}$  to  $4.7 \times 10^{-3}$  with an average at  $1.9 \times 10^{-3}$ . Most of the pumping tests revealed leaky confined aquifer conditions.

For the unconsolidated Holocene sands forming an unconfined aquifer, Kelbe and Rawlins (1992) used a specific yield of 35% and for the Port Durnford Formation a specific yield of 20% in their aquifer simulation studies.

## **3.2 Hydrochemisry and isotope studies**

### **3.2.1 *Ground water chemistry***

Chemical analyses have been done on a number of water samples collected during the project. Additional data have been obtained from other sources (National Groundwater Data Base, forestry companies, Richards Bay Minerals). Particularly from the report of Australian Groundwater Consultants (1975) a large number of analyses were supplied from their study area of interest near Richards Bay. The analyses have all been entered in a HYDROCOM data base, set up for the Zululand coastal plain. Boreholes where water analyses were available or where additional water samples could be collected are shown in **Figure 19**. The resulting data, representing all chemical ground water data for the Coastal Plain are presented as Piper, Durov, Schoeller, and SAR diagrams (**Figure 20**).

The overall quality of the water is good (conductivity generally <100 mS/m). The chemical pattern is generally similar to that of sea water with respect to Na, Cl, and  $\text{SO}_4$  ratios corresponding to rain water in more concentrated form. The products of carbonate dissolutions are added to the water only to a limited extent because of the low occurrence of carbonate in the area - particularly close to the sea. Low pH values are therefore common.

Some clear differences in ground water quality are evident. The analytical results from boreholes in the area between the Lakes Nhlabane and Mzingazi are characterized by high conductivity (>200 mS/m) and a clear Ca/Mg bicarbonate character. The search for an explanation for this distinct difference motivated the attempt to correlate water chemistry with geology, using statistical techniques.

The low number of samples (31) for which a specific geological association was known, prevented the use of standard multivariate statistical techniques (principal components,

cluster analysis, etc.). The chemical analyses of the available samples have therefore been subjected to a more qualitative method of data analyses which involves the construction of a 'fingerprint' table representing the ratio of concentrations of the different elements present in the samples. This method makes provision for the use of a small data set (i.e. relatively high uncertainties) in order to classify an unknown borehole water sample to either have originated from a specific lithological unit or to be a mixture of waters from different lithological units. The method entails making use of the 'fingerprint' table to determine strata of high probable origin following which a consideration of specific chemical ratios can yield the more probable geological association. A description of the data reduction and development of the 'fingerprint' table is given in **Appendix A**. The application is explained using some analyses selected from the Zululand water chemistry data base. The origin of some water samples thus determined is then compared with that of the geological borehole description and the depth from which the sample was taken.

From the examples in **Appendix A**, it follows that clear distinctions can be made between the more arenaceous units of the Upper Port Durnford, the lignite layer, and the Miocene sand and the argillaceous Lower Port Durnford, Uloa calcarenite and St Lucia mudstone. Difficulty was encountered in separating Lower Port Durnford from Uloa calcarenite due to the small difference in chemistry between their waters. The Upper Port Durnford was indistinguishable from the lignite layer. This could have been expected since the lignite layer is not an aquifer in the true sense of the word and the sample denoted as such is probably Upper Port Durnford water deriving chemical constituents from the lignite band. Most of the samples tested listed in **Appendix A** could indicate a single layer of the aquifer as the main source of the water.

### 3.2.2 *Isotopes in water*

#### Stable isotopes

Stable isotopes analyses of  $^{18}\text{O}$  and deuterium, were determined on most of the samples collected in the course of this project. Boreholes, and other water point locations where water samples were collected for isotope analyses are indicated on **Figure 21**. The aim was to characterize water types in the area. The initial work by Vogel and Van Urk (1975) near St Lucia, suggested that the isotopic composition of ground water might decrease from the coast inland. It appeared that this could be a useful tracer to follow ground water movement.

The accumulated data set of  $\delta^{18}\text{O}$  analyses in ground water indicated no significant isotopic variation (**Figure 22**). The isotope survey of rainfall also indicated such a constancy of isotope values throughout the area (see **Chapter 4.4**). The explanation for this lack of a "continental effect" must probably be sought in the very flat topography of the area and the episodic nature of the rain storms occurring in this area.

Surface waters (lake and rivers) show isotope enrichment with both  $^{18}\text{O}$  and deuterium (**Figure 24**). This is a generally known feature due to evaporation enrichment (Gat and Gonfiantini, 1981) during winter, but also during dry periods of summer. It appears that large lakes (e.g. Sibayi) have higher  $\delta^{18}\text{O}$  values than small pans. In the case of the latter, the depression (in this area at least) is essentially cutting below the water table and it appears that the water is just flowing through the pan system. The higher  $\delta^{18}\text{O}$  content of the large lakes was used as tracer to distinguish it from ground water to follow leakage of lake water towards the sea (see 3.3 below).

$\delta^{18}\text{O}$  and chloride time series were obtained from Lake Sibayi and Lake Bhangazi. These will be discussed below in the context of leakage studies from these lakes.

### Radiocarbon

A few ground water samples from existing (shallow) boreholes were collected for  $^{14}\text{C}$  analysis. The results (**Table 5**) indicated high  $^{14}\text{C}$  values typical of post-1960 recharge ( $^{14}\text{C} > 90\%$ ). This is in accordance with the high throughflow of water through the aquifer deduced from recharge estimates and modelling. The single lower  $^{14}\text{C}$  value (MT12) can be interpreted as considerably older (up to a few hundred years), but part of this  $^{14}\text{C}$  lowering is also due to the higher alkalinity of the sample (from carbonate solution). Overall, the high  $^{14}\text{C}$  values indicated that this isotope would not be very useful here, because of the high recharge rate.

The 120%  $^{14}\text{C}$  value of Lake Sibayi confirms the  $\delta^{18}\text{O}$  and modelling data that the lake water has a considerable residence time since it has had ample time for isotopic exchange of carbon and water with the atmosphere.

## 3.3 Ground water leakage to the sea

Stable isotopes were successfully used to indicate the movement of lake water through and below the dune cordon to the sea. The largest of the isolated lakes, Lake Sibayi (Allanson, 1979), is 70km<sup>2</sup> in extent, and separated from the sea by dunes which at places are up to 160m high and 1-2km wide, along a 10km length. The water level in the lake is approximately 20m above mean sea level and is in hydraulic contact with ground water levels in the sands around the lake. The average chloride content of the lake water (130 mg/l) is about three times that of the surrounding ground water, and remains very constant throughout the year. The  $\delta^{18}\text{O}$  content of the water is +2.2‰ SMOW, indicating that it represents a water body subject to extensive evaporation (Gat and Gonfiantini, 1981). This closed lake drains ground water from the inland areas, and the fact that its salinity remains low, suggests that a considerable water flow through the dune towards the sea must exist (Pitman and Hutchinson, 1975).

**Table 5:** Radiocarbon content of ground and surface water samples.

Sample no.	Name/Locality	Depth (m)	Analysis no.	$^{14}\text{C}$ (‰ modern)	Model age	$^{18}\text{O}$ (‰ SMOW)	$^{13}\text{C}$ (‰ PDB)
MT2	Ozabeno borehole	39m	Pta-4855	$103.5 \pm 0.8$	<30 year	-3.8	-21.1
MT10	Mftholweni borehole	40m	Pta-4845	$107.8 \pm 0.8$	<30 year	-3.6	-8.5
MT9	Phelendaba IDC borehole	29m	Pta-4849	$100.8 \pm 0.8$	<30 year	-1.0	-6.1
MT12	Mangusi Police borehole	30m	Pta-4893	$83.0 \pm 0.9$	<30 year	-2.2	-13.8
MT17	Mungu well	Shallow	Pta-4878	$116.7 \pm 0.9$	<30 year	-3.0	.11.7
MT18	Lake Sibayi	Surface	Pta-4861	$120.7 \pm 0.9$	<30 year	+2.1	-2.3

A set of water samples was collected over a two-year period by ourselves and by DWA&F staff servicing the water level gauge on the eastern end of Lake Sibayi. The very constant  $\delta^{18}\text{O}$  and chloride content (**Figure 24**) indicates that the lake is not sensitive to seasonal inflow and that the water body represents the throughflow of quite a number of years. This is consistent with the  $^{14}\text{C}$  content of 120% modern, which is higher than any of the ground water samples analyzed in the area and equal to the atmospheric value.

An occurrence of fresh-water seepage was found on the beach at Gobey's Point, opposite the southern end of Lake Sibayi. During Spring low tide, water emerges from under the dune onto the beach just above a horizontal sheet of calcified beach rock (**Figure 25**). A sample of the seepage water was found to have a  $\delta^{18}\text{O} = +1.85\text{‰}$  SMOW and a chlorinity of 6 g/l. Compared with the available values of Sibayi water ( $\delta^{18}\text{O} = +2.2\text{‰}$ ), local sea water ( $\delta^{18}\text{O} = +0.6\text{‰}$ ) and likely ground water ( $\delta^{18}\text{O} = -4$  to  $-2\text{‰}$ ) around the lake, it was evident from the position of the Gobey's Point sample on the possible mixing lines that the relatively fresh water seepage sampled on the beach was a mixture of Lake Sibayi water and sea water (**Figure 26**). There is no way that the normal ground water in the vicinity can be considered as the water source of the seepage, since its  $\delta^{18}\text{O}$  value is lower than any of the other components. This was confirmed with deuterium, where again the Gobey's Point sample located between Lake Sibayi and sea water (**Figure 27**), and away from the meteoric water line representing rain and ground water. The high salt content measured in the seepage is ascribed to sea water left behind in the beach sand during low tide which mixes with the fresh seepage water. See also **Chapter 5** for a discussion on the seepage from Lake Sibayi.

A similar fresh water occurrence along the coast near the Cape Vidal light house (north of St Lucia) has also been studied. Natal Parks Board staff supplied regular samples of this seepage and from Lake Bhangazi, just west of the dune from Cape Vidal. The  $\delta^{18}\text{O}$  and chloride data are more complex here compared to those of Lake Sibayi (**Figure 28**). Lake Bhangazi shows the effect of summer rains as a slow drop of the  $\delta^{18}\text{O}$  and Cl contents after January 1991. During the following (very dry) summer, the  $\delta^{18}\text{O}$  content rose markedly to values similar to Lake Sibayi (due to evaporation enrichment). The Cape Vidal seepage follows the lake water somewhat w.r.t.  $\delta^{18}\text{O}$ , without copying the major detail (**Figure 28**). Even though  $\delta^{18}\text{O}$  values are close to that of sea water, the low chloride contents of the seepage compared with sea water (19 000 mg/l) preclude the latter from being a major contributor (**Figure 29**). The combined evidence of  $\delta^{18}\text{O}$ , Cl and D suggest that this seepage is due to mixing between an evaporated water (Bhangazi) and local rain or ground water (**Figure 30**) with some occasional minor sea water addition to raise the chloride level.

The hydrology around Lake Bhangazi differs from that at Lake Sibayi, and probably causes the difference in the isotope character of seepage at Gobey's Point and Cape Vidal. At Lake Sibayi, a pressure head of approximately 20m exists, whereas at Lake Bhangazi it is only of the order of 6-7m. The surface area of Lake Bhangazi is about

3km<sup>2</sup>, compared with the ~70km<sup>2</sup> of Lake Sibayi. To the south of Lake Bhangazi, a large swamp area, the Mfabeni Swamp, is present which is an expression of the ground water level in the area. Lake Bhangazi is believed to act as a feeder to the Mfabeni Swamp, which eventually drains into Lake St Lucia. According to water levels measured in boreholes drilled during the Environmental Impact Assessment at Eastern Shores (CES, 1992), there is a ground water divide between Lake Bhangazi and the sea. The maximum piezometric head of this divide is, however, close to that of the water level in the lake. This may explain in part the different isotopic signature observed in the seepage water at Cape Vidal.

### 3.4 Rain water chemistry

#### 3.4.1 Sampling

After commencement of the project, the Steering Committee recommended that rainfall chemistry be included in the work programme. The object was to determine ion correlations in rain-water and ground water and use these to estimate the recharge to the aquifer.

A network of rainfall collecting stations was therefore established and operated for the largest part of three rainy seasons. That this period included the very dry 1991/92 season is in a sense useful, since it enabled the effect of wet/dry seasons to be investigated. The stations were selected to study the variation in rainfall chemistry over the area north of St Lucia and to provide a range of distances from the coast (Murgatroyd, 1983) and north/south variation with due regard to the availability of existing rain gauge stations and reliability of operators.

The locations of the six stations used are shown in **Figure 31** and relevant station details are indicated in **Table 6**.

Rainfall samples were collected as part of the standard weather observation routine. Daily precipitation samples were poured into a large container in the morning, when the rainfall for the past 24 hours was recorded. Once a month a 100ml sample from the monthly composite was dispatched to the laboratory for analysis. The rain gauges were standard Weather Bureau rain gauges (except at Phelendaba where an open cone gauge was used) and evaporation is considered to have been negligible. Initial experiments with monthly rainfall samplers were abandoned when it became evident that too much evaporation occurred in these samplers. At Phelendaba a few samples from large single rainstorms were also collected and compared with the monthly composites. No attempts were made to obtain onsite measurements of pH or other parameters, since this was deemed to be beyond the interest and capabilities of the sample collectors.



**Table 6:** Details of rainfall stations

Code	WB No.	Station	Authority
MBA	0412/180	Mbazwane Plantation	Kwazulu Department of Agriculture and Forestry
SOD	0376/302	Sodwana Bay	Natal Parks Board
MAK	0411/323	Makatini Agricultural Research Station	(then) Department of Development Aid Kwazulu
MAN	0412/466	Manzengwenya	Department of Agriculture and Forestry
PHE	0412/096	Phelendaba (Muzi)	IDC
TEM	0411/723	Tembe Elephant Park (Sihangwana)	Kwazulu Bureau of Natural Resources

The monthly composite samples were analyzed at the CSIR in Pretoria for  $^{18}\text{O}$  and deuterium, and for chemistry at the CSIR laboratory in Stellenbosch. Originally only the major cations and anions were analyzed, but others ( $\text{NH}_4$ ,  $\text{NO}_3$ , P) were added later to improve the ion balance.

Rainfall amounts were obtained from the samplers and confirmed from the authority to whom they have been reported. Good cooperation could be established with the samplers, resulting in a high collection reliability. For the period October 1989 to June 1992, between 86% and 100% of the rainfall at each station was collected.

### 3.4.2 Rain water chemistry

A data set of 157 useful rain-water chemistry analyses were obtained of which 95% showed cations and anions balanced to within 10% of each other. This is quite satisfactory in view of the low ion concentrations involved. The product of monthly rainfall amount and concentration yields the monthly salt deposition (expressed in kg/ha;  $1\text{kg/ha} = 0.1\text{g/m}$ ). This is the quantity relevant for salt balance and recharge calculations.

Statistical relations between the ion concentrations show good correlations between Na, Cl, Mg, and  $\text{SO}_4$  (**Table 7**). These are the main constituents of sea water and their correlation supports the model that seawater is the main source of salt in the rain. There is also a fair correlation between Ca and alkalinity identifying calcium carbonate as another salt source in rain. Principal component analysis of the same data set yielded a first principal component (PC1) weighted with Na, Cl, Mg, and  $\text{SO}_4$  a second one (PC2) weighted with Ca and alkalinity (**Figure 32**). Together these two principal components account for 84% of the variation of these ions in the rain samples analyzed.

A more direct composition model can be calculated by using the average of Na and Cl (suitably weighted) to indicate the sea water addition to the rain-water chemical

composition and then correcting Mg, SO<sub>4</sub>, Ca, and alkalinity proportionately. The average of the Ca and alkalinity remaining, is then used to indicate the CaCO<sub>3</sub> addition to the rain-water chemistry (Mamane, 1987). This simple addition model, similarly, accounts for 85% of the dissolved ions in the rain water with no obvious other relations in the remaining ion quantities.

**Table 7:** Correlation matrix of major constituents of rain-water (based on 157 analyses)

	Na	Cl	Mg	SO <sub>4</sub>	Ca	K	Alk
Na	1	0.99	0.97	0.74	0.61	0.57	0.50
Cl		1	0.96	0.71	0.59	0.53	0.43
Mg			1	0.81	0.66	0.65	0.55
SO <sub>4</sub>				1	0.59	0.65	0.36
Ca					1	0.47	0.74
K						1	0.64
Alk							1

Chemical concentrations of the collected rain water samples were used to calculate chloride deposition (**Appendix B**). Missing values (chloride, rainfall or samples not analyzed) were interpolated, using general features of these parameters. In this way, a data base covering three complete rainfall seasons (1989-1992) from August to July, was established, from which annual deposition rates were calculated.

Large variations of Ca and Cl deposition are evident from year to year through the very variable rainy periods encountered during the three-year sampling period (**Figures 33 and 34**). The annual chloride deposition rate relates to the rainfall amounts to some extent (**Figures 35**). The outlier chloride deposition of MAN in 1991/92 (compared with its annual rainfall) is due to two high chloride analyses (October 1991 and February 1992). While no sampling or analysis problems for these samples could be traced, the data look suspicious, and were reduced by a factor 3 for application in the three-year average used for recharge calculation (**Chapter 3**). The average values of the three complete seasons are then considered to represent a good long-term average.

The dominant feature of the ion distribution over the area is the rapid decrease of total salt deposition with distance inland (**Figure 36**). This was observed by earlier workers in the area (Murgatroyd, 1983; Archibald and Muller, 1987) and is a common feature worldwide (Junge and Werby, 1958; Hingston and Gailitis, 1976). The chemical character of the rain water composition changes by the rapid decrease of the sea water contribution, while the calcium carbonate contribution does not decrease all that much (**Figure 36**). This suggests that the CaCO<sub>3</sub> component could be a recirculated constituent, i.e. not a constituent transported from elsewhere. The source of this

carbonate is, however, not evident. The entire area is a typically acidic, non-calcretic humid environment where carbonate dust is not expected to occur in great abundance.

**Table 8:** Chloride deposition at rainfall stations (annual rainfall (mm) in brackets).

	Distance from sea (km)	Chloride deposition (in kg/ha/yr) and annual rainfall (in mm)			Average chloride deposition (kg/ha/yr)
		1989-90	1990-91	1991-92	
<b>Sodwana (SOD)</b>	0.5	114.8 (1516)	116.2 (1764)	51.8 (408)	94.3
<b>Manzingwenya (MAN)</b>	4	49.1 (986)	128.7 (1652)	137.7* (546)	74.6
<b>Mbazwane (MBA)</b>	8	57.6 (1239)	78.3 (1618)	48.0 (515)	61.3
<b>Phelendaba (PHE)</b>	24	27.2 (851)	28.2 (963)	25.0 (309)	26.8
<b>Makatini (MAK)</b>	44	24.0 (806)	20.3 (904)	10.0 (337)	18.1
<b>Tembe (TEM)</b>	50	22.5 (986)	20.8 (963)	18.5 (405)	20.6

Note: \* Probably too high by factor 3 (Figure 36). Corrected before averaging.

### 3.4.3 Isotopes in rainfall

Oxygen-18 analyses of the monthly rain water samples for all six collecting stations show a seasonal relation with low  $\delta^{18}\text{O}$  values during the summer and high values in winter (Figure 37). In some cases an inverse relation between rainfall and  $\delta^{18}\text{O}$  seems to exist (the so-called amount effect), but on a monthly basis, this is not very clear.

Deuterium analyses were also done on most rain water samples. The data show a good relation with  $\delta^{18}\text{O}$  along the known worldwide meteoric water-line (MWL) with only a few evaporated samples ( $\delta^{18}\text{O} > 0$ ) off the MWL (Figure 38). Most ground water samples are also located on this line (Figure 23).

The weighted (by precipitation amount) annual average  $\delta^{18}\text{O}$  content varies consistently from year to year at all the stations (Figure 39). This supports the "high  $^{18}\text{O}$  - arid season" linkage (Rozanski *et al.*, 1992) in a very convincing manner and suggest that, on an annual basis,  $\delta^{18}\text{O}$  could be used as rainfall indicator. Over the whole study area the variation of the mean annual  $\delta^{18}\text{O}$  content of rain varies less than 1‰ within the same year (Table 9).

The annual  $\delta^{18}\text{O}$  values can be combined in a weighted mean for the three year period for which measurements are available. If one assumes that only a representative portion of the rainfall above a certain cut-off point actually contributes to recharge (Bredenkamp, 1980), then the weighting is even more directed to higher rainfall years and subsequently lower  $\delta^{18}\text{O}$  values of recharge (**Table 9**). Cut-off values between 300 mm and 500 mm/annum produce  $\delta^{18}\text{O}$  values of recharge in the vicinity of -3.5‰ which correspond to the best estimate of  $\delta^{18}\text{O}$  in un-evaporated ground water (**Figure 22**).

**Table 9:** Three-year  $\delta^{18}\text{O}$  average weighted by annual rainfall less a cut-off value

	Cut-off 0	300 mm	500 mm
Sodwana (SOD)	-3.09	-3.33	-3.38
Manzengwenya (MAN)	-3.28	-3.60	-3.84
Mbazwana (MBA)	-3.51	-3.79	-3.90
Phelendaba (PHE)	-3.35	-3.78	-3.76
Makatini (MAK)	-2.60	-2.87	-2.95
Tembe (TEM)	-2.90	-3.03	-3.21

### 3.5 Ground water recharge estimates

Ground water recharge estimates have been reported by Worthington (1978) and Meyer and Kruger (1987). Worthington used a water balance approach and calculated that the recharge in the vicinity of Richards Bay is approximately 24% of the mean annual precipitation (MAP). Using a rainfall recharge relationship proposed by Bredenkamp (1985) which is based only on the MAP, Meyer and Kruger (1987) reported a recharge figure of approximately 21% of MAP.

The main aim of the rain water chemistry programme (**Chapter 3**) was to estimate ground water recharge by the salt increase method of Eriksson (Eriksson and Khunakasem, 1969; Eriksson, 1985). This method has been applied with a great deal of success in Botswana recently and led to the production of a map from which the recharge of ground water from rainfall can be deducted (Gieske, 1992). If  $C_p$  is the chloride (or any other conservative salt) content of rain water, then the evaporation of rain on and in the soil will cause the chloride content to rise to  $C_w$ . The recharge (as a fraction of rainfall) will then be

$$R = C_p / C_w.$$

Assumptions inherent in this technique are:

- (i) No production or removal of the specific salt by any other process, e.g. windblown salt, is recirculated.
- (ii) Dry salt deposition should be added to the total salt load. For this reason, the calculation is done from total salt deposition x annual rainfall (See **Appendix B** for a more detailed description of the recharge calculation procedure).
- (iii) It is assumed that the ground water chloride represents only vertically recharged water and not laterally transported salt. Adaptations for the latter situations can be made (Eriksson and Khunakasem, 1969).

In the Zululand coastal plain, it was considered that the above conditions would be valid and that reliable data could be obtained. A similar approach to obviate the problem of (iii) above, is to analyse the salt content of the soil moisture in the unsaturated zone just above the water table (Edmunds *et al.*, 1990; Bredenkamp, 1993). This is a more complex procedure, and requires that the water table be below the root zone.

Average chloride contents for rainfall were obtained from the chloride deposition rates and annual rainfall amounts (**Appendix B**). Chloride contents of ground water were estimated from borehole samples in the vicinity of the rainfall collection stations.

The resulting recharge data, which indicated that the recharge varies from 18% near the coast to about 5% at a distance of 50 km inland, are about half of those obtained by Bredenkamp (1993), using chloride profiles in the soil from the unsaturated zone. Bredenkamp's profiles were obtained to the east and west of Lake St Lucia. The chloride content of the soil moisture in the case of the St. Lucia data appears to be about half of that measured in the ground water of the northern Zululand coastal plain. Since Bredenkamp used the same chloride input quantities, the resulting recharge values are therefore about double. It is at this stage not certain whether the situation near St Lucia is that much different from the more northerly region of the present study. Our selection of boreholes near the rainfall stations was very limited and the computed recharge values of **Table 10** should be considered as lower limits. Whether a distinct cut-off point exists below which no recharge occurs is uncertain, since our work was concentrated along the higher rainfall area of the coastal zone. More data of this nature are constantly being generated for southern Africa (Gieske, 1992; Bredenkamp, 1993; Bredenkamp, 1995), and a better overall picture will hopefully soon emerge.

These calculated recharge values derived with the chloride method are lower than earlier reported values, but are believed to be more representative for the coastal plain conditions. The main difference in the techniques are that, whereas the previous methods used a fixed percentage of the MAP over the entire coastal plain region, the chloride method calculated recharge (as a percentage of the MAP) varies with rainfall.

**Table 10:** Three-year average recharge data.

Station	Sodwana (SOD)	Manzengwenya (MAN)	Mbazwana (MBA)	Phelendaba (PHE)	Makatini (MAK)	Tembe (TEM)
Rainfall (mm)	1229	1061	1124	708	683	785
Cl deposit (kg/ha/yr)	94.3	74.6	61.3	26.8	18.1	20.6
Ground water chloride (mg/l)	45	40	40	40	45	50
Recharge (% of annual rainfall)	17	18	14	9.5	5.9	5.2
Recharge (mm/yr)	210	187.1	153	67	40	41

### 3.6 Potential for ground water pollution

Due to the essentially unconsolidated nature of large aquifers on the coastal plain, the aquifer is extremely vulnerable to pollution. There are, however, mitigating factors that can lower the risk of pollution.

Ground water pollution can be classified as either regional or localized. Regional ground water pollution arises from polluted rivers which are losing water to the hydrogeological regime, from contaminated rainfall, and from saline intrusion as a result of the lowering of the potentiometric levels in coastal areas. Along the Zululand coastal plain these criteria need not be considered on the three grounds that the streams are mostly gaining, the coastal setting is not susceptible to contaminated rainfall despite the development of petrochemical complexes in the industrial area, the heavy mineral mining of the dunes, and the coastal barrier complex acts generally as a ground water divide which affords strong protection against marine intrusion. Consequently, only localized pollution of ground waters need to be considered.

In an urban environment, localized ground water pollution can be induced by such diverse factors as sewage effluents from septic tanks and fractured or overflowing sewers, effluents from refuse-disposal sites or mine-waste dumps, miscellaneous industrial wastes, infiltration from horticultural land that has been treated with fertilizers or insecticides, the presence of cemeteries, quarries and disused wells, and to a much

lesser extent, transport accidents. However, the vulnerability of the ground water regime to these various forms of pollution can only be ascertained by a consideration of appropriate geological and hydrogeological factors.

The relevant geological factors involve the depth of burial of the aquifer and the lithologies of the aquifer itself and the overlying deposits. In general, the risk of pollution to a given aquifer decreases as its depth of burial increases. The vulnerability of the ground water regime decreases as the depth to the potentiometric surface increases. Although pollution will spread more rapidly in an aquifer of high transmissivity, this condition will also be conducive to the more rapid dispersal of pollutants. For a given aquifer transmissivity, the rate of advance of the pollution front varies with the hydraulic gradient. The significance of a source of ground water pollution diminishes at greater distances from points of outlet from the ground water regime, e.a. abstraction boreholes or zones of seepage into gaining rivers. Consequently, the direction of ground water flow is important. The vulnerability to pollution of an aquifer system decreases as the hydraulic conductivity of the overlying deposits decreases.

Worthington (1978) analyzed the pollution potential of the aquifers in the Mzingazi catchment in great detail. He made an appraisal of those geological and geohydrological factors that control ground water vulnerability to pollution and emphasized the importance of perennial streams. Based on this he produced a pollution vulnerability map for the Mzingazi catchment (**Figure 40**). He classified the area into 5 different zones according to the criteria listed in **Table 11**. It is clear that to be able to do such a detailed classification, an extensive data set of the aquifer is required. For the regional approach adopted in the present study, it was therefore not possible to assess the pollution potential to the same detail.

This classification around Richards Bay is still valid and should be taken into account when planning new residential and industrial areas around Richards Bay.

On a regional scale two potential sources of aquifer contamination can be identified. These are undesirable land-use practices (e.g. agriculture) and sea-water intrusion. The first source will include such land-use practices as large increase in population and settlements on the plains where the ground water level is shallow, and extensive development of the agricultural potential of the region. The development of settlements will result in increased loads of waste water and sewage effluent that has to be disposed of. The pollution potential can be reduced by restricting development to the topographically higher lying areas where the water table is deeper. The potential pollution associated with agricultural land-use practices, will depend on the degree to which fertilizers, pesticides and herbicides will be applied. Again, the aquifer is extremely vulnerable to pollution from this source, as agricultural development would probably concentrate on the low lying area. Careful planning of both new settlements and agricultural practice would be required in future.

Sea water intrusion appears not to be a major threat as the elevated ground water levels near the coast and associated with the dune cordon, form an effective intrusion barrier. However, if large scale abstraction would occur anywhere near the coast, monitoring of water levels and quality is essential to determine whether a reversal of the ground water flow direction may occur.

**Table 11:** Classification of proposed development zones within the Mzingazi catchment (Worthington, 1978)

Zone	Strata thickness	Pollution vulnerability
1	Miocene aquifer <10m Middle Pleistocene >5m Upper Pleistocene >10m	Very low risk
2	Middle Pleistocene >5m Miocene aquifer and Upper Pleistocene (either both > or both <10m)	Low risk
3	Miocene aquifer >10m Middle Pleistocene >5m Upper Pleistocene >10m <b>OR</b> Miocene aquifer <10m Middle Pleistocene <5m Upper Pleistocene >10m	Low to Moderate risk
4	Middle Pleistocene >5m Miocene aquifer and Upper Pleistocene (either both > or both <10m)	Moderate risk
5	Miocene aquifer <10m Middle Pleistocene >5m Upper Pleistocene >10m	High risk



## CHAPTER 4

### MATHEMATICAL MODELLING OF THE COASTAL PLAIN AQUIFER

---

#### 4.1 General

The numerical simulation of physical and engineering problems has become a standard practice with the advent of fast, available computers. The simulation of ground water movement is thus no exception. However, the importance of using mathematical and numerical models in accordance with their accompanying assumptions, has again been stressed recently (Hassanizadeh and Carrera, 1992). The reliability of the numerical model depends, furthermore to a great extent, on the data used in the development and verification of such a model. The numerical modelling of the Zululand aquifer should therefore be evaluated against this background.

The borders of the region will be discussed in the next section, as well as the data used for the development of the model. The finite element model used for the study will then be considered, together with a discussion of the verification of the model. In order to show the potential of the numerical model, the effect of a hypothetical afforestation around Lake Sibayi will finally be simulated and discussed.

#### 4.2 Geohydrology

The Zululand aquifer, shown in **Figure 41**, was assumed to be the region just south of Richards Bay up to just north of lake Kosi, coinciding with the border of Mozambique. The coastal plain pinches out against the mountains in the west, which was then used as the western boundary of the aquifer. The four bigger lakes, that is Lake St Lucia, Lake Sibayi, Lake Mzingazi and Lake Kosi, as well as Richards Bay, are included in this region. All these areas of open water were taken into account in the numerical model.

Information on the piezometric heads in the region was restricted to data gathered from the boreholes drilled in the region. The distribution over the aquifer of the 140 boreholes where water level information was available for the study can also be seen in **Figure 41**.

These boreholes were, however, monitored only sporadically over the period 1972 to 1991, and in most cases, information of a single observation only at a borehole exists. In order to obtain a workable sample of piezometric heads to evaluate the region with, all of these boreholes were used. The piezometric heads were therefore, contrary to normal practice, not specified for a specific time. The motivation for this is that the change in heads over the regional scale is very small. This means that contours of the piezometric heads drawn over the region at different times are in agreement with one another.

The velocity vectors, calculated from the piezometric heads at 140 boreholes are shown in **Figure 42**. The general movement of ground water towards the lakes and coast is, as expected, evident.

#### **4.3 The finite element model**

The lack of sufficient data and the magnitude of the study area forced us to consider the aquifer on a regional scale. The implication of this is that, although the general movement of the ground water can be considered, predictions of the heads at individual boreholes cannot be done accurately.

A finite element grid was constructed over the region, containing 12 elements in the direction and 48 in the y-direction. This led to element sizes of one to five kilometres in the x-direction and two to four kilometres in the y-direction. The three bigger lakes, Lake St Lucia, Lake Kosi and Lake Sibayi, were excluded in the grid, shown in **Figure 43**. The final grid contained 618 nodes and 537 elements.

The boundary conditions implemented in the simulation were in accordance with the physical structure of the aquifer. That is along the coast, fixed heads or Dirichlet conditions of zero were specified, as well as for Lake St Lucia. The heads were kept at 20m at Lake Sibayi and at their initial values on the northern boundary. Due to the thinning of the aquifer on the western and southern boundaries, no-flow conditions or homogeneous Neumann conditions were used there.

The effect of rainfall was taken into account in the development of the numerical model. The average rainfall over the region varies between 1 200mm per annum at the coast to about 600mm inland, with the effective recharge varying between 18% and 5% in a similar way. The recharge to the aquifer in the model was therefore interpolated linearly between these two sets of figures.

In order to provide initial values for all the nodal points, the piezometric heads from the 140 known boreholes, although measured at different times, were interpolated to the 618 nodal points. The gradient interpolation methods, one of the features of the graphical package TRICON (Buys et al, 1992), proved to be very accurate, and was therefore used. The reason for using the heads measured at different times is, as stated above, due to lack of sufficient data. Contours of these initial nodal heads are presented in **Figure 44**.

#### **4.4 Results from the finite element model**

The aim of the regional model was to provide not only a model capable of simulating the global reaction of the aquifer, but also simulating the piezometric head movement at

boreholes where these data exist. A value of 100m<sup>2</sup>/d was selected for the transmissivity of the region and 0,15 for the storativity. The aquifer was simulated with the two-dimensional confined model, GCON (Botha et al, 1990) for a one-year period. The contours of the piezometric heads after this one-year period are presented in **Figure 45**. The agreement between **Figures 44 and 45** is evident.

The simulated heads along a few grid lines, parallel to the x-axis, were also considered. The initial heads are presented as solid lines, with the heads as simulated after one year shown as dots, according to the legend, in **Figure 46**. The line numbers in the figure are counted from the bottom of the finite element grid. The figure again shows the ability of the model to simulate the movement of the ground water.

In the final evaluation of this preliminary numerical model, the observed movement of the piezometric heads for seven nodes were compared against the simulated values. These comparisons are shown in **Table 12**.

**Table 12:** The movement of the piezometric level as observed at a few boreholes compared to the simulated values in a one-year period.

Borehole / Node		Piezometric head changes	
Borehole no.	Nodal no.	Observed	Simulated
ES277	176	-0.5	-0.13
ES280	189	0.90	1.65
ES308	206	0.09	-1.27
ES299	214	1.31	0.84
ES339	220	0.20	-3.37
ES298	232	0.40	0.92
ES296	245	-1.29	0.37

Although the simulated movements of nodes 176, 189, 214 and 232 are in accordance with the observed values, it is evident from the other nodes that some more refinements are needed for the model to be calibrated.

#### 4.5 The impact of afforestation on the aquifer: A hypothetical case study

The ability of the numerical model to simulate the behavior of the regional Zululand aquifer was furnished in the preceding discussion. However, the limitations of the model, for example the scarcity of geohydrological data and the resulting large elements, restrict its use in forecasting the movement of ground water on a detailed scale. It was therefore decided to apply the model on a hypothetical case study to demonstrate the abilities of the numerical model.

The effect of plantations on the ground water level and, via the ground water, on the lakes, has been the subject of numerous studies in the past (Lindley and Scott, 1987). It was therefore decided to use the numerical model with various, but feasible combinations of rainfall and water yield to demonstrate the effect of afforestation around Lake Sibayi. The region selected coincides with 28 elements on the finite element grid, and can be seen in **Figure 41**, marked around Lake Sibayi. The water level at the lake was kept constant at 20m for all the simulations.

The volume of water consumed by trees varies at large, partially because of differences in species, but also because of differences in the climate in which the plantation reside. Catchment studies (Lindley and Scott, 1987), and also present investigations at forest research centres, indicate an increase in evapotranspiration from grasslands to forests in the order of 200mm to 2000mm annually. The effect of normal rainfall and variations of these evapotranspiration rates were therefore used in the numerical model to show their potential effect on Lake Sibayi.

The cases investigated, were recharge by rainfall of 150 mm per year, combined with evaporation rates, measured per unit area per annum, of 0 mm, 200 mm, 1 000 mm, 1 500 mm and 2 000 mm. The effect of one of these scenarios, that of 150 mm recharge and 2 000mm evapotranspiration, on the ground water levels, is shown in **Figure 47**.

The effect of the high water usage of the plantation on the ground water levels in the vicinity of the lake, can be seen by comparing **Figure 47** with **Figure 45**. Although the differences in the contours are restricted to the area where the plantation was specified, the simulation was done for one year only, and the effect of the plantation on the ground water levels will increase with time.

However, it is difficult to evaluate the effect of the different evapotranspiration rates on the large scale contour map. Two sections were therefore drawn through the lake, one parallel to the coastline and the other perpendicular to the coastline, marked AA' and BB' respectively on **Figure 43**. The simulated ground water levels for the five different evaporation rates, that is 0, 200, 1 000, 1 500 and 2 000 mm per annum, per unit area are compared in **Figures 48 and 49**.

The section perpendicular to the coastline, presented in **Figure 48**, shows a large natural gradient towards Lake Sibayi and the sea. However, this gradient decreases with an increase in the evaporation rate. This means less ground water will flow towards the lake, resulting in an eventual lowering of the water level in Lake Sibayi. **Figure 49** depicts the section parallel to the coast. Under normal conditions, that is with no evapotranspiration, ground water flows from both sides into the Lake. However, all the other cases shows a gradient out of Lake Sibayi, in a southerly direction.

The two sections show that an evapotranspiration rate of 1 000 mm per annum already causes a severe lowering in the ground water level around Lake Sibayi. The larger evapotranspiration figures, which can also be interpreted by being periods of continuous lower annual precipitation, only exaggerates these conditions.

The effect of the evapotranspiration can also be seen by comparing the direction of flow around the lake. In **Figure 50**, the direction of the flow of ground water around the lake and through the simulation area can be seen under normal conditions, that is of rainfall only. A mass balance of flow to and from Lake Sibayi, calculated with the simulation computer program, shows an equilibrium situation.

The extreme case of 150mm recharge, but 2 000mm evapotranspiration, or an effective discharge of 1 850mm per unit area, per year, can be seen in **Figure 51**. The flow vectors are drawn mostly away from the Lake. In this case, the mass balance shows a net outflow of  $8 \times 10^3 \text{ m}^3/\text{d}$  from Lake Sibayi. Therefore, Lake Sibayi will provide water to the plantation, resulting in a severe lowering of the water level in the lake.

#### **4.6 Conclusions**

A numerical model for the Zululand aquifer was developed which could at least, on a regional scale, be used to make some predictions on the availability and movement of ground water in the aquifer. However, before detailed evaluations with the model can be undertaken, it has to be calibrated with and verified against a comprehensive set of geohydrological data for the region. This should include transmissivity and storativity values and ground water levels measured over a two- to three-year period, from a representative set of boreholes over the region.

The possible danger of over-utilization of the ground water by large commercial forests, especially during periods of drought, was outlined in a hypothetical case study. The ability of the ground water to act as a water reservoir is well-known and also illustrated in the hypothetical study. However, as with any ground water resource, it has a limited capacity, and should be managed as such.

## CHAPTER 5

### WATER BALANCE CALCULATIONS AND UTILIZATION OF THE GROUND WATER RESOURCES

---

Following the recharge estimates calculated from the chloride balance in **Chapter 3** above, and combining it with the water level contour data presented in **Chapter 4**, it is possible to derive a first estimate of a water balance for the northern part (surface area approximately 330 km<sup>2</sup>) of the study area. For this purpose that area of the coastal plain between the Mocambique border and the northern limit of Lake St. Lucia was chosen.

Using the available data, a water balance can be derived in two ways. Firstly by using the recharge estimates and secondly, using the ground water flow equation.

#### 5.1 Recharge driven water balance

In **Chapter 3** the recharge rate as a percentage of the mean annual precipitation and the distance from the coast was estimated. This ranges from 19% at the coast to 5% in the interior (**Table 10, Chapter 3**). The decrease of MAP with distance from the coast has been obtained from the MAP maps produced by Dent et al (1989). The rainfall onto this part of the Zululand coastal plain has been calculated to be  $3.3 \times 10^8$  m<sup>3</sup>/year. By integrating the MAP maps with the percentage recharge distribution an average figure for recharge (11%) and rainfall (900mm) over this area could be obtained. This results in an annual nett recharge to the coastal plain aquifer of about  $3.28 \times 10^8$  m<sup>3</sup>/y. If it is accepted that this total volume exits the coastal plain as seepage along the coast, a figure of  $3.28 \times 10^5$  m<sup>3</sup>/ y/km of coastline results.

#### 5.2 Flow equation derived water balance

A comprehensive set of permeability determinations of the sediments of the Coastal Plain is not available. Permeability values have been determined by Australian Groundwater Consultants (1975), Worthington (1978), Simmonds (1990) and Davies Lynn and Partners (1992). The most comprehensive set of permeabilities was derived for the EIA study the Eastern Shores area of Lake St. Lucia. Geologically the coastal dune cordon divided stratigraphically into "Cover sands", "Older aeolian sands", "Interlayered deposits" and Port Durnford Formation resting on a floor of Cretaceous age siltstones. Permeabilities determined for these different sequences are:

Cover sands	15.6 m/d
Older aeolian sands	0.87 m/d
Port Durnford Formation	4.3 m/d

By using the water level contour map (**Figure 44**) an average gradient towards the coast of 1:250 can be derived. Taking into account the relative thicknesses of the different geological formations, an average permeability of 5m/d is a realistic figure. This value compares favourably with that cited by Pitman and Hutchinson (1975). Worthington (1978) established an average permeability of 2.5m/d through pumping tests in the Richards Bay area. For an average aquifer thickness of 50m above the impermeable Cretaceous floor, a total flow from the northern part of the coastal plain aquifer towards the sea is calculated to be  $4.4 \times 10^7 \text{ m}^3/\text{y}$  or  $3.7 \times 10^5 \text{ m}^3/\text{y}/\text{km}$  of coastline. Although there is a fair agreement between the flow volumes derived with the two techniques, these values must be seen as a first approximation as the parameters used for the calculations are average values.

### 5.3 Preferential flow paths to the sea

There are selected areas where the ground water flow towards the sea is considerably more. One known area is the outflow from lake Sibayi. The geophysical results have revealed the presence of a deep erosion channel east of Lake Sibayi. Although untested by drilling, this erosional channel is believed to be filled with approximately 120-140m of Holocene age sediments with a permeability probably of the same order as that of the Cover sands at St. Lucia. Based on the difference in head between Lake Sibayi and the sea (approximately 20m) and assuming permeability values derived from pumping tests at Richards Bay, Pitman Hutchinson (1975) calculated that the seepage from the lake towards the sea to be between  $1 \times 10^5 \text{ m}^3/\text{y}$  and  $4 \times 10^5 \text{ m}^3/\text{y}$  per kilometre of the coast. However, these figures were based on the elevation of the impermeable floor being at -25m below mean sea level. The geophysical derived depth of the impermeable floor is on average -100m below mean sea level and the width of the palaeo-channel approximately 20 km. Using these figures and the same permeability values as Pitman and Hutchinson, the outflow is calculated to be between  $1.1 \times 10^8 \text{ m}^3/\text{y}/\text{km}$  and  $4.4 \times 10^8 \text{ m}^3/\text{y}/\text{km}$ . This is equivalent to  $5.4 \times 10^6 \text{ m}^3/\text{y}/\text{km}$  to  $2.2 \times 10^7 \text{ m}^3/\text{y}/\text{km}$  of coast. These figures should be compared to the volume of the lake calculated to be  $9.81 \times 10^8 \text{ m}^3$  (Ramsey, 1990). The ratio between the annual seepage from the lake volume in the lake, indicates a turnaround time of between approximately 2½ and 10 years. This estimate is consistent with the stable isotope data which indicated that the  $\delta^{18}\text{O}$  and chloride concentrations of lake water show almost no seasonal changes. This constant feature is an indication that the water remains in the lake for a number of years (See **Chapter 4**)

At least one more known occurrence of a similar type palaeo-channel is known to occur along the coast of northern Zululand. During drilling to establish the geological succession of the Eastern Shores area as part of the Environmental Impact Assessment study of mining on the Eastern Shores, a palaeo-channel south of Mission Rocks was discovered. The floor of this channel is believed to be at about -80 m below sea level. There are, however, no fresh water seepages occurring along this section of the coastline.

#### 5.4 Utilization of ground water resource

Currently substantial amounts of ground water are only abstracted in two areas. These are in the flood plain of the Mhlatuze where ground water is used for irrigating the sugar cane field and in the vicinity of the Richard Bay Minerals mining operation.

The latter is mainly used as an emergency supply in times of drought. Depending on the pumping costs involved and the permits issued by DWA&F&F for abstraction from Lake Mzingazi and Nhlabane, this ground water abstraction scheme may become a permanent source of water. No information is, however, available on the volume of water pumped from this well field or the yield from the individual wells.

As the main aquifers are the Uloa and Port Durnford Formations, the exact distribution of these formations need to be known. Due to the regional nature of the study, it is possible to identify accurately individual wellfield development areas. Based on all available geohydrological information, a classification of low, medium and high ground water potential was devised. Factors that influence the classification of an area, thickness of sediments above the Cretaceous, depth to water level, quality of water, expected development of Uloa and Port Durnford Formation in an area and the proximity (lateral) of outcrops of Cretaceous siltstones. These areas are marked on **Figure 52**. This map must however be treated only as a rough approximation of potential development areas and before any development of ground water resources is planned, further study and exploration drilling and borehole testing will be necessary.



## CHAPTER 6

### CONCLUSIONS AND RECOMMENDATIONS

---

#### 6.1 Conclusions

The objectives for the project as stated in the contract conditions, and listed in the introduction to this report, have been met, with the exception of all the exploration drilling and test pumping originally envisaged. This was due to the build up of political unrest in the area which made the area unsafe for the drilling and test pumping crews.

The earlier statement that the Zululand Coastal Plain Aquifer can be regarded as one of the largest alluvial aquifers in South Africa has been confirmed by the additional information collected during this investigation. Although the investigation has also led to a better understanding of the aquifer system, several aspects warrant more study. In this regard the interaction between vegetation, whether it be natural or commercial (forestry and agriculture for example), and the ground water regime needs to be assessed thoroughly before any large scale development of the ground water resource is envisaged.

There exists a fine balance between the ecology of the region and the ground water regime. Any future development plans for the region, whether development for tourism, rural settlements, agriculture, mining or afforestation have to take into account the delicate balance of the ecosystem.. Ground water plays a crucial role in this ecosystem and any change in the ground water conditions may influence the ecosystem negatively.

Some specific conclusions emanating from this study are listed below:

- The thickness of the aquifers stratigraphically above the Cretaceous age sediments, was mapped over the entire coastal plain using geophysical techniques calibrated against a limited amount of borehole information.
- The electrical resistivity sounding technique used to determine the depth to the top of the Cretaceous age formations is more appropriate than the electromagnetic techniques to determine the thickness of the different units in the geological succession.
- Depth penetration by EM techniques is restricted due to the decrease in resistivity with depth of the different geological units and the very conductive nature of the sedimentary succession.
- Interpretation of DC soundings is complicated also because of the continuous decrease of the resistivity with depth.
- Resolution of individual geological units with geophysical methods proved not always to be successful. The depth to the top of the Cretaceous formations can, however, be determined with a large degree of confidence.

- Borehole geophysical measurements also failed to clearly identify different geological horizons.
- Gravity surveys were not able to detect palaeo-channels subsequently filled with younger sediments.
- Two palaeo-channels were detected through which increased seepage towards the sea can occur. One of these is situated opposite Lake Sibayi and the other one is near Mission Rocks opposite Lake St Lucia.
- A water level contour map was constructed for the entire coastal plain using measured water levels and applying statistical techniques to infer elevations in areas where data points were sparse.
- A ground water divide, roughly parallel to the coastline, could clearly be identified from this map.
- From the available water level information, three different water level scenarios in the vicinity of the coastal dune cordon could be identified. These are at Lake Sibayi, Eastern Shores of Lake St Lucia, and at Richards Bay.
- A regional mathematical simulation model was designed to simulate steady state conditions. This model was used to determine ground water flow directions and velocities over the entire coastal plain.
- It was further used to simulate the effect of an afforested area around Lake Sibayi to determine the effect on lake and ground water levels. This model indicates that if evapotranspiration by the plantations exceeds 1 000 mm/ha/a, water levels in the lake may already be affected. A number of assumptions have, however, been made during this simulation. These figures should therefore be regarded as provisional.
- A rainfall-recharge relationship was established which varies with distance from the coast. Recharge as a percentage of MAP varies from 18 % at the coast to 5 % at a distance of 50 km inland.
- The rainfall-recharge relationship was used as input to the mathematical simulation exercise.
- The Cl concentration in rainfall decreases rapidly from the coast to the inland.
- Ground water quality over the entire coastal plain is generally of good quality. There are, however, regional differences in the chemical character.
- A "fingerprinting" technique was developed successfully to correlate the water chemistry with the geological horizon from which it originates.
- Stable isotopes were used to great advantage to distinguish between seepage from lakes and ground water. Stable isotopes also confirmed a considerable residence time for water in the larger lakes like Sibayi and Bhangazi.
- No seasonal isotopic variation was recognized in rainwater. Isotope analyses could also not be used to trace the movement of ground water due to insignificant variations observed.
- Carbon-14 analyses indicated that the ground water recharge is mostly post-1960. This is in accordance with the high through-flow of water through the aquifer deduced from recharge estimates and modelling.

- Isotope analyses confirmed that the fresh water occurrence along the coast opposite Lake Sibayi originates from the lake.
- Sea-water intrusion into the aquifer is unlikely to occur due to an effective above sea level piezometric head along the coastal dune cordon.
- The aquifer is highly vulnerable to surface sources of pollution.

## 6.2 Recommendations

In view of the ecologically sensitive nature of the area and the dominating role that ground water plays in maintaining the balance, a number of important recommendations are made. These include that:

- the water level monitoring program should be maintained;
- the interaction between the ground water and the vegetation in the area be investigated in detail and that a research program to address this aspect be compiled as soon as possible;
- this research program should include input from ecologists, the Department of Water Affairs and Forestry, the commercial forestry sector, nature conservation officials, tourism authorities and regional planners;
- further work is required to quantify the effect of afforestation on the ground water conditions in more detail;
- the mathematical simulation model should be refined and updated once more data becomes available;
- the pollution vulnerability of the aquifer should be brought to the attention of the planners.

## LIST OF REFERENCES

---

- ALLANSON, B R (1979). Lake Sibayi. W Junk, The Hague, 364p.
- ARCHIBALD, C G M and MULLER M S (1987). Physical and chemical characteristics of bulk precipitation in the Richards Bay area. SA J of Sci, **83**, 700-704.
- AUSTRALIAN GROUNDWATER CONSULTANTS (PTY) LTD (1975). Richards Bay Groundwater Investigations - Richards Bay Heavy Minerals Project. Confidential Report.
- BOTHA J F, VERWEY J P, BUYS, J, TREDoux G, MOODIE J W and HODGKISS M (1990). Modelling Groundwater Contamination in the Atlantis aquifer. WRC Report No 175/1/90, Water Research Commission, Pretoria.
- BREDENKAMP, D B (1980). Kwantitatiewe ramings van grondwateraanvulling met behulp van eenvoudige hidrologiese modelle. Ground water 1980 Symposium, 7-9 July, Pretoria.
- BREDENKAMP, D B (1985). Estimation of ground water recharge in dolomitic aquifers. Abstract, Ground Water '85 Symposium, Pretoria, 98-107.
- BREDENKAMP, D B (1993). Recharge estimation based on chloride profiles. Dept. of Water Affairs and Forestry, Pretoria, Report GH 3804 (Draft copy), 22p.
- BREDENKAMP, D B, BOTHA, L J, VAN TONDER, G J and VAN RENSBURG, H J (1995). Manual on quantitative estimation of recharge and aquifer storativity based on practical hydro-logical methods. Water Research Commission Report TT 73/95.
- BUYS J, BOTHA J F and MESSERSCHMIDT, H J (1992). Triangular irregular meshes and their application in the graphical representation of geohydrological data. WRC Report No 271/2/92, Water Research Commission, Pretoria.
- COASTAL AND ENVIRONMENTAL SERVICES (1992). Specialist Reports. In: Environmental Impact Assessment, Eastern Shores of Lake St Lucia, Kingsa/Tojan Lease. Area. Volume 1, Part 1, Grahamstown, pp 1-20.
- COETSEE, VdA (1991). Bepaling van gesteente hidrologiese en geoëlektriese eienskappe. CSIR Internal Report No EMA-I 9113.
- COOPER, M R and MCCARTHY, M J (1988). The stratigraphy of the Uloa Formation. Abstracts Geocongress '88, Geol. Soc. S. Afr., Durban.

- DAVIES, LYNN AND PARTNERS. (1992) Landform geomorphology and geology. In: Environmental Impact Assessment, Eastern Shores of Lake St. Lucia, Kingsa/Tojan Lease Area, Vol. I, Part 1, Specialist Reports. Coastal and Environmental Services, Grahamstown, SR2., 21-62.
- DINGLE, R V, SIESSER, W G and NEWTON, A R (1983). Mesozoic and Tertiary geology of Southern Africa. Rotterdam. Balkema.
- DU PREEZ, J W and WOLMARANS, L G (1986). S. Afr. Geol. Surv. Map Explanation Sheet 2632 (Kosi Bay). Government Printer, Pretoria.
- EDMUNDS, W M, DARLING, W G and KINNIBURGH, D G (1990). Solute profiling techniques for recharge estimation in semi-arid and arid terrain. In: D N Lerner, A S Issar, I Simmers (ed)., Groundwater Recharge, Verlag Heinz Hesse, Hannover, Germany.
- ERIKSSON, E and KHUNAKASEM, V (1969). Chloride concentrations in groundwater. Recharge rate and rate of deposition of chloride in the Israel coastal plain. J of Hydrology, 7, 178-197.
- FOCKEMA, P D (1986). The heavy mineral deposits of Richards Bay, 2301-2307. In: Anhaeusser, C.R. and Maske, S., (eds.), Mineral Deposits of Southern Africa, Vol. 2, 2335pp.
- FRANKEL, J J (1960). Late Mesozoic and Cenozoic events in Natal, South Africa. Trans. N.Y. Acad. Sc., Ser. II, Vol. 22, No. 8, 565-577.
- FRANKEL, J J (1966). Basal rocks of the Tertiary at Uloa, Zululand, South Africa. Geol. Mag., 103, 214-230.
- GAT, J R and GONFIANTINI (1981). Stable isotope hydrology. Tech. Report 210, IAEA, Vienna, pp 337.
- GIESKE, A S M (1992). Dynamics of groundwater recharge. PhD Thesis, Free Univ. Amsterdam, 289p.
- HASSANIZADEH, S M and CARRERA, J (1992). Editorial. Advances in Water Research, 15, 1-3.
- HOBDAV, D K and ORME, A R (1974). The Port Durnford Formation. A major barrier lagoon complex along the Zululand coast. Trans. Geol. Soc. S. Afr. 77, 141-149.
- HOBDAV, D K and JACKSON, M P A (1979). Transgressive shorezone sedimentation and depositional deformation in the Pleistocene of Zululand, South Africa. Journ. Sediment. Petrol. 49, 145-158.

- HINGSTON, F J and GAILITIS, V (1976). The geographic variation of salt precipitated over western Australia. *Australian J. Soil Res*, 14, 319-335.
- HUTCHISON, I P G and PITMAN, W V (1973). Climatology and Hydrology of the St Lucia Lake System. Hydrological Research Unit, Report 1/73, University of the Witwatersrand, Johannesburg.
- JUNGE, C E and WERBY, R T (1958). The concentration of chloride, sodium, potassium, calcium and sulphate in rain water over the United States. *J Meteorol*, 15, 417-425.
- KELBE, B and RAWLINS, B K (1992). Hydrology. In: Environmental Impact Assessment, Eastern Shores of Lake St. Lucia, Kingsa/Tojan Lease Area, Vol. I, Part 1, Specialist Reports. Coastal and Environmental Services, Grahamstown, SR3, 63-124.
- KENNEDY, W J, and KLINGER, H C (1975). Cretaceous faunas from Zululand and Natal, South Africa. Introduction. *Stratigraphy. Brit. Mus. (Nat. Hist.) Bull. Geol.* No 25.
- KRUGER, G P and MEYER, R (1988). A sedimentological model for the northern Zululand Coastal Plain. Abstracts Geocongress '88, Geol. Soc. S. Afr., Durban, 423-425.
- KRUGER, G P (1986). An investigation into the feasibility of rice cultivation on the Ngwavuma Coastal Plain, northern Natal. A report on the results of a hydrogeological and geomorphological Survey. IDC Confidential Internal Report, 42 pp.
- LINDLEY, A J and SCOTT, D F (1987). The impact of pine plantations on the ground-water resources of the Eastern Shores of Lake St Lucia. SAFRI Report No. JFRC 87/01.
- MAMANE, Y (1987). Chemistry of precipitation in Israel. *Science of the Total Environment*, 61, 1-13.
- MAUD, R R (1961). A preliminary review of the structure of coastal Natal. *Trans. Geol. Soc. S. Afr.*, 64, 247-256.
- MAUD, R R and ORR, W N (1975). Aspects of post-Karoo geology in the Richards Bay area. *Trans. Geol. Soc. S. Afr.*, 78, 101-109.
- MCCARTHY, M J (1988). Some observations on the occurrence of "Berea-type" Red Sand along the Natal coast. Abstracts Geocongress '88, Geol. Soc. of S. Afr., Durban. 403b-d.
- MCCARTHY, M J (1992). Unpublished notes prepared on Geological Excursion in the Durban area, 31p.

- MCMILLAN, I K (1987). The genus *Ammonia* Brunnich, 1772 (Foraminiferida) and its potential for elucidating the latest Cainozoic stratigraphy of South Africa. *S. Afr. J. Sc.* 83, 32-42.
- MEYER, R and DE BEER, J H (1981). A geophysical study of the Cape Flats aquifer. *Trans. Geol. Soc. S. Afr.*, 84, 107-114.
- MEYER R, DE BEER J H and BLUME, J (1982). A geophysical-geohydrological study of an area around Lake Sibayi, northern Zululand. Confidential CSIR Report Kon/Gf/81/1.
- MEYER, R, DUVENHAGE, A W A, BLUME, J, VALLENDUUK, J W and HUYSEN, R M J (1983). Report on a geophysical and geohydrological investigation of the ground water potential between Lambert's Bay and Graafwater and the coastal region between Lambert's Bay and Elands Bay. Confidential CSIR Report No. Kon/Gf/79/1.
- MEYER, R, HUYSEN, R M J, COETSEE, VdA and AUCAMP, J J (1987). A geoelctrical survey of an area between Lake Sibayi and Lake Kosi, Northern Zululand. CSIR Confidential Report C-FIS 129.
- MEYER, R and KRUGER, G P (1987). Geophysical and geohydrological investigations along the Zululand coastal plain. Abstract, Hydrological Sciences Symposium Proceedings: Volume I, Rhodes University, Grahamstown, South Africa, 299-311.
- MEYER, R, COETSEE, VdA en TALMA, A S (1989). Tussentydse verslag, WNK-projek K5/221 Geohidrologiese ondersoek en evaluasie van die Zoelandse kusakwifoor. WNNR Vertroulike Verslag nr. EMA-C 8928.
- MEYER, R, DUVENHAGE A W A and AUCAMP, J J (1989). Final report on the geoelectrical investigation of an area around Port Durnford on the Zululand coastal plain. Confidential report No. EMA-C 88115.
- MEYER, R, MCCARTHY, M J and EGLINGTON, B M (1993). Further investigation of the geology and geohydrology of the dune cordon on the eastern shores of Lake St Lucia. Report No. EMAP-C-93032.
- MURGATROYD, A L (1983). Spatial variations in precipitation chemistry over Natal, South Africa. *SA J Sci*, 79, 408-410.
- ORME, A R (1973). Barrier and lagoon systems along the Zululand coast, South Africa. In: D.R.Coates (Ed.) *Coastal Geomorphology*. New York: N.Y. State Univ. Press., 181--217.
- ORR, W N and CHAPMAN, J R (1974). Danian (Palaeocene) marine rocks at Richards Bay, South Africa. *S. Afr. J. Sci.* 70, 247-249.

- PITMAN, W V and HUTCHINSON, I P G (1975). A preliminary hydrological study of Lake Sibaya. Report 4/75. Hydrol. Res. Unit, Univ. of the Witwatersrand, Johannesburg, pp35.
- RAWLINS B K (1991). A geohydrological assessment of the behaviour and response of the Zululand Coastal Plain to both environmental influences and human activity. Unpublished MSc thesis, University of Zululand.
- RAWLINS, B K and KELBE, B E (1990). A geohydrological study of the behaviour and response of the Zululand Coastal Plain to both environmental influence and human activity. Annual Report. University of Zululand.
- ROZANSKI, K, ARAGUAS, L A and GONFIANTINI, R (1992). Relation between long-term trends of oxygen-18 isotopic composition of precipitation and climate. *Science*, **258**, 981-985.
- SIMMONDS, A L E (1990). Investigations into possible saline intrusion at lake Mzingazi, Richard Bay. Department of Water Affairs and Forestry, Directorate geohydrology, Report No. GH 3711.
- STAPLETON, R P (1975). Planktonic foraminifera and calcareous nannofossils at the Cretaceous-Tertiary contact in Zululand. *Palaeont. afr.* **18**, 53-69.
- STAPLETON, R P (1977) Planctonic foraminifera and the age of the Uloa Pecten Bed. *Geol. Surv. S. Afr. Bull.*, **60**, 11-15.
- TINLEY, K L (1985). Coastal dunes of South Africa. *S. Afr. Nat. Sci. Programme Report No.* 109.
- VAN TONDER, G J, BOTHA, J F, and MULLER, J (1986). The problem of sea water intrusion near Lake Mzingazi at Riochards Bay. *Water S.A.*, **12**(2), 83-88.
- VAN WYK, W L (1963). Groundwater studies in northern Natal, Zululand and surrounding areas. *S. Afr. Geol. Surv. Mem.* No. 52.
- VAN ZIJL, J S V (1971). Results of an electrical sounding profile, Eastern Shores area, St Lucia. Confidential NPRL, CSIR Report, Pretoria.
- VOGEL, J C and VAN URK, H (1975). Isotopic investigation of Lake St Lucia. Internal NPRL, CSIR Report, Pretoria.
- WOLMARANS, L G and DU PREEZ, J W (1986). *S. Afr. Geol. Surv. Map Explanation Sheet* 271/232 (St. Lucia).



WORTHINGTON, P F (1978). Groundwater conditions in the Zululand coastal plain around Richards Bay. CSIR Report, FIS 182, 209pp.

WRIGHT, C I and MASON, T R (1990). The sedimentation of Lake Sibaya, North KwaZulu. Unpublished Joint Geological Survey - University of Natal Report No. 1990-0147, 25pp.

## FIGURES

## **APPENDIX A**

### **GEOCHEMICAL CLASSIFICATION OF ZULULAND GROUND WATER**

**APPENDIX B**

**GROUND WATER RECHARGE CALCULATIONS**

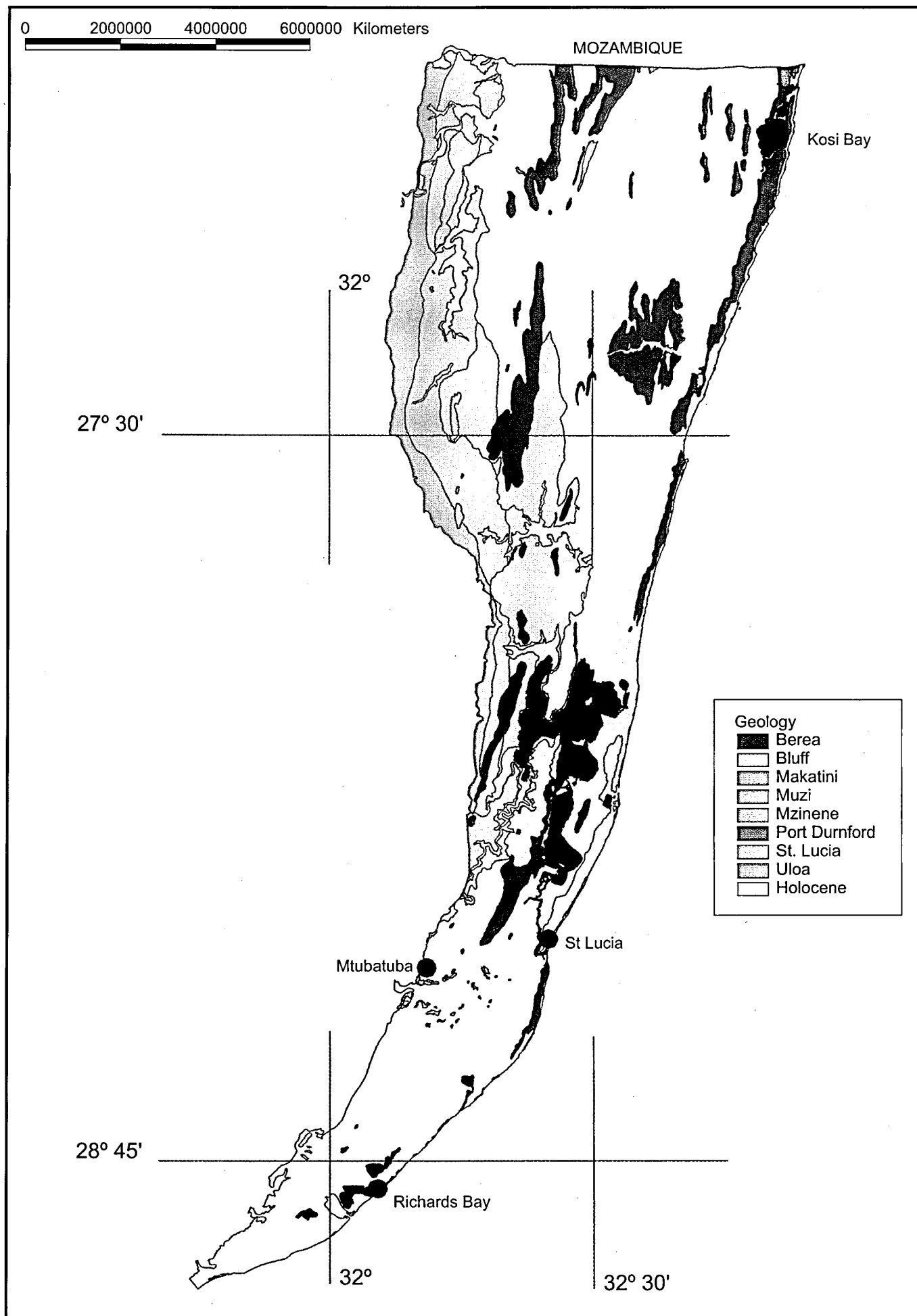


Figure 1. Geological map of the Zululand Coastal area.

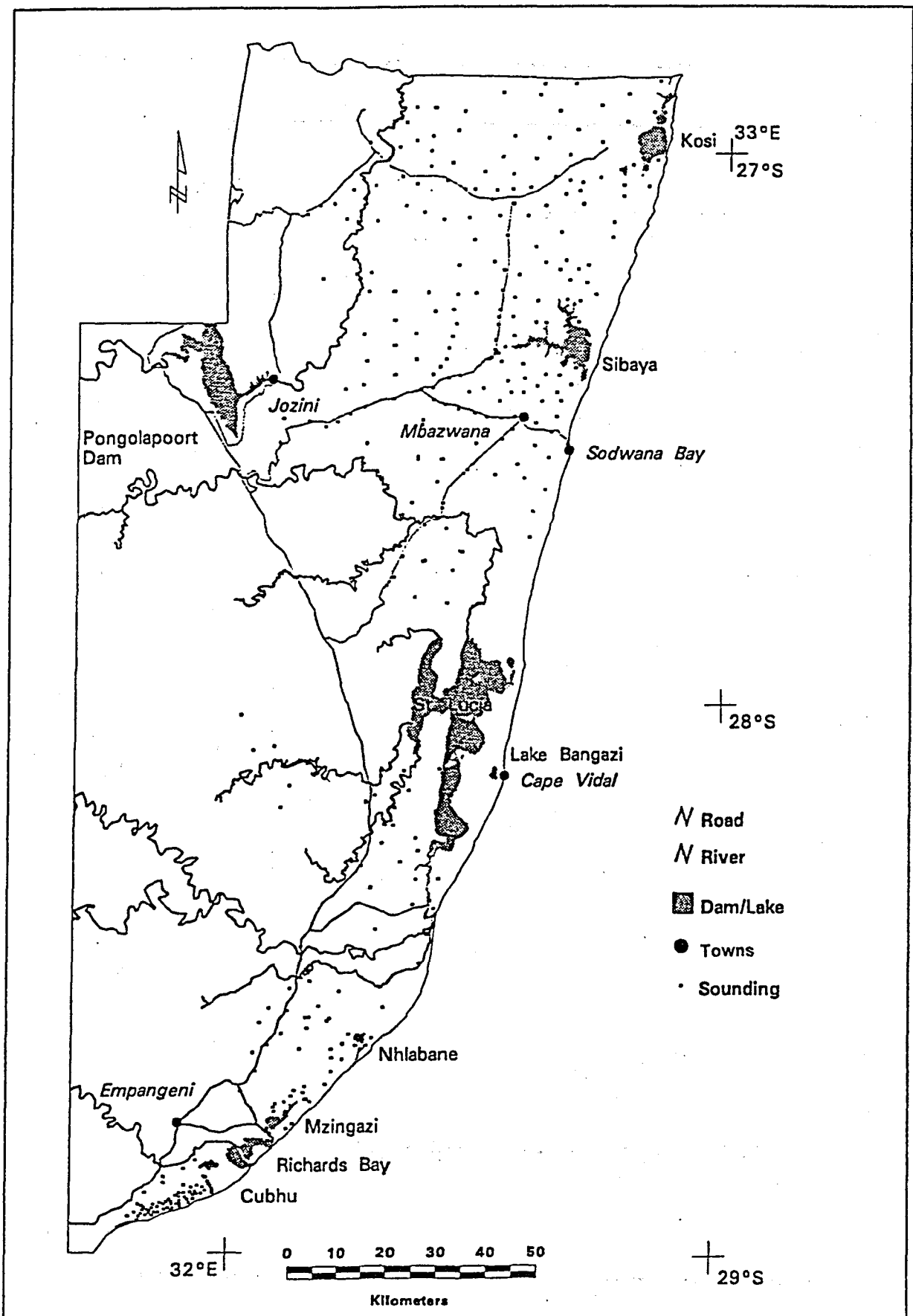


Figure 2: Resistivity sounding locations.

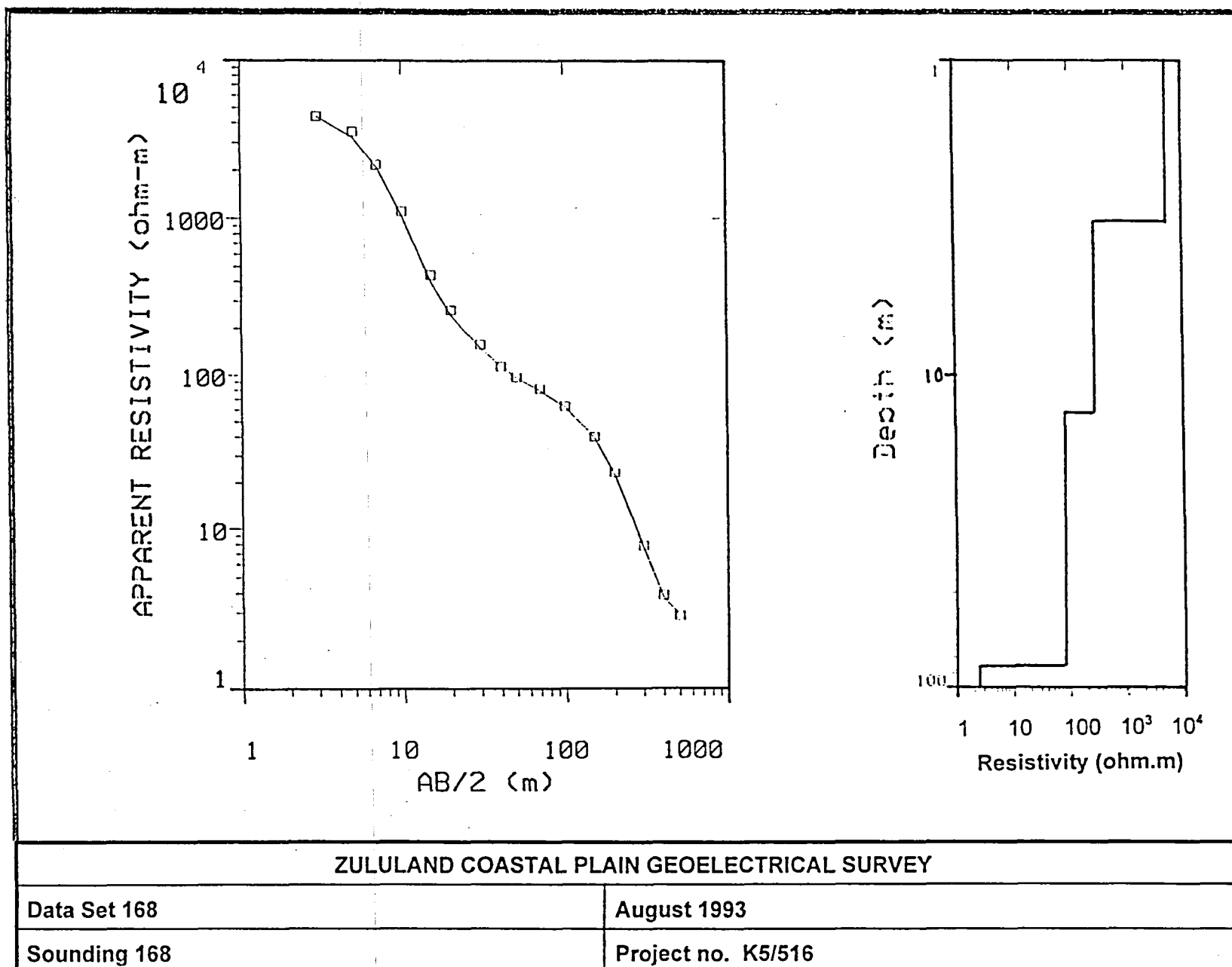


Figure 3: A typical direct current (DC) resistivity sounding curve and interpretation.

ES 85

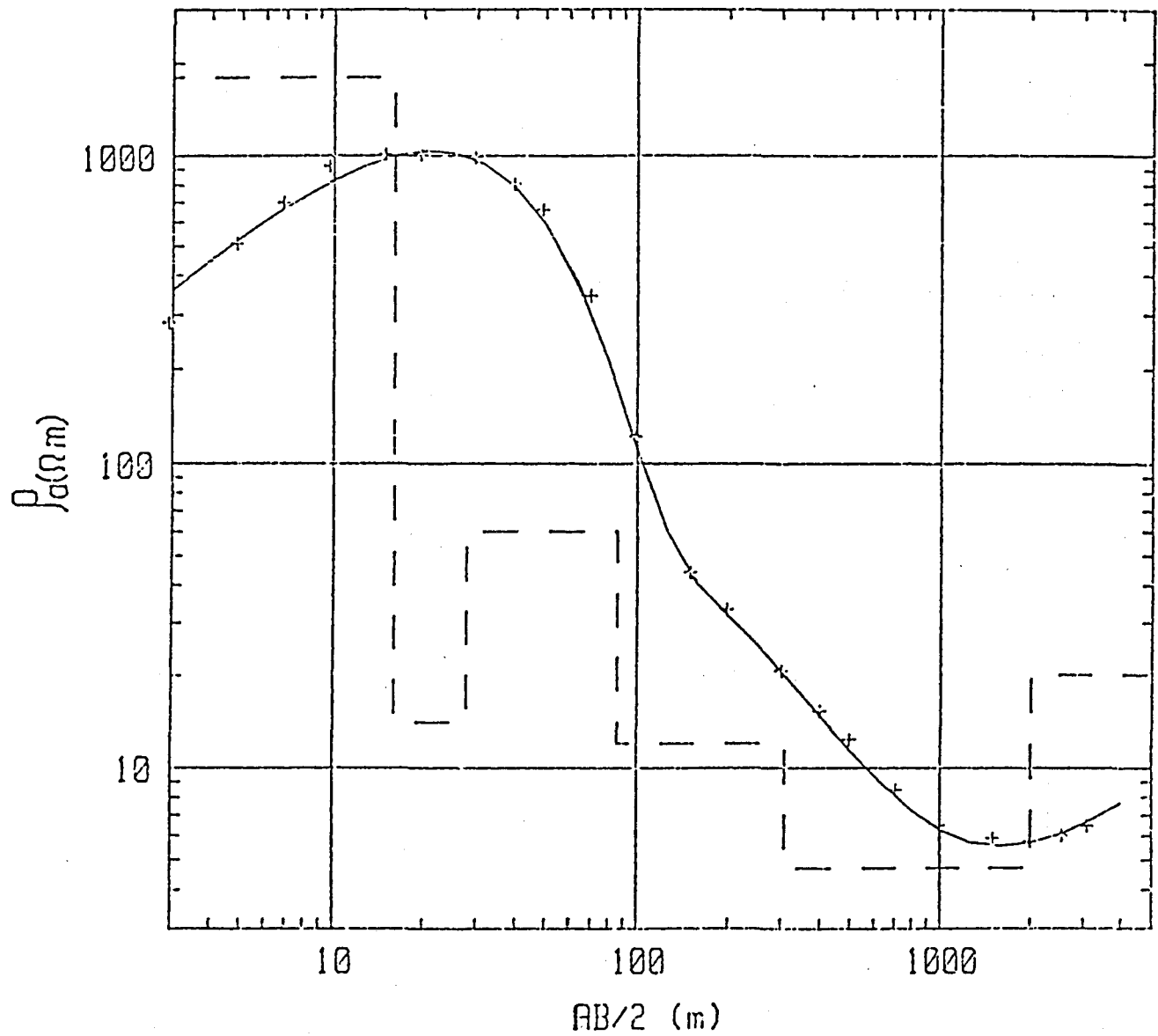


Figure 4: Sounding curve and model for resistivity sounding ES 85.



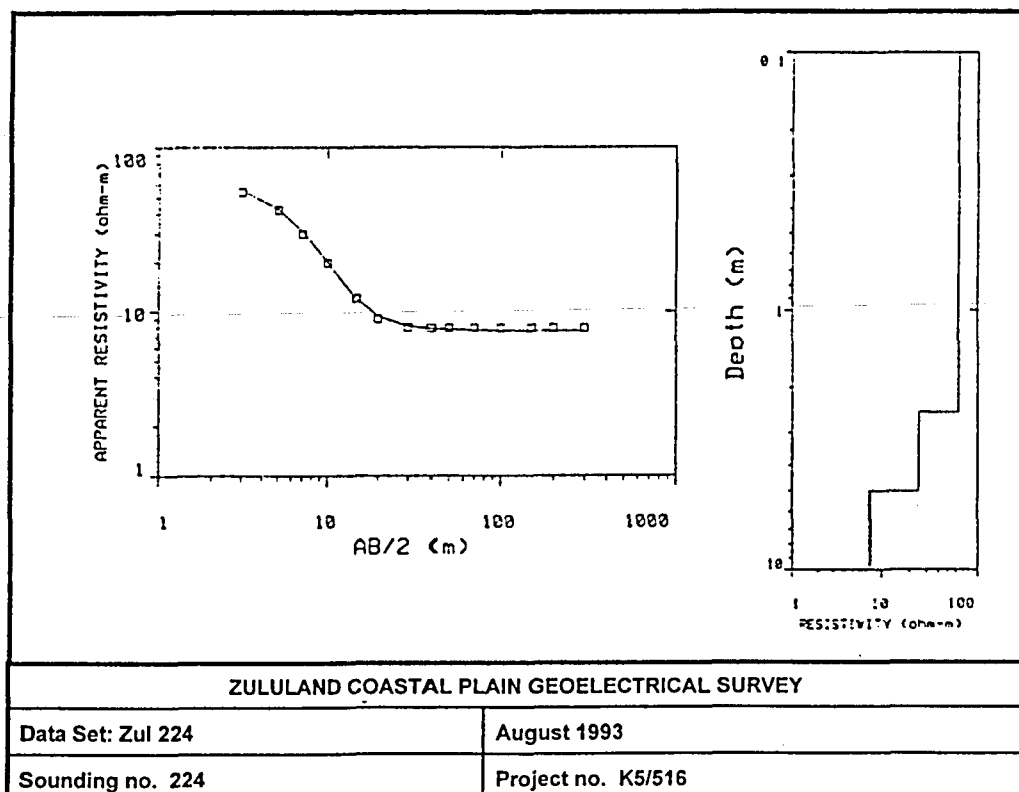
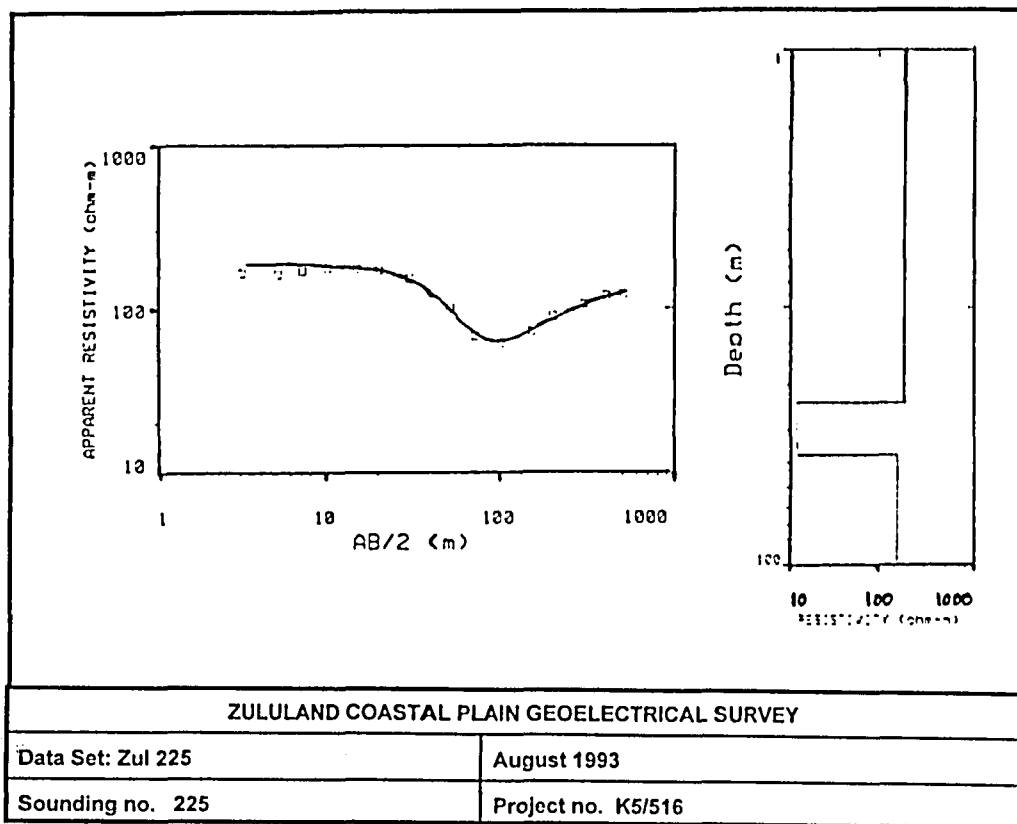


Figure 5: DC sounding curve and interpretations for ES 235 (Lebombo Group) and ES 224 Makatini Formation).

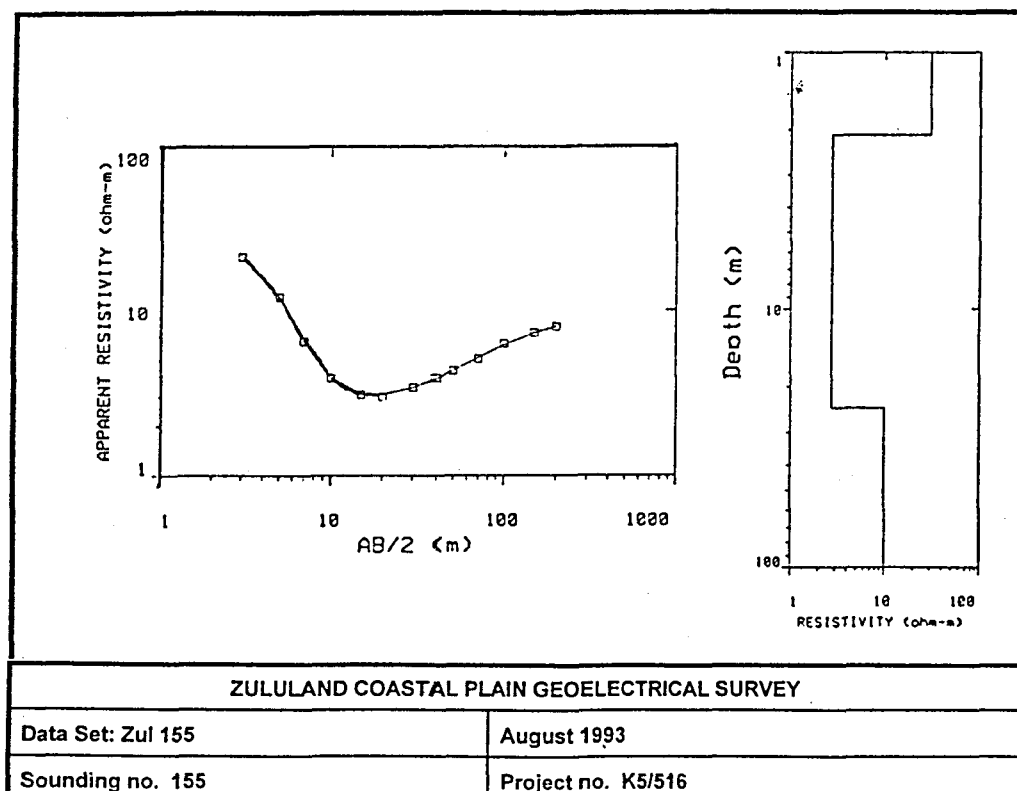
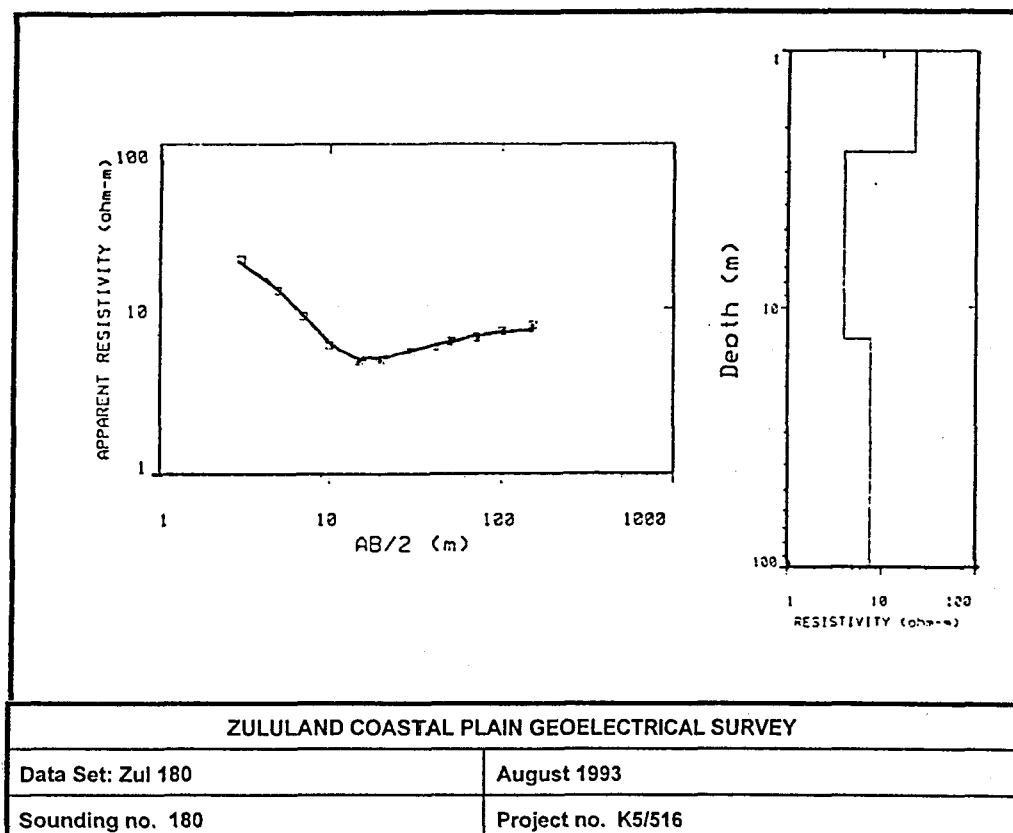


Figure 6: DC sounding curve and interpretations for ES 180 (Mzineni Formation) and ES 155 (St Lucia Formation).

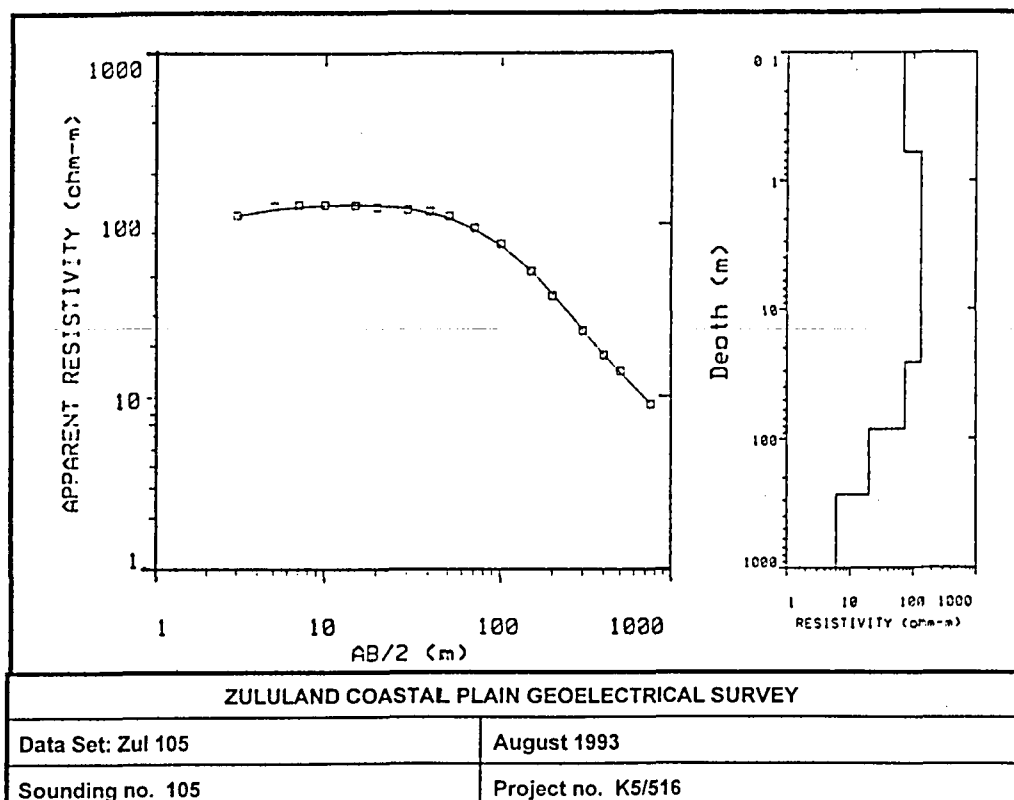
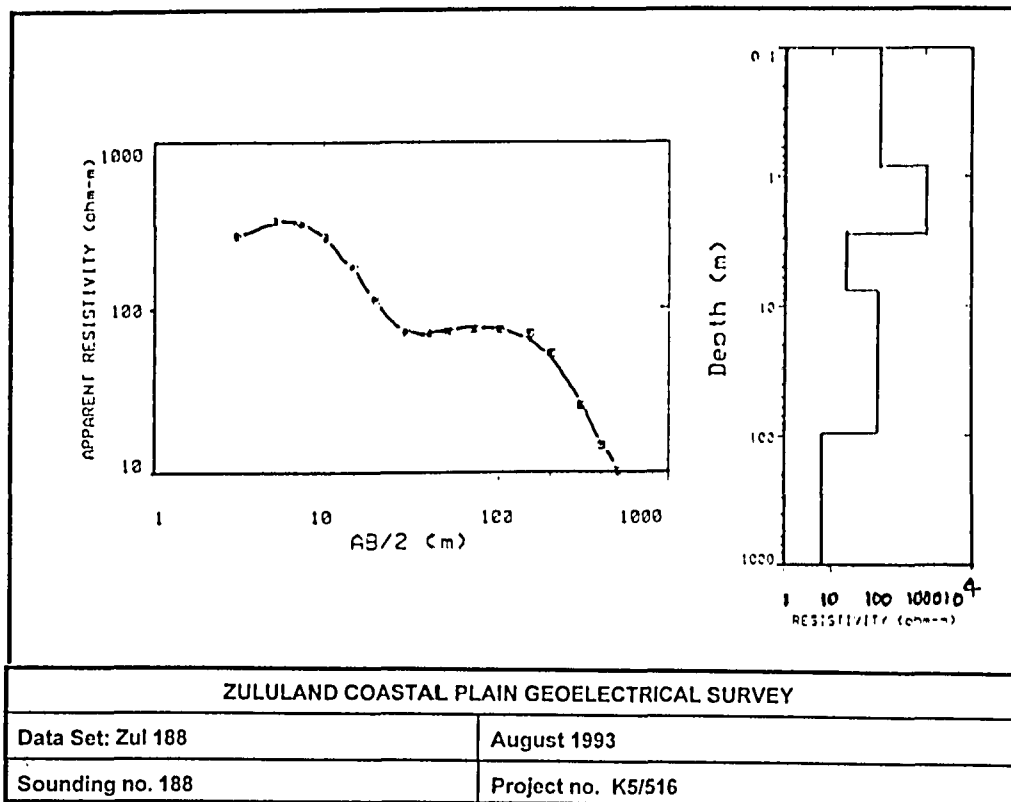


Figure 7: DC sounding curve and interpretations for ES 188 (Uloa Formation) and ES 105 (Port Durnford Formation).

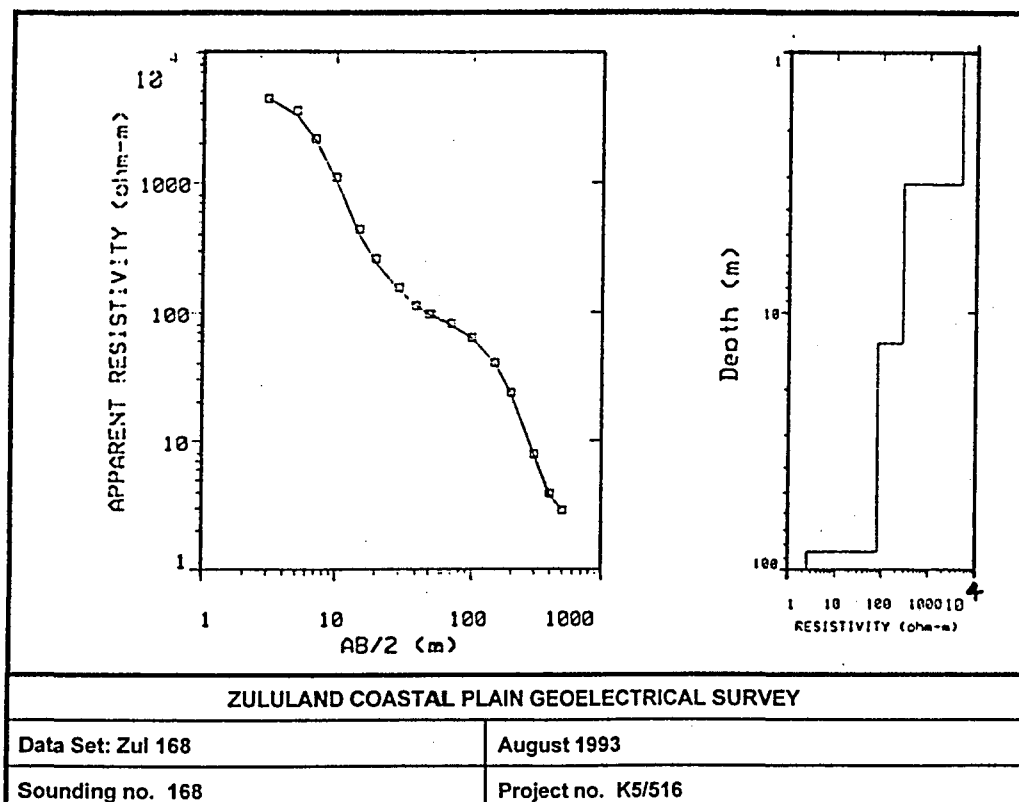
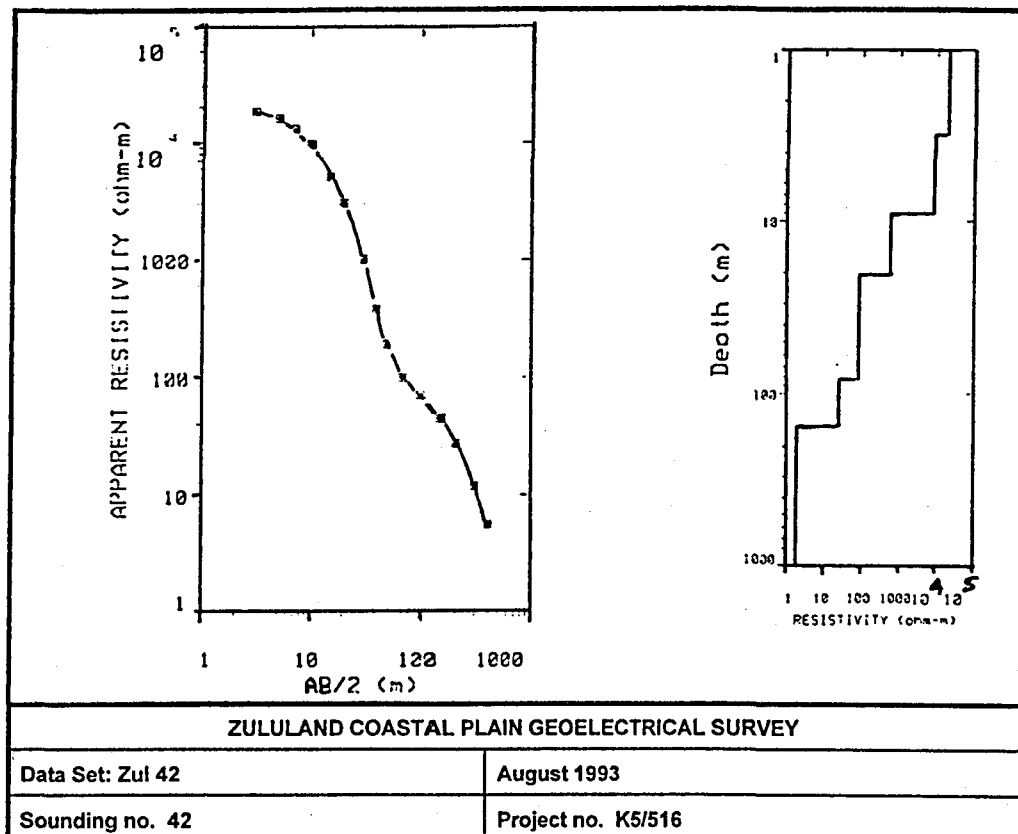
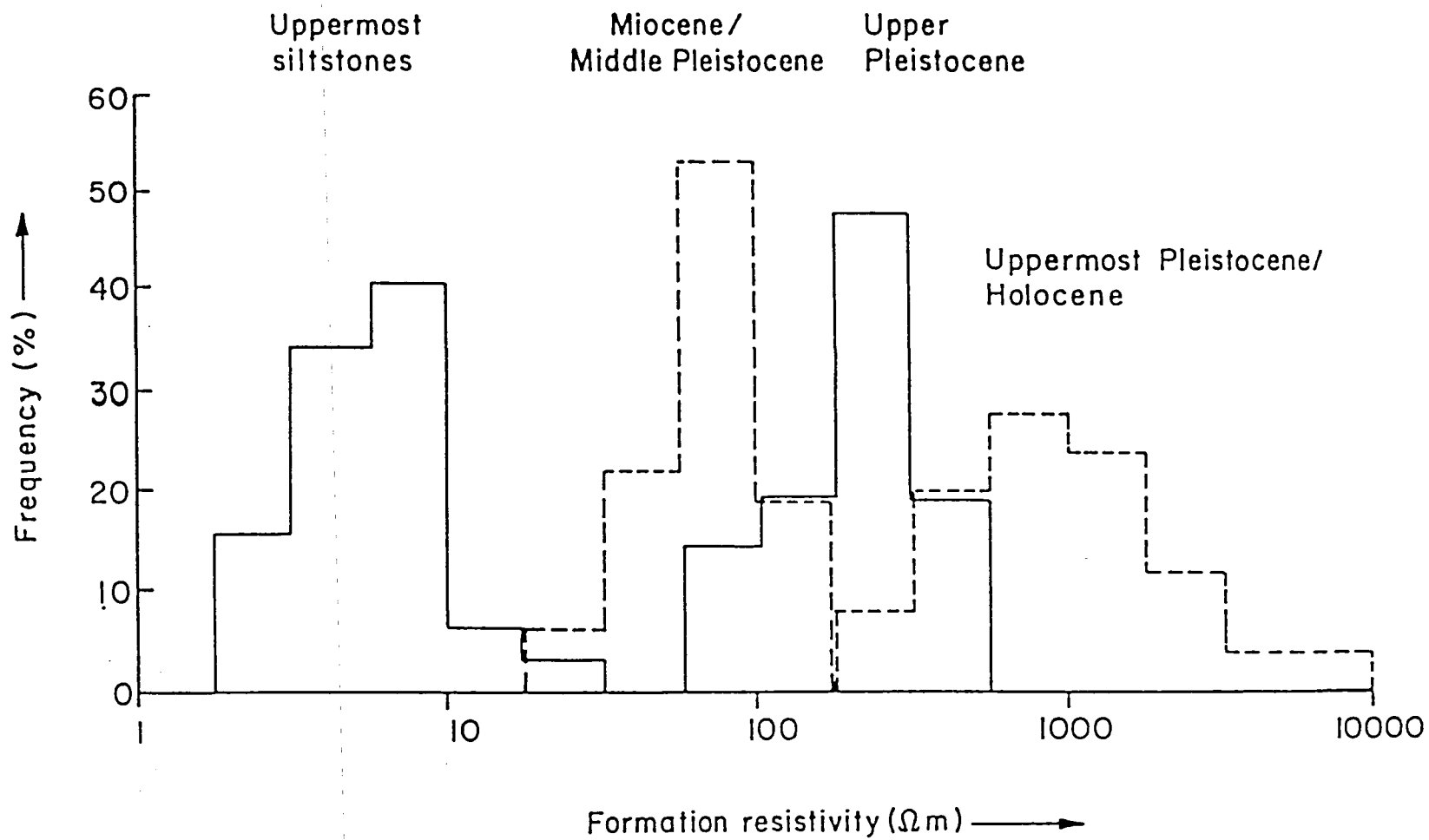
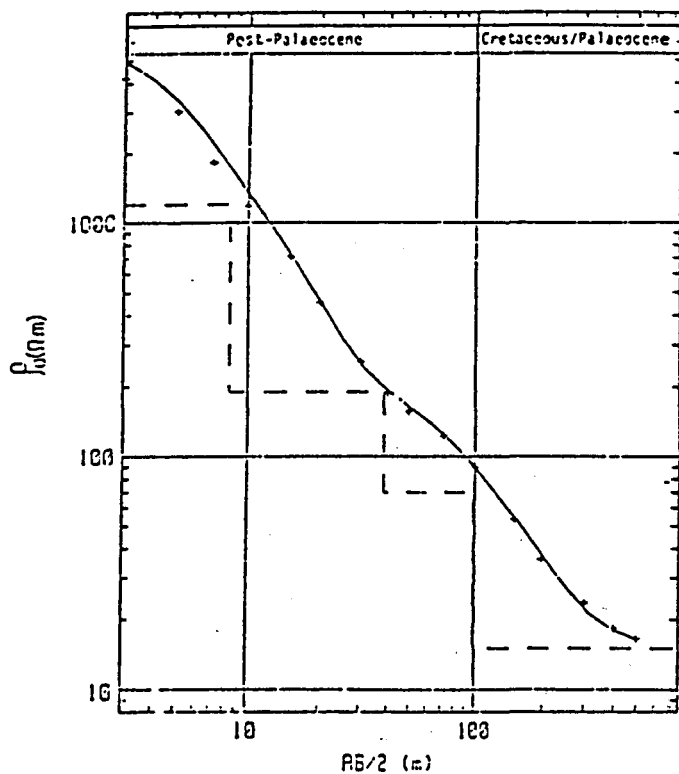


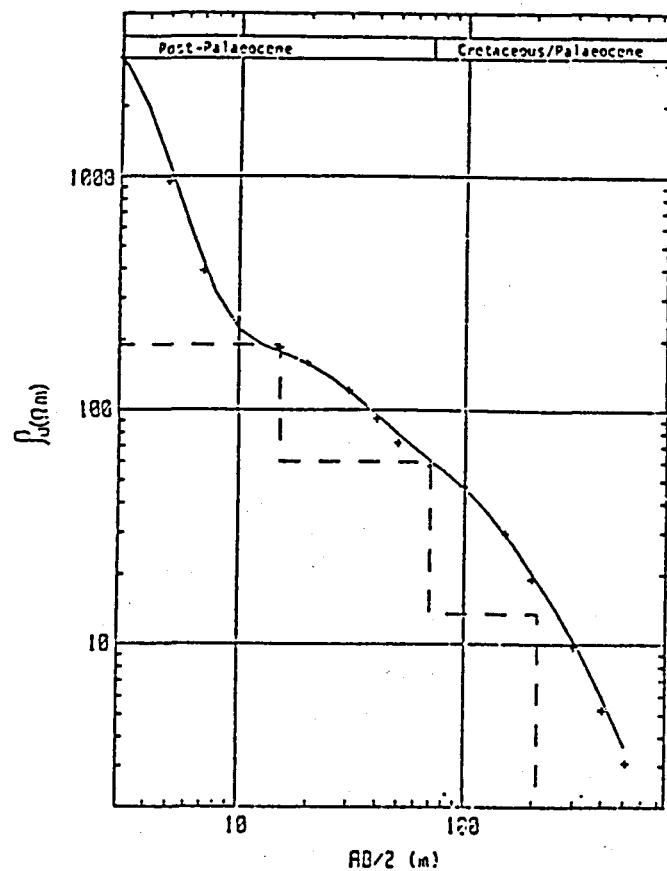
Figure 8: DC sounding curve and interpretations for ES 42 (Berea-type Red Sand) and ES 168 (Holocene sands).



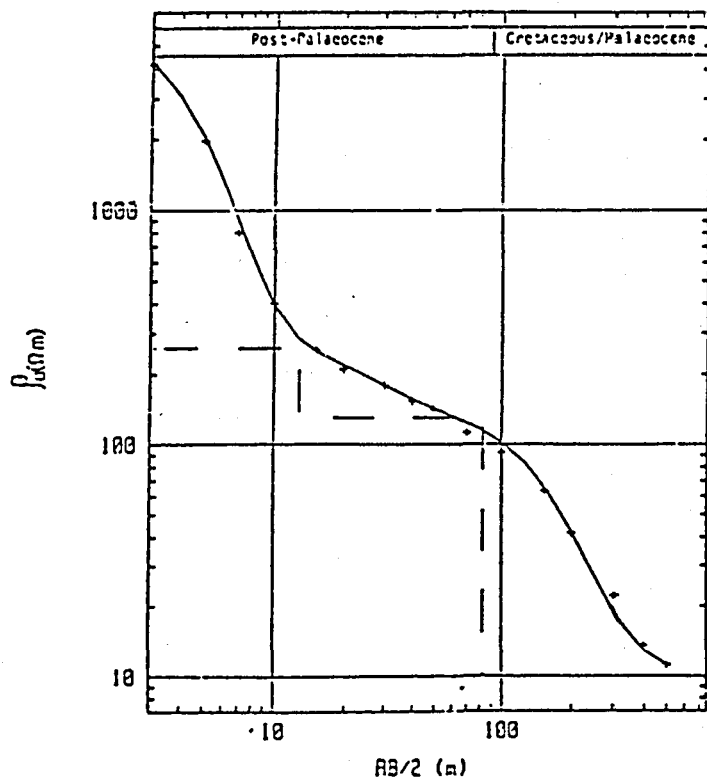
**Figure 9:** Histogram of surface measured formation resistivities based on calibration soundings (Worthington, 1979).



Sounding curve and model for ES 1 measured at Soekor borehole ZF 1/72



Sounding curve and model for ES 2 measured at Soekor borehole ZG 1/72



Sounding curve and model for ES 4 measured at Soekor borehole ZE 1/71

Figure 10: Sounding curves and models for ES 1, ES 2 and ES 4.

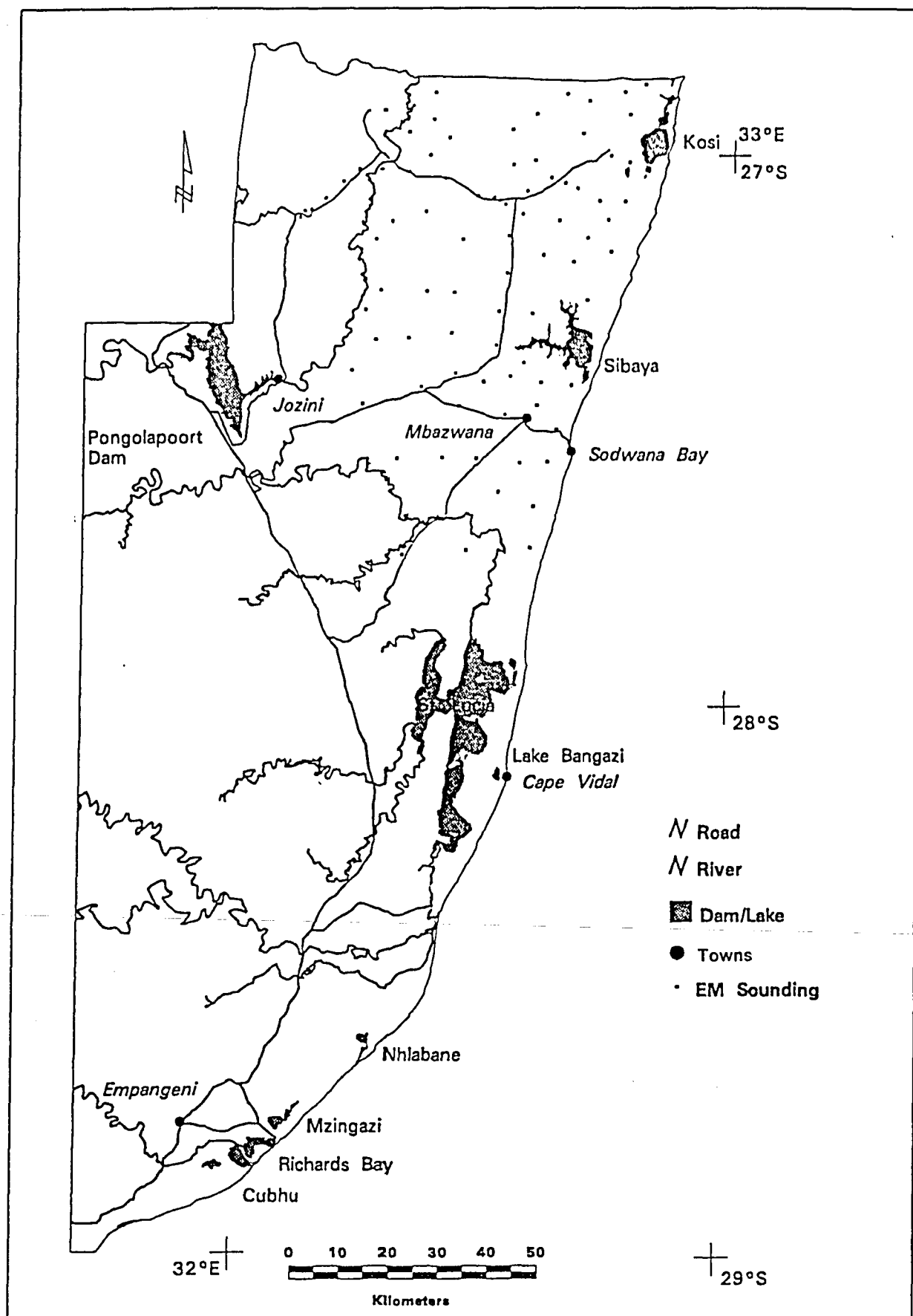
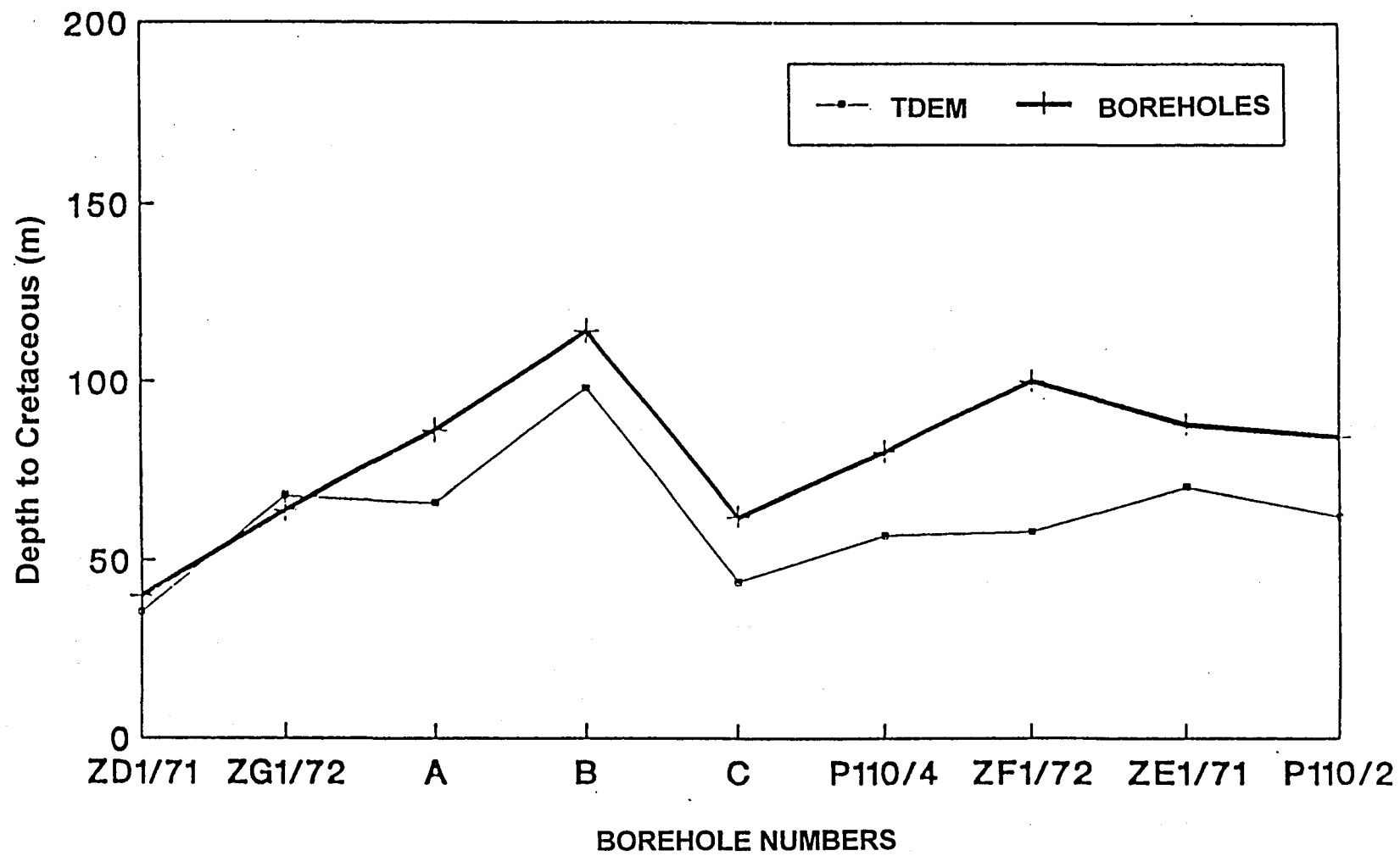


Figure 11: Electromagnetic sounding (EM-37) Sounding locations.



**Figure 12:** Comparison between the results of time domain electromagnetic sounding interpretations (TDEM) and drilling results.



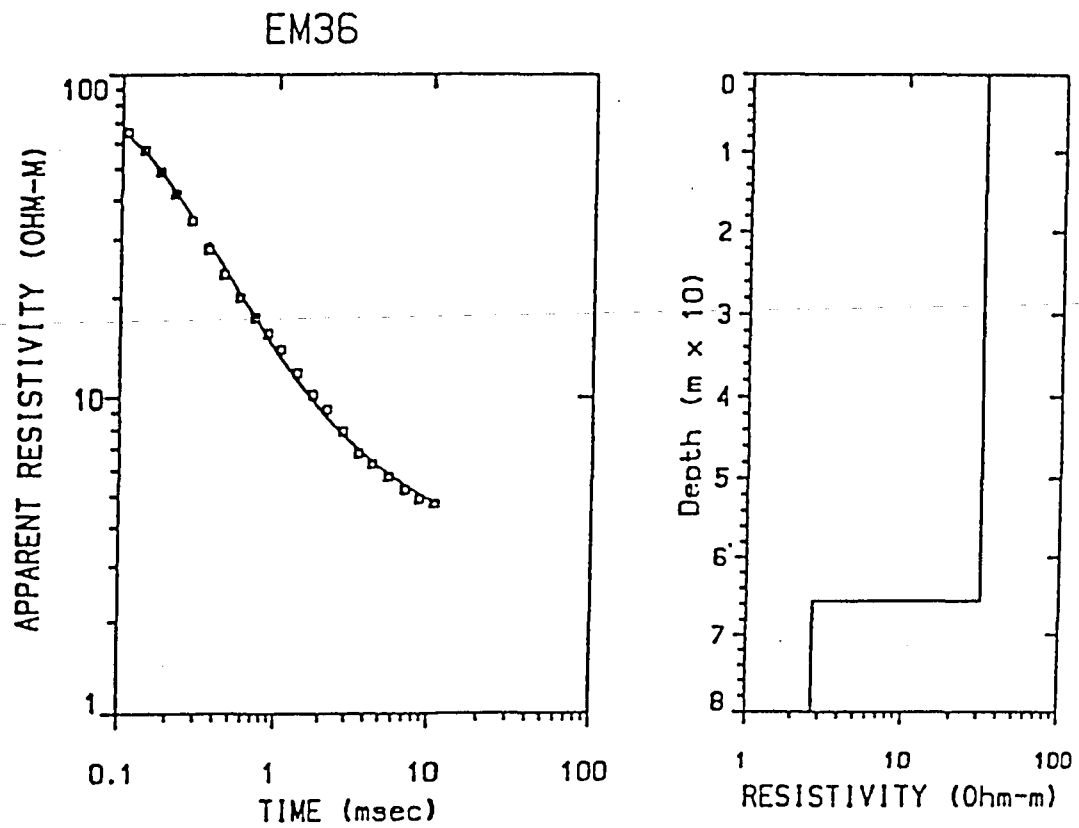
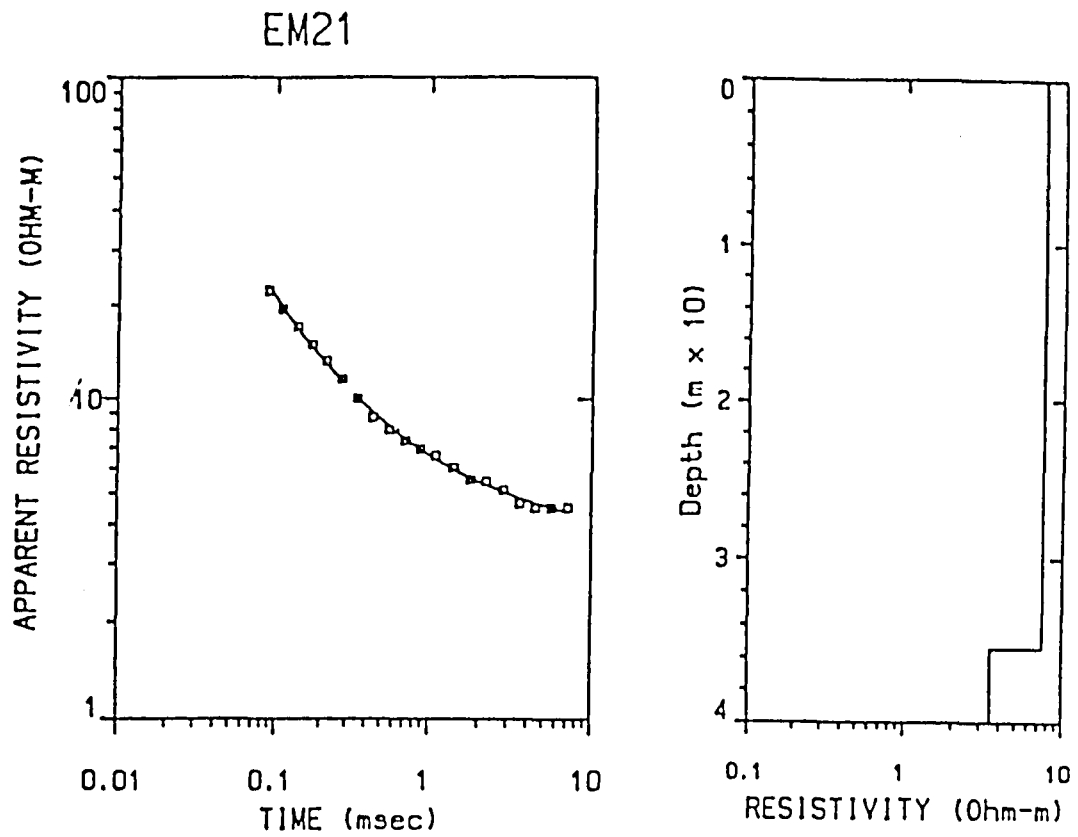


Figure 13: Transient electromagnetic sounding curves and models for soundings EM 21 and EM 36.

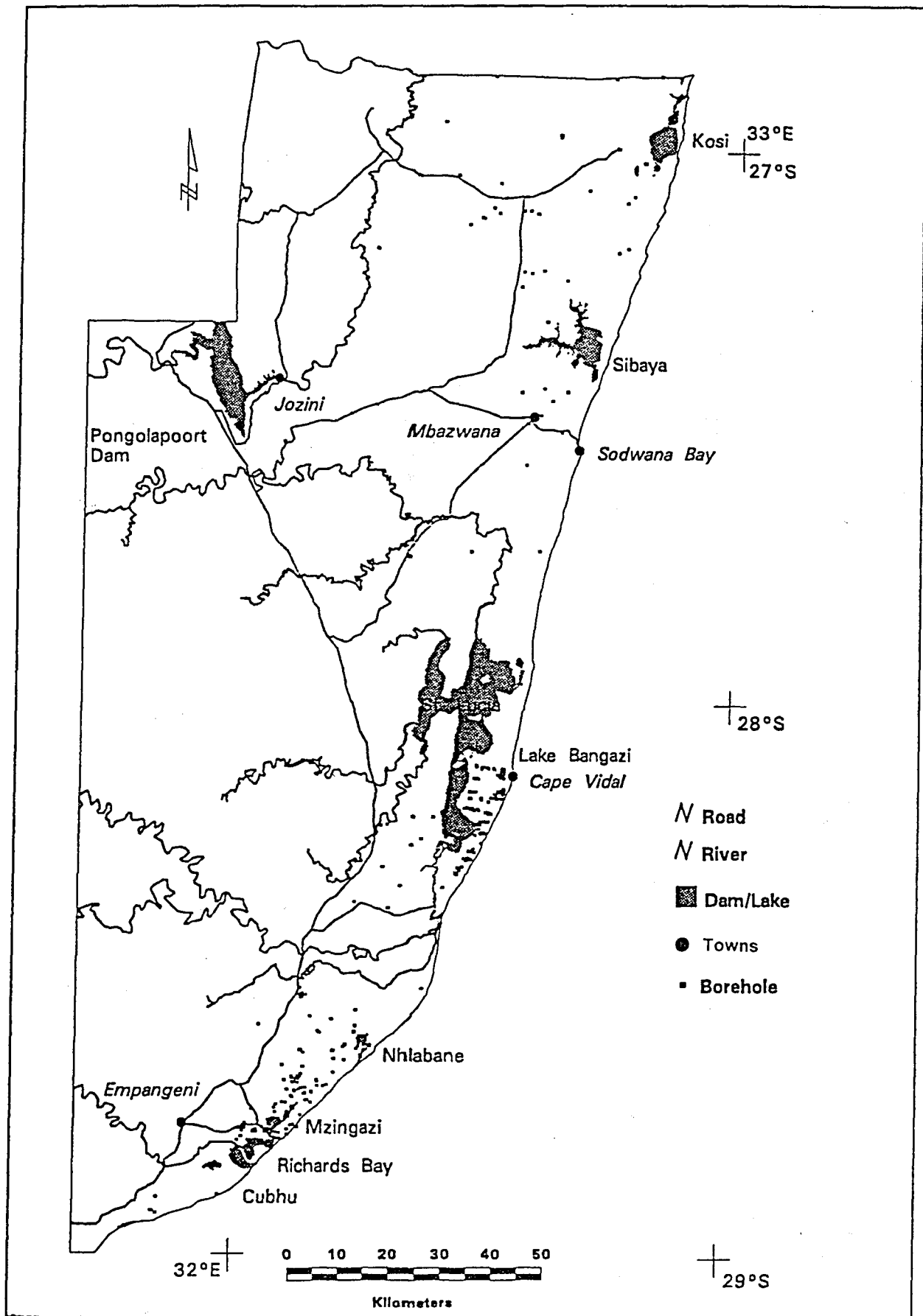


Figure 14: Borehole positions on the Zululand Coastal Plain.

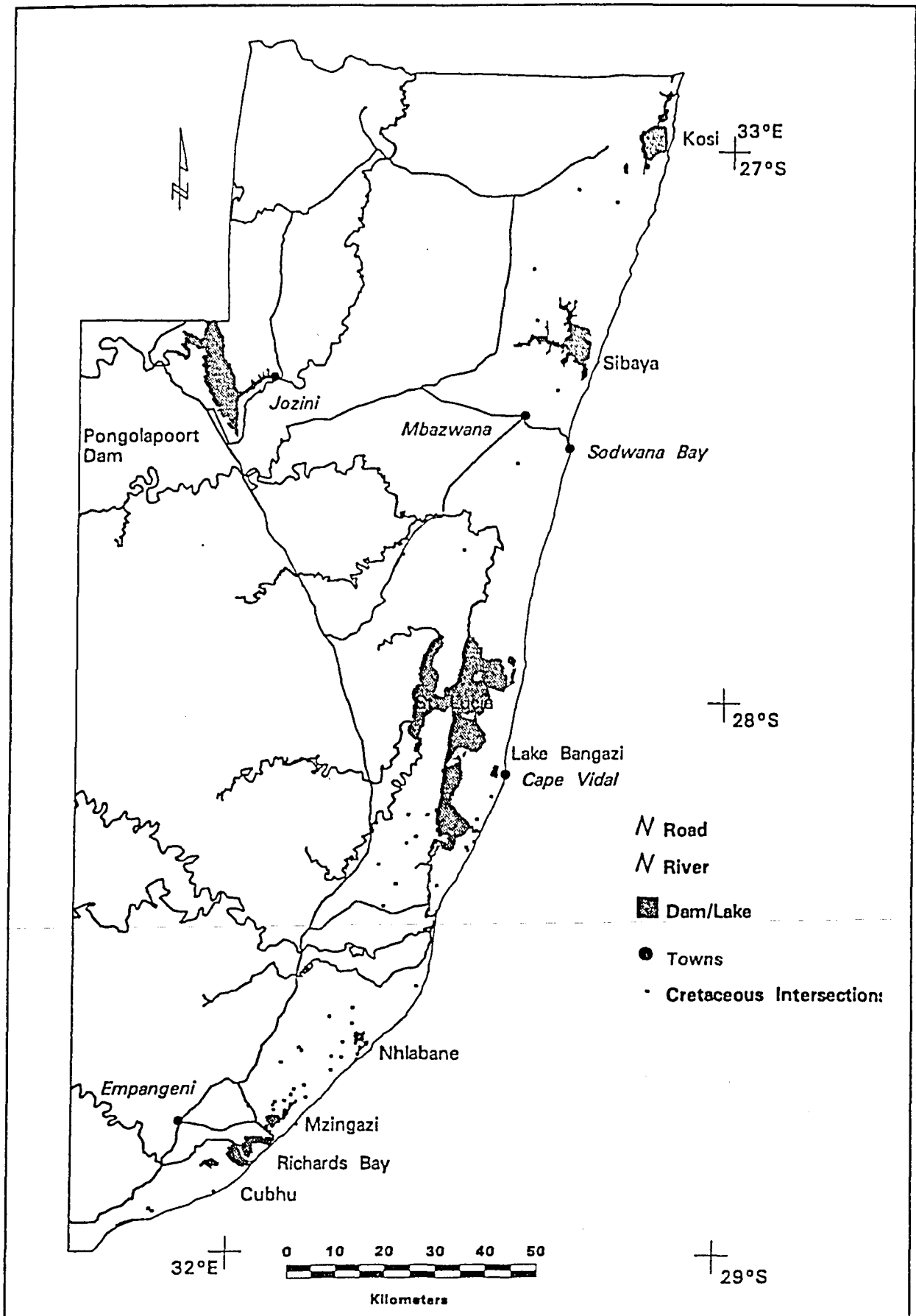


Figure 15: Boreholes where Cretaceous age rocks were intersected.

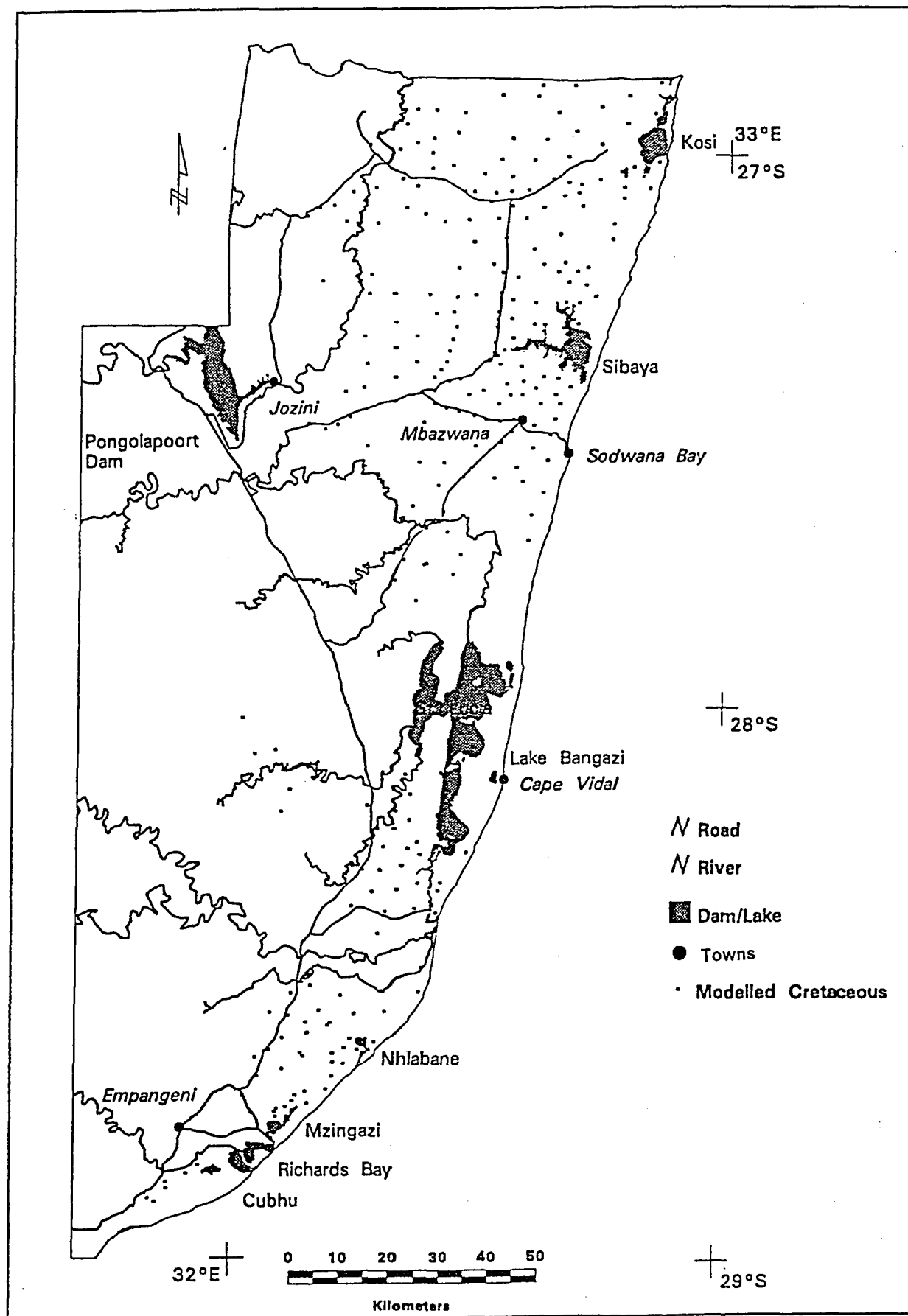


Figure 16: Positions of modeled depths to Cretaceous.

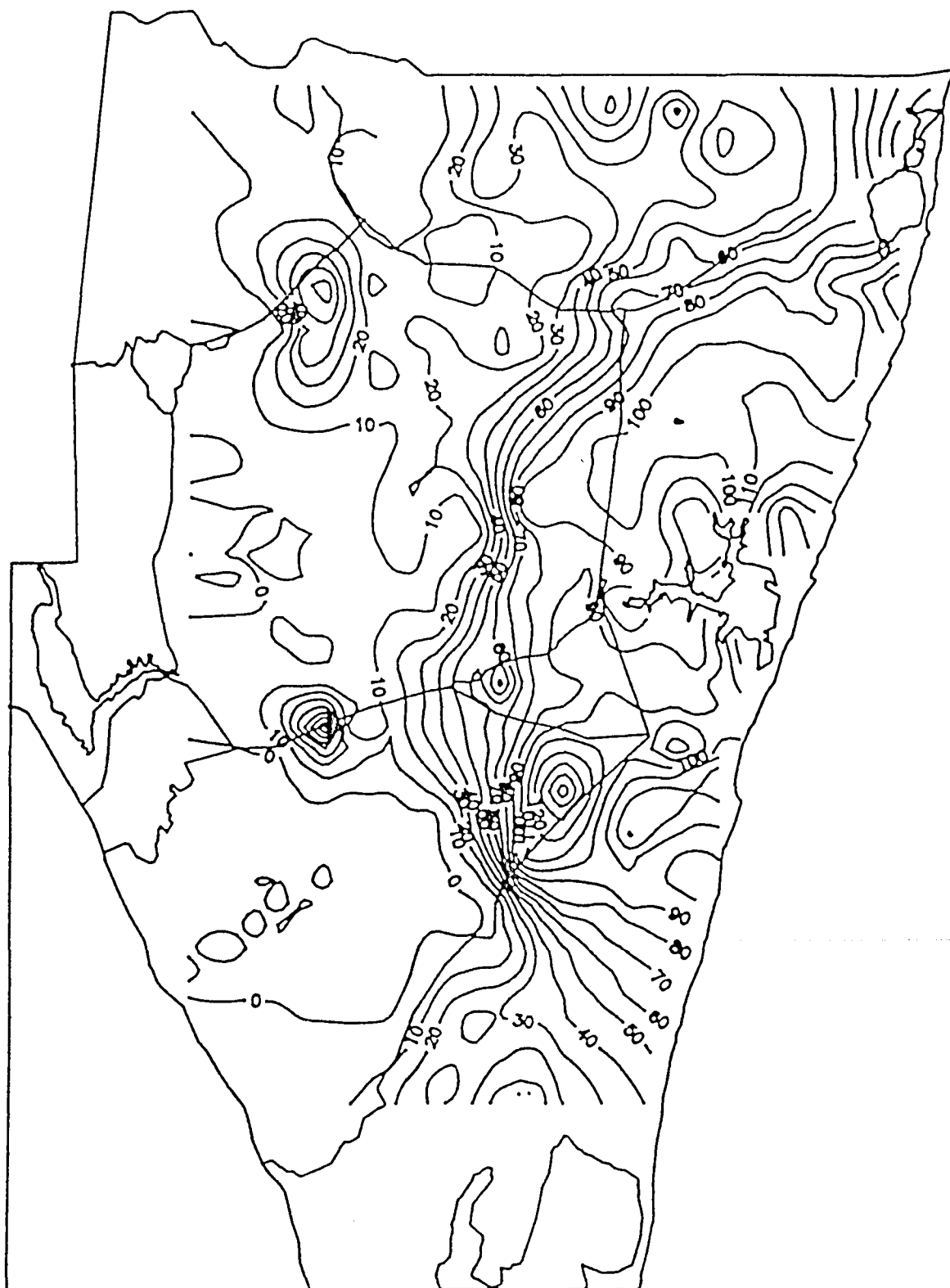
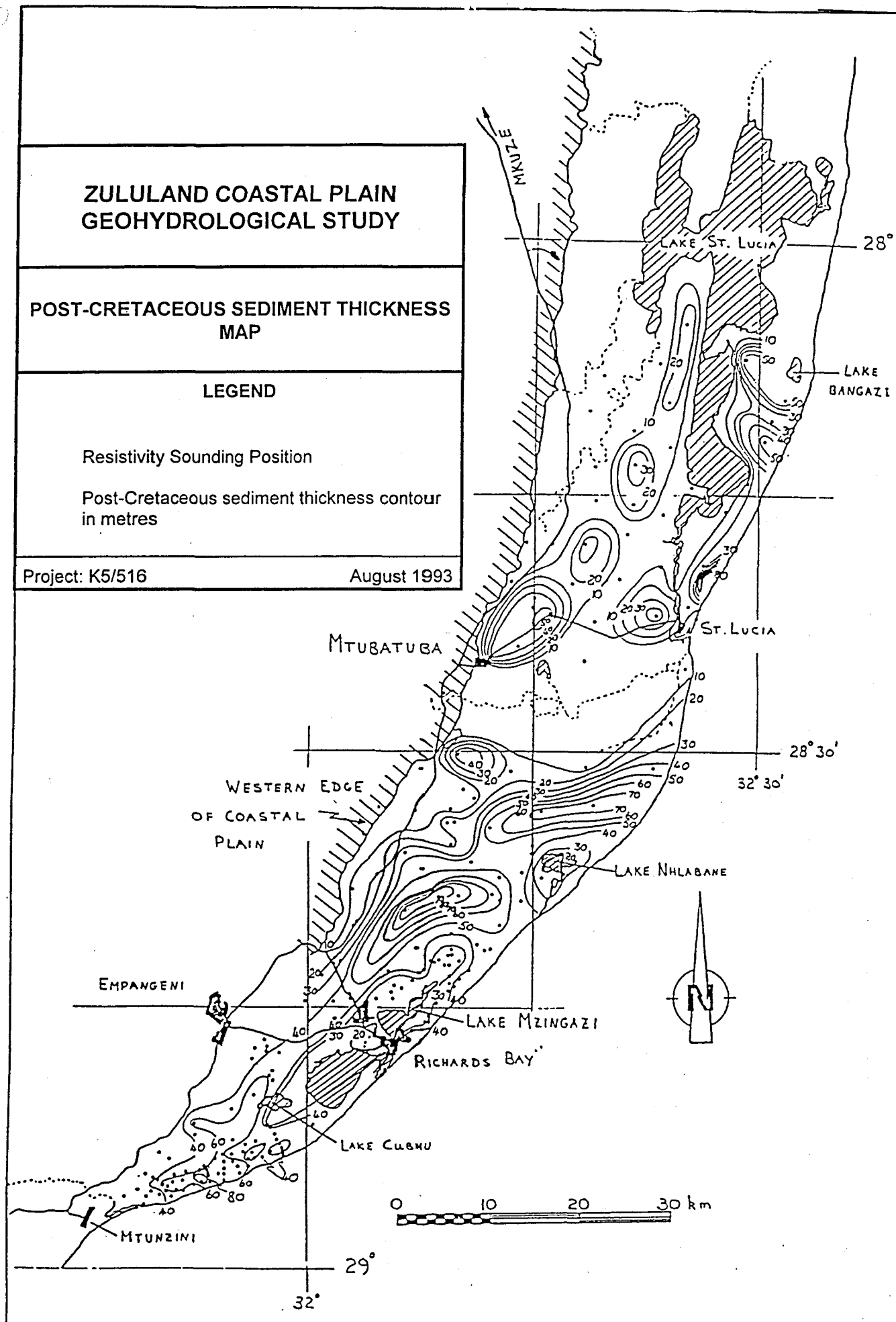


Figure 17: Post Cretaceous sediment thickness north of Lake St Lucia.



**Figure 18:** Post-Cretaceous sediment thickness on the Zululand Coastal Plain south of

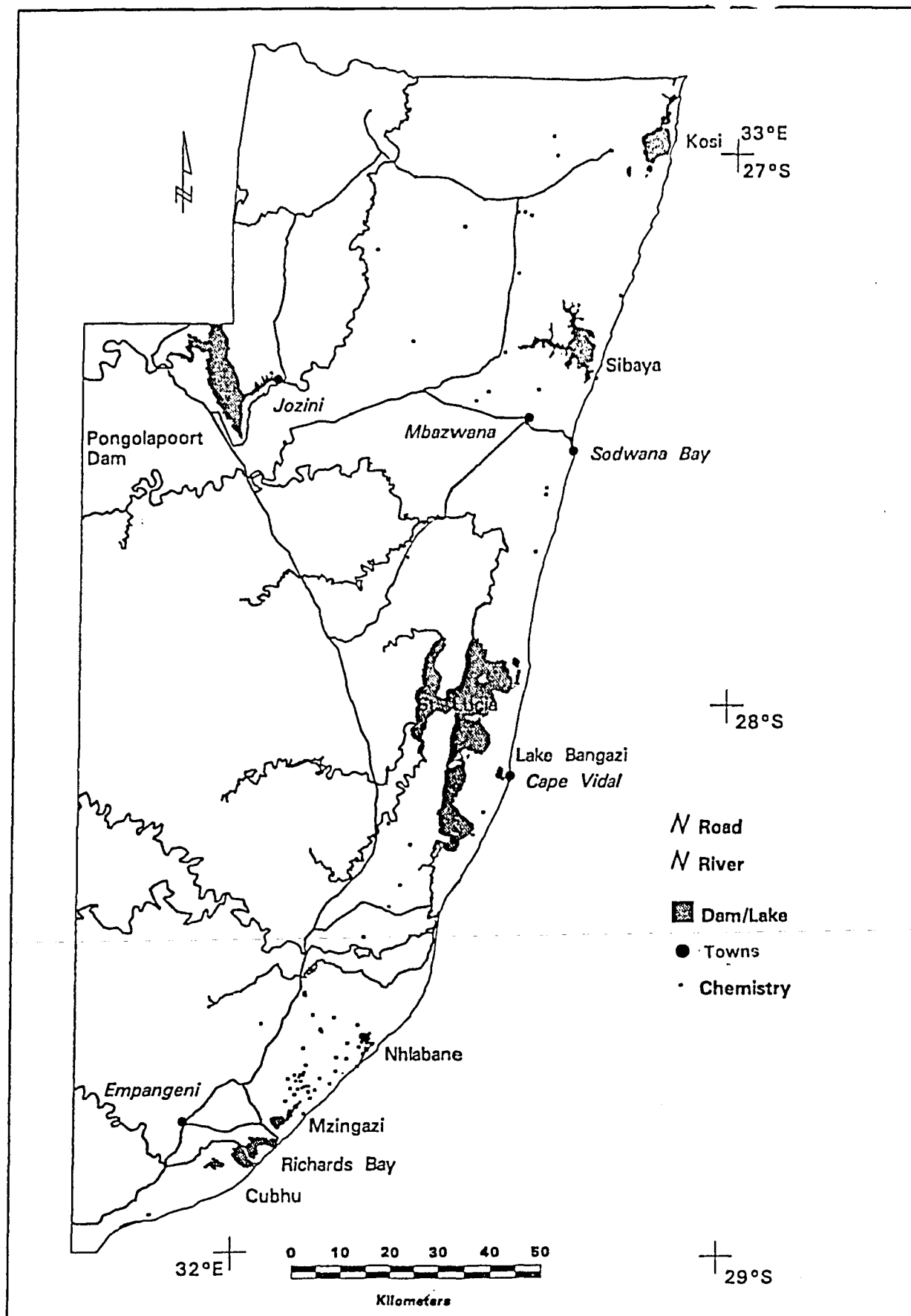


Figure 19: Boreholes sampled for water chemistry.

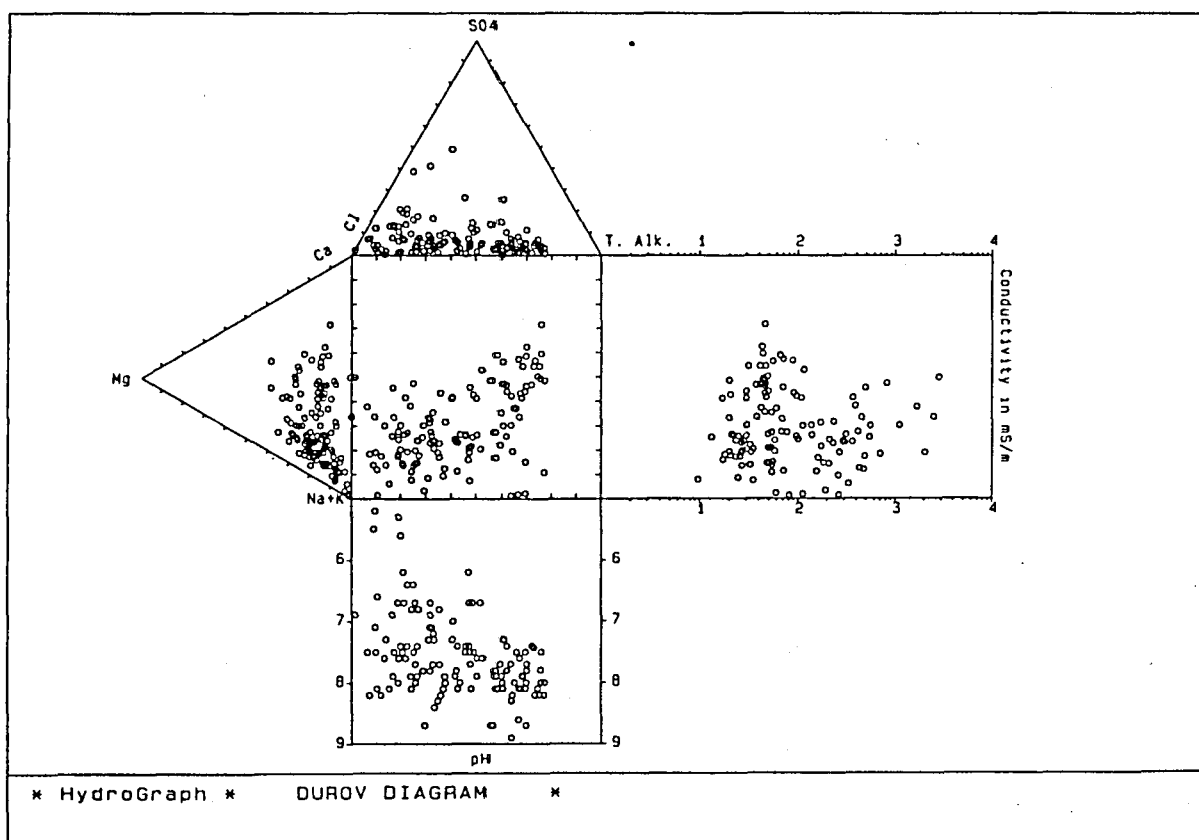
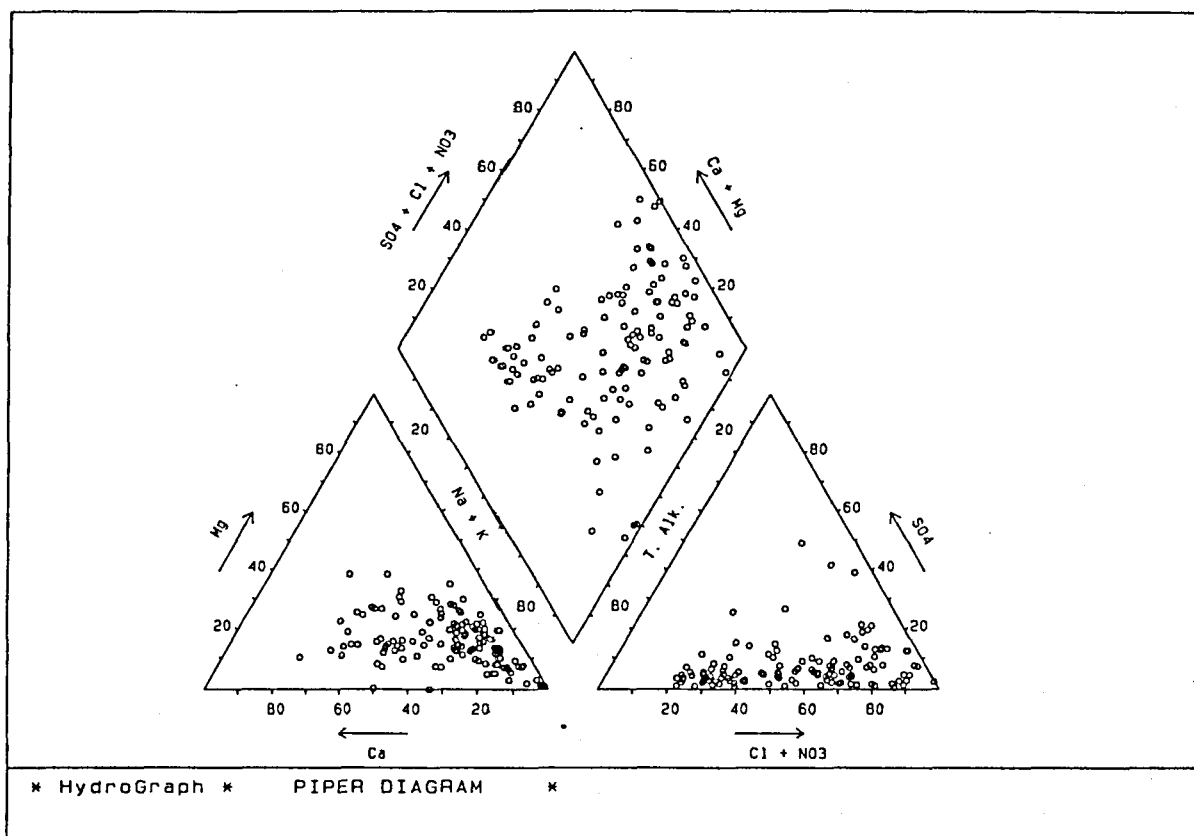
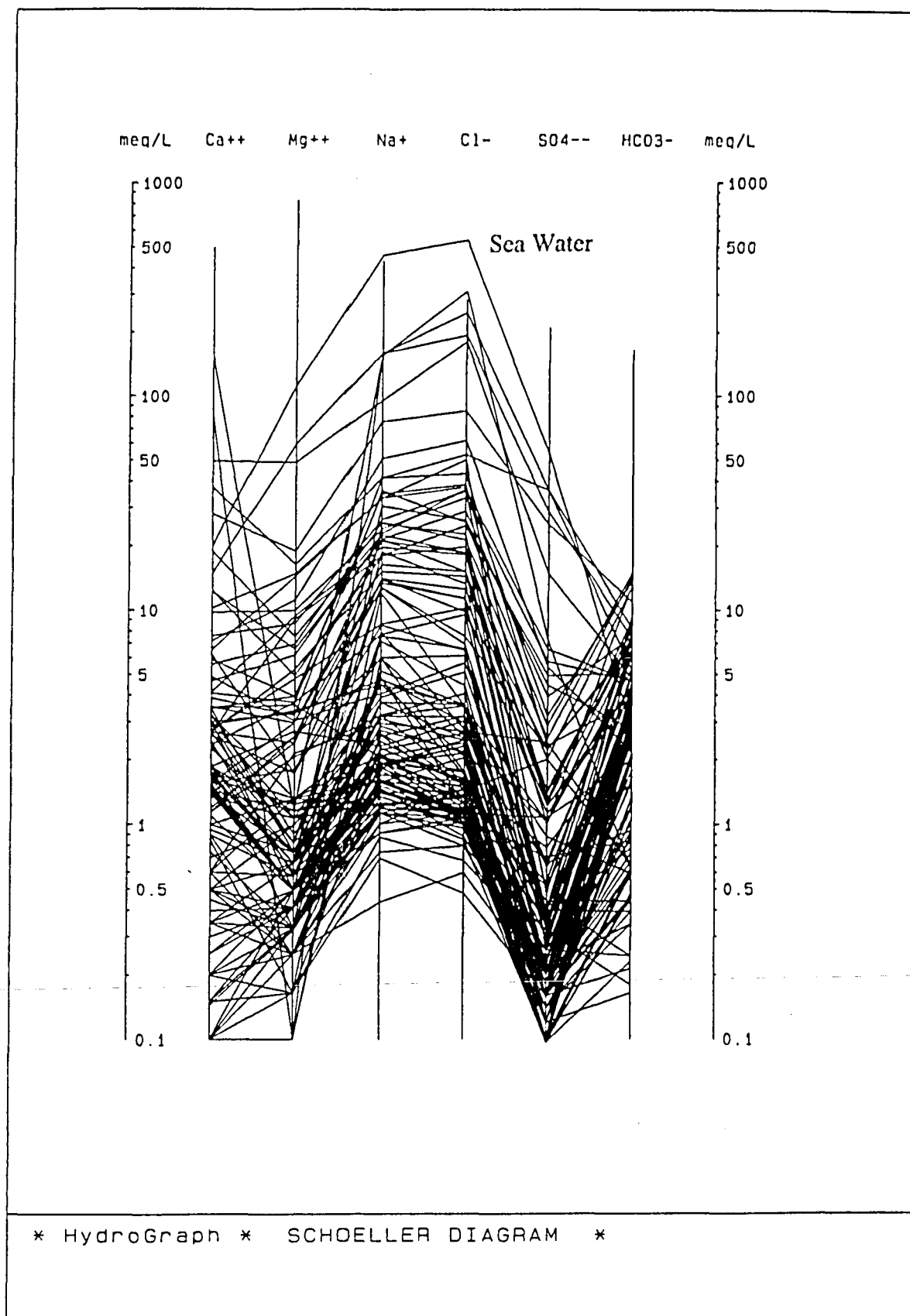


Figure 20a: Results of chemical analyses of all water samples entered into the Hydrocom database. Data are represented as Piper and Durov diagrams.





**Figure 20b:** Results of chemical analyses of all water samples entered into the Hydrocom database. Data are represented on a Schoeller diagram.



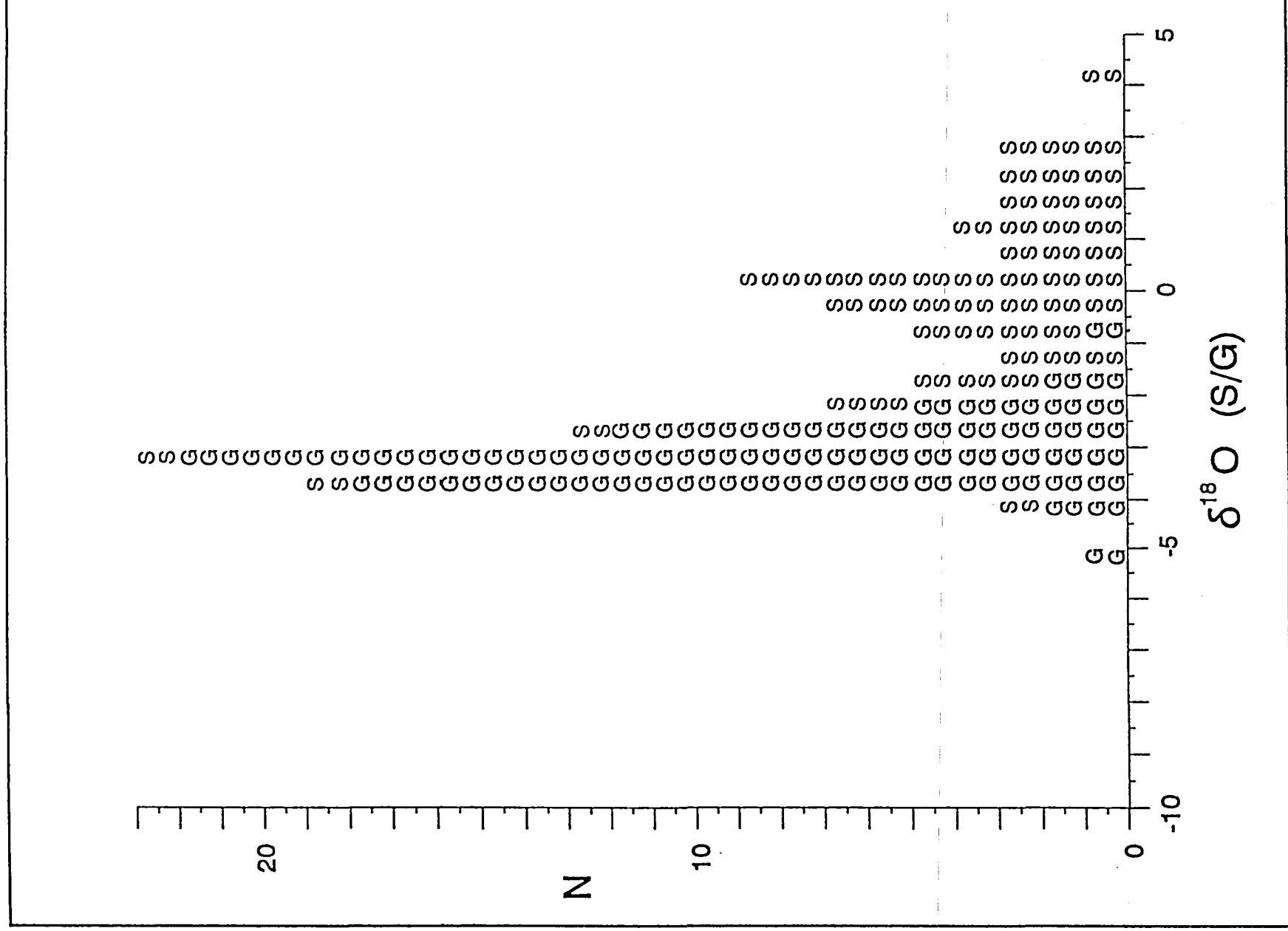


**Figure 22:** Distribution of  $\delta^{18}\text{O}$  levels on ground water and surface water in the study area.  
Surface waters show the effect of isotope enrichment due to evaporation.

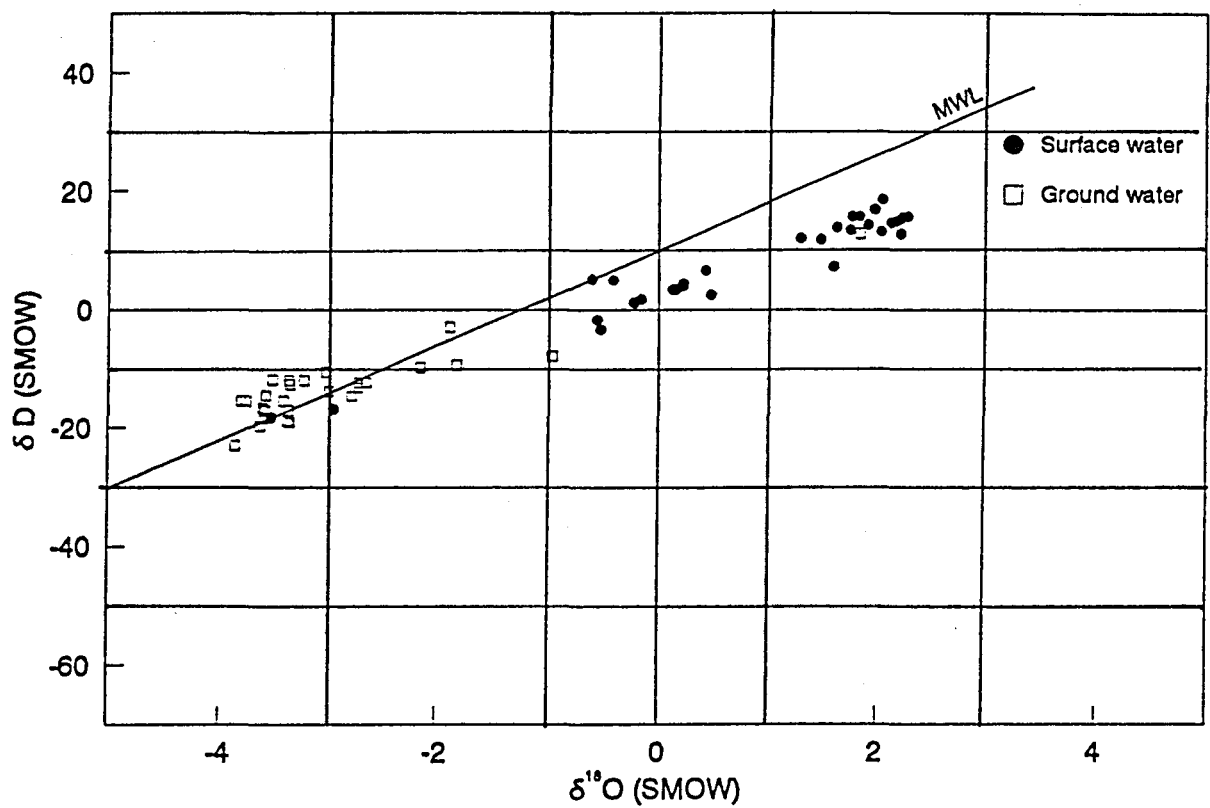


**Figure 23:** Relation between  $^{18}\text{O}$  and deuterium in ground water and surface water. Ground water falls on the Meteoric Water Line (MWL) following a general pattern. Deviations from the MWL by surface water are due to evaporation enrichment.

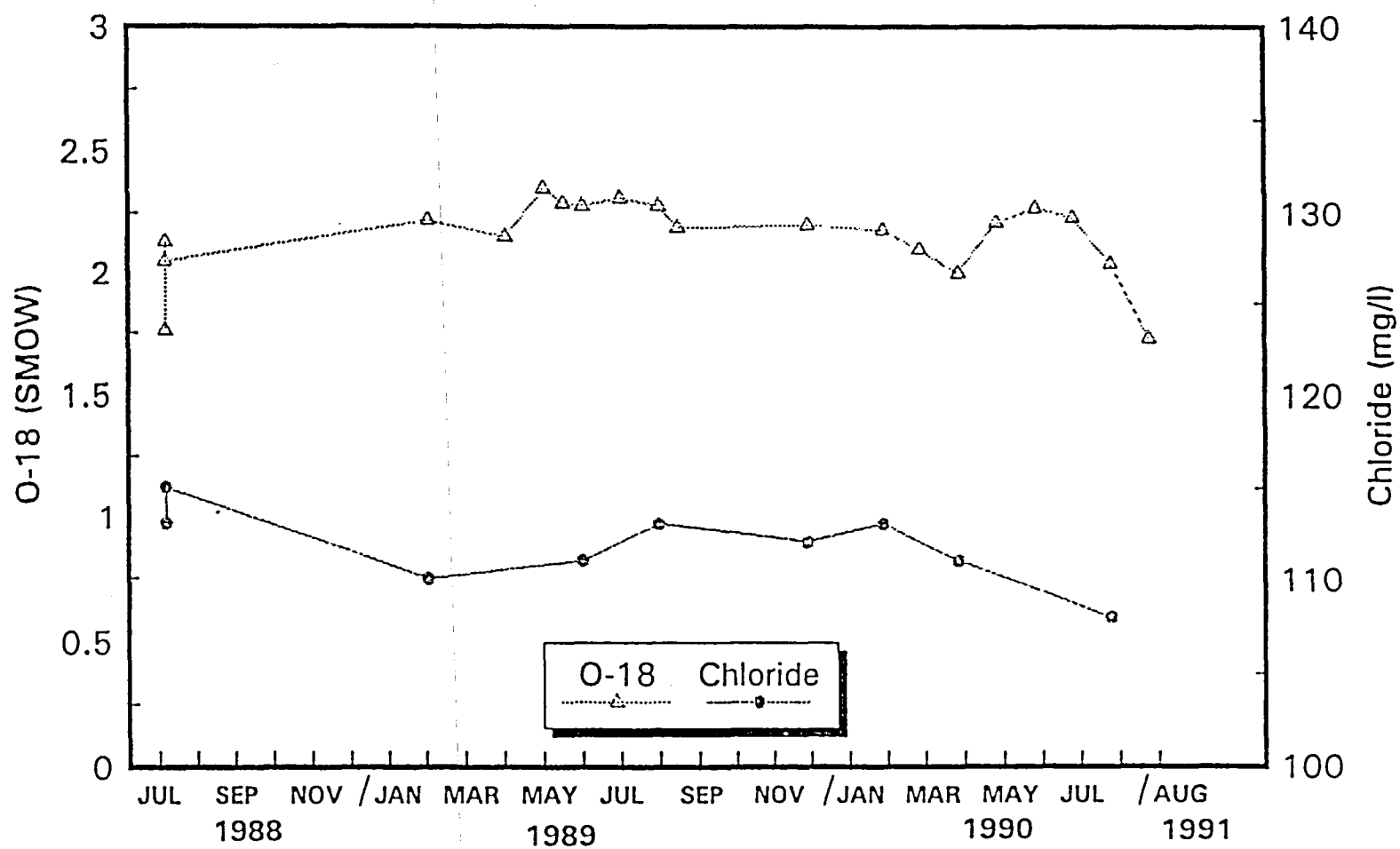


**Figure 24:** Time series of chloride (Cl) and  $^{18}\text{O}$  in Lake Sibayi. The overall constancy of both parameters indicates that the annual (rain/ground) water inflow is small compared with the lake volume.

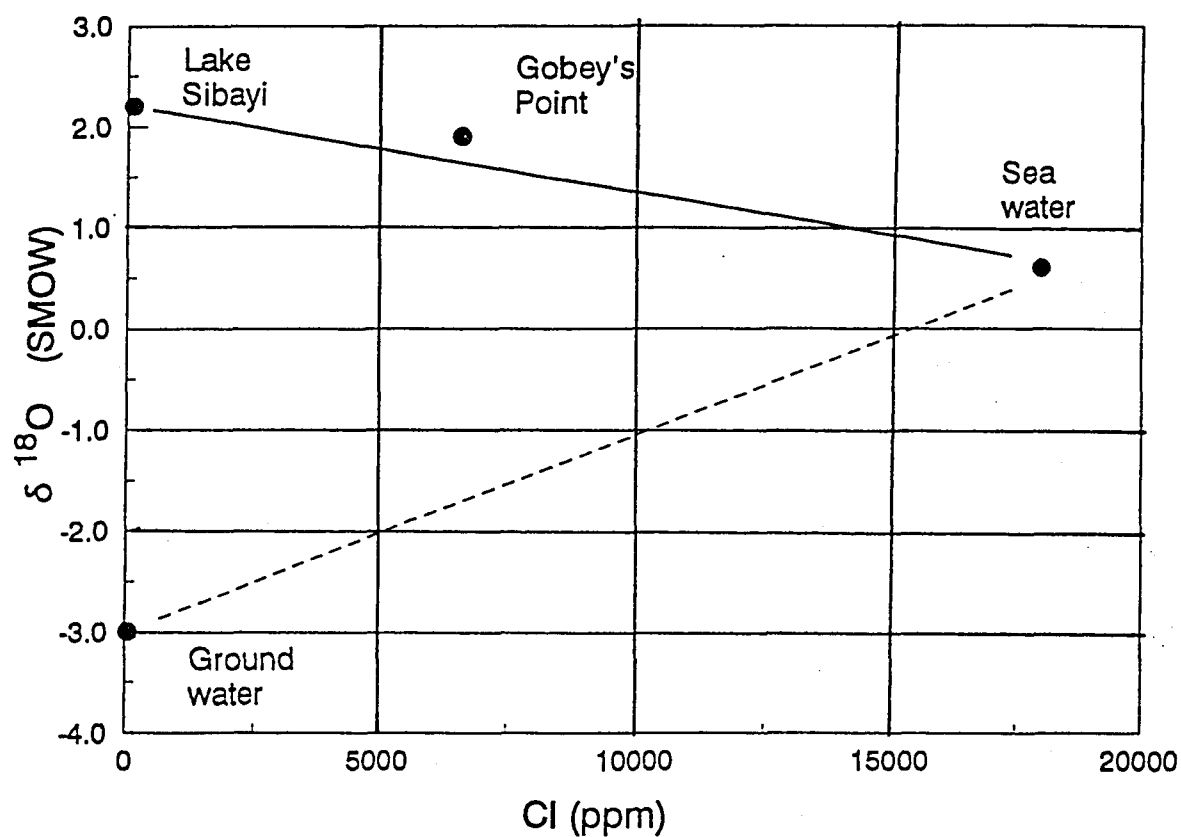


**Figure 25:**  $^{18}\text{O}$  and chloride relation for the Gobey's Point seepage and the waters likely to be its sources.

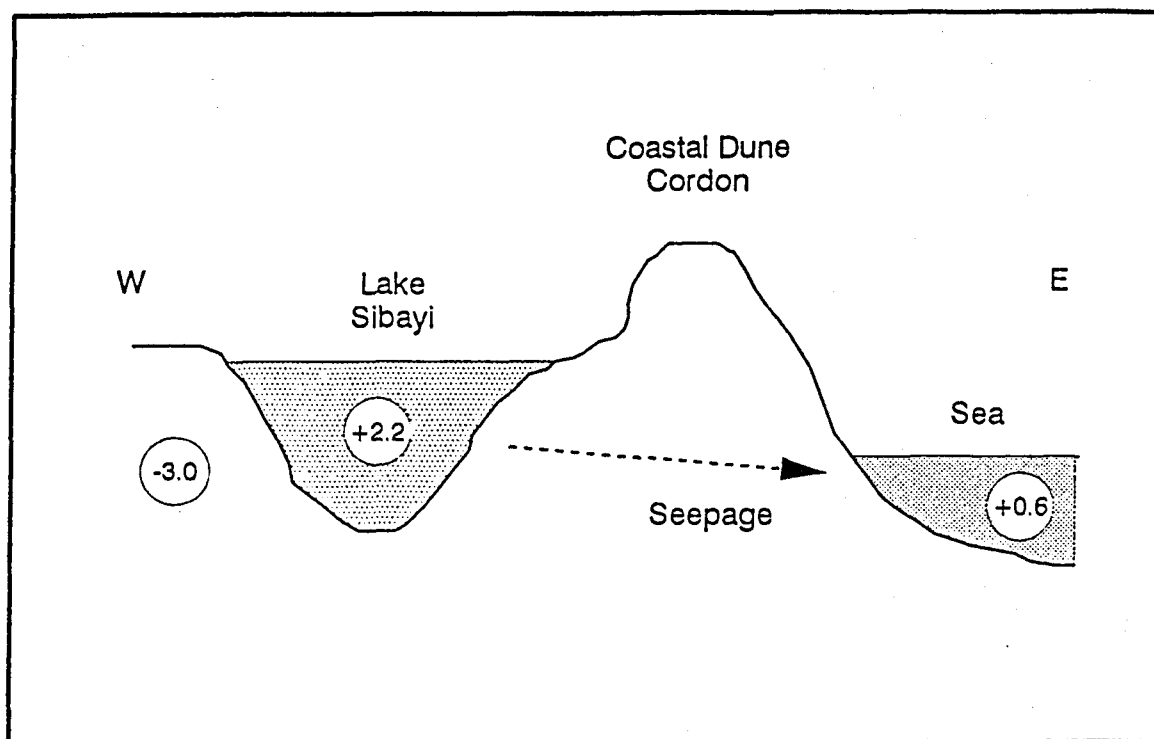


**Figure 26:** Schematic cross-section through the coastal dune between Lake Sibayi and the sea.

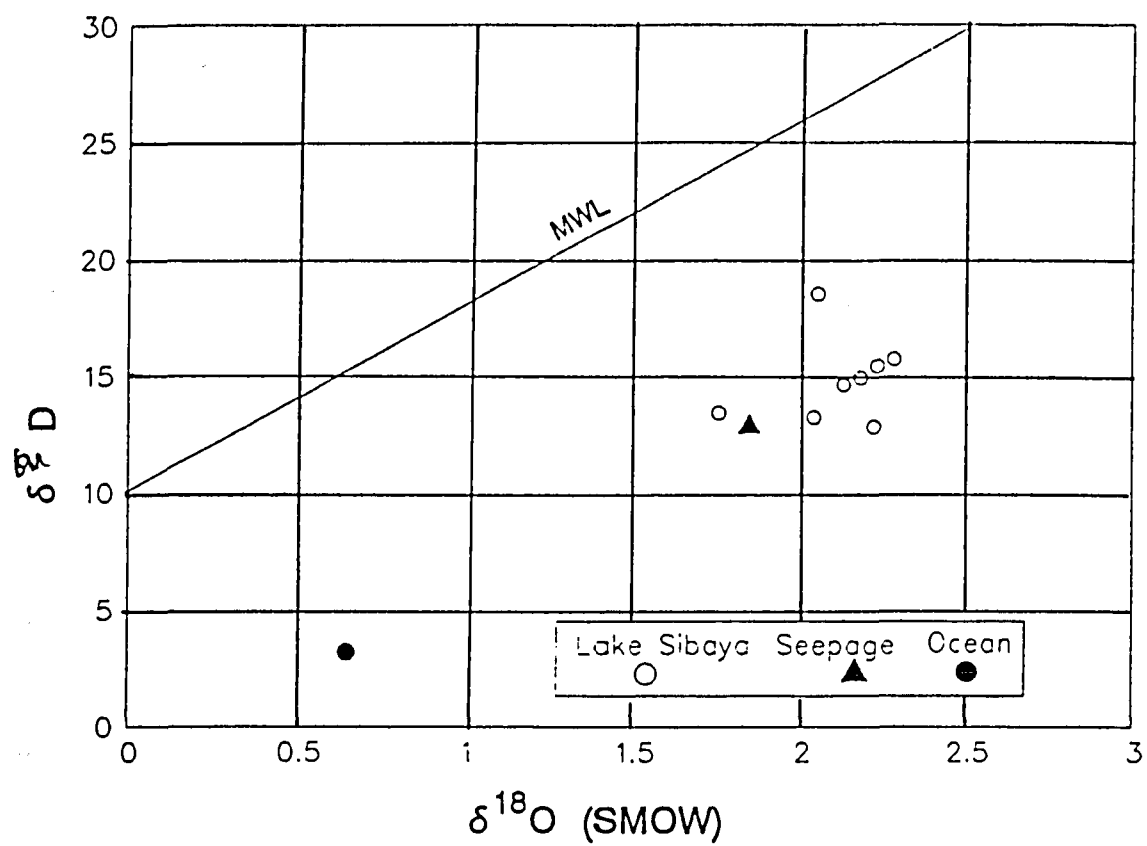


**Figure 27:**  $^{18}\text{O}$  and deuterium relation for Gobey's Point seepage and its likely sources. The seepage is also located directly on the mixing line between lake and sea water and distinctly different from the MWL representing rain and ground water.

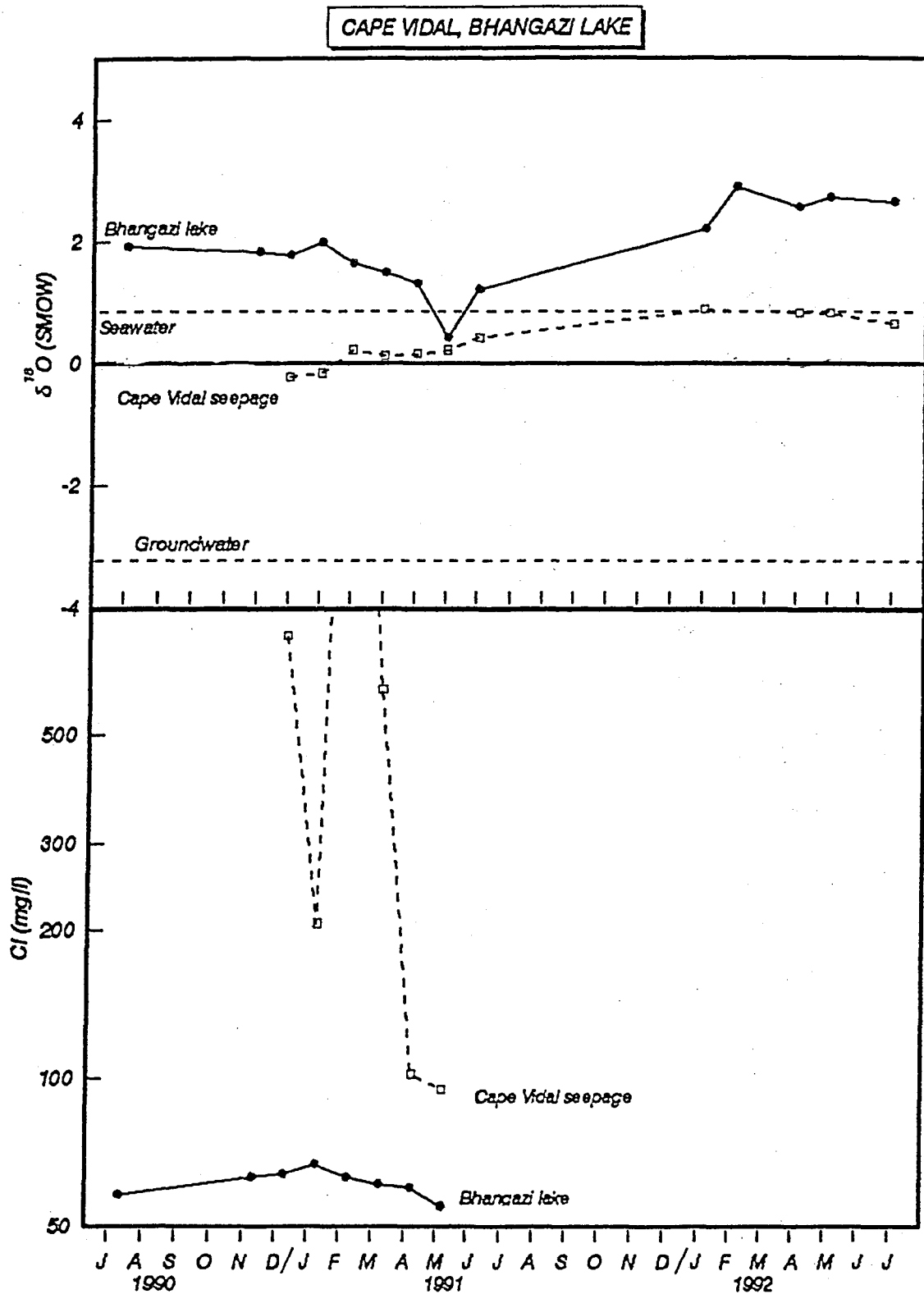


**Figure 28:**  $^{18}\text{O}$  and chloride time series of Lake Bhangazi and the Cape Vidal seepage water. The average  $^{18}\text{O}$  content of ground water is shown for comparison.



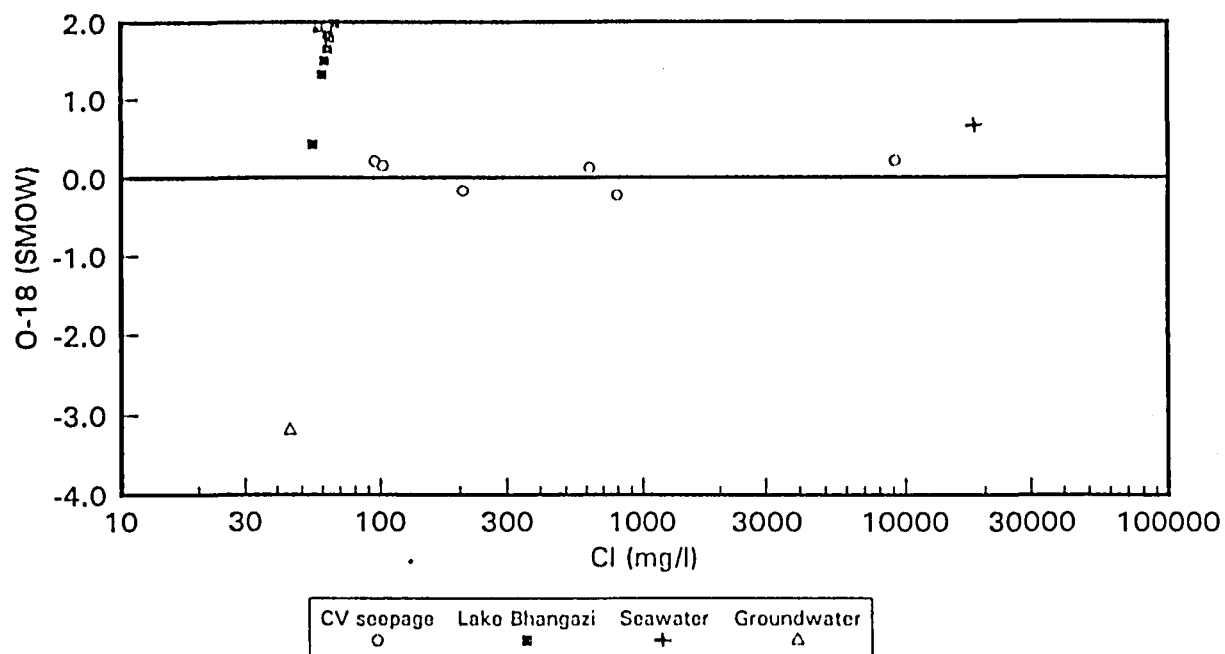


**Figure 29:** Comparison of  $^{18}\text{O}$  and Cl in the Cape Vidal/Bhangazi system. Average values for ground water in the area are taken from Breckenkamp (1993). Cape Vidal seepage can be seen to be a mixture between Lake Bhangazi water and ground water with occasional sea water contributions. Note the logarithmic scale.

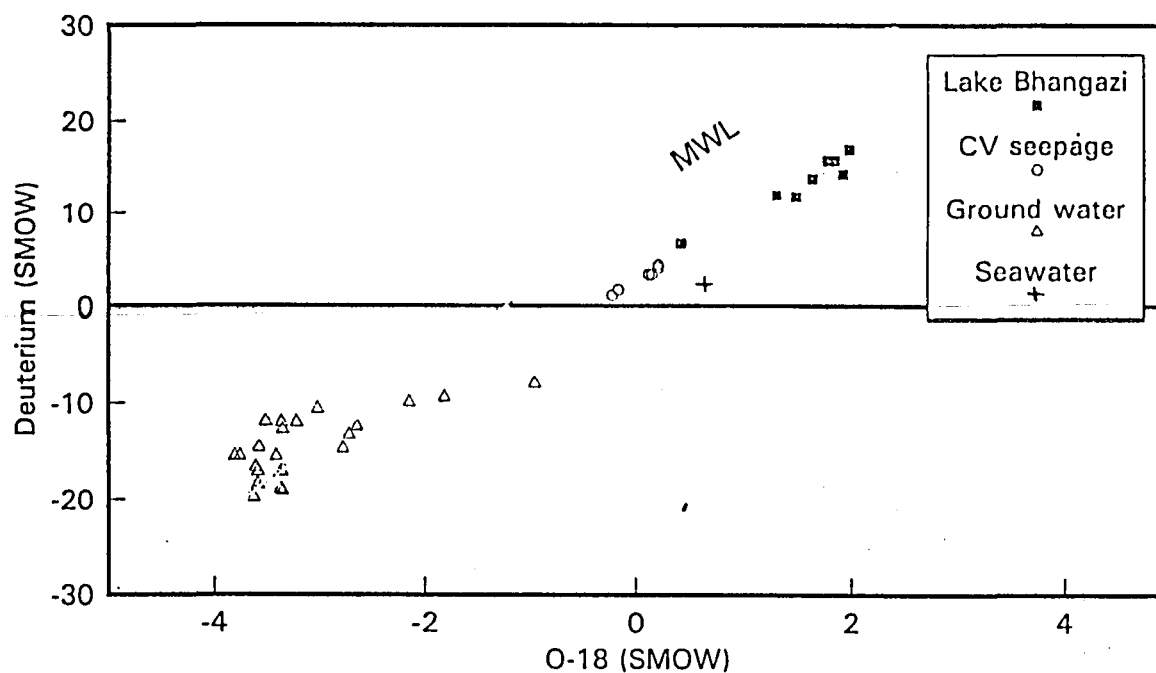


**Figure 30:**  $^{18}\text{O}$  and deuterium relation for water in the Cape Vidal/Lake Bhangazi system. The interpretation of Cape Vidal seepage as mixing between Lake Bhangazi water and local ground water is evident.

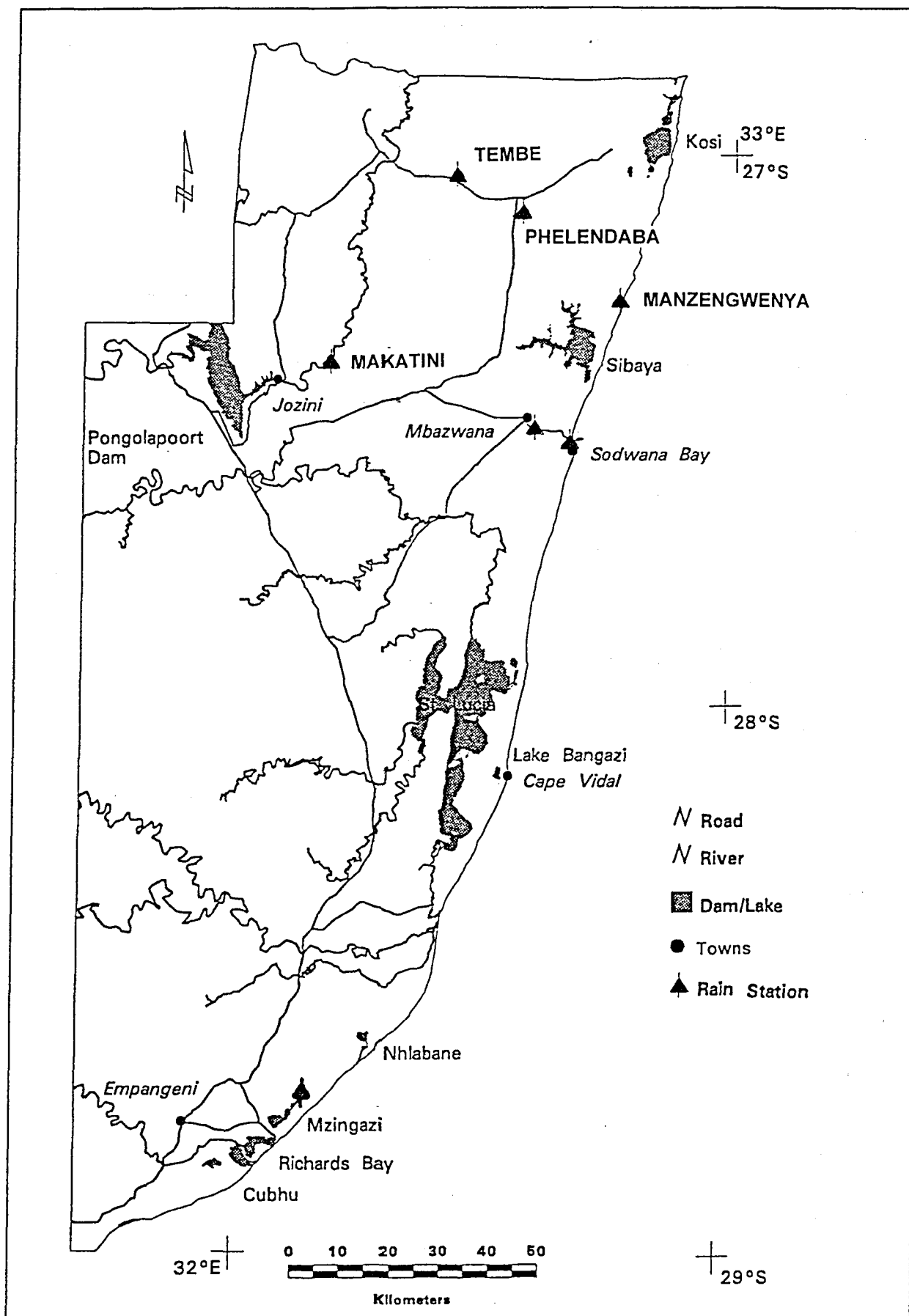


Figure 31: Rainfall monitoring stations used for this study.

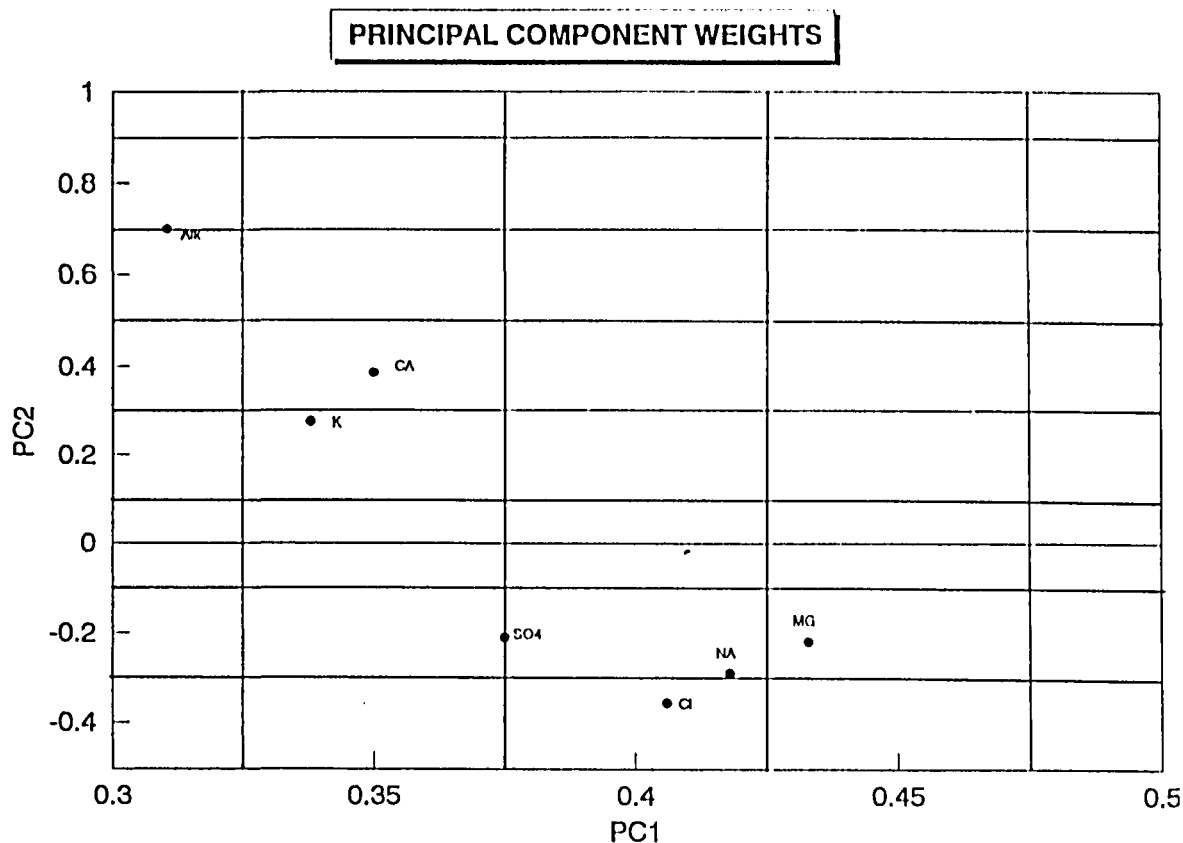


Figure 32: Results of principle component analysis of the rainfall chemistry data. The weights of the various ions contributing to the first two principle components are shown.

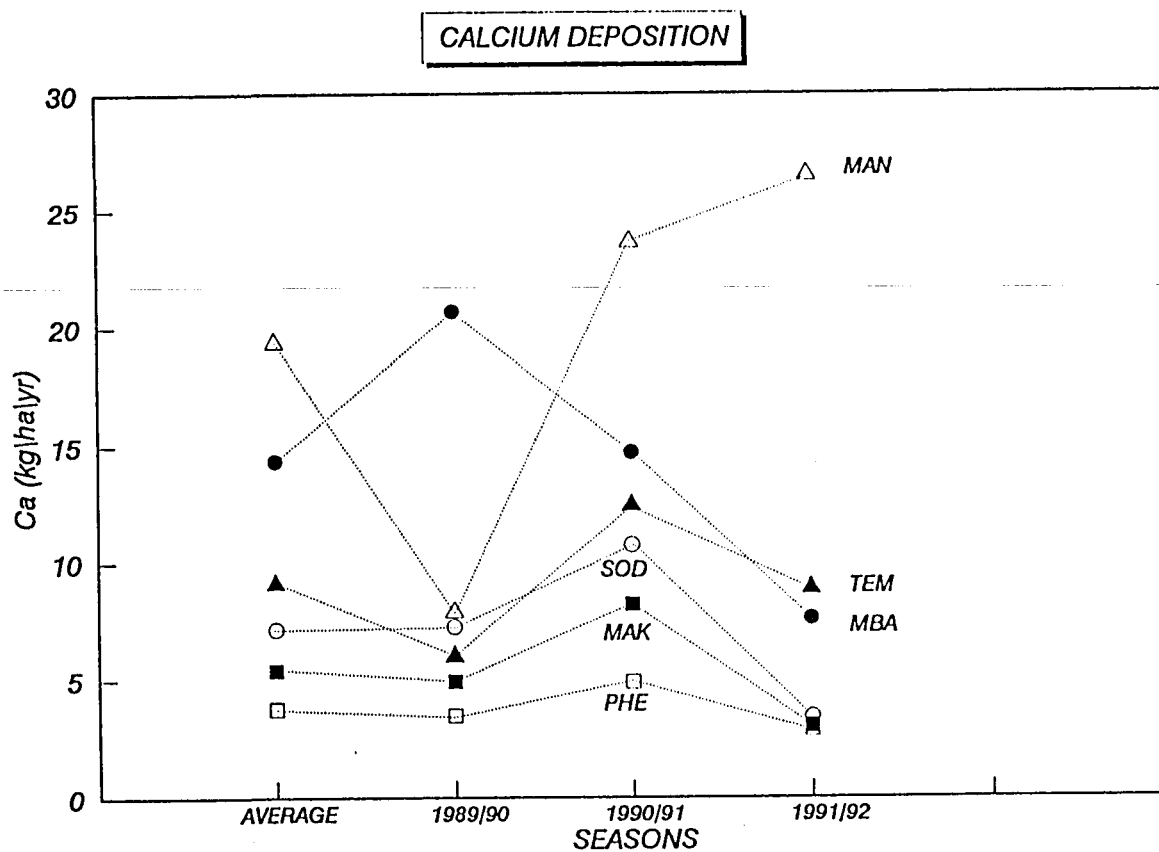


Figure 33: Annual calcium deposition rates for the three sampling years.

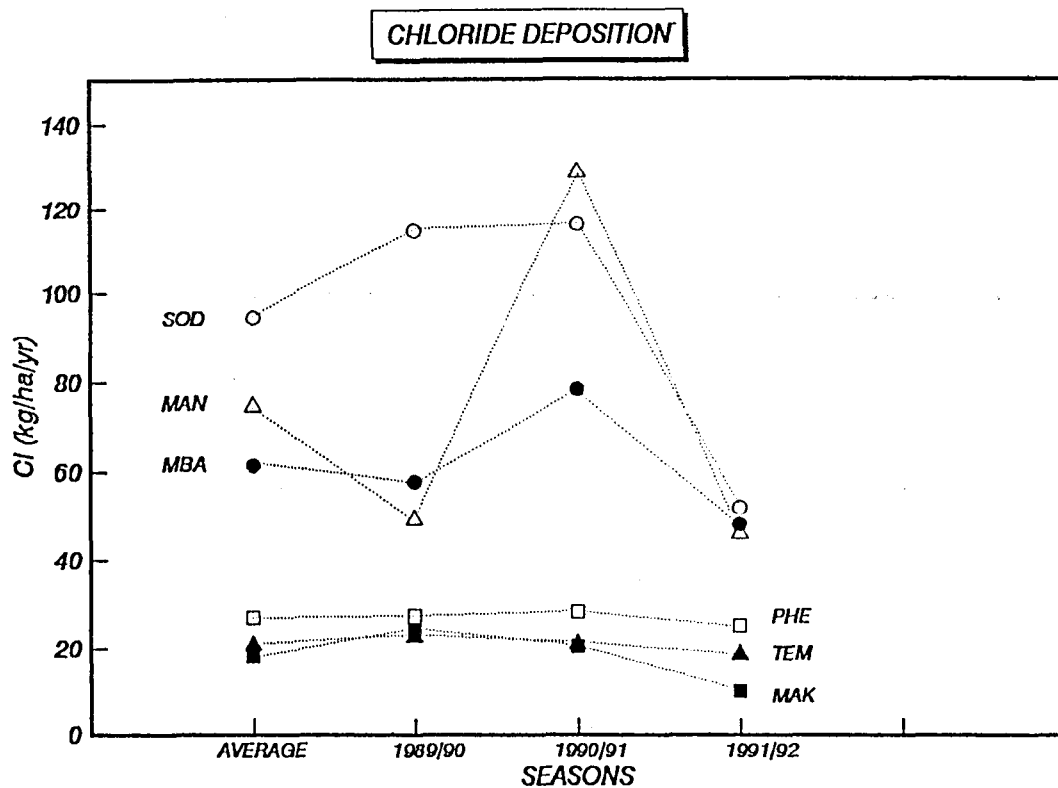


Figure 34: Annual chloride deposition rates for the three sampling years. The coastal stations (SOD, MBA, MAN) show more annual variations than do the inland stations.

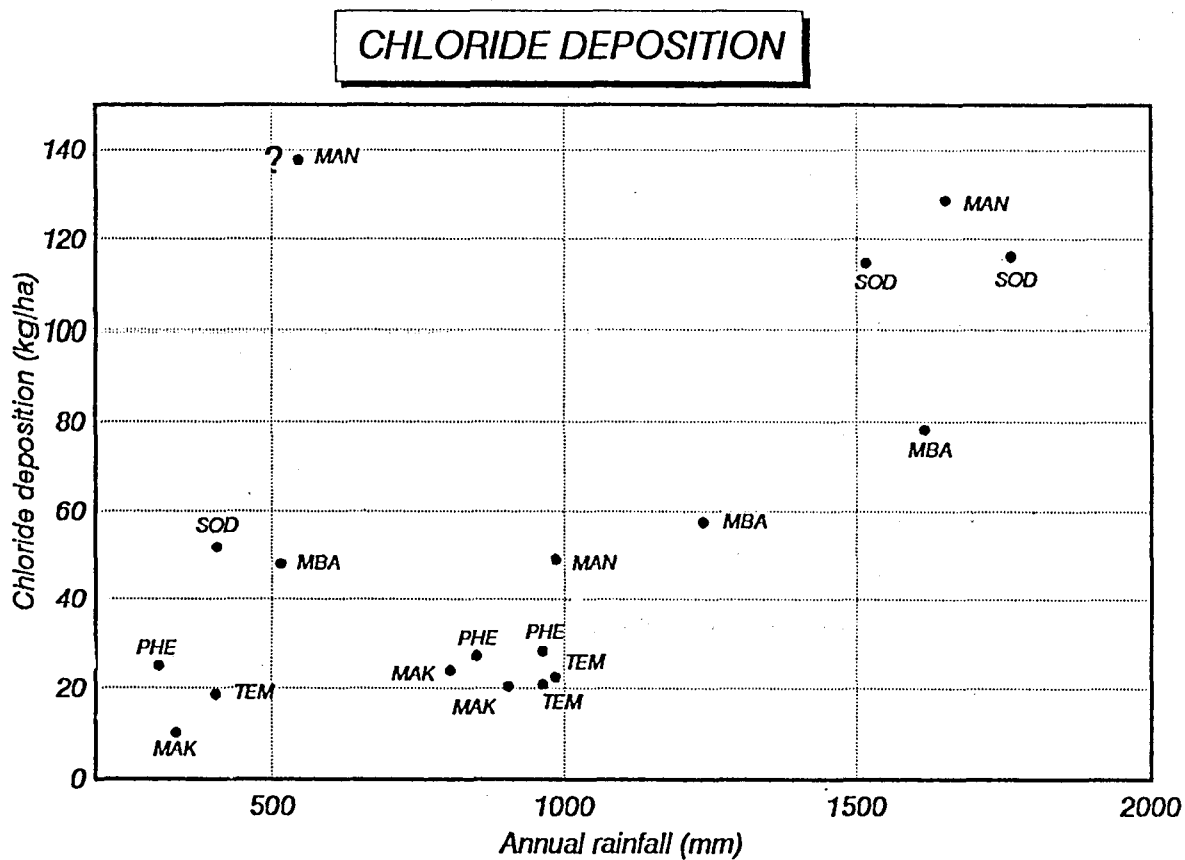


Figure 35: Relation between annual chloride deposition (for each of the three years) and the rainfall of that year.

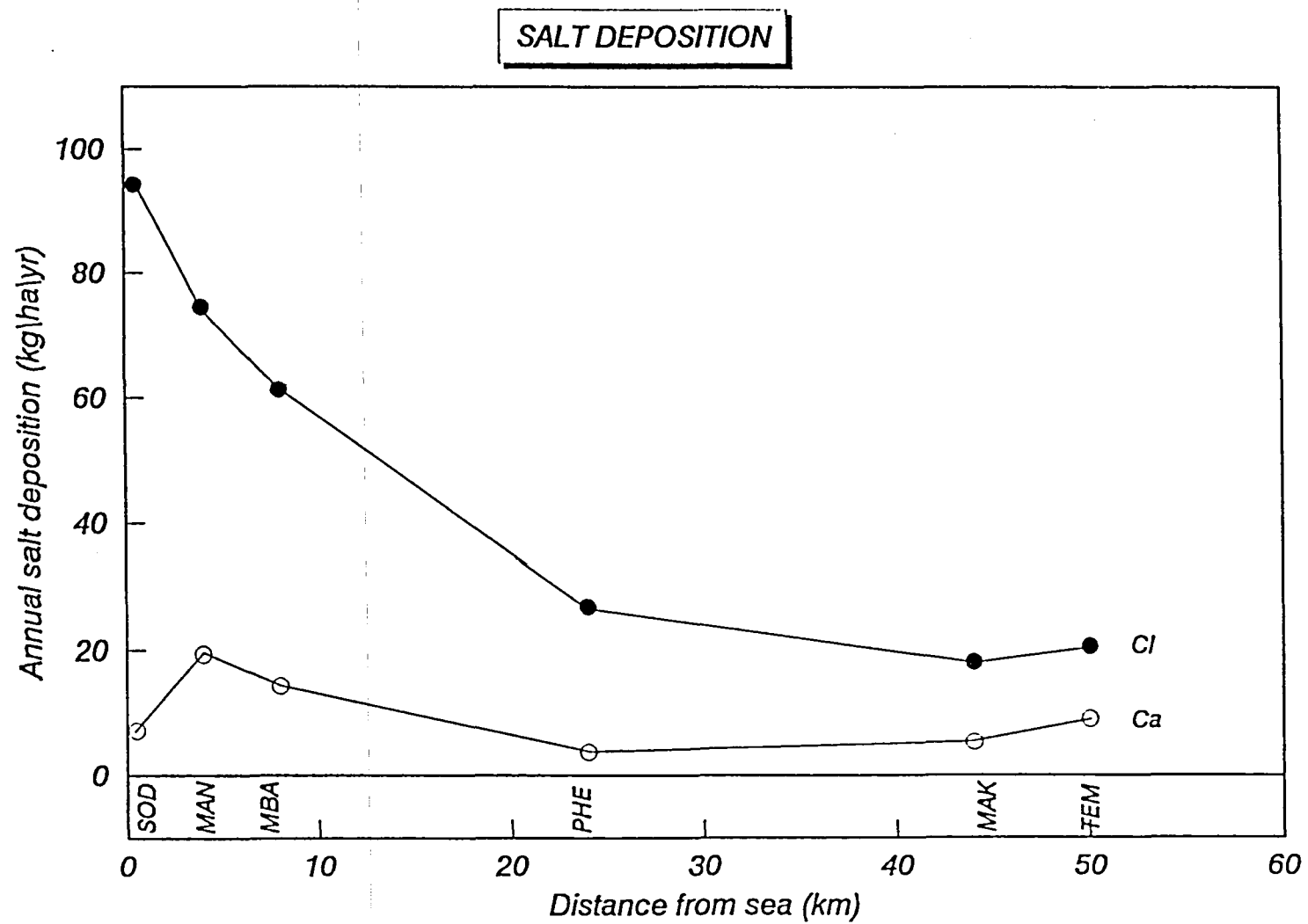


Figure 36: Average (three years) chloride and calcium deposition with distance inland.

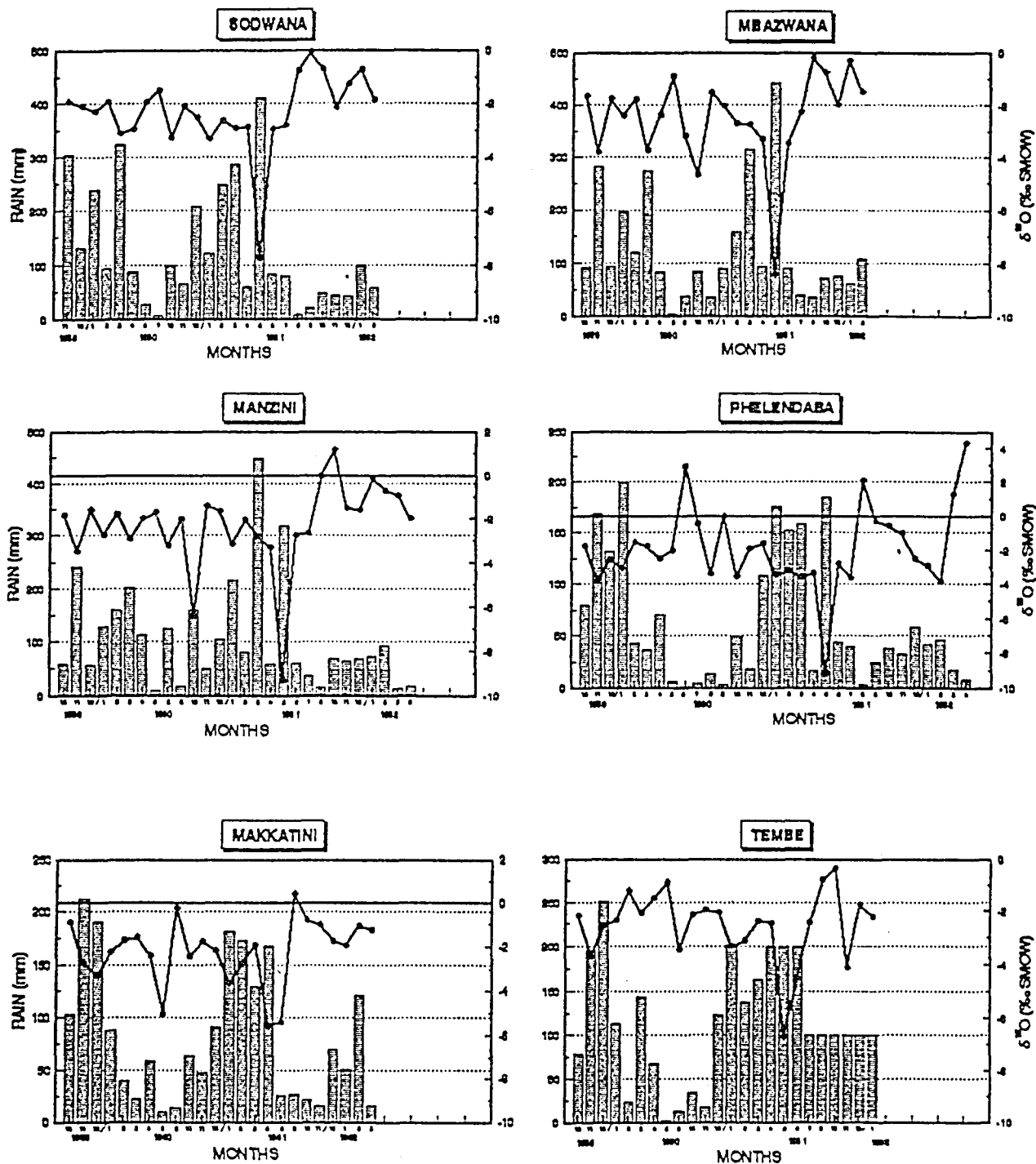


Figure 37: Seasonal pattern of rainfall and its  $^{18}\text{O}$  content for the six rainfall stations (October 1989 to January 1992).

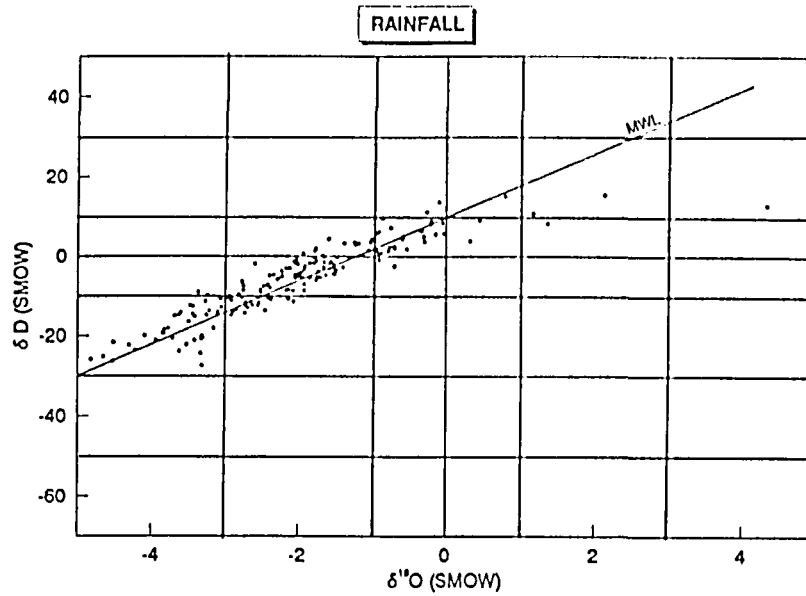


Figure 38:  $^{18}\text{O}$  deuterium relation for rainfall. Most are located on the MWL ( $\delta\text{D} = 8\delta^{18}\text{O} + 10$ ) which holds worldwide (Gat and Giofanti, 1981).

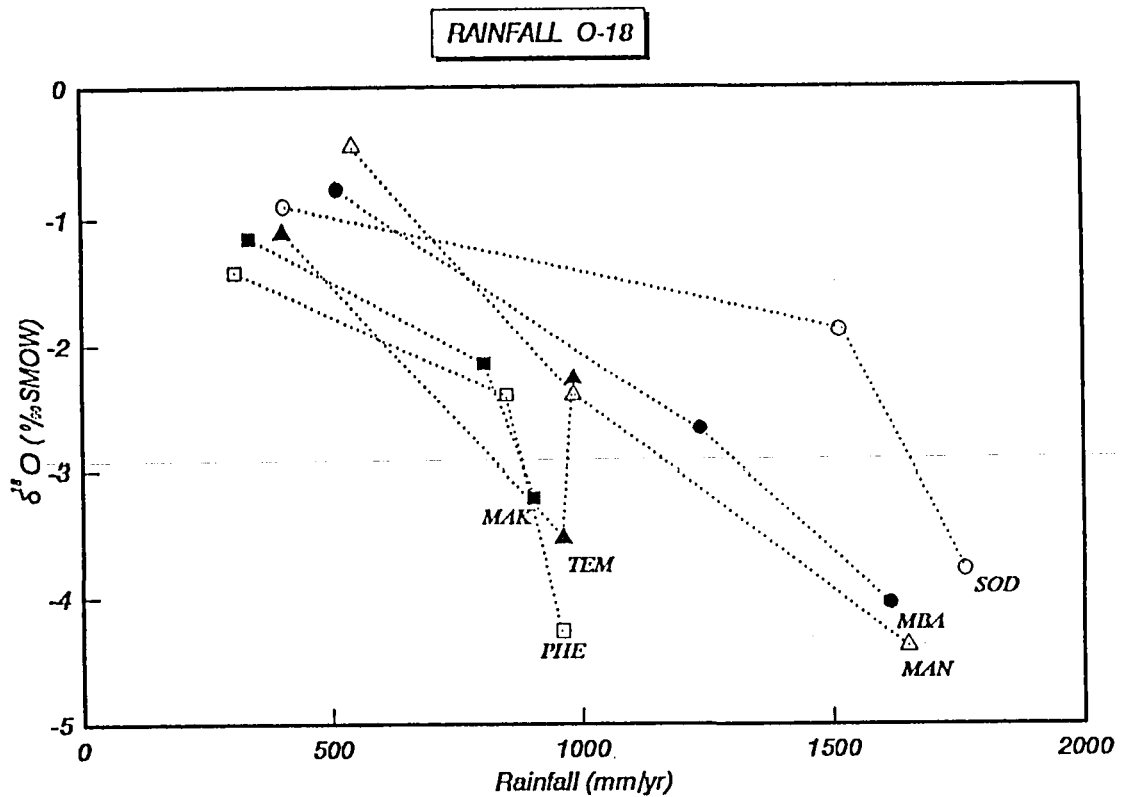
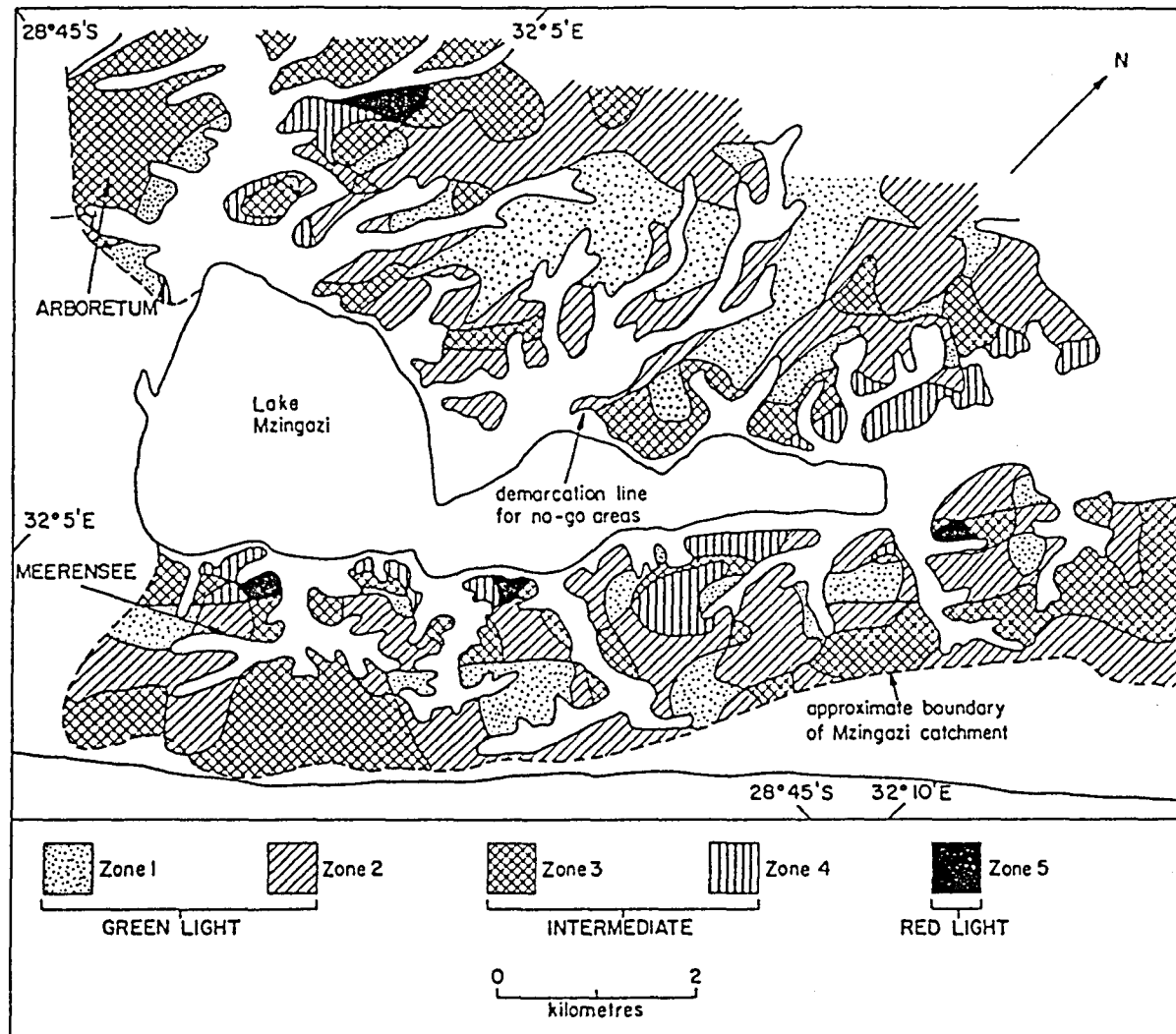
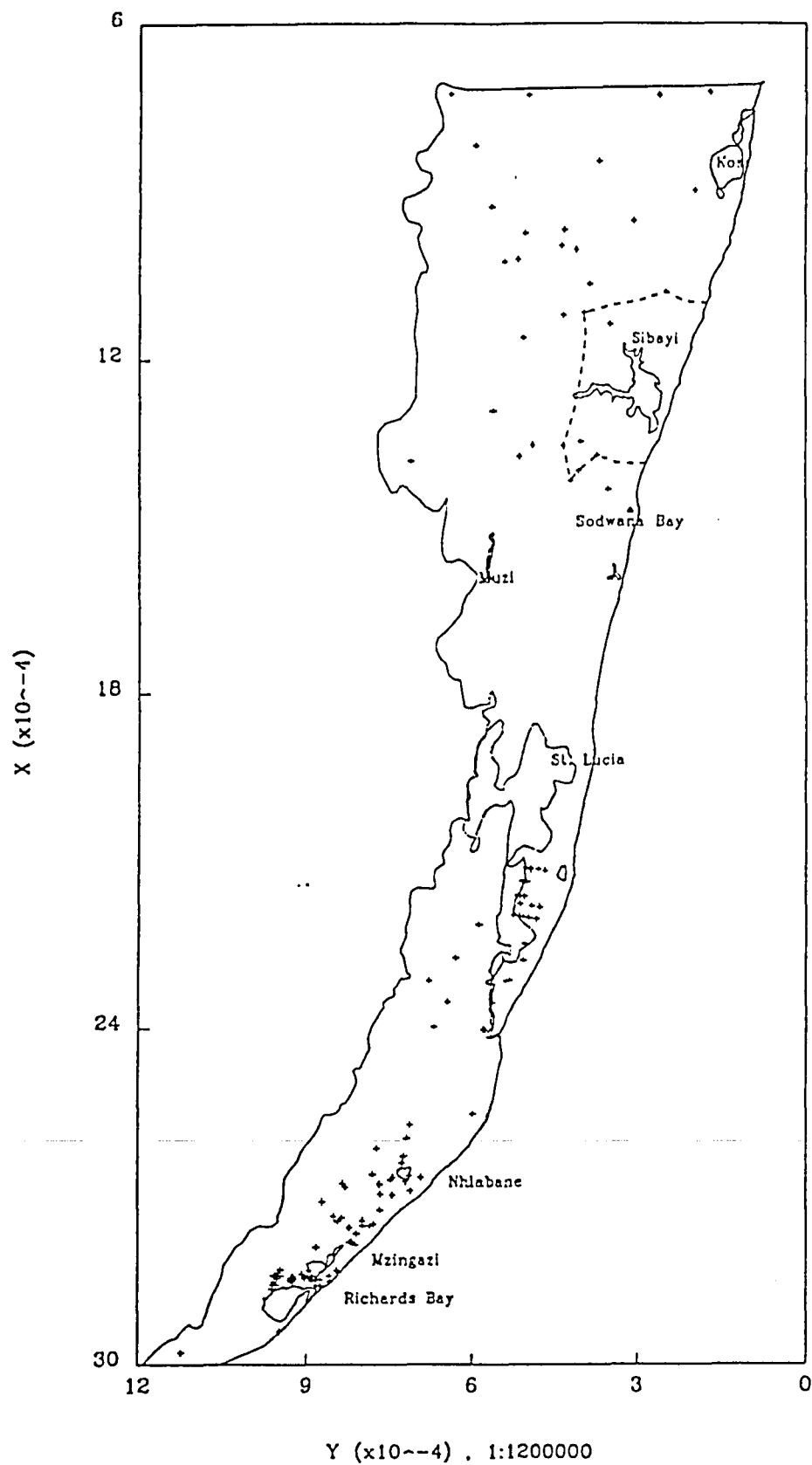


Figure 39: Relation between weighted annual  $^{18}\text{O}$  content in rain and the total rainfall for that year. Note the large difference (especially for the coastal stations SOD, MAN, MBA) and the driest year (1991/92).



**Figure 40:** Pollution vulnerability map for the fresh waters of the inner catchment of Lake Mzingazi (Worthington, 1978).





**Figure 41:** The borders of the Zululand aquifer, as well as the positions of the lakes and boreholes used in this study, are shown. The hypothetical afforestation around Lake Sibayi is also shown.

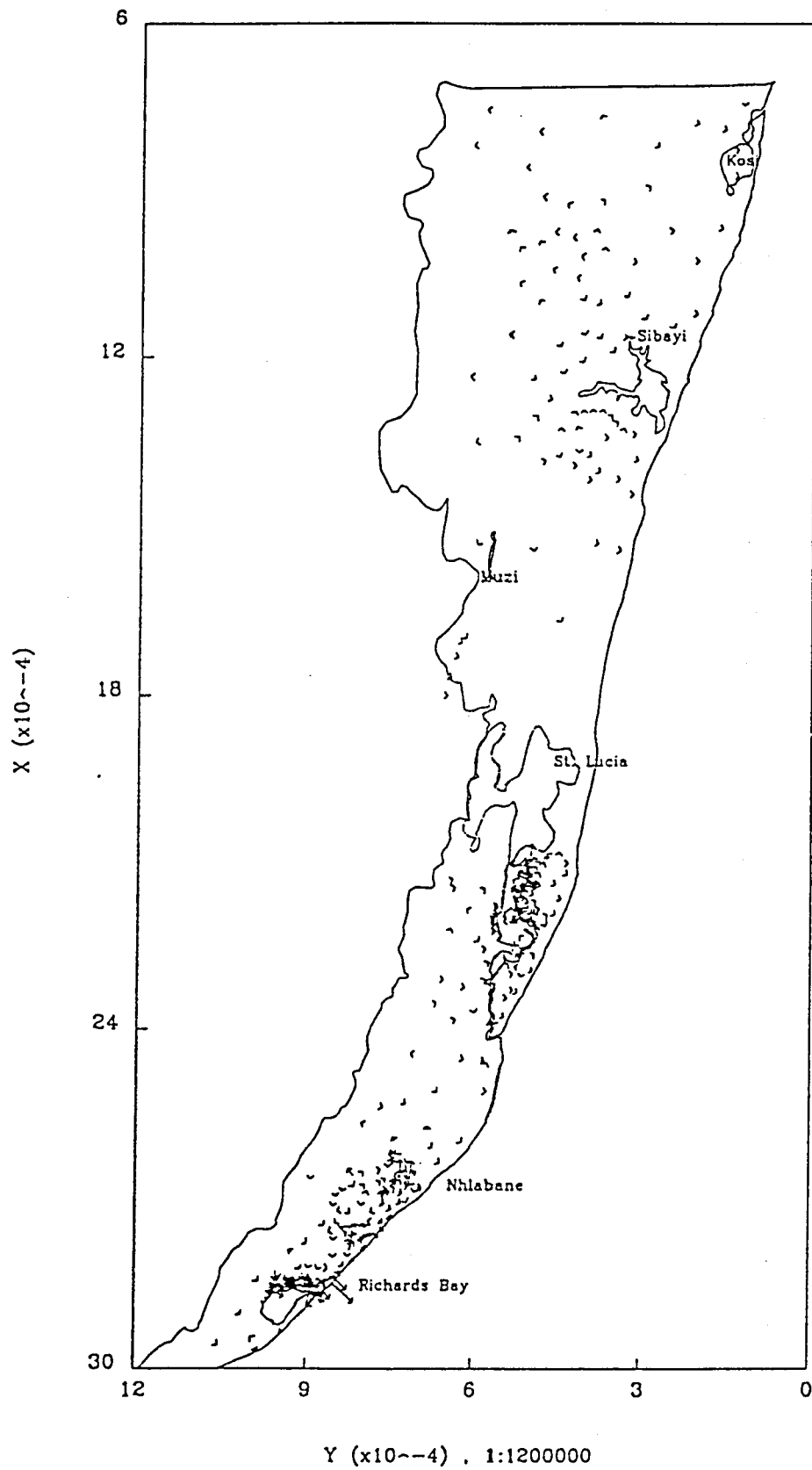


**Figure 42:** The ground water velocities in the Zululand aquifer, as computed from the 140 boreholes.

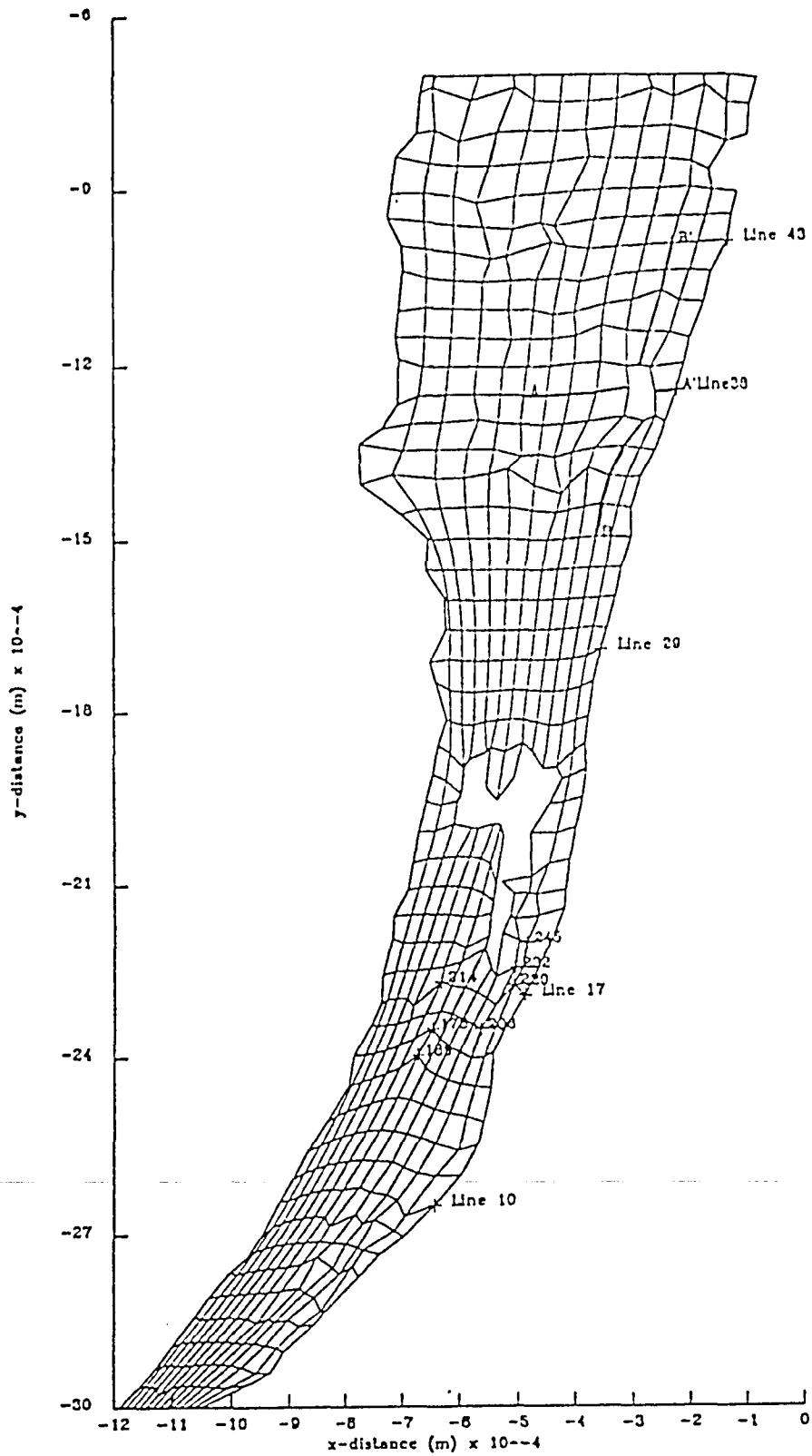


**Figure 43:** The finite element grid drawn over the Zululand aquifer. The grid excludes the three lakes, Lake St Lucia, Lake Sibayi and Lake Kosi.

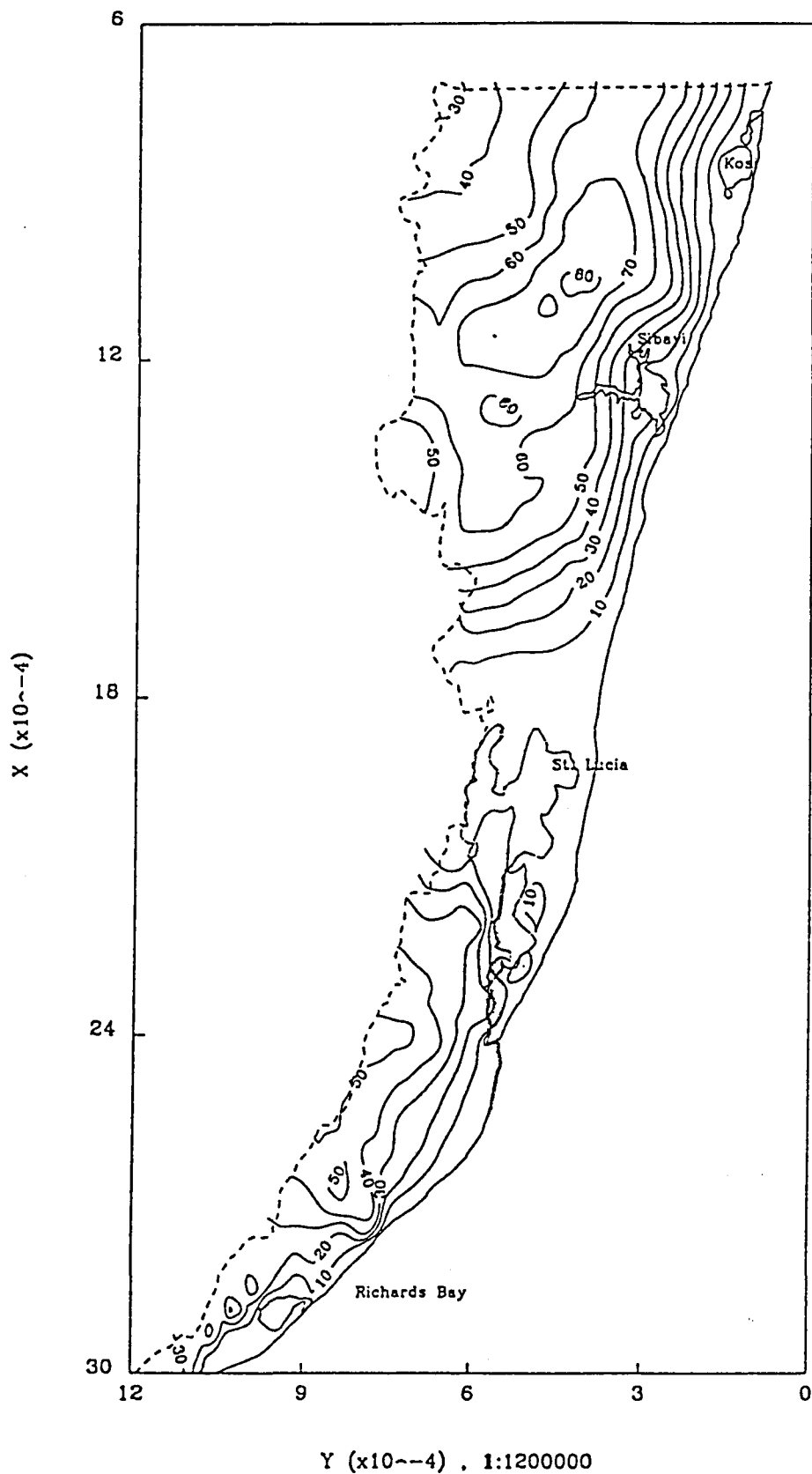


**Figure 44:** The piezometric heads from the 140 boreholes were interpreted to all the nodes of the finite element grid, resulting in head contours as shown.

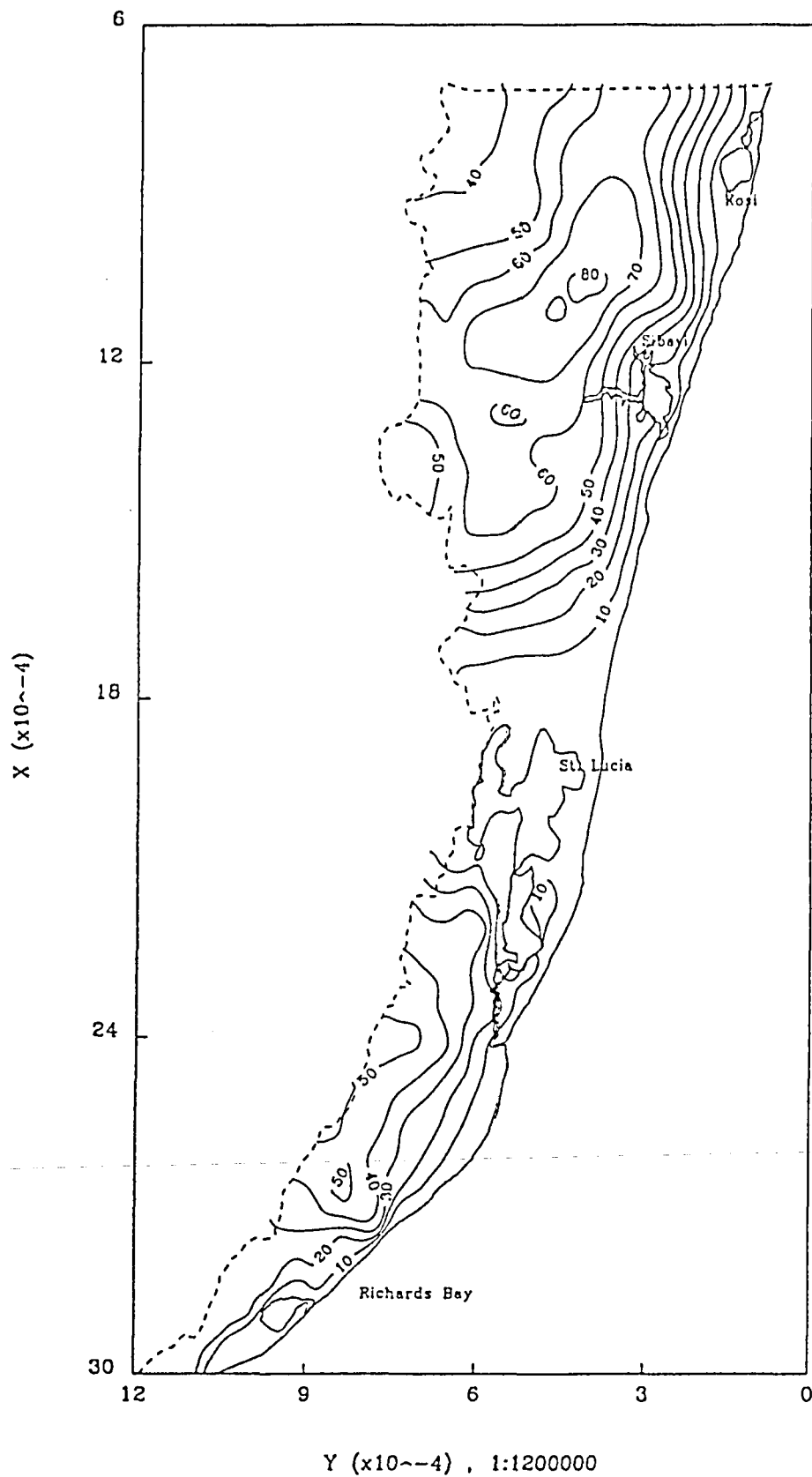


**Figure 45:** Contours from the simulated piezometric heads for the Zululand aquifer after a simulation period of one year.

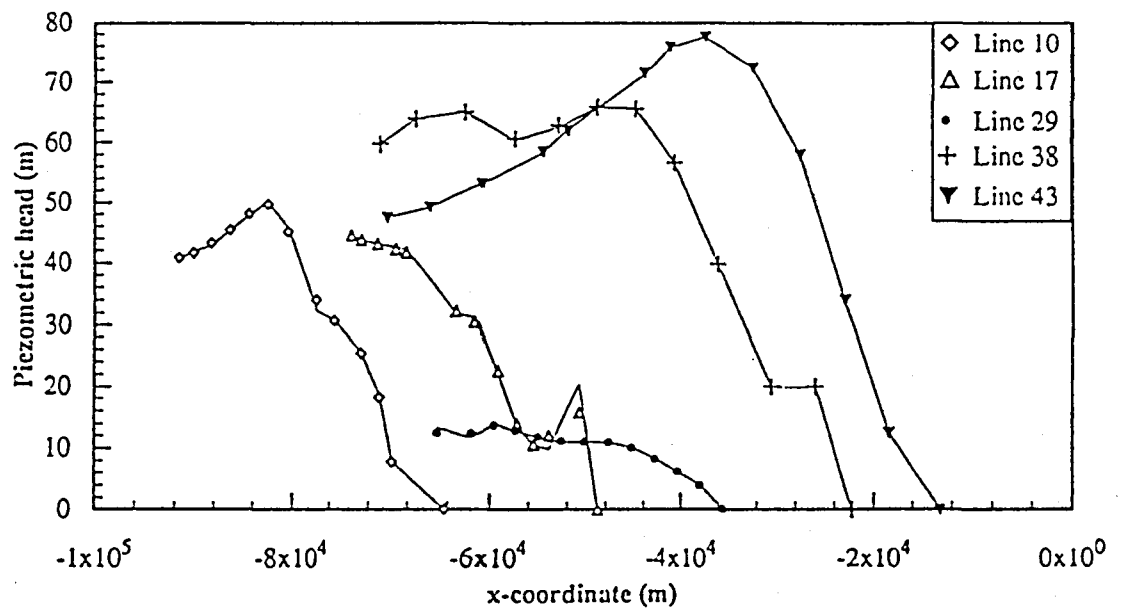


**Figure 46:** A comparison of the initial (solid lines) and simulated (dots) piezometric heads of the numerical model, taken at a few sections parallel to the x-axis. The line numbers are according to the finite element model of Figure 47, counted from the bottom of the grid.

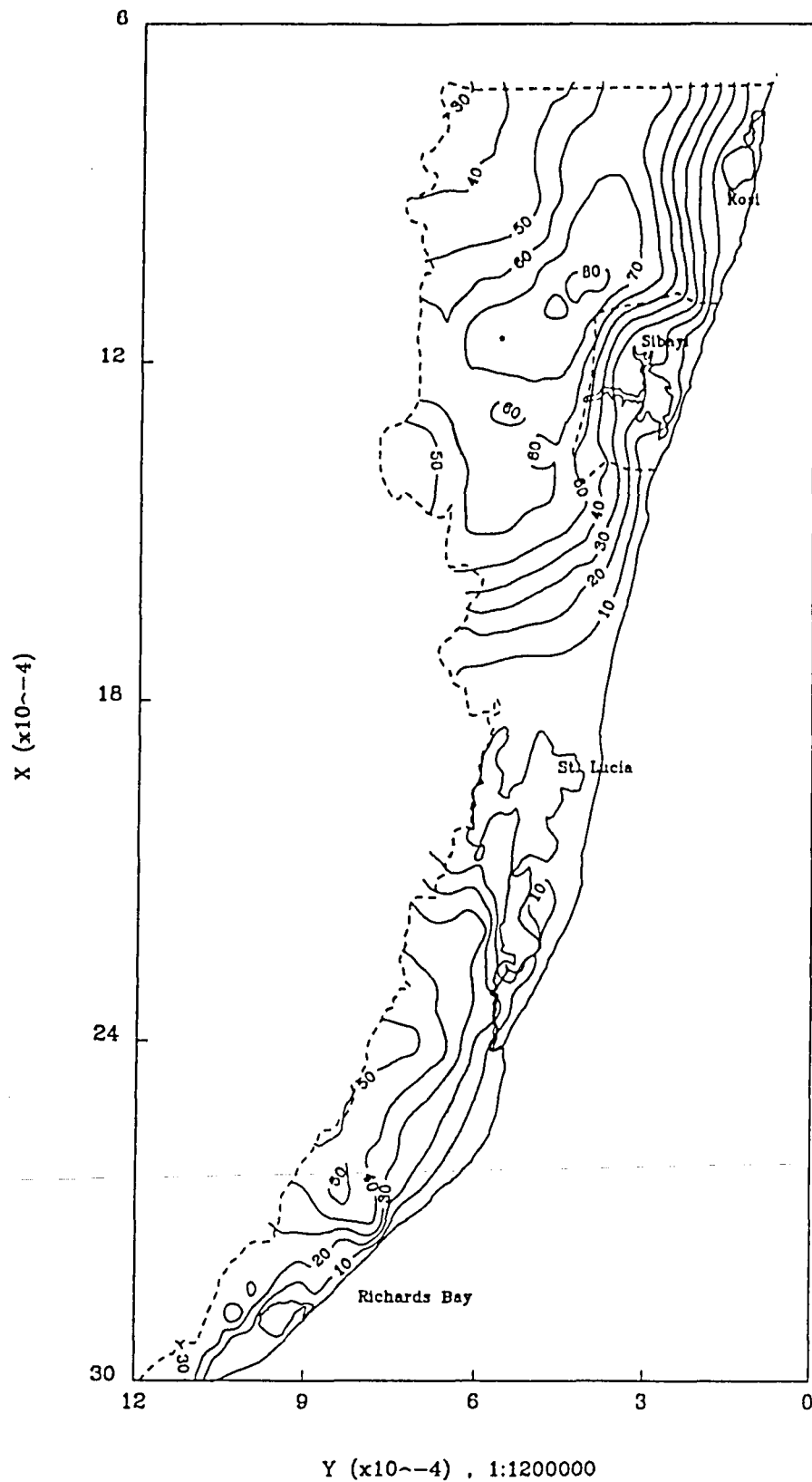


**Figure 47:** Contours of the water levels, simulated for one year, with hypothetical; recharge and evaporation figures of 150 mm/year and 200 mm/year respectively. Contours passing through the lakes are due to the coarse finite element grid used.

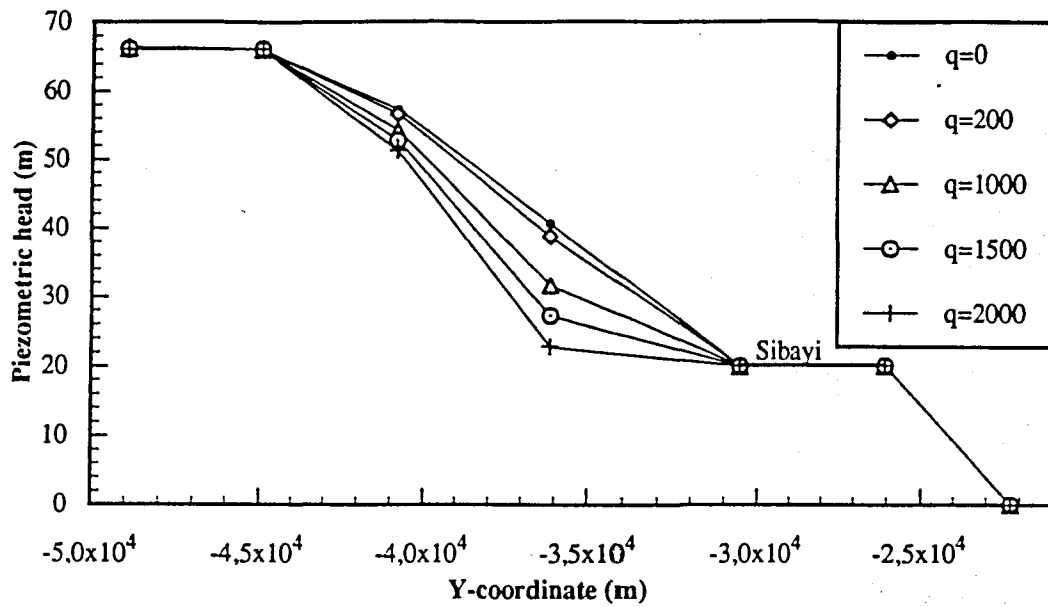


**Figure 48:** Section AA' through Lake Sibayi, perpendicular to the coast, showing the effect of a variation in evapotranspiration values. The evapotranspiration specified for the cases was 0, 200, 1 000, 2 000 and 4 000 mm per annum, per unit area.

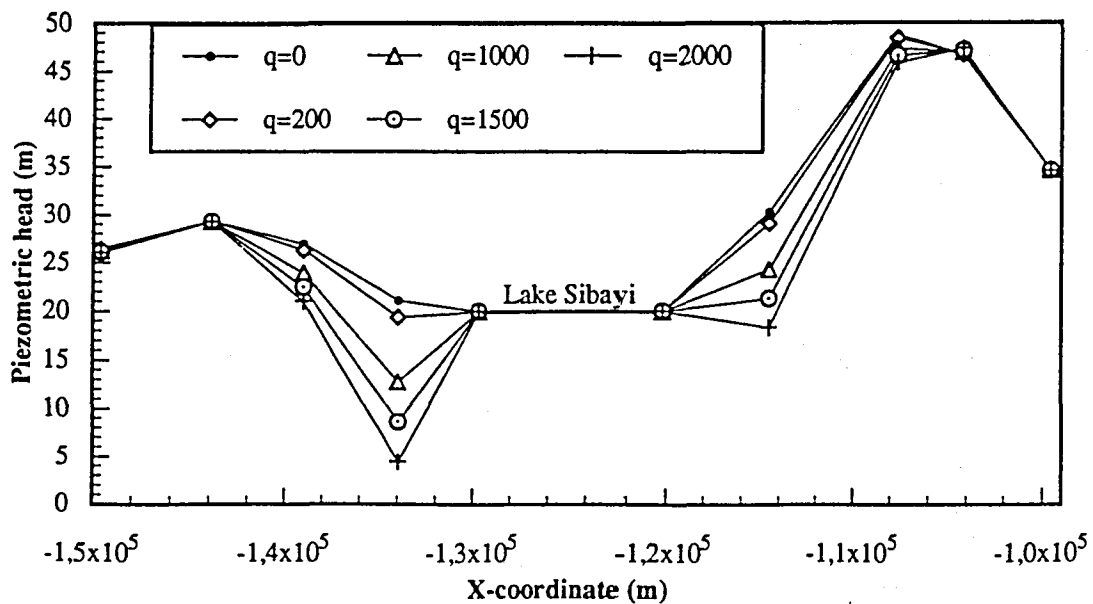


**Figure 49:** Section BB' through Lake Sibayi, parallel to the coast, showing the effect of a variation in evapotranspiration values. The evapotranspiration specified for the cases was 0, 200, 1 000, 2 000 and 4 000 mm per annum, per unit area.



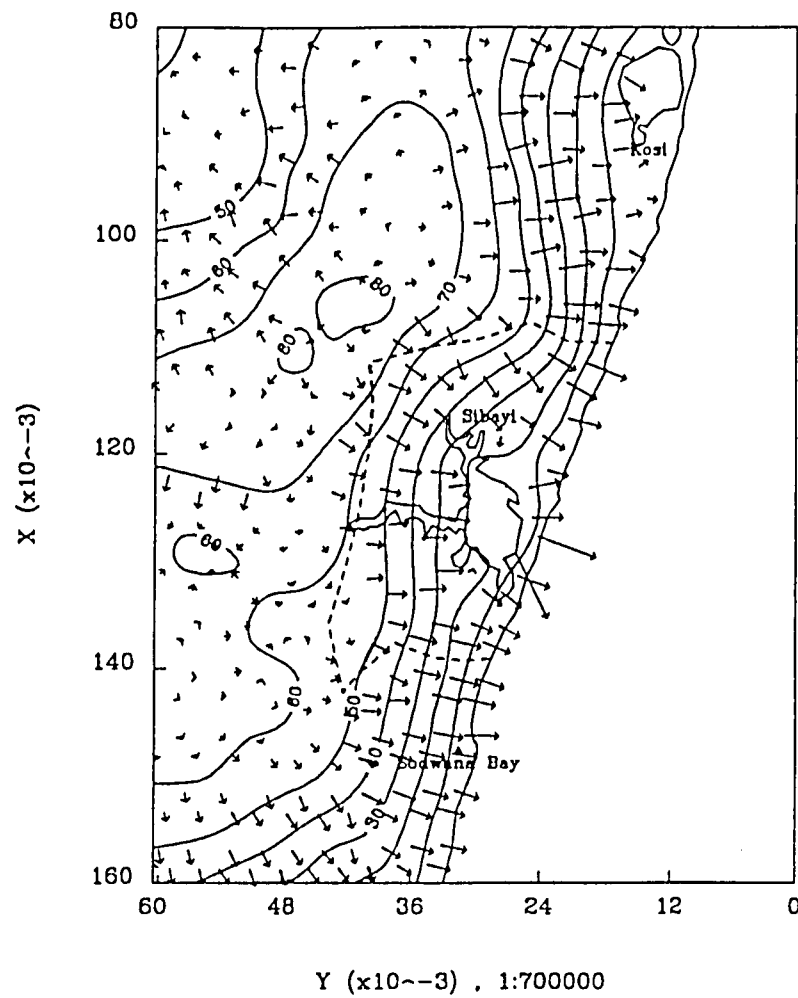


**Figure 50:** The direction of flow of ground water around Lake Sibayi and through the simulation area under normal conditions of 150 mm recharge per year.

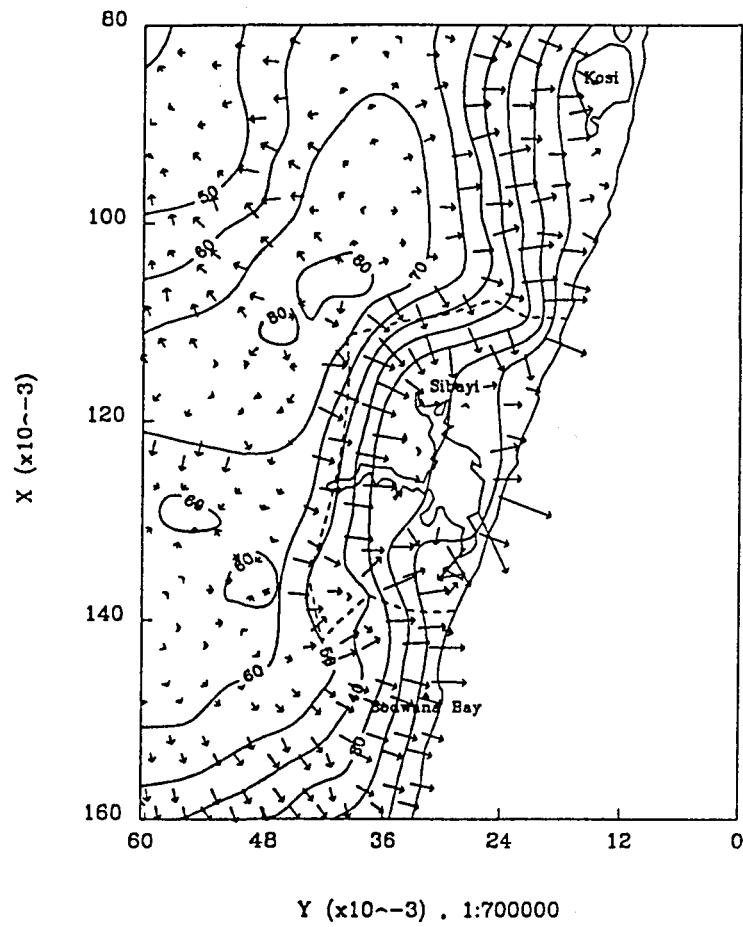


**Figure 51:** The direction of flow of ground water around Lake Sibayi and through the simulation area under extreme conditions of an effective discharge of 2 500 mm per year.

# Aquifer Potential

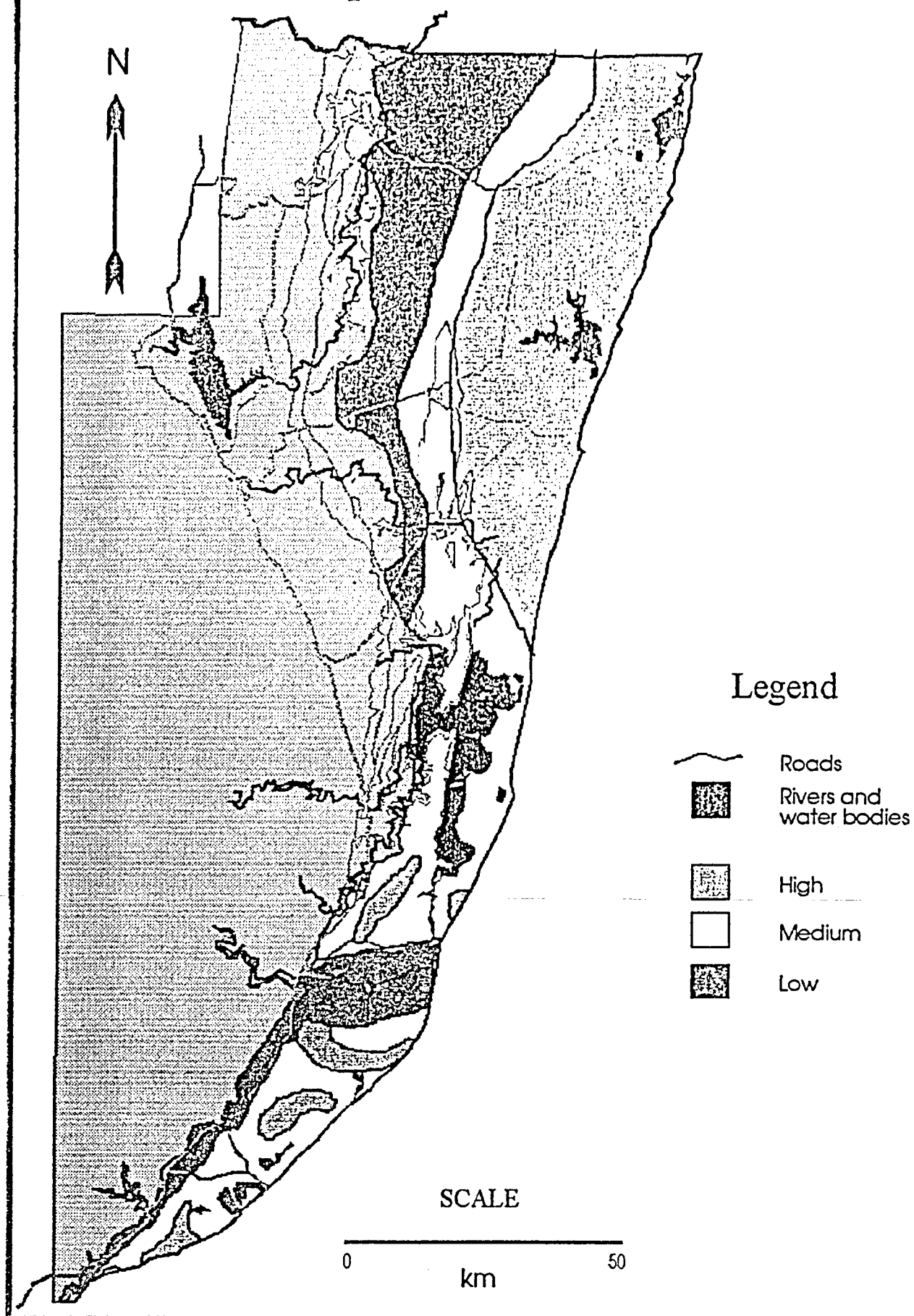


**Figure 52:** Map indicating the aquifer potential in different parts of the Zululand Coastal Plain.

## **APPENDIX A**

### **GEOCHEMICAL CLASSIFICATION OF ZULULAND GROUND WATER**

**Table A1: Lithological units from which water samples were collected.**

Geological formation or position in stratigraphic column	Lithological description	No of samples
Upper Port Durnford	Sandstone	7
Lower Port Durnford	Argillaceous sandstone	2
Lignite band	Lignite	3
Upper Miocene Unit	Sandstone	3
Uloa Formation	Calcarenite	12
St Lucia	Mudstone	4

This method makes provision for the use of a small data set (i.e. relatively high uncertainties) in order to classify any unknown unpolluted ground water sample to either have originated from a specific lithological unit or to be a mixture of waters from different lithological units. The method entails making use of the 'fingerprint' table to determine strata of high probable origin following which a consideration of specific chemical ratios would yield the most probable of the high probability cases.

A description of the data reduction and development of the 'fingerprint' table is given below. The application is then explained using some analyses selected from the available Zululand water chemistry data base. The origin of the water sample so determined is then compared with that of the geological borehole description and the depth from which the sample was taken.

### **A.3 SORTING AND DATA REDUCTION**

All available analyses of water samples collected from specific geological units were sorted according to geological origin. The chemical analyses in both mg/l and meq/l, depth from which sample was taken as well as the ratios of concentration of all elements to each other (in meq/l) for each stratigraphic unit and means of these parameters have been compiled. The mean values of the chemical parameters and a summary of the Element/TDS ratios values for each geological unit are listed in **Table A.2**. The mass % ratio of all elements with respect to the total dissolved solids were also calculated.

### **A.4 GRAPHICAL AND STATISTICAL MANIPULATION**

Schoeller diagrams were drawn for each of the boreholes with depth data. Note that these Schoeller diagrams are essentially similar to the 'fingerprinting' technique to be discussed, yet are a much simplified version of this technique. These diagrams also have elemental concentrations in meq/l and the slope of any line between two adjacent elements represents the ratio between them. Its application is limited, however, since

only a limited number of elements are represented, since direct relations are shown only between adjacent elements, and since only a limited number of analyses can be portrayed without cluttering. Yet these diagrams still show the typical chemical fingerprint of a specific layer, even though nothing is shown about the variation of any parameter about its mean.

Complete statistics including mean, variance, standard deviation and percentiles were further performed for the following:

- a) All physical and chemical parameters for each layer separately.
- b) All ratios of elements to other elements for each layer separately.
- c) All ratios of elements to TDS for each stratum separately.

Tables II and III present the means and standard deviations for each of these parameters for comparison purposes.

## **A.5 EXAMPLE TO ILLUSTRATE THE APPLICATION OF THE METHOD**

### **A.5.1 Setting up the 'Fingerprint' table**

To set up the 'fingerprint' table, the statistical distribution of parameters as defined by the mean and standard deviation, are used. This is illustrated by the following example:

From **Table A.2** the values of Ca/TDS means and standard deviations were used to produce the distribution graph in **Figure A1**. From the graph 'good' resolution can be seen between samples A, B, D, and samples E, C with F covering the whole range. Consider the ranges where  $\text{Ca/TDS} \geq 10\%$ ,  $\geq 20\%$ ,  $\leq 10\%$ . An analysis of unknown origin with

- 1)  $\text{Ca/TDS} \geq 10\%$  can belong to C, E, F or A, maybe even B, but definitely not D.
- 2)  $\text{Ca/TDS} \geq 20\%$  can belong to C and F maybe even E, but not A, B, or D.
- 3)  $\text{Ca/TDS} \leq 10\%$  can belong to either A, B, D, F but not E or C.

(1) and (2) are examples of maximum fingerprinting with (3) being a minimum fingerprint. This means that an unknown analysis with  $\text{Ca/TDS} \geq 20\%$  has a much higher probability to belong to groups C and F than to A, B, D.

This example forms the basis of the method presented here. If sufficient information is available it should be possible to distinguish and designate any unknown analysis to a specific origin.

Two questions that may come to mind at this stage are:

- Are the mean and standard deviation good indicators for such a small sample?
- What is the resolution of the method (i.e. how well can be distinguished between water resident in different geological units)?

The answer to these questions is to consider as many ratios as possible and to carefully consider the data at hand before making any deductions.

#### A.5.2 Use of the 'fingerprint' table

To illustrate how the origin of an unknown water sample is determined from the 'fingerprint' table, first determine all the possible ratios (in meq/l) and then test these by means of the fingerprint table (**Table A3**). As an example, a water sample from the Richards Bay area is taken (sample number 2832CA00033, from Zululand Hydrocom data base).

From the Fingerprint Test Table (**Table A5**)

- $\text{Ca/TDS} = 6,82 \%$
- $\text{Mg/TDS} = 3,71 \%$
- $\text{Na/TDS} = 19,62 \%$

Using the fingerprint table (**Table A3**) the sample is grouped in the following classes:

- $\text{Ca/TDS}$  not larger than 10%
- $\text{Mg/TDS}$  larger than 3,5% but not 5%
- $\text{Na/TDS} \geq 15\%$  but not larger than 20%

From these three ratios the following deductions are made:

- $\text{Mg/TDS} \geq 3,5\%$  implies that the sample may belong to A, B, D, or E.
- $\text{Na/TDS} \geq 15\%$  implies that the sample was most likely derived from A, B, D, E, or F.
- The method is not directly reversible and the  $\text{Ca/TDS}$  ratio is of no use here.

This process of testing is now applied to all the parameters as set out in the fingerprint table. The total score for each lithological unit is the number of times that the given data set satisfied the testing parameters.

*(Note: Elements not denoted as a ratio to another element on the table should be read as element/TDS in %)*

For this sample the scores were:

A = 26	D = 14
B = 20	E = 14
C = 11	F = 13

It is clear that the probability of the sample being A (Upper Port Durnford Formation) is quite good, yet for the case when more than one stratum has very high probability (i.e. when its score  $\geq$  average score), a more detailed look at the probability strata needs to be taken.

This phenomenon can be caused by two factors - mixture of waters (should especially be suspected if two adjacent strata are concerned) or the two statistical distribution chemistries are too close to be properly resolved. The two most probable strata can now be tested by looking at specific ratios where these two layers have minimum distribution overlap.

In the case of the example, the Na/TDS ratio distribution is shown in **Figure A2**. It should be clear that the sample originated from A, yet the more the ratios that can be used to distinguish between the layers the better. If no clear distinction can be made between two layers of high probability one would need to look at other information such as borehole depth screen position and geological borehole descriptions in order to determine whether the sample is a mixture of waters from two strata or just a lack of resolution feature. Thus by using the method described, the example could be assigned to a specific layer; in this case the Upper Port Durnford Formation.

## **A.6 MORE EXAMPLES OF IDENTIFYING ORIGIN WITH 'FINGERPRINT' TECHNIQUES**

Additional samples obtained during the pump testing of boreholes recently drilled around Lake Mzingazi by the Department of Water Affairs (Table V), were also subjected to this fingerprint analysis technique. The results are discussed below.

As noted in the text the method followed may, and possibly will, yield more than one probable origin. The examples given below are all of known origin and the testing was done to ensure the efficiency of the method and also to give an idea of the resolution of the method. The samples were treated as unknowns and only after testing were the results compared to the actual origin.

### **A.6.1 Example 1: Water sample 2832CB0004 from Zululand Hydrocom data base**

Only B, E, and F were considered.

B was discounted due to low Ca/TDS and low  $\text{HCO}_3/\text{TDS}$ .

E rejected due to low Cl/TDS and K/TDS.

Conclude source to be F, which is correct.



A.6.2 Example 2: Water sample 2832CA00038 from Zululand Hydrocom data base

Consider only C and E.

E discounted due to generally lower Si/TDS and higher Na/TDS.

Conclude source to be C, which is correct.

A.6.3 Example 3: Water sample 2832CA00033 from Zululand Hydrocom data base

Consider A and B. No good separation could be made between these two layers; the sample is in fact from A yet it must be kept in mind that layer B (Lignite layer) is not a true aquifer and that water denoted as B probably consists of 'A' water with leaching products from B.

Therefore these two layers will be considered as being the same for the rest of the examples.

A.6.4 Example 4: Water sample 2832CA00032 from Zululand Hydrocom data base

Consider A, B, and D.

A and B were rejected due to their low Ca/TDS and high Si/TDS.

C and E difficult to separate yet Na/TDS and  $\text{SO}_4/\text{TDS}$  point towards E.

Conclude the source to be E, which is correct.

A.6.5 Example 5: Water sample 2832CA00030 from Zululand Hydrocom data base

Consider A, B, and F.

F discounted due to its Na/TDS, K/TDS, and  $\text{HCO}_3$  being too high.

A and B indistinguishable.

The sample is actually from B.

A.6.6 Example 6: Water sample 2832CA00015 from Zululand Hydrocom data base

Consider A, B, and D.

Both high Si/TDS and very high  $\text{NO}_3/\text{TDS}$  point towards D.

Conclude source to be D, which is correct.

A.6.7 Example 7: Water sample 39422

Consider A, B, and E.

Low Si/TDS and high Ca/TDS of sample discounts A and B whilst high Cl/TDS discounts C.

Conclude source to be E, which is correct.

A.6.8 Example 8: Water sample 39421

Consider A, B, and E.

A and B rejected as above, and C on account of high Si/TDS.

Concluded source to be E. In this case the sample was a mixture of waters from 9 m Uloa (E) and 2 m St Lucia (F). The major component was identified as the source yet the F fingerprint could not be seen. This may be due to either poor resolution or lack of contribution from F. (*Note that thicknesses quoted only signify the length of the screen in each stratum.*)

A.6.9 Example 9: Water sample 39254

Consider A, B, and E.

No distinction could be made using Ca/TDS and Si/TDS yet both HCO<sub>3</sub>/TDS and Cl/TDS point towards A.

Conclude A to be source. In this case the sample from 6 m Port Durnford (A) and 2 m St Lucia (F). Again only the major component could be identified.

A.6.10 Example 10 Water sample 39250

Consider A, B, and F.

Ca/TDS point to A, B, E, and F.

Si/TDS points to E and F.

Mg/TDS points to F.

Na/TDS points to A, B, E, and F.

K/TDS points to A, B, and E.

HCO<sub>3</sub>/TDS points to A.

Cl/TDS points to A and F.

No proper distinction could be made and the sample was concluded to be a mixture of A, E, and F. The sample was reported to have come from a borehole in which 10 m of Port Durnford (A), 9 m of Uloa (E), and 7 m of St Lucia (F) was intersected. This indicates that a mixture with no dominant species cannot readily be identified as representing a particular geological horizon.

## A.8 CONCLUSIONS

A qualitative method for the determination of the probable origin of water of any specific chemistry based on quantitative statistical studies on a small data set was developed with special reference to the Zululand aquifer. For the Zululand data presented it was found that the fingerprint table set up gave good first approximations which could then be narrowed down by considering specific parameters.

From the examples it follows that when in high probabilities, clear distinctions could be made between the more arenaceous units of the Upper Port Durnford, the lignite layer, and the Miocene sand and the argillaceous Lower Port Durnford, Uloa Calcarenite and St Lucia Mudstone, by only considering Ca/TDS, Si/TDS, and  $\text{HCO}_3/\text{TDS}$  ratio.

Difficulty was encountered in separating Lower Port Durnford from Uloa Calcarenite due to the small difference in chemistry between their waters, yet Na/TDS, Si/TDS,  $\text{SO}_4/\text{TDS}$ , and  $\text{NO}_3/\text{TDS}$  may show a separation for these strata.

The Upper Port Durnford was indistinguishable from the lignite layer yet this could have been expected since the lignite layer is not an aquifer in the true sense of the word and the sample denoted as such is probably Upper Port Durnford water deriving chemical constituents from the lignite band.

Most of the samples tested indicated a single layer of the aquifer as the main source of the water except in the case of sample 39250 where the origin was indistinguishable due to approximately equal contributions to the sample from three aquifer horizons. It can be seen that all the contributing strata show high probability, yet separate ratios pointed to all the possible strata and no clear deduction, else than it being a mixture, could be drawn.

The method discussed was thus used with relative success in predicting the aquifer layer where any ground water sample could have originated. In Figures A3, A4, and A5 the hydrochemical character of water samples from the different geological units within the Zululand aquifer are given.

TABLE A.1

Zululand Groundwater Chemistry  
Means of Physical and Chemical Parameters

Stratigraphic position	pH	EC mS/m	TDS mg/l	Ca mg/l	Mg mg/l	Na mg/l	K mg/l	Si mg/l	HCO3 mg/l	SO4 mg/l	Cl mg/l	NO3 mg/l
Pleistocene Upper Pt Durnford	6.70	20.67	136.00	13.26	4.10	26.44	2.93	16.56	41.99	13.21	46.54	4.55
Lignite	6.53	31.10	238.67	16.37	13.33	32.60	11.47	11.73	116.30	22.17	51.60	3.86
Pleistocene Lower Pt Durnford	7.55	39.00	271.00	54.85	7.15	22.75	6.70	25.25	187.75	8.25	44.00	0.44
Miocene sand (Uloa)	6.27	19.83	136.67	6.73	4.80	29.60	5.80	29.00	55.53	17.60	42.60	19.59
Miocene Calcarenite (Uloa)	7.30	45.88	317.25	50.61	10.52	45.03	7.82	15.32	217.07	24.68	57.89	3.34
Cretaceous mudstone (St.Lucia)	7.65	39.13	267.00	36.43	3.33	76.13	26.05	12.70	195.35	25.88	77.98	3.07

TABLE A.2

Zululand Chemistry  
Ratio(Element/TDS)

Stratigraphic position		Ca	Mg	Na	K	Si	HCO3	SO4	Cl	NO3
Pleistocene Upper Pt Durnford	Mean	8.13	3.28	20.86	2.30	11.24	27.73	11.07	37.20	4.24
	St.Dev.	7.11	1.05	5.35	1.21	6.09	15.03	7.96	11.38	5.05
Lignite	Mean	7.16	4.17	14.45	5.83	6.24	42.45	9.70	24.21	1.85
	St.Dev.	2.96	4.39	2.42	6.91	4.34	27.08	5.39	8.52	0.69
Pleistocene Lower Pt Durnford	Mean	20.56	2.66	8.35	2.58	9.54	70.43	3.12	16.28	0.17
	St.Dev.	4.43	0.30	0.73	1.41	3.20	16.26	1.09	0.52	0.02
Miocene sand (Uloa)	Mean	4.68	3.42	21.90	4.25	22.41	40.32	13.11	32.32	14.62
	St.Dev.	3.12	0.79	1.97	0.35	9.35	8.86	1.81	8.87	4.74
Miocene Calcarenite (Uloa)	Mean	16.05	3.29	14.34	2.57	4.83	68.83	7.70	18.37	1.08
	St.Dev.	4.09	1.02	4.52	1.86	1.61	12.39	4.49	4.52	0.90
Cretaceous mudstone (St.Lucia)	Mean	15.37	1.38	27.66	11.46	5.24	78.17	9.97	29.46	0.97
	St.Dev.	10.82	0.77	8.27	10.84	3.19	28.18	2.18	3.33	1.36

Zululand Groundwater Chemistry  
Patio Comparison File

Stratigraphy	Ca/Mg meq/meq	Ca/Na meq/meq	Ca/K meq/meq	Ca/Si meq/meq	Ca/AlO <sub>3</sub> meq/meq	Ca/SO <sub>4</sub> meq/meq	Ca/Cl meq/meq	Ca/NO <sub>3</sub> meq/meq	Ca/F meq/meq	Mg/Na meq/meq	Mg/K meq/meq	Mg/Si meq/meq	Mg/AlO <sub>3</sub> meq/meq	Mg/SO <sub>4</sub> meq/meq	Mg/Cl meq/meq	Mg/NO <sub>3</sub> meq/meq	Mg/F meq/meq	Na/K meq/meq	Na/Si meq/meq	Na/AlO <sub>3</sub> meq/meq	Na/NO <sub>3</sub> meq/meq	Na/Cl meq/meq
B = Pleistocene Upper Pt. Durnford (Hem.)	Mean St. Dev.	2.06 1.51	0.55 0.37	0.80 0.69	0.29 0.22	0.90 0.66	3.06 4.18	0.52 0.56	50.22 82.15	126.00 114.55	0.30 0.04	5.14 2.29	0.23 0.16	0.84 0.53	2.17 2.60	0.26 0.06	12.61 13.10	32.00 4.24	17.00 8.61	0.75 0.43	2.87 1.94	0.43 1.37
B = Lignite	Mean St. Dev.	1.06 1.33	0.50 0.23	6.94 5.97	0.70 0.62	0.66 0.34	2.32 1.69	0.58 0.29	13.27 7.36	"	0.63 0.75	10.40 15.62	1.37 2.18	0.46 0.23	2.24 2.50	0.73 0.96	18.17 25.26	"	10.42 8.52	1.24 1.19	1.47 1.37	1.47 1.37
C = Pleistocene Lower Pt. Durnford (Hem.)	Mean St. Dev.	4.65 0.46	2.06 0.86	17.34 6.00	0.77 0.10	0.89 0.01	15.84 2.03	2.23 0.42	273.50 20.31	273.50 20.31	0.61 0.13	3.82 1.67	0.17 0.04	0.20 0.02	3.45 0.78	0.48 0.04	59.00 1.51	59.00 1.41	6.68 4.11	0.29 0.12	0.33 0.11	0.33 0.11
D = Miocene sand + silt (Uloa)	Mean St. Dev.	0.83 0.54	0.25 0.18	2.19 1.65	0.09 0.08	0.33 0.15	0.87 0.59	1.27 0.21	33.33 28.11	33.33 28.11	0.30 0.00	2.55 0.55	0.10 0.04	0.44 0.16	1.05 0.37	0.33 0.15	1.30 0.57	39.33 15.18	8.68 0.63	0.32 0.09	1.49 0.38	1.49 0.38
E = Miocene Calcareite (Uloa)	Mean St. Dev.	3.30 1.43	1.53 0.97	16.36 7.25	1.27 0.51	0.70 0.08	20.93 43.79	1.71 0.81	70.40 98.03	223.00 70.70	0.49 0.27	6.45 4.75	0.41 0.14	0.25 0.09	6.16 13.94	0.54 0.16	23.44 28.49	101.00 21.41	14.23 10.94	0.98 0.33	0.58 0.24	0.58 0.24
F = Oretaceous mudstone (St. Lucia)	Mean St. Dev.	6.29 1.48	0.81 0.77	3.29 2.71	1.12 0.81	0.56 0.29	3.62 2.53	0.93 0.67	13.50 11.17	59.84 34.17	0.11 0.09	0.49 0.28	0.17 0.09	0.09 0.03	0.53 0.27	0.14 0.08	2.64 2.21	11.50 6.36	6.50 4.33	2.12 1.50	1.08 0.61	1.08 0.61

	Na/SO <sub>4</sub>	Na/Cl	Na/NO <sub>3</sub>	Na/F	K/Si	K/NO <sub>3</sub>	K/SO <sub>4</sub>	K/Cl	K/NO <sub>3</sub>	K/F	Si/NO <sub>3</sub>	Si/Cl	Si/NO <sub>3</sub>	Si/F	NO <sub>3</sub> /SO <sub>4</sub>	NO <sub>3</sub> /Cl	NO <sub>3</sub> /NO <sub>3</sub>	NO <sub>3</sub> /F	SO <sub>4</sub> /Cl	SO <sub>4</sub> /NO <sub>3</sub>	SO <sub>4</sub> /F	Cl/NO <sub>3</sub>	Cl/F	NO <sub>3</sub> /F	SR	
A	Mean	5.83	0.09	46.17	129.50	0.05	0.16	0.06	3.19	6.00	4.37	11.40	2.02	151.45	248.00	4.43	0.57	45.83	77.00	0.21	9.29	36.00	49.50	151.50	6.49	1.85
	Std.Dev.	7.08	0.12	51.63	4.95	0.04	0.10	0.52	0.03	3.68	2.97	10.51	2.23	243.57	114.55	4.74	0.58	70.14	76.37	0.11	8.88	19.80	53.34	7.79	0.92	0.49
B	Mean	3.63	0.97	22.61	"	0.15	0.55	0.59	0.18	4.35	2.54	4.70	1.16	25.75	"	4.67	1.31	31.43	"	0.30	7.21	"	32.94	"	7.72	1.71
	Std.Dev.	1.68	0.23	7.90	"	0.10	0.86	0.44	0.19	4.64	3.05	3.73	0.60	12.79	"	3.53	1.24	33.40	"	0.12	3.50	"	3.54	"	0.69	0.56
C	Mean	5.91	0.80	98.00	99.00	0.05	0.06	0.95	0.14	17.00	1.16	20.55	2.96	359.50	359.50	17.00	2.52	309.00	309.00	0.15	17.50	17.50	124.00	124.00	6.95	0.77
	Std.Dev.	2.49	0.09	22.63	22.63	0.01	0.02	0.21	0.07	7.07	0.13	0.07	0.91	71.42	71.42	1.98	0.52	29.29	29.29	0.05	3.54	3.54	14.14	14.14	0.98	0.25
D	Mean	3.52	1.09	4.35	129.00	0.03	0.17	0.41	0.12	0.50	5.09	11.49	3.43	13.79	413.33	2.45	0.76	3.25	91.00	0.31	1.26	36.67	4.12	120.33	6.85	2.26
	Std.Dev.	0.33	0.20	1.44	16.70	0.01	0.05	0.07	0.04	0.16	2.56	3.79	3.39	3.90	81.59	0.59	0.26	2.07	30.45	0.04	0.50	3.51	1.44	7.02	0.47	0.41
E	Mean	0.24	1.20	37.42	197.80	0.10	0.06	1.14	0.13	4.35	12.00	20.78	1.38	63.72	230.40	27.19	2.79	93.76	317.60	0.30	9.40	57.29	37.55	171.80	6.93	1.54
	Std.Dev.	10.81	0.24	21.77	80.96	0.08	0.04	2.06	0.08	4.62	5.00	53.50	0.52	111.75	90.30	53.82	1.06	105.32	51.27	0.16	6.32	35.33	37.44	31.22	0.47	0.58
F	Mean	6.01	1.45	62.30	310.50	0.36	0.21	1.29	0.34	6.07	31.00	0.56	3.50	126.00	"	6.16	1.54	37.34	298.00	0.25	8.60	37.00	36.34	165.00	6.79	3.92
	Std.Dev.	2.45	0.45	44.27	210.50	0.13	0.12	0.91	0.28	4.15	22.63	0.17	1.55	5.57	125.87	1.60	0.48	21.87	189.71	0.03	7.35	9.80	29.23	99.00	1.99	2.68

## TABLE A.4

- 1)  $\text{Ca} \geq 10\%$
- 2)  $\text{Mg} \geq 3.5\%$
- 3)  $\text{Na} \geq 15\%$
- 4)  $\text{K} \geq 5\%$
- 5)  $\text{Si} \geq 10\%$
- 6)  $\text{HCO}_3 \geq 50\%$
- 7)  $\text{SO}_4 \geq 70\%$
- 8)  $\text{Cl} \geq 10\%$
- 9)  $\text{NO}_3 \geq 3\%$
- 10)  $\text{Ca:Mg} \geq 4.5$
- 11)  $\text{Ca:Na} \geq 2$
- 12)  $\text{Ca:K} \geq 20$
- 13)  $\text{Ca:Si} \geq 1$
- 14)  $\text{Ca:HCO}_3 \geq 0.5$
- 15)  $\text{Ca:HCO}_3 \geq 1.0$
- 16)  $\text{Ca:Cl} \geq 10$
- 17)  $\text{Ca:Cl} \geq 1$
- 18)  $\text{Mg:Na} \geq 0.5$
- 19)  $\text{Mg:K} \geq 5$
- 20)  $\text{Mg:Si} \geq 10$
- 21)  $\text{Mg:HCO}_3 \geq 0.5$
- 22)  $\text{Mg:HCO}_3 \geq 1$
- 23)  $\text{Mg:SO}_4 \geq 2$
- 24)  $\text{Mg:Cl} \geq 0.8$
- 25)  $\text{Na:K} \geq 15$
- 26)  $\text{Na:Si} \geq 1$
- 27)  $\text{Na:HCO}_3 \geq 1$
- 28)  $\text{Na:HCO}_3 \geq 2$
- 29)  $\text{Na:SO}_4 \geq 6$
- 30)  $\text{Na:SO}_4 \geq 10$
- 31)  $\text{Na:Cl} \geq 1.5$
- 32)  $\text{K:Si} \geq 0.1$
- 33)  $\text{K:Si} \geq 0.35$
- 34)  $\text{K:HCO}_3 \geq 0.2$
- 35)  $\text{K:HCO}_3 \geq 0.4$
- 36)  $\text{K:SO}_4 \geq 1$
- 37)  $\text{K:Cl} \geq 0.3$
- 38)  $\text{Si:HCO}_3 \geq 2$
- 39)  $\text{Si:SO}_4 \geq 10$
- 40)  $\text{Si:SO}_4 \geq 20$
- 41)  $\text{Si:Cl} \geq 3$
- 42)  $\text{HCO}_3:\text{SO}_4 \geq 10$
- 43)  $\text{SO}_4:\text{Cl} \geq 2.5$
- 44)  $\text{SO}_4:\text{Cl} \geq 0.25$
- 45)  $\text{SO}_4:\text{Cl} \geq 0.4$

A = Upper Port Durnford  
B = Lignite Layer  
C = Lower Port Durnford  
D = Miocene Sand  
E = Uloa Calcarenite  
F = Cretaceous Mud St. I

TABLE A.5

Sample														STRATIGRAPHY											
Sample														Sample											
Sample														Sample											
Sample														Sample											
Sample														Sample											
Sample														Sample											
Sample														Sample											
Sample														Sample											
Sample														Sample											
Sample														Sample											
Sample														Sample											
Sample														Sample											
Sample														Sample											
Sample														Sample											
Sample														Sample											
Sample														Sample											
Sample														Sample											
Sample														Sample											
Sample														Sample											
Sample														Sample											
Sample														Sample											
Sample														Sample											
Sample														Sample											
Sample														Sample											
Sample														Sample											
Sample														Sample											
Sample														Sample											
Sample														Sample											
Sample														Sample											
Sample														Sample											
Sample														Sample											
Sample														Sample											
Sample														Sample											
Sample														Sample											
Sample														Sample											
Sample														Sample											
Sample														Sample											
Sample														Sample											
Sample														Sample											
Sample														Sample											
Sample														Sample											
Sample														Sample											
Sample														Sample											
Sample														Sample											
Sample														Sample											
Sample														Sample											
Sample														Sample											
Sample														Sample											
Sample														Sample											
Sample														Sample											
Sample														Sample											
Sample														Sample											
Sample														Sample											
Sample														Sample											
Sample														Sample											
Sample														Sample											
Sample														Sample											
Sample														Sample											
Sample														Sample											
Sample														Sample											
Sample														Sample											
Sample														Sample											
Sample														Sample											
Sample														Sample											
Sample														Sample											
Sample														Sample											
Sample														Sample											
Sample														Sample											
Sample														Sample											
Sample														Sample											
Sample														Sample											
Sample														Sample											
Sample														Sample											
Sample														Sample											
Sample														Sample											
Sample														Sample											
Sample														Sample											
Sample														Sample											
Sample														Sample											
Sample														Sample											
Sample														Sample											
Sample														Sample											
Sample														Sample											
Sample														Sample											
Sample														Sample											
Sample														Sample											
Sample														Sample											
Sample														Sample											
Sample														Sample											
Sample														Sample											
Sample														Sample											
Sample														Sample											
Sample														Sample											
Sample														Sample											
Sample														Sample											
Sample														Sample											
Sample														Sample											
Sample														Sample											
Sample														Sample											
Sample														Sample											
Sample														Sample											
Sample														Sample											
Sample														Sample											
Sample														Sample											
Sample														Sample											
Sample														Sample											
Sample														Sample											
Sample														Sample											
Sample														Sample											
Sample														Sample											
Sample														Sample											
Sample														Sample											
Sample														Sample											
Sample														Sample											
Sample														Sample											
Sample														Sample											
Sample														Sample											
Sample														Sample											
Sample														Sample											
Sample														Sample											
Sample														Sample											
Sample														Sample											
Sample														Sample											
Sample														Sample											
Sample														Sample											
Sample														Sample											
Sample														Sample											
Sample														Sample											
Sample														Sample											
Sample														Sample											
Sample														Sample											
Sample														Sample											
Sample														Sample											
Sample														Sample											
Sample														Sample											
Sample														Sample											
Sample														Sample											
Sample														Sample											
Sample														Sample											
Sample														Sample											
Sample														Sample											
Sample														Sample											
Sample														Sample											
Sample														Sample											
Sample														Sample											
Sample														Sample											
Sample														Sample											
Sample														Sample											
Sample														Sample											
Sample														Sample											
Sample														Sample											
Sample														Sample											
Sample														Sample											
Sample														Sample											
Sample														Sample											
Sample														Sample											
Sample														Sample											
Sample														Sample											
Sample														Sample											
Sample														Sample											
Sample														Sample											
Sample														Sample											
Sample														Sample											
Sample														Sample											
Sample														Sample											
Sample														Sample											
Sample														Sample											
Sample														Sample											
Sample														Sample											
Sample														Sample											
Sample														Sample											
Sample														Sample											
Sample														Sample											
Sample														Sample											
Sample														Sample											
Sample														Sample											
Sample														Sample											
Sample														Sample											
Sample														Sample											
Sample														Sample											
Sample														Sample											
Sample														Sample											
Sample														Sample											
Sample														Sample											
Sample														Sample											
Sample														Sample											
Sample														Sample											
Sample														Sample											
Sample														Sample											
Sample														Sample											
Sample														Sample											
Sample														Sample											
Sample														Sample											
Sample														Sample											
Sample														Sample											
Sample														Sample											
Sample														Sample											
Sample														Sample											
Sample														Sample											
Sample														Sample											
Sample														Sample											
Sample														Sample											
Sample														Sample											
Sample														Sample											
Sample</																									

## B. GROUND WATER RECHARGE CALCULATIONS

---

If the salt (chloride) concentration in precipitation water (rain water) is given by  $C_p$  (in mg/l) and the precipitation amount is  $P_m$  (mm/month), then the salt deposition rate  $S_m$  is:

$$S_m = (C_p P_m) / 100 \quad [\text{kg/ha/month}]$$

or

$$S_m = (C_p P_m) / 10 \quad [\text{g/m}^2/\text{month}]$$

Summing and averaging the salt deposition rates yields an annual average salt deposition rate  $S_a$  (kg/ha/year). If  $C_w$  is the salt concentration in ground water, then the recharge will be:

$$R = (S_a / C_p) \times 100 \quad (\text{mm/year})$$

and the percentage recharge will be

$$\% \text{ recharge} = R / P_a.$$

*Note:*  $100 \text{ mg/m}^2 = 0.1 \text{ g/m}^2 = 1 \text{ kg/ha}$



---

# **GEOHYDROLOGICAL INVESTIGATION AND EVALUATION OF THE ZULULAND COASTAL AQUIFER**

---

**Report to the  
WATER RESEARCH COMMISSION**

by

**R Meyer<sup>1</sup>, A S Talma<sup>1</sup>, A W A Duvenhage<sup>1</sup>, B M Eglington<sup>1</sup>,  
J Taljaard<sup>1</sup>, J F Botha<sup>2</sup>, J Verwey<sup>2</sup> and I van der Voort<sup>2</sup>**

<sup>1</sup>Environmentek, CSIR

<sup>2</sup>University of the Free State

## EXECUTIVE SUMMARY

### 1. INTRODUCTION

The Zululand coastal plain, with a surface area of approximately 7 000 km<sup>2</sup> in South Africa, is located on the north east coast of Kwazulu-Natal and extends from Mtunzini in the south to the Mocambique border in the north. This is a distance of about 250 km whereas the Coastal Plain stretches for another almost 1000 km in Mozambique. It constitutes the largest primary coastal aquifer in South Africa. From a ground water perspective this aquifer has until a few years ago received little attention. Several large lakes, some of which have a direct connection to the ocean while others are isolated from the ocean, occur along this stretch of land and form an integral part of this delicate ecosystem.

During the 1960's the town of Richards Bay was proclaimed a national growth point and has developed over the years into an industrial city along the coast. Developments such as this and the expansion of the agricultural, forestry and tourism industry, together with the development of large industrial factories is placing unprecedented demands on this environmentally sensitive area. The proposed mining of heavy minerals along the Eastern Shores of Lake St Lucia in the early 1990s, has again raised the sensitivity and complexity of the area in terms of the functioning of the environment in this region.

Large gaps in our knowledge base, and thus our understanding of the functioning of the system, has prompted this study. Despite several mostly unrelated studies of the ground water resources on the Zululand Coastal Plain have been done over the years. This project was initiated to address some of the many interesting geohydrological features of the coastal plain that are fundamental to our understanding of this aquifer and its associated environment and to integrate the knowledge that already exists for the area. Because of the extent of the large extent of the aquifer (250km north-south and 60km maximum east-west), the aim was not to understand the detailed geohydrology of this rather complex area, but to add to the already existing data base of knowledge of the aquifer in order to obtain a conceptual model of the aquifer system.

The report is divided into 6 chapters of which **Chapter 1** contains mainly background information to this study. This is followed by a chapter (**Chapter 2**) which describes the geology and the geophysical investigations that were conducted and the results of the geophysical surveys. In **Chapter 3** various aspects of the geohydrology, such as a description of the aquifer, ground water quality and isotope studies, thickness of the

aquifer succession, hydraulic characteristics of the aquifer, recharge and pollution vulnerability, are described. The development of a mathematical simulation model and the results from modelling various ground water utilization options for the Coastal Plain including the effect of afforestation on the aquifer, is described in **Chapter 4**. This is followed by **Chapter 5** which contains water balance calculations and a description of the utilization of the ground water resource. Conclusions and recommendations emanating from the project are contained in **Chapter 6**.

## **2. STUDY OBJECTIVES**

The objectives of the study as stated in the original project proposal were

- to determine the extent and geohydrological conditions of the aquifer associated with the Zululand coastal plain between Richards Bay and the Mocambique border by means of geophysical surveys and subsequent drilling and pump testing;
- to determine the regional ground water flow pattern;
- to determine the vulnerability to pollution of the aquifer and the associated effect it may have on pollution of the inland lake systems;
- to determine the amount of ground water recharge to the aquifer under current land-use practices and the role that the inland lake systems play in this regard;
- to evaluate the response of the aquifer to large scale abstraction of ground water as well as the interaction between ground water, forestry and the lake systems through a mathematical simulation;
- to determine what amounts of ground water can be abstracted from the aquifer without causing negative effects on the ground water system;
- to evaluate the possibility of sea water intrusion into the aquifer; and
- to determine a water balance for the Coastal Plain.

## **3. METHODOLOGY**

In the course of the study the Steering Committee decided that the application of stable isotopes determinations, in conjunction with the ground water chemistry to study the recharge to the coastal aquifer would add significantly to our understanding of the recharge pattern across the study area. The continuous monitoring of the isotopic and chemical character of the rainfall and water from the lakes over a three-year period was therefore initiated as a way to determine the recharge to the aquifer.

Due to the deterioration of the security situation on the coastal plain, both in the northern areas as well as the area around Kwambonambi, the drilling programme had

to be curtailed before all exploration boreholes could be completed. No production boreholes for pump testing were therefore drilled apart from a few around Lake Mzingazi drilled by the Department of Water Affairs and Forestry for assessing the flow conditions around this lake. The result was that all objectives (for example determining the sustainable yield of the aquifer) could not be fully achieved.

Crucial to the understanding of the geohydrology of the coastal plain, is a knowledge of the thickness of the alluvial succession defining the aquifer. The study area is underlain by alluvial deposits of Holocene age (<100 00 years), and rocks of Tertiary and Quaternary age (<65 million years). Geophysical techniques provide one way of determining the thickness of these successions. The application and success of the direct current resistivity and time domain electromagnetic exploration techniques to study the geological successions has already been proven on the Zululand coastal plain and were therefore further applied to map the geological succession overlying the Cretaceous floor rocks over the entire coastal plain. Initially an area on the coastal plain had been selected where the different aspects influencing the geohydrological conditions could be studied. These included the lake systems, dunes, plantations, geological succession, etc. The following step then was to extend the study to eventually cover the entire coastal plain. The thickness and lateral extent of the post-Cretaceous sedimentary succession was studied using geophysical techniques followed by the drilling of boreholes in selected localities for calibration purposes.

Water samples were collected from boreholes and other water sources for chemical and isotopic analyses to identify different ground water types and to contribute to our understanding of the recharge characteristics. The chemical and isotopic characteristics of rainfall and ground water were studied in depth to produce a recharge relationship for the coastal aquifer. Eventually all the collected information was integrated and a conceptual geohydrological model was formulated. This model was then developed further into a mathematical simulation model with which different geohydrological scenarios could be tested on a regional scale.

#### **4. SUMMARY OF MAJOR RESULTS AND CONCLUSIONS**

The objectives for the project as stated in the contract conditions, and listed in the introduction to this report, have been met, with the exception of all the exploration drilling and test pumping originally envisaged. This was due a deteriorating security situation which made the area unsafe for the drilling and test pumping crews. This had the effect that the sustainability of the aquifer in terms of abstraction could not be assessed over the entire coastal plain.

The earlier statement that the Zululand Coastal Plain Aquifer can be regarded as one of the largest alluvial aquifers in South Africa has been confirmed by the additional information collected during this investigation. Although the investigation has also led to a better understanding of the aquifer system, several aspects warrant more study. In this regard the interaction between vegetation, whether it be natural or commercial (forestry and agriculture for example), and the ground water regime needs to be assessed thoroughly before any large scale development of the ground water resource is envisaged.

There exists a fine balance between the ecology of the region and the ground water regime. Any future development plans for the region, whether development for tourism, rural settlements, agriculture, mining or afforestation have to take into account the delicate balance of the ecosystem. Ground water plays a crucial role in this ecosystem and any change in the ground water conditions may influence the ecosystem negatively.

Some specific conclusions emanating from this study are listed below:

- The thickness of the aquifers stratigraphically above the Cretaceous age sediments, was mapped over the entire coastal plain using geophysical techniques. Confidence in the thickness determinations was achieved by calibrating the interpreted thicknesses against known borehole information.
- The electrical resistivity sounding technique used to determine the depth to the top of the Cretaceous age formations is more appropriate than the electromagnetic techniques to determine the thickness of the different units in the geological succession.
- Interpretation of direct current (dc) soundings is complicated because of the continuous decrease of the resistivity with depth. Similarly depth penetration by Electromagnetic (EM) techniques was also found to be restricted due to the decrease in resistivity with depth of the different geological units and the very conductive nature of the sedimentary succession.
- Resolution of individual geological units with geophysical methods proved not always to be successful. The depth to the top of the Cretaceous formations can, however, be determined with a large degree of confidence.
- Borehole geophysical measurements also failed to clearly identify different geological horizons.
- Gravity surveys were not able to detect palaeo-channels subsequently filled with younger sediments.
- Two palaeo-channels were detected geophysically and by drilling, through which increased seepage towards the sea can and does occur. One of these is situated opposite Lake Sibayi and the other one is near Mission Rocks opposite Lake St Lucia.

- A water level contour map was constructed for the entire coastal plain using measured water levels and applying statistical techniques to infer elevations in areas where data points were sparse.
- A ground water divide, roughly parallel to the coastline, could clearly be identified from this map.
- From the available water level information, three different water level scenarios in the vicinity of the coastal dune cordon could be identified. These are at Lake Sibayi, Eastern Shores of Lake St Lucia, and at Richards Bay.
- A regional mathematical simulation model was designed to simulate steady state conditions. This model was used to determine ground water flow directions and velocities over the entire coastal plain.
- It was further used to simulate the effect of an afforested area around Lake Sibayi to determine the effect on lake and ground water levels. This model indicates that if evapotranspiration by the plantations exceeds 1 000 mm/ha/a, water levels in the lake may already be affected. A number of assumptions have, however, been made during this simulation. These figures should therefore be regarded as provisional.
- An important rainfall-recharge relationship was established which varies with distance from the coast. Recharge as a percentage of MAP varies from 18 % at the coast to 5 % at a distance of 50 km inland.
- The rainfall-recharge relationship was used as input to the mathematical simulation exercise.
- Ground water quality over the entire coastal plain is generally of good quality. There are, however, due to changing geological conditions, regional differences in the chemical character.
- A hydrochemical "fingerprinting" technique was developed and used successfully to correlate the water chemistry with the geological horizon from which it originates.
- Stable isotopes were used to great advantage to distinguish between seepage from lakes and ground water. Stable isotopes also confirmed a considerable residence time for water in the larger lakes like Sibayi and Bhangazi.
- No seasonal isotopic variation was recognized in rainwater. Isotope analyses could also not be used to trace the movement of ground water due to insignificant variations observed
- Carbon-14 analyses indicated that the ground water recharge is mostly post-1960. This is in accordance with the high through-flow of water through the aquifer deduced from recharge estimates and modelling.  
Isotope analyses confirmed that the fresh water occurrence along the coast opposite Lake Sibayi originates from the lake.
- Sea-water intrusion into the aquifer is unlikely to occur due to an effective above sea level piezometric head along the coastal dune cordon.
- The aquifer is highly vulnerable to surface sources of pollution.

In view of the ecologically sensitive nature of the area and the dominating role that ground water plays in maintaining the balance has again been reiterated by the results obtained during this investigation. Based on the result attained, a number of important recommendations for future studies and development initiatives on the Coastal Plain are made. These include that:

- A water level monitoring programme should be initiated and maintained to document the long term character of the regional water level and ground water quality.
- The interaction between the ground water and the vegetation in the area be investigated in detail and that a research program to address this aspect be compiled as soon as possible. This would assist to better understand the effect of large scale development projects (for example extensive commercial forestry) on the aquifer and the ecology of the region as a whole.
- This research program should include input from ecologists, the Department of Water Affairs and Forestry, the commercial forestry sector, nature conservation officials, tourism authorities and regional planners.
- Further work is required to quantify the effect of afforestation on the ground water conditions in more detail.
- The mathematical simulation model should be refined and updated once more data becomes available.
- The pollution vulnerability of the aquifer should be brought to the attention of the planners.

## ACKNOWLEDGMENTS

The research described in this report emanated from a project funded by the Water Research Commission and entitled:

### **“GEOHYDROLOGICAL INVESTIGATION AND EVALUATION OF THE ZULULAND COASTAL AQUIFER”**

Contributions throughout the duration of the project by members of the Steering Committee are gratefully acknowledged. The Steering Committee responsible for this project consisted of the following persons:

Mr A G Reynders	Water Research Commission (Chairman)
Mr H M du Plessis	Water Research Commission
Mr R Bush	Department of Water Affairs and Forestry
Dr J H de Beer	Environmentek, CSIR
Mr F Bosman	Richards Bay Municipality
Mr P Conant	Kwazulu Bureau of Natural Resources
Prof J F Botha	Institute for Ground-water Studies, University of the Orange Free State
Dr D B Bredenkamp	Department of Water Affairs and Forestry

The authors further wish to thank the many individuals, institutions and companies who contributed to the project, by supplying information, either in the form of fruitful discussions or from reports and publications. All this information in some way or another contributed to the success of the project.

We would like to acknowledge the contributions made by the following individuals or institutions:

Prof B Kelbe, University of Zululand  
Richards Bay Minerals  
Natal Parks Board  
Kwazulu Department of Natural Resources  
Department of Water Affairs and Forestry  
Council for Geoscience  
Industrial Development Corporation  
Forestry Industry  
Borough of Richards Bay  
Atomic Energy Corporation  
Davies, Lynn and Partners, Durban  
Mr M J McCarthy, Durban



## TABLE OF CONTENTS

Executive Summary .....	i
Acknowledgments .....	vii
Table of Contents .....	viii
List of Appendices .....	ix
List of Figures .....	x
List of Tables .....	xii

<b>CHAPTER 1: INTRODUCTION AND SUMMARY OF PREVIOUS GEOHYDROLOGICAL STUDIES OF THE COASTAL PLAIN .....</b>	<b>1</b>
<b>1.1 Introduction .....</b>	<b>1</b>
<b>1.2 Research objectives .....</b>	<b>2</b>
<b>1.3 Approach to study .....</b>	<b>2</b>
<b>1.4 Report layout .....</b>	<b>3</b>
<b>1.5 Summary of previous geohydrological studies on the Coastal Plain ..</b>	<b>3</b>
 <b>CHAPTER 2: GEOLOGY OF THE COASTAL PLAIN AND GEOPHYSICAL INVESTIGATIONS .....</b>	 <b>6</b>
<b>2.1 Information Sources .....</b>	<b>6</b>
<b>2.2 Geological Succession .....</b>	<b>8</b>
2.2.1 <i>Basement rocks (Cretaceous age)</i> .....	8
2.2.2 <i>Tertiary age sediments</i> .....	8
2.2.3 <i>Pleistocene deposits</i> .....	9
2.2.4 <i>Younger unconsolidated deposits</i> .....	9
<b>2.3 Geophysical Investigation and Techniques used .....</b>	<b>10</b>
<b>2.4 Electrical Methods .....</b>	<b>10</b>
2.4.1 <i>Direct Current Resistivity Technique (Schlumberger Array)</i> .....	10
2.4.2 <i>Types of sounding curves</i> .....	11
2.4.3 <i>Geoelectric layer resistivities</i> .....	11
2.4.4 <i>Calibration soundings</i> .....	11
<b>2.5 Electromagnetic Soundings .....</b>	<b>13</b>
2.5.1 <i>General</i> .....	13
2.5.2 <i>Calibration soundings</i> .....	13
<b>2.6 Gravity Survey .....</b>	<b>14</b>
<b>2.7 Results of Geophysical Investigation .....</b>	<b>14</b>
2.7.1 <i>Geoelectrical Techniques</i> .....	14
2.7.2 <i>Geophysical Borehole Logging</i> .....	15

<b>CHAPTER 3: GEOHYDROLOGY OF THE ZULULAND COASTAL PLAIN</b> .....	17
<b>3.1 Aquifer description</b> .....	17
<b>3.2 Hydrochemisry and Isotope Studies</b> .....	18
3.2.1 <i>Ground Water Chemistry</i> .....	18
3.2.2 <i>Isotopes in Water</i> .....	19
Stable isotopes .....	19
Radiocarbon .....	20
<b>3.3 Ground Water Leakage to the Sea</b> .....	20
<b>3.4 Rain Water Chemistry</b> .....	23
3.4.1 <i>Sampling</i> .....	23
3.4.2 <i>Rain water chemistry</i> .....	24
3.4.3 <i>Isotopes in rainfall</i> .....	26
<b>3.5 Ground Water Recharge Estimates</b> .....	27
<b>3.6 Potential for Ground Water Pollution</b> .....	29
 <b>CHAPTER 4: MATHEMATICAL MODELLING OF THE COASTAL PLAIN AQUIFER</b> ..	32
<b>4.1 General</b> .....	32
<b>4.2 Geohydrology</b> .....	32
<b>4.3 The Finite Element Model</b> .....	33
<b>4.4 Results from the Finite Element Model</b> .....	33
<b>4.5 The Impact of Afforestation on the Aquifer: A Hypothetical Case Study</b> .....	34
<b>4.6 Conclusions</b> .....	36
 <b>CHAPTER 5: WATER BALANCE CALCULATIONS</b> .....	37
<b>5.1 Recharge Driven Water Balance</b> .....	37
<b>5.2 Flow Equation Derived Water Balance</b> .....	37
<b>5.3 Preferential Flow Paths to the Sea</b> .....	38
<b>5.4 Utilization of Ground Water Resource</b> .....	39
 <b>CHAPTER 6: CONCLUSIONS AND RECOMMENDATIONS</b> .....	40
<b>6.1 Conclusions</b> .....	40
<b>6.2 Recommendations</b> .....	42
 <b>LIST OF REFERENCES</b> .....	43

## LIST OF APPENDICES

**APPENDIX A: Geochemical classification of ground water on the Zululand Coastal Plain**

**APPENDIX B: Ground water recharge calculations**

## LIST OF FIGURES

- Figure 1:** Geological map of the Zululand Coastal area.
- Figure 2:** Resistivity sounding locations.
- Figure 3:** A typical direct current (DC) resistivity sounding curve and interpretation.
- Figure 4:** Sounding curve and model for resistivity sounding ES 85.
- Figure 5:** DC sounding curve and interpretations for ES 235 (Lebombo Group) and ES 224 (Makatini Formation).
- Figure 6:** DC sounding curve and interpretations for ES 180 (Mzineni Formation) and ES 155 (St Lucia Formation).
- Figure 7:** DC sounding curve and interpretations for ES 188 (Uloa Formation) and ES 105 (Port Durnford Formation).
- Figure 8:** DC sounding curve and interpretations for ES 42 (Berea-type Red Sand) and ES 168 (Holocene sands).
- Figure 9:** Histogram of surface measured formation resistivities based on calibration soundings (Worthington, 1979).
- Figure 10:** Sounding curves and models for ES 1, ES 2 and ES 4.
- Figure 11:** Electromagnetic sounding (EM-37) Sounding locations.
- Figure 12:** Comparison between the results of electromagnetic sounding interpretations and drilling results .
- Figure 13:** Transient electromagnetic sounding curves and models for soundings EM 21 and EM 36.
- Figure 14:** Borehole positions on the Zululand Coastal Plain.
- Figure 15:** Boreholes where Cretaceous age rocks were intersected.
- Figure 16:** Positions of modeled depths to Cretaceous.
- Figure 17:** Post Cretaceous sediment thickness north of Lake St Lucia.
- Figure 18:** Post-Cretaceous sediment thickness on the Zululand Coastal Plain south of Lake St Lucia.
- Figure 19:** Boreholes sampled for water chemistry.
- Figure 20a:** Results of chemical analyses of all water samples entered into the Hydrocom database. Data are represented as Piper and Durov diagrams.
- Figure 20b:** Results of chemical analyses of all water samples entered into the Hydrocom database. Data are represented as a Schoeller diagram.
- Figure 21:** Ground water sampling positions for isotope analyses.
- Figure 22:** Distribution of  $\delta^{18}\text{O}$  levels on ground water and surface water in the study area. Surface waters show the effect of isotope enrichment due to evaporation.
- Figure 23:** Relation between  $^{18}\text{O}$  and deuterium in ground water and surface water. Ground water falls on the Meteoric Water Line (MWL) following a general pattern. Deviations from the MWL by surface water are due to evaporation enrichment.
- Figure 24:** Time series of chloride (Cl) and  $^{18}\text{O}$  in Lake Sibayi. The overall constancy of both parameters indicates that the annual (rain/ground) water inflow is small compared with the lake volume.

- Figure 25:**  $^{18}\text{O}$  and chloride relation for the Gobey's Point seepage and the waters likely to be its sources.
- Figure 26:** Schematic cross-section through the coastal dune between Lake Sibayi and the sea.
- Figure 27:**  $^{18}\text{O}$  and deuterium relation for Gobey's Point seepage and its likely sources. The seepage is also located directly on the mixing line between lake and sea water and distinctly different from the MWL representing rain and ground water.
- Figure 28:**  $^{18}\text{O}$  and chloride time series of Lake Bhangazi and the Cape Vidal seepage water. The average  $^{18}\text{O}$  content of ground water is shown for comparison.
- Figure 29:** Comparison of  $^{18}\text{O}$  and Cl in the Cape Vidal/Bhangazi system. Average values for ground water in the area are taken from Bredenkamp (1993). Cape Vidal seepage can be seen to be a mixture between Lake Bhangazi water and ground water with occasional sea water contributions. Note the logarithmic scale.
- Figure 30:**  $^{18}\text{O}$  and deuterium relation for water in the Cape Vidal/Lake Bhangazi system. The interpretation of Cape Vidal seepage as mixing between Lake Bhangazi water and local ground water is evident.
- Figure 31:** Rainfall monitoring stations used for this study.
- Figure 32:** Results of principle component analysis of the rainfall chemistry data. The weights of the various ions contributing to the first two principle components are shown.
- Figure 33:** Annual calcium deposition rates for the three sampling years.
- Figure 34:** Annual chloride deposition rates for the three sampling years. The coastal stations (SOD, MBA, MAN) show more annual variations than do the inland stations.
- Figure 35:** Relation between annual chloride deposition (for each of the three years) and the rainfall of that year.
- Figure 36:** Average (three years) chloride and calcium deposition with distance inland.
- Figure 37:** Seasonal pattern of rainfall and its  $^{18}\text{O}$  content for the six rainfall stations.
- Figure 38:**  $^{18}\text{O}$  deuterium relation for rainfall. Most are located on the MWL ( $\delta\text{D} = 8\delta^{18}\text{O} + 10$ ) which holds worldwide (Gat and Giofanti, 1981).
- Figure 39:** Relation between weighted annual  $^{18}\text{O}$  content in rain and the total rainfall for that year. Note the large difference (especially for the coastal stations SOD, MAN, MBA) and the driest year (1991/92).
- Figure 40:** Pollution vulnerability map for the fresh waters of the inner catchment of Lake Mzingazi (Worthington, 1978).
- Figure 41:** The borders of the Zululand aquifer, as well as the positions of the lakes and boreholes used in this study, are shown. The hypothetical afforestation around Lake Sibayi is also shown.
- Figure 42:** The ground water velocities in the Zululand aquifer, as computed from the 140 boreholes.
- Figure 43:** The finite element grid drawn over the Zululand aquifer. The grid excludes the three lakes, Lake St Lucia, Lake Sibayi and Lake Kosi.
- Figure 44:** The piezometric heads from the 140 boreholes were interpreted to all the nodes of the finite element grid, resulting in head contours as shown.

- Figure 45:** Contours from the simulated piezometric heads for the Zululand aquifer after a simulation period of one year.
- Figure 46:** A comparison of the initial (solid lines) and simulated (dots) piezometric heads of the numerical model, taken at a few sections parallel to the x-axis. The line numbers are according to the finite element model of Figure 47, counted from the bottom of the grid.
- Figure 47:** Contours of the water levels, simulated for one year, with hypothetical; recharge and evaporation figures of 150 mm/year and 2000 mm/year respectively
- Figure 48:** Section AA' through Lake Sibayi, perpendicular to the coast, showing the effect of a variation in evapotranspiration values. The evapotranspiration specified for the cases was 0, 200, 1 000, 2 000 and 4 000 mm per annum, per unit area.
- Figure 49:** Section BB' through Lake Sibayi, parallel to the coast, showing the effect of a variation in evapotranspiration values. The evapotranspiration specified for the cases was 0, 200, 1 000, 2 000 and 4 000 mm per annum, per unit area.
- Figure 50:** The direction of flow of ground water around Lake Sibayi and through the simulation area under normal conditions of 150 mm recharge per year.
- Figure 51:** The direction of flow of ground water around Lake Sibayi and through the simulation area under extreme conditions of an effective discharge of 2 500 mm per year.
- Figure 52:** Map indicating the aquifer potential in different parts of the Zululand Coastal Plain.

## LIST OF TABLES

- Table 1:** Simplified geological sequence: Zululand Coastal Plain
- Table 2:** Correlation of the biostratigraphic, lithostratigraphic and geoelectrical subdivisions of the Cenozoic and late Mesozoic succession on the Zululand Coastal Plain (Adapted and extended from Worthington, 1978).
- Table 3:** Porosity determinations using "Archie's Law" where  $F = \rho_r / \rho_w = a^{-m}$  (with  $a=1$  and  $m=1.5$ ).
- Table 4:** Porosity values for different geological sequences as derived from geophysical borehole logging and other techniques
- Table 5:** Radiocarbon content of ground and surface water samples.
- Table 6:** Details of rainfall stations.
- Table 7:** Correlation matrix of major constituents of rain water (based on 157 analyses).
- Table 8:** Chloride deposition at rainfall stations (annual rainfall in millimetres in brackets).
- Table 9:** Three year  $^{18}\text{O}$  average weighted by annual rainfall less a cut-off value.
- Table 10:** Three year average ground water recharge data.
- Table 11:** Classification of proposed development zones within the Mzingazi catchment (Worthington, 1978)
- Table 12:** The movement of the piezometric level as observed at a few boreholes compared to the simulated values in a one year period.

## CHAPTER 1

### INTRODUCTION AND SUMMARY OF PREVIOUS GEOHYDROLOGICAL STUDIES OF THE COASTAL PLAIN

---

#### 1.1 Introduction

The Zululand coastal plain is an environmentally sensitive region located on the coast of northern Natal. The Zululand coastal plain, with a surface area of approximately 7 000 km<sup>2</sup> in South Africa, extends from Mtunzini in the south to the Mocambique border in the north and forms the largest primary coastal aquifer in South Africa. Despite several isolated studies of the aquifer, the vast ground water resources are, however, only exploited on a very limited scale for urban water supply and intermittently as an additional source of water for the coastal mining operations. Several large lakes, some of which have a direct connection to the ocean while others are isolated from the ocean, occur along this stretch of land and form an integral part of this delicate ecosystem. The inland lakes are in direct hydraulic contact with the ground water system.

During the 1960's the town of Richards Bay was proclaimed a national growth point and has developed over the years into an industrial city along the coast. Developments such as this and the expansion of the agricultural and forestry industry, together with the development of large industrial factories is placing unprecedented demands on this environmentally sensitive area. The proposed mining of heavy minerals along the Eastern Shores of Lake St Lucia and along the coast south of Richards Bay, as well as the proclamation of the Greater St Lucia Wetland Park, has again increased the awareness of the sensitivity and complexity of the area in terms of the functioning of this ecosystem.

Large gaps in our knowledge base, and thus our understanding of the functioning of the system, has prompted this study. The CSIR has been involved in several investigations and research projects along the coastal plain for many years ( Van Zijl, 1971; Vogel and Van Urk, 1975; Worthington, 1978; Meyer *et al*, 1982; Kruger and Meyer, 1986; Meyer *et al*, 1989; Meyer *et al*, 1993). The most extensive contributions to our understanding of the geohydrology of the coastal plain, was the work done by Australian Groundwater Consultants (1975) and Worthington (1978), and more recently by Kelbe and Rawlins (1992). Extensive studies have also been conducted around Lake Sibayi, the largest South African inland fresh water lake, by Pitman and Hutchinson (1975).

This project was initiated to address some of the many interesting geohydrological features of the coastal plain that are fundamental to our understanding of this aquifer and its associated environment and to integrate the knowledge that already exists for the area.

## 1.2 Research objectives

The objectives of the study as stated in the original project proposal were

- to determine the extent and geohydrological conditions of the aquifer associated with the Zululand coastal plain between Richards Bay and the Mocambique border by means of geophysical surveys and subsequent drilling and pump testing;
- to determine the regional ground water flow pattern;
- to determine the vulnerability to pollution of the aquifer and the associated effect it may have on pollution of the inland lake systems;
- to determine the amount of ground water recharge to the aquifer under current land-use practices and the role that the inland lake systems play in this regard;
- to evaluate the response of the aquifer to large scale abstraction of ground water as well as the interaction between ground water, forestry and the lake systems through a mathematical simulation;
- to determine what amounts of ground water can be abstracted from the aquifer without causing negative effects on the ground water system;
- to evaluate the possibility of sea water intrusion into the aquifer; and
- to determine a water balance for the Coastal Plain.

In the course of the study the Steering Committee decided that the application of stable isotopes determinations, in conjunction with the ground water chemistry to study the recharge to the coastal aquifer would add significantly to our understanding of the recharge pattern across the study area. The continuous monitoring of the isotopic and chemical character of the rainfall and water from the lakes over a three-year period was therefore initiated as a way to determine the recharge to the aquifer.

Due to the deterioration of the security situation on the coastal plain, both in the northern areas as well as the area around Kwambonambi, the drilling programme had to be curtailed before all exploration boreholes could be completed. No production boreholes for pump testing were therefore drilled apart from a few around Lake Mzingazi drilled by the Department of Water Affairs and Forestry for assessing the flow conditions around this lake. The result was that all objectives (for example determining the sustainable yield of the aquifer) could not be fully achieved. This prompted the collation of all existing geological and borehole information available on the coastal plain. Although many boreholes were located, well documented information on these hardly existed.

## 1.3 Approach to study

Crucial to the understanding of the geohydrology of the coastal plain, is a knowledge of the thickness of the alluvial succession defining the aquifer. The study area is underlain by alluvial deposits of Holocene age (<100 00 years), and rocks of Tertiary and

Quaternary age (<65 million years). Geophysical techniques provide one way of determining the thickness of these successions. The application and success of the direct current resistivity and time domain electromagnetic exploration techniques to study the geological successions has already been proven on the Zululand coastal plain and were therefore further applied to map the geological succession overlying the Cretaceous floor rocks over the entire coastal plain (Worthington, 1978; Meyer and Kruger, 1987; Meyer *et al.*, 1982; 1987; 1989). Initially an area on the coastal plain had been selected where the different aspects influencing the geohydrological conditions could be studied. These included the lake systems, dunes, plantations, geological succession, etc. The following step then was to extend the study to eventually cover the entire coastal plain. The thickness and lateral extent of the post-Cretaceous sedimentary succession was studied using geophysical techniques followed by the drilling of boreholes in selected localities for calibration purposes.

Water samples were collected from boreholes and other water sources for chemical and isotopic analyses to identify different ground water types and to contribute to our understanding of the recharge characteristics. The chemical and isotopic characteristics of rainfall and ground water were studied in depth to produce a recharge relationship for the coastal aquifer. Eventually all the collected information was integrated and a conceptual geohydrological model was formulated. This model was then developed further into a mathematical simulation model with which different geohydrological scenarios could be tested on a regional scale.

#### **1.4 Report layout**

The report is divided into 6 chapters of which **Chapter 1** contains mainly background information to this study. This is followed by a chapter (**Chapter 2**) which describes the geology and the geophysical investigations that were conducted and the results of the geophysical surveys. In **Chapter 3** various aspects of the geohydrology, such as a description of the aquifer, ground water quality and isotope studies, thickness of the aquifer succession, hydraulic characteristics of the aquifer, recharge and pollution vulnerability, are described. The development of a mathematical simulation model and the results from modelling various ground water utilization options for the Coastal Plain including the effect of afforestation on the aquifer, is described in **Chapter 4**. This is followed by **Chapter 5** which contains water balance calculations and a description of the utilization of the ground water resource. Conclusions and recommendations emanating from the project are contained in **Chapter 6**. A comprehensive list of references follows after Chapter 6.

#### **1.5 Summary of previous geohydrological studies on the Coastal Plain**

Over the years, several geohydrological investigations of different scales have been conducted on parts of the Zululand coastal plain. Some of the more important investigations were those by Van Wyk (1963), Australian Groundwater Consultants



(1975), Worthington (1978), Meyer *et al.* (1982), Kruger (1986), Kelbe and Rawlins (1992), and some more recent detailed investigations of well field developments east of Kwambonambi (Johnson, personal communication). In addition, a number of hydrological studies were also done on the lake systems so frequently found on the coastal plain. These were mainly done by the Hydrological Research Unit of the University of the Witwatersrand, and concentrated on Lakes St Lucia and Sibayi (Hutchinson and Pitman, 1973; Pitman and Hutchinson, 1975).

The reports by Van Wyk (1963), Worthington (1978), Australian Groundwater Consultants (1975) and Kruger (1986) were perhaps the most extensive studies over this period. Van Wyk's and Kruger's studies concentrated on the northern part of the coastal plain, whereas those by the Australian Groundwater Consultants and Worthington concentrated on the area around Richards Bay, Lake Mzingazi and Lake Nhlabane.

Worthington's approach was that of an integrated geophysical and geohydrological investigation directed at a detailed evaluation of the hydrological conditions around Richards Bay and Lake Mzingazi. Worthington (1978) used the results of some 900 direct current Schlumberger resistivity soundings to establish the geological succession above the extensive and impermeable siltstone of Cretaceous and Palaeocene age. He concluded that the compacted coquina and calcarenite of Miocene age overlying the siltstones in places, constitutes the major aquifer and attains thicknesses in excess of 20m in places. This view was also shared by Australian Groundwater Consultants (1975). The younger Pleistocene succession of fine-grained sands, clays and lignites generally give rise to leaky confined aquifer conditions in the Richards Bay area.

The interpretation of the geoelectric data, supported by calibration soundings and lithostratigraphic records from borehole logs, provided an adequate definition of the mode of occurrence of the Miocene aquifer which is present discontinuously and irregularly within the southern part of the Zululand coastal plain. The average hydraulic conductivity and storage coefficient of the Miocene Formation was established through pumping tests to be 4,5m/d and  $2 \times 10^{-4}$  respectively.

Within the area surveyed by Worthington, the potentiometric levels show a striking correlation with topography, a feature he interpreted as a direct consequence of the relatively low permeability of the Pleistocene succession, and which, through the presence of the coastal dune barrier complex, affords strong protection against saline water intrusion. This conclusion was also reached by Simmonds (1990) and Botha *et al.* (1989). Recent intensive studies around the Eastern Shores and dune cordon east of Lake St Lucia as part of the Environmental Impact Report for the proposed heavy mineral mining at Eastern Shores, Lake St Lucia, provided detailed information on the geohydrology associated with the dune cordon (Davies, Lynn and Partners, 1992; Kelbe and Rawlins, 1992; Meyer *et al.*, 1993). An intensive drilling programme across the dune cordon revealed that the dunes, which reach an elevation of up to 130m amsl at Mt Tabor, are virtually dry, and do not contain any perched water tables (Meyer *et al.*, 1993). In addition, and contrary to expectations and general belief (Van Zijl, 1971;

Pitman and Hutchison, 1975), the dunes do not support a ground water mound. The phreatic surface has nowhere been found to be in excess of 10m amsl and the ground water divide is situated to the west of the dune cordon between the dunes and the eastern shore of Lake St Lucia.

The distribution of aquifer transmissivity has been used by Worthington (1978) in conjunction with the map of potentiometric levels to estimate the subsurface seepage into Lake Mzingazi. His calculations indicated that ground water seepage accounts for over 30% of the total replenishment of Lake Mzingazi. The base flow was calculated to be about 80 000m<sup>3</sup>/day. He also predicted that the base flow would be severely affected, if significant ground water abstraction takes place in the Mzingazi catchment. Worthington also studied the pollution vulnerability of the aquifer and based on hydraulic properties of the aquifer, thickness of aquifer units, and depth to water table, subdivided the area into six zones; from a "green-light" area (favorable for urban development) to a "red-light" area where urban development is not recommended. He further warned that, because of the effectively steady-state conditions in the area, any serious change to the water balance by excessive surface and ground water abstraction, will cause a significant interaction between the different fresh water regimes which might, in turn, have undesirable consequences from the point of view of pollution vulnerability. A steady-state finite element ground water simulation model indicated that the two lakes, Nhlabane and Mzingazi, are hydrologically independent.

The procedure of combining geophysical and geohydrological information adopted in the study by Worthington was suggested as a future strategy for optimum ground water exploration in similar coastal regions. One reason why this approach was successful, was the high density of geoelectrical sounding positions.

Lindley and Scott (1987), Rawlins and Kelbe (1990) and Rawlins (1991) conducted investigations into the geohydrology of the area between the coastal dune cordon and the Eastern Shores of Lake St Lucia. As this area is covered by extensive timber plantations, the prime objectives of these investigations were to determine the influence of the plantations on the ground water regime. A comprehensive network of shallow boreholes, meteorological stations with continuous rainfall monitoring and stream gauging was installed and operated for a period of three years. Lindley and Scott (1987) concluded that pine plantations, and in particular *Pinus elliottii*, are responsible for an additional annual evapotranspiration loss of approximately 2 100 m<sup>3</sup>/ha. Rawlins (1991) arrived at an evapotranspiration loss figure for pine plantations ranging between 1 500m<sup>3</sup>/ha/yr and 1 750m<sup>3</sup>/ha/yr. He calculated that the commercial plantations at Eastern Shores account for an estimated total annual inflow reduction of water to Lake St Lucia of between 37 x 10<sup>6</sup>m<sup>3</sup> and 43 x 10<sup>6</sup>m<sup>3</sup> or 10% to 12% of the fresh water inflow to the Lake. This would affect the water balance to the Lake seriously and with reduced fresh water inflow into the Lake, the salinity balance of the Lake will be changed. This in turn, will have a direct impact on the flora and fauna of the Lake and its environments.

## CHAPTER 2

### GEOLOGY OF THE COASTAL PLAIN AND GEOPHYSICAL INVESTIGATIONS

---

#### 2.1 Information sources

The study area is covered by two 1:250 000 scale geological maps 2632 Kosi Bay and 27½32 St Lucia. In general, Quaternary geology has been neglected in South African geology, with the main emphasis being placed on the older economically more interesting geology. The Zululand coastal plain, being one of the main areas of Quaternary geology, has also suffered from the lack of attention. Over the last decade or two, a considerable amount of geological research has been done on the southern part of the coastal plain, south of Lake St Lucia. As a result of the heavy mineral mining activities north of Richards Bay and the proposed mining along the dune cordon east of Lake St Lucia, a substantial amount of new information has been accumulated for the coastal dune cordon and in its immediate vicinity (Fockema, 1986). In addition, the development of the town of Richards Bay and all the infrastructure associated with this development in the late 1960's and early 1970's, has provided a wealth of information on engineering geological aspects.

The northern half of the coastal plain, north of Lake St Lucia, and which includes the largest part of the coastal plain, has not been so fortunate in terms of new geological information. The information on post-Cretaceous geology is almost exclusively restricted to the records of a few deep oil exploration boreholes (Wolmarans and Du Preez, 1986; Du Preez and Wolmarans, 1986) and boreholes drilled for a geohydrological study of a small portion in the Muzi swamp area north of Lake Sibayi (Kruger and Meyer, 1988).

Some of the more important sources of information on the geology of the Zululand coastal plain, apart from the ones mentioned above, are by the following authors: Frankel (1960), Maud (1961), Van Wyk (1963), Frankel (1966), Orme (1973), Hobday and Orme (1974), Maud and Orr (1975), Stapleton (1977), Worthington (1978), Hobday and Jackson (1979), Dingle *et al* (1983), Tinley (1985), Fockema (1986), Kruger and Meyer (1988), McCarthy (1988) and Davies *et al* (1992). Reference is also made to unpublished reports made available by the Department of Water Affairs and Forestry, the Geological Survey of South Africa and numerous internal reports of consultants. A geological map, compiled from the 1:250 000 map sheets, is shown in **Figure 1**. A description of the geological succession is listed in **Table 1**.

**Table 1:** Simplified geological sequence for the Zululand Coastal Plain

Age (ma)	System/Period	Series/Epoch	Etage	Group	Formation	Lithology
0.1	Quaternary	Holocene (Recent)				Alluvium, dune, aeolian and beach sands
<1.6		Pleistocene	Upper Pleistocene		Berea	Sand, red clay rich sand
			Middle Upper Pleistocene		Bluff	Calcareous sandstone
			Lower Pleistocene		Upper Port Durnford	Sand and sandstone
						Lignite
					Lower Port Durnford	Clay rich sandstone
1.6 - 65	Tertiary	Late Miocene to Pleistocene			Uloa	Calcareous sandstone and coquina
		Palaeocene	Thanetian - Danian		Zululand	St Lucia
65 - 146	Cretaceous	Late Cretaceous	Albian - Cenomanian	Mzinene		Glauconitic siltstone
		Early Cretaceous	Upper Barremian - Upper Aptian	Makatini		Conclomerate, sandstone and siltstone
146 - 208	Jurassic			Lebombo	Mpilo/Movene	Amygdaloidal trachybasalt
					Jozini	Riodacite and rhyolite
					Letaba	Basalt and rhyolitic lava

## 2.2 Geological succession

### 2.2.1 *Basement rocks (Cretaceous age)*

For the purpose of this study, the rocks of Cretaceous and Palaeocene age can be regarded as the "basement rocks". This succession of mainly siltstones, conglomerates and sandstones is collectively known as the Zululand Group and comprises three formations; the St Lucia, Mzinene and Makatini Formations. The fine siltstones are virtually uniform with occasional thin bands of hard sandy limestone. Apart from having a very low permeability, the quality and quantity of ground water encountered in these formations is extremely poor (TDS >8 000 mg/l), and therefore are regarded as the "basement" rocks for this study. The siltstones range in age from late Cretaceous to early Palaeocene (Orr and Chapman, 1974). Kennedy and Klinger (1975) introduced the name St Lucia Formation for all the Cretaceous bedrock in the Zululand coastal plain. Since the lower Palaeocene strata possess an identical lithology, and there is no evidence of a pronounced unconformity at the Cretaceous/Palaeocene interface, the Palaeocene, for practical purposes may be regarded as part of the St Lucia Formation. On the geological map 27½32 St Lucia, the term Richards Bay Formation has been introduced to describe these Palaeocene age siltstones. According to Stapleton (1975), the Palaeocene deposits are thought to have originated during times of climatic changes. Although these siltstones are lithologically very similar, it does appear that a geoelectrical distinction can be made based on the interpretations of geoelectrical sounding data (see Section 6). The strike direction of the Cretaceous formations is roughly parallel to the coast and dipping towards the coast at an angle of 3-5°.

### 2.2.2 *Tertiary age sediments*

The Cretaceous age sediments are overlain by a sequence of mainly calcarenites in turn overlying basal boulder beds. These relatively thin Miocene age sediments are geohydrologically very important as they can be regarded as one of the main aquifers in the succession (Worthington, 1978). The best outcrops of these rocks occur at Uloa, Sapolwana (Umfolozzi plain) and Lake View along the Pongola River. Maud and Orr (1975) have described the Miocene strata as comprising a lower coquina and an upper calcarenite. Because of the outcrops at Uloa, this sequence was given the name Uloa Formation. The coquina rests unconformably on the siltstones, is hard and coarse and contains abundant fossils. The upper surface of the coquina has apparently been subject to karst solution weathering prior to the deposition of the overlying calcarenite. Cooper and McCarthy (1988) are of the opinion that the Uloa Formation, which grades up into the overlying aeolianites is the result of marine regression. The age of the Uloa Formation is currently disputed. Most authors are of the opinion that the Uloa is of Miocene age (~20 Ma), although a much younger middle Pleistocene age is attributed to this formation by McMillan (1987, 1993). Following an intensive geohydrological investigation in the Richards Bay region, Worthington (1978) was of the opinion that the Uloa Formation occurs in lower lying areas or valleys eroded into Cretaceous age rocks.

### 2.2.3 Pleistocene deposits

The Miocene sediments are extensively overlain by a thick succession of loosely consolidated sands, silts, clays and lignite. The lower late Middle Pleistocene age sediments are known as the Port Durnford Formation and are described in detail by Hobday and Orme (1974). The Port Durnford Formation has been described in the Richards Bay area as comprising of a lower, more argillaceous layer, separated from an upper arenaceous layer by a persistent but discontinuous lignite band. This lignite band was formed over larger areas and was observed in a borehole near Kosi Bay by Kruger and Meyer (1988). The Port Durnford Formation is found in boreholes along the entire coastal dune cordon. The upper surface varies between about 40m amsl near Richards Bay to about 50m amsl near Mbazwana (Fockema, 1986; Kruger and Meyer, 1988; Davies *et al*, 1992). The total thickness of the Port Durnford has been recorded as 25-30m by Worthington (1978) in the Richards Bay area. However, Davies *et al* (1992) reported thicknesses of up to 70m in boreholes north of St Lucia.

### 2.2.4 Younger unconsolidated deposits

The Port Durnford Formation is overlain by fluvial and aeolian sands of Middle to Upper Pleistocene and Holocene age. These sands are predominantly fine grained, contain an average of about 5 % silt and clay (Davies *et al*, 1992; Meyer *et al*, 1993) and are largely unconsolidated. Extensive exposures of clayey red sand, especially more inland, has been termed the Berea-type clayey red sand (McCarthy, 1992). These red sands are the result of intense weathering of dune rock. Although it has mainly formed from late Tertiary aeolianites, it is also known to have formed from younger aeolianites. Weathering and oxidation of minor iron-bearing silicate minerals in the sand form clay and hematite, the latter producing the deep red pigmentation of the weathered mantle.

The Zululand coastal plain is known for its numerous palaeo-dune cordons. In the northern part of the coastal plain six dune cordons can be distinguished progressively increasing in age away from the coast. The most pronounced and youngest of these is the coastal dune cordon stretching all the way from Port Durnford in the south up to the Mocambique border in the north. These dunes are up to 60m amsl. An extensive description of these dunes is given by Davies *et al*, (1992) and Meyer *et al*, (1993). Davies *et al*, (1992) described the typical dune succession at Eastern Shores as follows: "*Deposited onto the Port Durnford Formation are interlayered calcareous sandstones and uncemented sands which are up to 40m thick in places. These are followed by what is termed 'Older aeolian sands' which in turn is overlain by 'Coversands'*". The coversands are mined for their heavy mineral content and contain occasional calcrete nodules. No layering of any form has been observed during an extensive drilling program at Eastern Shores (Davies *et al*, 1992; Meyer *et al*, 1993). These coversands are most probably of Holocene age and extend to depths exceeding 70m. The "older aeolian sands" possess a marginally higher fraction of silt and clay particles and are considered to be of Late Pleistocene age (Davies *et al*, 1992).

## 2.3 Geophysical investigation and techniques used

Previous experience on the Zululand coastal plain and in other similar situations, has indicated that because of the contrast in resistivity and low contact resistance, depth penetration capabilities and the speed of operation, electrical techniques are the most suitable and cost effective geophysical techniques to apply in the circumstances (Van Zijl, 1971; Australian Groundwater Consultants, 1975; Worthington, 1978; Meyer and De Beer, 1981; Meyer *et al* 1982; Meyer *et al*, 1983; Meyer *et al*, 1987; Coetsee, 1991). Therefore the emphasis was placed on the direct current and electromagnetic sounding techniques. The Directorate Geohydrology of the Department of Water Affairs and Forestry suggested that the gravity method also be applied to detect some palaeo-erosion features. In the Environmental Impact Report (EIA) regarding the proposed mining along the Eastern Shores of Lake St Lucia, it is mentioned that the Ground Penetrating Radar technique has been tried without success to determine the internal dune structure of the coastal dunes (Coastal and Environmental Services, 1992).

## 2.4 Electrical methods

### 2.4.1 Direct current resistivity technique (Schlumberger array)

The method of Schlumberger electrical sounding essentially involves the passage of an applied current  $I$  into the ground through two current electrodes and the measurement of the resulting potential difference  $\nabla V$  between a second electrode pair. From a knowledge of the geometry of the electrode arrangement it is possible to calculate the apparent resistivity of the subsurface as viewed by the configuration. By expanding the electrode configuration about a fixed reference point, a sequence of apparent resistivity values can be obtained which relate to progressively greater, and therefore deeper, volumes of earth. These data are plotted as a sounding curve which depicts the variation of apparent resistivity with current-electrode spacing, the latter serving as a pseudo-depth. The object is to obtain, by graphic or analytical interpretation of the sounding curve, the vertical distribution of electrical resistivity beneath the reference point in the form of a horizontal layering of discrete intrinsic resistivities.

The sounding data compiled for this report consist of 408 sounding curves (**Figure 2**). The majority of these soundings were done during the first phases of this project but work done previously in the area was also used extensively (Van Zijl, 1971; Australian Groundwater Consultants, 1975; Worthington, 1978; Meyer *et al*, 1987; Meyer *et al*, 1989a; 1989b). Most of the electrical soundings were expanded to maximum current electrode (AB) spacings of 1km, but several, especially those used for calibration purposes at boreholes had longer AB spacings, with AB = 6 km being the maximum used.

#### 2.4.2 *Types of sounding curves*

Sounding curves are predominantly of the descending type (or Q, QQ and QQQ type) which indicates a decrease in resistivity with the depth. **Figure 3** shows a typical example. At short current electrode spacings, corresponding to a small depth of investigation, the apparent resistivity is high ( $>4\,000\text{ ohm.m}$ ) indicating the dry surface sand (Holocene age). Following this, the resistivity decreases with depth with indications of a thick layer with a resistivity below  $100\text{ ohm.m}$  (the Upper Pleistocene?) and finally the sounding curve flattens out at large current electrode spacings to approach a value of around  $4\text{ ohm.m}$ . This layer indicates the Cretaceous/Palaeocene siltstone unit.

In some of the longer soundings, the presence of the resistive basement could be observed at the longest AB spacings. The sounding curve at ES 85, where the maximum current electrode spacing (AB) was 6 km, is a good example (**Figure 4**). The minimum value the curve attains is  $5.5\text{ ohm.m}$  which means that the true resistivity must be somewhat lower. This conductive layer represents the Cretaceous/Palaeocene siltstone unit. The final segment of the curve, however, rises again and is the manifestation of the more resistive rocks of the Lebombo Group which are expected to underlie the siltstones in this region.

Representative sounding curves measured on outcrops of the different geological formations or sequences are given in **Figures 5 to 8** (Lebombo, Makatini, Mzinene, St Lucia, Uloa, Port Durnford, Berea formations and Holocene sediments).

#### 2.4.3 *Goelectric layer resistivities*

Using all the geoelectric data available Worthington (1978) compiled a histogram of surface-measured formation resistivities and divided the geological succession into four geoelectric units. These are shown in **Figure 9**. With additional data collected after Worthington's survey, it became apparent that the Middle-Palaeocene/Late Cretaceous siltstones (geoelectric Unit 4), with a resistivity range of  $3\text{--}15\text{ ohm.m}$  can, however, often be divided into two units, an upper more resistive unit, and a lower, more conductive unit. Otherwise the classification scheme used by Worthington still holds. The extended biostratigraphic, lithostratigraphic and geoelectric subdivision of the Cenozoic and Mesozoic succession is given in **Table 2**.

#### 2.4.4 *Calibration soundings*

Electrical resistivity soundings were done near all existing boreholes where reliable geological control was available in order to be able to calibrate the interpretations. The interpretations (layer resistivities and thicknesses) were adjusted to correspond to the geological borehole information until a good fit to the field data was obtained. In this way a narrow range of resistivity values were obtained for the different geological formations and these were then used to interpret the rest of the sounding curves.



**Table 2:** Correlation of the biostratigraphic, lithostratigraphic and geoelectrical subdivisions of the Cenozoic and late Mesozoic succession on the Zululand Coastal Plain (Adapted and extended from Worthington, 1978).

Biostratigraphic range	Lithostratigraphic range	Geoelectric Unit	Resistivity range (ohm.m)	Approximate position of geological formations
Holocene - latest Pleistocene	Dune and beach sand	Surficial Units 1(a) and 1(b)	250 - 7 500	----- Berea Formation
Late Pleistocene	Fine-grained aeolian quartz sand	Upper Pleistocene Unit 2	90 - 350	Bluff Formation
Middle Pleistocene	very fine-grained quartz sand	Middle Pleistocene Unit 3(a)	24 - 75	Port Durnford and Uloa Formations
Middle Palaeocene	Calcarenite, coquina	Miocene Unit 3(b)		
Late Cretaceous	Glauconite	Palaeocene? Unit 4(a)	8 - 15	St Lucia Formation
	Siltstone	Late Cretaceous Unit 4(b)	3 - 8	Mzinene Formation?

Examples of interpreted calibration curves are given in **Figure 10**. All borehole information, together with the sounding results obtained from DC soundings done on outcrops of the various geological formations, were used to compile a list of the variation in the apparent resistivity of the different geological formations (**Table 2**).

## **2.5 Electromagnetic soundings**

### **2.5.1 General**

A total of 68 Transient Electromagnetic Soundings (TEM) were conducted in the northern part of the Zululand coastal area. A Geonics EM-37 instrument was used for this survey. The results of 23 additional TEM soundings done previously are also included in this report. The localities of TEM soundings are shown on **Figure 11**.

To evaluate the TEM sounding results with the direct current (DC) results, a number of the TEM soundings were done at the same location as the DC soundings. The interpretation of some of the TEM soundings proved to be of a complex nature, due to the fact that the depth of investigation attained with the TEM method was restricted by conductive, near surface layers. A factor that reduces the effective use of the TEM method in the Zululand coastal area is that the TEM method is very effective in recognizing conductive layers, whereas the DC method recognizes both conductive and resistive layers as long as they are well defined in terms of thicknesses. Furthermore, it is well known that the absolute interpreted conductivity value for a certain layer differs, depending on the geophysical method that is being used. This makes a direct correlation between the two methods difficult. The successful application for the TEM method in the Zululand coastal area was further restricted by the fact that the conductive lower Port Durnford Formation was absent in certain areas. The TEM method defines the depth to the first conductive layer with a high degree of confidence, but it was often uncertain whether this conductive layer represents the lower Port Durnford, the Muzi or the Cretaceous Formations.

### **2.5.2 Calibration soundings**

The results of TEM measurements near boreholes in the northern part of the investigation area is shown in **Figure 12**. It was possible to achieve an excellent correlation between the TEM results and the actual borehole results for the depth to the Cretaceous floor in two cases, namely at boreholes ZD 1/71 and ZG 1/72 (**Figure 13**). In all the other cases, the Cretaceous floor was more than 20 m deeper than the interpreted depth to the conductive layer from the TEM results (**Figure 12**).

In the early phase of this investigation, the Uloa Formation was regarded as having a conductive character and that the top of this formation could be used as a conductive marker when dealing with the TEM method. However, as the investigation was extended to cover the whole of the Zululand coastal area, it became evident from

borehole and DC results that the lower Port Durnford and the Cretaceous formations are much more conductive than the Uloa Formation. The resistivity of the Uloa Formation falls in a range of 40-100 ohm.m, i.e. within the range of geoelectric Unit 3 (**Table 2**).

## **2.6 Gravity survey**

The Directorate Geohydrology, Department of Water Affairs and Forestry conducted a short gravity survey in the vicinity of St Lucia. The objective was to establish whether the gravity method could be used successfully to locate the palaeo-channels eroded into the Cretaceous and which have subsequently been filled with younger sediments. The survey was, however, unsuccessful due to the steep gradient of the gravity field observed along large sections of the South African coastline. Unless the regional gravity field can be removed successfully from the survey data, small perturbations on the gravity field, as would be expected under the conditions in Zululand, cannot be recognized successfully. The survey was abandoned after two profiles did not reveal the presence of a palaeo-channel identified by the drilling results.

## **2.7 Results of geophysical investigation**

### **2.7.1 Geoelectrical techniques**

As was discussed in the previous chapter, the electrical techniques gave the best results in terms of the depth to the Cretaceous basement. Although both these techniques result in a geoelectrical layered interpretation of the geological succession, it was not possible to unambiguously relate the different geological formations/units to specific geoelectrical layers. This is also clearly illustrated in **Table 2** which indicates a large range in and a large degree of overlap of the resistivities allocated to different geoelectrical/geological units.

From a comparison between the results of the resistivity (DC) and the electromagnetic (TEM) surveys in determining the depth to Cretaceous, it appears that with the TEM technique the top of the Uloa Formation could be mapped, whereas at the same locality the DC technique indicated the depth to the top of the Cretaceous. By combining the interpretations of the two techniques, the thickness of the Uloa Formation could therefore theoretically be resolved.

Our knowledge of the extent and occurrence of the Uloa Formation is, however, not sufficient to collect an extensive set of correlation soundings to be able to use the two techniques in a complimentary way to resolve the presence and thickness of the Uloa Formation across the Zululand coastal plain. The application of the TEM technique was therefore only restricted to the northern part of the coastal plain.

In view of the uncertainties associated with the results of the TEM interpretations, these interpretations were not used in the compilation of an elevation map of the top of the Cretaceous. **Figure 14** shows all boreholes drilled on the Coastal Plain where geological information was available, whereas **Figure 15** indicates those boreholes that intersected Cretaceous sediments and which were used for calibrating the resistivity and EM sounding interpretations. **Figure 16** shows those localities where the depth to Cretaceous could be confidently interpreted from the sounding curves. By combining all DC sounding interpretations and borehole information, separate contour maps of the depth to Cretaceous were compiled for the northern and southern parts of the Coastal Plain (**Figures 17 and 18**). These maps must, however, be seen as first approximations of the post Cretaceous topography as there are still several unresolved issues with regard to the interpretation of the geophysical data.

One significant feature, not revealed by the contour map, is the presence of an extremely wide palaeo-channel eroded into the Cretaceous floor rocks and subsequently filled by younger deposits. This channel is situated between Lake Sibayi and the coast. Interpretations of the geoelectrical data indicates an erosional depth to approximately ~120 m below mean sea level. This channel is almost 20 km wide and occurs over the entire length of Lake Sibayi. The existence of this channel could not be proved by drilling due to access and drilling restrictions, but the geoelectrical character of the material deposited in this area, differs significantly from that found to the north and south of Lake Sibayi. The implications this channel has on the seepage of water from Lake Sibayi is discussed later (**Chapter 5.3**).

### 2.7.2 *Geophysical borehole logging*

Geophysical borehole logging was not able to resolve the interfaces between the different geological formations uniquely. This is due to a lack of sufficient contrast in physical properties of the different units in the succession. The electrical logs were, however, used to calculate porosity values for the geological units using Archie's Law. The results are presented in **Table 3**. As can be seen from this table, a wide variation in the values calculated for porosity were observed. Because of the many assumptions made when applying Archie's Law, the porosity values should only be used as an indication of the relative porosity of the different horizons.

The unrealistically high value for the Uloa Formation (**Table 3**) may in part be due to karstified conditions developed in the formation. In comparison, the values listed by Davies, Lynn and Partners (1992) for the Eastern Shores area of St Lucia are also listed in **Tables 3 and 4**.

**Table 3:** Porosity determinations using "Archie's Law" where  $F = \rho_r / \rho_w = a\phi^m$  (with  $a=1$  and  $m=1.5$ )

Borehole	Depth interval	$\rho_r$ (ohm.m)	$\rho_w$ (ohm.m)	$\phi$ (%) ( $m = 1.5$ )	Geology	$\phi$ (%) Average
P110/1	0-8	430	19	12.4	0-15m Holocene deposits 15-31m Upper Port Durnford Formation	21
	8-12	160	19	24		
	12-16	160-60	19	24-46		55
	16-30	40	19	60.7		
	30-42	10	19	-		
	42-47	30	19	73.886	31-47m Uloa Formation	
P110/2	0-40	100	11	22.8	0-7m Holocene deposits	23
	40-54	100-20	11	22.8-67	7-55m Upper Port Durnford Formation	29
	54-72	25	11	57.7		
	72-78	52	11	35.3	55-84m Uloa Formation	49
	78-84	38	11	43.6		
P110/3	0-5	250	23	20.3	0-14m Holocene deposits	27
	5-16	140	23	29.8	14-54m Upper Port Durnford Formation	
	16-28	170	23	25.2		37
	28-33	170-110	23	26.2-52.6		
	33-57	110-60	23	35-52.6		69
	57-71	40	23	69	89-98 Upper Cretaceous	-
	71-87	62	23	51.5		
	87-98	15	23	-		
P110/4	0-2.5	50	55	-	0-2.5m Holocene deposits	31
	2.5-11	320	55	30.9	2.5-12m Upper Port Durnford Formation	
	11-17	40	55	-	12-17m Peat	
P110/5	0-7	66	5	17.8	0-16 Holocene deposits	16
	7-16	95	5	13.9	16-41m Upper Port Durnford Formation	
	16-21	140	5	10.7		
	21-28	70	5	17.1		
	28-41	64	5	18.1		16
P110/6	0-5	300	23	6917.9	Holocene deposits	28
	5-12	110	23	35	Upper Port Durnford Formation	27.5
	12-30	220	23	22		
	30-56	130	23	31.3	Uloa Formation	
	56-68	55	23	55.8		61
	68-75	40	23	69		

Average: Holocene ~23%; Port Durnford Formation ~31%; Uloa Formation > 50%(?)

**Table 4:** Porosity values for different geological sequences as derived from geophysical borehole logging and other techniques

Geological unit	Resistivity logging derived porosity	Porosity (as per Davies Lynn and Partners report (1992))
Holocene deposits	~23%	
"Cover sands" (Holocene)		38%
Older aeolian sands		36%
Port Durnford Formation	~31%	
Uloa Formation	~50%	42%

## CHAPTER 3

### GEOHYDROLOGY OF THE ZULULAND COASTAL PLAIN

---

#### 3.1 Aquifer description

Because all the formations above the Cretaceous floor rocks are composed of mainly quartzitic sands, many of which are unconsolidated to consolidated, they can all be treated as potential aquifer units. The report by Davies, Lynn and Partners (1992) indicated that the grain size distribution, as well as the porosity of the young Holocene age cover sands, the underlying more cemented aeolian sands and the Port Durnford Formation are virtually the same. The variation in permeability of these three units, listed by Davies, Lynn and Partners (1992) (from 0.8 m/d to 17 m/d) can in part be explained by the small variation (a few percent only) in the silt and clay content of the samples.

Borehole data, as well as hand dug wells and shallow augering have indicated that the arenaceous succession is generally fully saturated from the interface with the Cretaceous formations up to a frequently shallow water level. The data set of water levels collected during the study indicated a close relationship to the topography. This suggests that the near surface deposits possess a relatively low hydraulic permeability. This mimic of the topography by the water level, was used to interpolate water level information in areas where little or no data was available (see **Chapter 4**).

The many shallow wells (mainly hand dug) that exploit this shallow aquifer, have a low yield and are often equipped with hand pumps.

The next aquifer unit in the succession is the Upper Port Durnford Formation. This aquifer has not been exploited to any great extent, although north of Richards Bay new well fields have been developed recently in this formation with good success. Hydraulic permeability of the Port Durnford Formation has been determined for the Eastern Shores of Lake St Lucia and found to be around 4 - 5 m/d.

The study by Australian Groundwater Consultants (1975) and Worthington (1978) identified the Uloa Formation to be the most promising aquifers unit in the region. As described above, this formation consists of a coarse-grained shelly sandstone with calcarenite associated with it. The calcarenite has been observed in borehole core samples to contain some dissolution channels which increases its porosity significantly. This layer is however usually only a few metres thick and is not present everywhere. Thicknesses of up to 25 m have been reported. Worthington (1978) is of the opinion that the mode of distribution of this Miocene succession is determined to a large extent by the undulations in the erosion surface of the underlying Palaeocene siltstones.

Pumping tests results from this aquifer reported by Australian Groundwater Consultants (1975), Worthington (1978) and Simmonds (1990) indicated yields of up to 25 l/s in areas where this layer is more than 20m thick.

The permeabilities obtained from pumping tests are within the range of 0.5 - 23.6 m/d with an average of 4.5 m/d. Values for the storage coefficient range from  $1.9 \times 10^{-5}$  to  $4.7 \times 10^{-3}$  with an average at  $1.9 \times 10^{-3}$ . Most of the pumping tests revealed leaky confined aquifer conditions.

For the unconsolidated Holocene sands forming an unconfined aquifer, Kelbe and Rawlins (1992) used a specific yield of 35% and for the Port Durnford Formation a specific yield of 20% in their aquifer simulation studies.

## **3.2 Hydrochemisry and isotope studies**

### **3.2.1 Ground water chemistry**

Chemical analyses have been done on a number of water samples collected during the project. Additional data have been obtained from other sources (National Groundwater Data Base, forestry companies, Richards Bay Minerals). Particularly from the report of Australian Groundwater Consultants (1975) a large number of analyses were supplied from their study area of interest near Richards Bay. The analyses have all been entered in a HYDROCOM data base, set up for the Zululand coastal plain. Boreholes where water analyses were available or where additional water samples could be collected are shown in **Figure 19**. The resulting data, representing all chemical ground water data for the Coastal Plain are presented as Piper, Durov, Schoeller, and SAR diagrams (**Figure 20**).

The overall quality of the water is good (conductivity generally  $<100$  mS/m). The chemical pattern is generally similar to that of sea water with respect to Na, Cl, and  $\text{SO}_4$  ratios corresponding to rain water in more concentrated form. The products of carbonate dissolutions are added to the water only to a limited extent because of the low occurrence of carbonate in the area - particularly close to the sea. Low pH values are therefore common.

Some clear differences in ground water quality are evident. The analytical results from boreholes in the area between the Lakes Nhlabane and Mzingazi are characterized by high conductivity ( $>200$  mS/m) and a clear Ca/Mg bicarbonate character. The search for an explanation for this distinct difference motivated the attempt to correlate water chemistry with geology, using statistical techniques.

The low number of samples (31) for which a specific geological association was known, prevented the use of standard multivariate statistical techniques (principal components,

cluster analysis, etc.). The chemical analyses of the available samples have therefore been subjected to a more qualitative method of data analyses which involves the construction of a 'fingerprint' table representing the ratio of concentrations of the different elements present in the samples. This method makes provision for the use of a small data set (i.e. relatively high uncertainties) in order to classify an unknown borehole water sample to either have originated from a specific lithological unit or to be a mixture of waters from different lithological units. The method entails making use of the 'fingerprint' table to determine strata of high probable origin following which a consideration of specific chemical ratios can yield the more probable geological association. A description of the data reduction and development of the 'fingerprint' table is given in **Appendix A**. The application is explained using some analyses selected from the Zululand water chemistry data base. The origin of some water samples thus determined is then compared with that of the geological borehole description and the depth from which the sample was taken.

From the examples in **Appendix A**, it follows that clear distinctions can be made between the more arenaceous units of the Upper Port Durnford, the lignite layer, and the Miocene sand and the argillaceous Lower Port Durnford, Uloa calcarenite and St Lucia mudstone. Difficulty was encountered in separating Lower Port Durnford from Uloa calcarenite due to the small difference in chemistry between their waters. The Upper Port Durnford was indistinguishable from the lignite layer. This could have been expected since the lignite layer is not an aquifer in the true sense of the word and the sample denoted as such is probably Upper Port Durnford water deriving chemical constituents from the lignite band. Most of the samples tested listed in **Appendix A** could indicate a single layer of the aquifer as the main source of the water.

### 3.2.2 *Isotopes in water*

#### Stable isotopes

Stable isotopes analyses of  $^{18}\text{O}$  and deuterium, were determined on most of the samples collected in the course of this project. Boreholes, and other water point locations where water samples were collected for isotope analyses are indicated on **Figure 21**. The aim was to characterize water types in the area. The initial work by Vogel and Van Urk (1975) near St Lucia, suggested that the isotopic composition of ground water might decrease from the coast inland. It appeared that this could be a useful tracer to follow ground water movement.

The accumulated data set of  $\delta^{18}\text{O}$  analyses in ground water indicated no significant isotopic variation (**Figure 22**). The isotope survey of rainfall also indicated such a constancy of isotope values throughout the area (see **Chapter 4.4**). The explanation for this lack of a "continental effect" must probably be sought in the very flat topography of the area and the episodic nature of the rain storms occurring in this area.



Surface waters (lake and rivers) show isotope enrichment with both  $^{18}\text{O}$  and deuterium (**Figure 24**). This is a generally known feature due to evaporation enrichment (Gat and Gonfiantini, 1981) during winter, but also during dry periods of summer. It appears that large lakes (e.g. Sibayi) have higher  $\delta^{18}\text{O}$  values than small pans. In the case of the latter, the depression (in this area at least) is essentially cutting below the water table and it appears that the water is just flowing through the pan system. The higher  $\delta^{18}\text{O}$  content of the large lakes was used as tracer to distinguish it from ground water to follow leakage of lake water towards the sea (see 3.3 below).

$\delta^{18}\text{O}$  and chloride time series were obtained from Lake Sibayi and Lake Bhangazi. These will be discussed below in the context of leakage studies from these lakes.

### Radiocarbon

A few ground water samples from existing (shallow) boreholes were collected for  $^{14}\text{C}$  analysis. The results (**Table 5**) indicated high  $^{14}\text{C}$  values typical of post-1960 recharge ( $^{14}\text{C} > 90\%$ ). This is in accordance with the high throughflow of water through the aquifer deduced from recharge estimates and modelling. The single lower  $^{14}\text{C}$  value (MT12) can be interpreted as considerably older (up to a few hundred years), but part of this  $^{14}\text{C}$  lowering is also due to the higher alkalinity of the sample (from carbonate solution). Overall, the high  $^{14}\text{C}$  values indicated that this isotope would not be very useful here, because of the high recharge rate.

The 120%  $^{14}\text{C}$  value of Lake Sibayi confirms the  $\delta^{18}\text{O}$  and modelling data that the lake water has a considerable residence time since it has had ample time for isotopic exchange of carbon and water with the atmosphere.

## 3.3 Ground water leakage to the sea

Stable isotopes were successfully used to indicate the movement of lake water through and below the dune cordon to the sea. The largest of the isolated lakes, Lake Sibayi (Allanson, 1979), is 70km<sup>2</sup> in extent, and separated from the sea by dunes which at places are up to 160m high and 1-2km wide, along a 10km length. The water level in the lake is approximately 20m above mean sea level and is in hydraulic contact with ground water levels in the sands around the lake. The average chloride content of the lake water (130 mg/l) is about three times that of the surrounding ground water, and remains very constant throughout the year. The  $\delta^{18}\text{O}$  content of the water is +2.2‰ SMOW, indicating that it represents a water body subject to extensive evaporation (Gat and Gonfiantini, 1981). This closed lake drains ground water from the inland areas, and the fact that its salinity remains low, suggests that a considerable water flow through the dune towards the sea must exist (Pitman and Hutchinson, 1975).

**Table 5:** Radiocarbon content of ground and surface water samples.

Sample no.	Name/Locality	Depth (m)	Analysis no.	$^{14}\text{C}$ (‰ modern)	Model age	$^{18}\text{O}$ (‰ SMOW)	$^{13}\text{C}$ (‰ PDB)
MT2	Ozabeno borehole	39m	Pta-4855	$103.5 \pm 0.8$	<30 year	-3.8	-21.1
MT10	Mftholweni borehole	40m	Pta-4845	$107.8 \pm 0.8$	<30 year	-3.6	-8.5
MT9	Phelendaba IDC borehole	29m	Pta-4849	$100.8 \pm 0.8$	<30 year	-1.0	-6.1
MT12	Mangusi Police borehole	30m	Pta-4893	$83.0 \pm 0.9$	<30 year	-2.2	-13.8
MT17	Mungu well	Shallow	Pta-4878	$116.7 \pm 0.9$	<30 year	-3.0	.11.7
MT18	Lake Sibayi	Surface	Pta-4861	$120.7 \pm 0.9$	<30 year	+2.1	-2.3

A set of water samples was collected over a two-year period by ourselves and by DWA&F staff servicing the water level gauge on the eastern end of Lake Sibayi. The very constant  $\delta^{18}\text{O}$  and chloride content (**Figure 24**) indicates that the lake is not sensitive to seasonal inflow and that the water body represents the throughflow of quite a number of years. This is consistent with the  $^{14}\text{C}$  content of 120% modern, which is higher than any of the ground water samples analyzed in the area and equal to the atmospheric value.

An occurrence of fresh-water seepage was found on the beach at Gobey's Point, opposite the southern end of Lake Sibayi. During Spring low tide, water emerges from under the dune onto the beach just above a horizontal sheet of calcified beach rock (**Figure 25**). A sample of the seepage water was found to have a  $\delta^{18}\text{O} = +1.85\text{‰}$  SMOW and a chlorinity of 6 g/l. Compared with the available values of Sibayi water ( $\delta^{18}\text{O} = +2.2\text{‰}$ ), local sea water ( $\delta^{18}\text{O} = +0.6\text{‰}$ ) and likely ground water ( $\delta^{18}\text{O} = -4$  to  $-2\text{‰}$ ) around the lake, it was evident from the position of the Gobey's Point sample on the possible mixing lines that the relatively fresh water seepage sampled on the beach was a mixture of Lake Sibayi water and sea water (**Figure 26**). There is no way that the normal ground water in the vicinity can be considered as the water source of the seepage, since its  $\delta^{18}\text{O}$  value is lower than any of the other components. This was confirmed with deuterium, where again the Gobey's Point sample located between Lake Sibayi and sea water (**Figure 27**), and away from the meteoric water line representing rain and ground water. The high salt content measured in the seepage is ascribed to sea water left behind in the beach sand during low tide which mixes with the fresh seepage water. See also **Chapter 5** for a discussion on the seepage from Lake Sibayi.

A similar fresh water occurrence along the coast near the Cape Vidal light house (north of St Lucia) has also been studied. Natal Parks Board staff supplied regular samples of this seepage and from Lake Bhangazi, just west of the dune from Cape Vidal. The  $\delta^{18}\text{O}$  and chloride data are more complex here compared to those of Lake Sibayi (**Figure 28**). Lake Bhangazi shows the effect of summer rains as a slow drop of the  $\delta^{18}\text{O}$  and Cl contents after January 1991. During the following (very dry) summer, the  $\delta^{18}\text{O}$  content rose markedly to values similar to Lake Sibayi (due to evaporation enrichment). The Cape Vidal seepage follows the lake water somewhat w.r.t.  $\delta^{18}\text{O}$ , without copying the major detail (**Figure 28**). Even though  $\delta^{18}\text{O}$  values are close to that of sea water, the low chloride contents of the seepage compared with sea water (19 000 mg/l) preclude the latter from being a major contributor (**Figure 29**). The combined evidence of  $\delta^{18}\text{O}$ , Cl and D suggest that this seepage is due to mixing between an evaporated water (Bhangazi) and local rain or ground water (**Figure 30**) with some occasional minor sea water addition to raise the chloride level.

The hydrology around Lake Bhangazi differs from that at Lake Sibayi, and probably causes the difference in the isotope character of seepage at Gobey's Point and Cape Vidal. At Lake Sibayi, a pressure head of approximately 20m exists, whereas at Lake Bhangazi it is only of the order of 6-7m. The surface area of Lake Bhangazi is about

3km<sup>2</sup>, compared with the ~70km<sup>2</sup> of Lake Sibayi. To the south of Lake Bhangazi, a large swamp area, the Mfabeni Swamp, is present which is an expression of the ground water level in the area. Lake Bhangazi is believed to act as a feeder to the Mfabeni Swamp, which eventually drains into Lake St Lucia. According to water levels measured in boreholes drilled during the Environmental Impact Assessment at Eastern Shores (CES, 1992), there is a ground water divide between Lake Bhangazi and the sea. The maximum piezometric head of this divide is, however, close to that of the water level in the lake. This may explain in part the different isotopic signature observed in the seepage water at Cape Vidal.

### **3.4 Rain water chemistry**

#### **3.4.1 Sampling**

After commencement of the project, the Steering Committee recommended that rainfall chemistry be included in the work programme. The object was to determine ion correlations in rain-water and ground water and use these to estimate the recharge to the aquifer.

A network of rainfall collecting stations was therefore established and operated for the largest part of three rainy seasons. That this period included the very dry 1991/92 season is in a sense useful, since it enabled the effect of wet/dry seasons to be investigated. The stations were selected to study the variation in rainfall chemistry over the area north of St Lucia and to provide a range of distances from the coast (Murgatroyd, 1983) and north/south variation with due regard to the availability of existing rain gauge stations and reliability of operators.

The locations of the six stations used are shown in **Figure 31** and relevant station details are indicated in **Table 6**.

Rainfall samples were collected as part of the standard weather observation routine. Daily precipitation samples were poured into a large container in the morning, when the rainfall for the past 24 hours was recorded. Once a month a 100ml sample from the monthly composite was dispatched to the laboratory for analysis. The rain gauges were standard Weather Bureau rain gauges (except at Phelendaba where an open cone gauge was used) and evaporation is considered to have been negligible. Initial experiments with monthly rainfall samplers were abandoned when it became evident that too much evaporation occurred in these samplers. At Phelendaba a few samples from large single rainstorms were also collected and compared with the monthly composites. No attempts were made to obtain onsite measurements of pH or other parameters, since this was deemed to be beyond the interest and capabilities of the sample collectors.

**Table 6:** Details of rainfall stations

Code	WB No.	Station	Authority
MBA	0412/180	Mbazwane Plantation	Kwazulu Department of Agriculture and Forestry
SOD	0376/302	Sodwana Bay	Natal Parks Board
MAK	0411/323	Makatini Agricultural Research Station	(then) Department of Development Aid Kwazulu
MAN	0412/466	Manzengwenya	Department of Agriculture and Forestry
PHE	0412/096	Phelendaba (Muzi)	IDC
TEM	0411/723	Tembe Elephant Park (Sihangwana)	Kwazulu Bureau of Natural Resources

The monthly composite samples were analyzed at the CSIR in Pretoria for  $^{18}\text{O}$  and deuterium, and for chemistry at the CSIR laboratory in Stellenbosch. Originally only the major cations and anions were analyzed, but others ( $\text{NH}_4$ ,  $\text{NO}_3$ , P) were added later to improve the ion balance.

Rainfall amounts were obtained from the samplers and confirmed from the authority to whom they have been reported. Good cooperation could be established with the samplers, resulting in a high collection reliability. For the period October 1989 to June 1992, between 86% and 100% of the rainfall at each station was collected.

### 3.4.2 Rain water chemistry

A data set of 157 useful rain-water chemistry analyses were obtained of which 95% showed cations and anions balanced to within 10% of each other. This is quite satisfactory in view of the low ion concentrations involved. The product of monthly rainfall amount and concentration yields the monthly salt deposition (expressed in kg/ha; 1kg/ha = 0.1g/m). This is the quantity relevant for salt balance and recharge calculations.

Statistical relations between the ion concentrations show good correlations between Na, Cl, Mg, and  $\text{SO}_4$  (Table 7). These are the main constituents of sea water and their correlation supports the model that seawater is the main source of salt in the rain. There is also a fair correlation between Ca and alkalinity identifying calcium carbonate as another salt source in rain. Principal component analysis of the same data set yielded a first principal component (PC1) weighted with Na, Cl, Mg, and  $\text{SO}_4$  a second one (PC2) weighted with Ca and alkalinity (Figure 32). Together these two principal components account for 84% of the variation of these ions in the rain samples analyzed.

A more direct composition model can be calculated by using the average of Na and Cl (suitably weighted) to indicate the sea water addition to the rain-water chemical

composition and then correcting Mg, SO<sub>4</sub>, Ca, and alkalinity proportionately. The average of the Ca and alkalinity remaining, is then used to indicate the CaCO<sub>3</sub> addition to the rain-water chemistry (Mamane, 1987). This simple addition model, similarly, accounts for 85% of the dissolved ions in the rain water with no obvious other relations in the remaining ion quantities.

**Table 7:** Correlation matrix of major constituents of rain-water (based on 157 analyses)

	Na	Cl	Mg	SO <sub>4</sub>	Ca	K	Alk
Na	1	0.99	0.97	0.74	0.61	0.57	0.50
Cl		1	0.96	0.71	0.59	0.53	0.43
Mg			1	0.81	0.66	0.65	0.55
SO <sub>4</sub>				1	0.59	0.65	0.36
Ca					1	0.47	0.74
K						1	0.64
Alk							1

Chemical concentrations of the collected rain water samples were used to calculate chloride deposition (**Appendix B**). Missing values (chloride, rainfall or samples not analyzed) were interpolated, using general features of these parameters. In this way, a data base covering three complete rainfall seasons (1989-1992) from August to July, was established, from which annual deposition rates were calculated.

Large variations of Ca and Cl deposition are evident from year to year through the very variable rainy periods encountered during the three-year sampling period (**Figures 33 and 34**). The annual chloride deposition rate relates to the rainfall amounts to some extent (**Figures 35**). The outlier chloride deposition of MAN in 1991/92 (compared with its annual rainfall) is due to two high chloride analyses (October 1991 and February 1992). While no sampling or analysis problems for these samples could be traced, the data look suspicious, and were reduced by a factor 3 for application in the three-year average used for recharge calculation (**Chapter 3**). The average values of the three complete seasons are then considered to represent a good long-term average.

The dominant feature of the ion distribution over the area is the rapid decrease of total salt deposition with distance inland (**Figure 36**). This was observed by earlier workers in the area (Murgatroyd, 1983; Archibald and Muller, 1987) and is a common feature worldwide (Junge and Werby, 1958; Hingston and Gailitis, 1976). The chemical character of the rain water composition changes by the rapid decrease of the sea water contribution, while the calcium carbonate contribution does not decrease all that much (**Figure 36**). This suggests that the CaCO<sub>3</sub> component could be a recirculated constituent, i.e. not a constituent transported from elsewhere. The source of this

carbonate is, however, not evident. The entire area is a typically acidic, non-calcretic humid environment where carbonate dust is not expected to occur in great abundance.

**Table 8:** Chloride deposition at rainfall stations (annual rainfall (mm) in brackets).

	Distance from sea (km)	Chloride deposition (in kg/ha/yr) and annual rainfall (in mm)			Average chloride deposition (kg/ha/yr)
		1989-90	1990-91	1991-92	
<b>Sodwana (SOD)</b>	0.5	114.8 (1516)	116.2 (1764)	51.8 (408)	94.3
<b>Manzingwenya (MAN)</b>	4	49.1 (986)	128.7 (1652)	137.7* (546)	74.6
<b>Mbazwane (MBA)</b>	8	57.6 (1239)	78.3 (1618)	48.0 (515)	61.3
<b>Phelendaba (PHE)</b>	24	27.2 (851)	28.2 (963)	25.0 (309)	26.8
<b>Makatini (MAK)</b>	44	24.0 (806)	20.3 (904)	10.0 (337)	18.1
<b>Tembe (TEM)</b>	50	22.5 (986)	20.8 (963)	18.5 (405)	20.6

Note: \* Probably too high by factor 3 (Figure 36). Corrected before averaging.

### 3.4.3 Isotopes in rainfall

Oxygen-18 analyses of the monthly rain water samples for all six collecting stations show a seasonal relation with low  $\delta^{18}\text{O}$  values during the summer and high values in winter (**Figure 37**). In some cases an inverse relation between rainfall and  $\delta^{18}\text{O}$  seems to exist (the so-called amount effect), but on a monthly basis, this is not very clear.

Deuterium analyses were also done on most rain water samples. The data show a good relation with  $\delta^{18}\text{O}$  along the known worldwide meteoric water-line (MWL) with only a few evaporated samples ( $\delta^{18}\text{O} > 0$ ) off the MWL (**Figure 38**). Most ground water samples are also located on this line (**Figure 23**).

The weighted (by precipitation amount) annual average  $\delta^{18}\text{O}$  content varies consistently from year to year at all the stations (**Figure 39**). This supports the "high  $^{18}\text{O}$  - arid season" linkage (Rozanski *et al.*, 1992) in a very convincing manner and suggest that, on an annual basis,  $\delta^{18}\text{O}$  could be used as rainfall indicator. Over the whole study area the variation of the mean annual  $\delta^{18}\text{O}$  content of rain varies less than 1‰ within the same year (**Table 9**).

The annual  $^{18}\text{O}$  values can be combined in a weighted mean for the three year period for which measurements are available. If one assumes that only a representative portion of the rainfall above a certain cut-off point actually contributes to recharge (Bredenkamp, 1980), then the weighting is even more directed to higher rainfall years and subsequently lower  $\delta^{18}\text{O}$  values of recharge (Table 9). Cut-off values between 300 mm and 500 mm/annum produce  $\delta^{18}\text{O}$  values of recharge in the vicinity of -3.5‰ which correspond to the best estimate of  $\delta^{18}\text{O}$  in un-evaporated ground water (Figure 22).

**Table 9:** Three-year  $\delta^{18}\text{O}$  average weighted by annual rainfall less a cut-off value

	Cut-off 0	300 mm	500 mm
<b>Sodwana (SOD)</b>	-3.09	-3.33	-3.38
<b>Manzengwenya (MAN)</b>	-3.28	-3.60	-3.84
<b>Mbazwana (MBA)</b>	-3.51	-3.79	-3.90
<b>Phelendaba (PHE)</b>	-3.35	-3.78	-3.76
<b>Makatini (MAK)</b>	-2.60	-2.87	-2.95
<b>Tembe (TEM)</b>	-2.90	-3.03	-3.21

### 3.5 Ground water recharge estimates

Ground water recharge estimates have been reported by Worthington (1978) and Meyer and Kruger (1987). Worthington used a water balance approach and calculated that the recharge in the vicinity of Richards Bay is approximately 24% of the mean annual precipitation (MAP). Using a rainfall recharge relationship proposed by Bredenkamp (1985) which is based only on the MAP, Meyer and Kruger (1987) reported a recharge figure of approximately 21% of MAP.

The main aim of the rain water chemistry programme (Chapter 3) was to estimate ground water recharge by the salt increase method of Eriksson (Eriksson and Khunakasem, 1969; Eriksson, 1985). This method has been applied with a great deal of success in Botswana recently and led to the production of a map from which the recharge of ground water from rainfall can be deducted (Gieske, 1992). If  $C_p$  is the chloride (or any other conservative salt) content of rain water, then the evaporation of rain on and in the soil will cause the chloride content to rise to  $C_w$ . The recharge (as a fraction of rainfall) will then be

$$R = C_p / C_w.$$

Assumptions inherent in this technique are:



- (i) No production or removal of the specific salt by any other process, e.g. windblown salt, is recirculated.
- (ii) Dry salt deposition should be added to the total salt load. For this reason, the calculation is done from total salt deposition x annual rainfall (See **Appendix B** for a more detailed description of the recharge calculation procedure).
- (iii) It is assumed that the ground water chloride represents only vertically recharged water and not laterally transported salt. Adaptations for the latter situations can be made (Eriksson and Khunakasem, 1969).

In the Zululand coastal plain, it was considered that the above conditions would be valid and that reliable data could be obtained. A similar approach to obviate the problem of (iii) above, is to analyse the salt content of the soil moisture in the unsaturated zone just above the water table (Edmunds *et al.*, 1990; Bredenkamp, 1993). This is a more complex procedure, and requires that the water table be below the root zone.

Average chloride contents for rainfall were obtained from the chloride deposition rates and annual rainfall amounts (**Appendix B**). Chloride contents of ground water were estimated from borehole samples in the vicinity of the rainfall collection stations.

The resulting recharge data, which indicated that the recharge varies from 18% near the coast to about 5% at a distance of 50 km inland, are about half of those obtained by Bredenkamp (1993), using chloride profiles in the soil from the unsaturated zone. Bredenkamp's profiles were obtained to the east and west of Lake St Lucia. The chloride content of the soil moisture in the case of the St. Lucia data appears to be about half of that measured in the ground water of the northern Zululand coastal plain. Since Bredenkamp used the same chloride input quantities, the resulting recharge values are therefore about double. It is at this stage not certain whether the situation near St Lucia is that much different from the more northerly region of the present study. Our selection of boreholes near the rainfall stations was very limited and the computed recharge values of **Table 10** should be considered as lower limits. Whether a distinct cut-off point exists below which no recharge occurs is uncertain, since our work was concentrated along the higher rainfall area of the coastal zone. More data of this nature are constantly being generated for southern Africa (Gieske, 1992; Bredenkamp, 1993; Bredenkamp, 1995), and a better overall picture will hopefully soon emerge.

These calculated recharge values derived with the chloride method are lower than earlier reported values, but are believed to be more representative for the coastal plain conditions. The main difference in the techniques are that, whereas the previous methods used a fixed percentage of the MAP over the entire coastal plain region, the chloride method calculated recharge (as a percentage of the MAP) varies with rainfall.

**Table 10:** Three-year average recharge data.

Station	Sodwana (SOD)	Manzengwenya (MAN)	Mbazwana (MBA)	Phelendaba (PHE)	Makatini (MAK)	Tembe (TEM)
Rainfall (mm)	1229	1061	1124	708	683	785
Cl deposit (kg/ha/yr)	94.3	74.6	61.3	26.8	18.1	20.6
Ground water chloride (mg/l)	45	40	40	40	45	50
Recharge (% of annual rainfall)	17	18	14	9.5	5.9	5.2
Recharge (mm/yr)	210	187.1	153	67	40	41

### 3.6 Potential for ground water pollution

Due to the essentially unconsolidated nature of large aquifers on the coastal plain, the aquifer is extremely vulnerable to pollution. There are, however, mitigating factors that can lower the risk of pollution.

Ground water pollution can be classified as either regional or localized. Regional ground water pollution arises from polluted rivers which are losing water to the hydrogeological regime, from contaminated rainfall, and from saline intrusion as a result of the lowering of the potentiometric levels in coastal areas. Along the Zululand coastal plain these criteria need not be considered on the three grounds that the streams are mostly gaining, the coastal setting is not susceptible to contaminated rainfall despite the development of petrochemical complexes in the industrial area, the heavy mineral mining of the dunes, and the coastal barrier complex acts generally as a ground water divide which affords strong protection against marine intrusion. Consequently, only localized pollution of ground waters need to be considered.

In an urban environment, localized ground water pollution can be induced by such diverse factors as sewage effluents from septic tanks and fractured or overflowing sewers, effluents from refuse-disposal sites or mine-waste dumps, miscellaneous industrial wastes, infiltration from horticultural land that has been treated with fertilizers or insecticides, the presence of cemeteries, quarries and disused wells, and to a much

lesser extent, transport accidents. However, the vulnerability of the ground water regime to these various forms of pollution can only be ascertained by a consideration of appropriate geological and hydrogeological factors.

The relevant geological factors involve the depth of burial of the aquifer and the lithologies of the aquifer itself and the overlying deposits. In general, the risk of pollution to a given aquifer decreases as its depth of burial increases. The vulnerability of the ground water regime decreases as the depth to the potentiometric surface increases. Although pollution will spread more rapidly in an aquifer of high transmissivity, this condition will also be conducive to the more rapid dispersal of pollutants. For a given aquifer transmissivity, the rate of advance of the pollution front varies with the hydraulic gradient. The significance of a source of ground water pollution diminishes at greater distances from points of outlet from the ground water regime, e.a. abstraction boreholes or zones of seepage into gaining rivers. Consequently, the direction of ground water flow is important. The vulnerability to pollution of an aquifer system decreases as the hydraulic conductivity of the overlying deposits decreases.

Worthington (1978) analyzed the pollution potential of the aquifers in the Mzingazi catchment in great detail. He made an appraisal of those geological and geohydrological factors that control ground water vulnerability to pollution and emphasized the importance of perennial streams. Based on this he produced a pollution vulnerability map for the Mzingazi catchment (**Figure 40**). He classified the area into 5 different zones according to the criteria listed in **Table 11**. It is clear that to be able to do such a detailed classification, an extensive data set of the aquifer is required. For the regional approach adopted in the present study, it was therefore not possible to assess the pollution potential to the same detail.

This classification around Richards Bay is still valid and should be taken into account when planning new residential and industrial areas around Richards Bay.

On a regional scale two potential sources of aquifer contamination can be identified. These are undesirable land-use practices (e.g. agriculture) and sea-water intrusion. The first source will include such land-use practices as large increase in population and settlements on the plains where the ground water level is shallow, and extensive development of the agricultural potential of the region. The development of settlements will result in increased loads of waste water and sewage effluent that has to be disposed of. The pollution potential can be reduced by restricting development to the topographically higher lying areas where the water table is deeper. The potential pollution associated with agricultural land-use practices, will depend on the degree to which fertilizers, pesticides and herbicides will be applied. Again, the aquifer is extremely vulnerable to pollution from this source, as agricultural development would probably concentrate on the low lying area. Careful planning of both new settlements and agricultural practice would be required in future.

Sea water intrusion appears not to be a major threat as the elevated ground water levels near the coast and associated with the dune cordon, form an effective intrusion barrier. However, if large scale abstraction would occur anywhere near the coast, monitoring of water levels and quality is essential to determine whether a reversal of the ground water flow direction may occur.

**Table 11:** Classification of proposed development zones within the Mzingazi catchment (Worthington, 1978)

Zone	Strata thickness	Pollution vulnerability
1	Miocene aquifer <10m Middle Pleistocene >5m Upper Pleistocene >10m	Very low risk
2	Middle Pleistocene >5m Miocene aquifer and Upper Pleistocene (either both > or both <10m)	Low risk
3	Miocene aquifer >10m Middle Pleistocene >5m Upper Pleistocene >10m <b>OR</b> Miocene aquifer <10m Middle Pleistocene <5m Upper Pleistocene >10m	Low to Moderate risk
4	Middle Pleistocene >5m Miocene aquifer and Upper Pleistocene (either both > or both <10m)	Moderate risk
5	Miocene aquifer <10m Middle Pleistocene >5m Upper Pleistocene >10m	High risk

## CHAPTER 4

### MATHEMATICAL MODELLING OF THE COASTAL PLAIN AQUIFER

---

#### 4.1 General

The numerical simulation of physical and engineering problems has become a standard practice with the advent of fast, available computers. The simulation of ground water movement is thus no exception. However, the importance of using mathematical and numerical models in accordance with their accompanying assumptions, has again been stressed recently (Hassanizadeh and Carrera, 1992). The reliability of the numerical model depends, furthermore to a great extent, on the data used in the development and verification of such a model. The numerical modelling of the Zululand aquifer should therefore be evaluated against this background.

The borders of the region will be discussed in the next section, as well as the data used for the development of the model. The finite element model used for the study will then be considered, together with a discussion of the verification of the model. In order to show the potential of the numerical model, the effect of a hypothetical afforestation around Lake Sibayi will finally be simulated and discussed.

#### 4.2 Geohydrology

The Zululand aquifer, shown in **Figure 41**, was assumed to be the region just south of Richards Bay up to just north of lake Kosi, coinciding with the border of Mozambique. The coastal plain pinches out against the mountains in the west, which was then used as the western boundary of the aquifer. The four bigger lakes, that is Lake St Lucia, Lake Sibayi, Lake Mzingazi and Lake Kosi, as well as Richards Bay, are included in this region. All these areas of open water were taken into account in the numerical model.

Information on the piezometric heads in the region was restricted to data gathered from the boreholes drilled in the region. The distribution over the aquifer of the 140 boreholes where water level information was available for the study can also be seen in **Figure 41**.

These boreholes were, however, monitored only sporadically over the period 1972 to 1991, and in most cases, information of a single observation only at a borehole exists. In order to obtain a workable sample of piezometric heads to evaluate the region with, all of these boreholes were used. The piezometric heads were therefore, contrary to normal practice, not specified for a specific time. The motivation for this is that the change in heads over the regional scale is very small. This means that contours of the piezometric heads drawn over the region at different times are in agreement with one another.

The velocity vectors, calculated from the piezometric heads at 140 boreholes are shown in **Figure 42**. The general movement of ground water towards the lakes and coast is, as expected, evident.

### **4.3 The finite element model**

The lack of sufficient data and the magnitude of the study area forced us to consider the aquifer on a regional scale. The implication of this is that, although the general movement of the ground water can be considered, predictions of the heads at individual boreholes cannot be done accurately.

A finite element grid was constructed over the region, containing 12 elements in the direction and 48 in the y-direction. This led to element sizes of one to five kilometres in the x-direction and two to four kilometres in the y-direction. The three bigger lakes, Lake St Lucia, Lake Kosi and Lake Sibayi, were excluded in the grid, shown in **Figure 43**. The final grid contained 618 nodes and 537 elements.

The boundary conditions implemented in the simulation were in accordance with the physical structure of the aquifer. That is along the coast, fixed heads or Dirichlet conditions of zero were specified, as well as for Lake St Lucia. The heads were kept at 20m at Lake Sibayi and at their initial values on the northern boundary. Due to the thinning of the aquifer on the western and southern boundaries, no-flow conditions or homogeneous Neumann conditions were used there.

The effect of rainfall was taken into account in the development of the numerical model. The average rainfall over the region varies between 1 200mm per annum at the coast to about 600mm inland, with the effective recharge varying between 18% and 5% in a similar way. The recharge to the aquifer in the model was therefore interpolated linearly between these two sets of figures.

In order to provide initial values for all the nodal points, the piezometric heads from the 140 known boreholes, although measured at different times, were interpolated to the 618 nodal points. The gradient interpolation methods, one of the features of the graphical package TRICON (Buys et al, 1992), proved to be very accurate, and was therefore used. The reason for using the heads measured at different times is, as stated above, due to lack of sufficient data. Contours of these initial nodal heads are presented in **Figure 44**.

### **4.4 Results from the finite element model**

The aim of the regional model was to provide not only a model capable of simulating the global reaction of the aquifer, but also simulating the piezometric head movement at

boreholes where these data exist. A value of  $100\text{m}^2/\text{d}$  was selected for the transmissivity of the region and 0,15 for the storativity. The aquifer was simulated with the two-dimensional confined model, GCON (Botha et al, 1990) for a one-year period. The contours of the piezometric heads after this one-year period are presented in **Figure 45**. The agreement between **Figures 44 and 45** is evident.

The simulated heads along a few grid lines, parallel to the x-axis, were also considered. The initial heads are presented as solid lines, with the heads as simulated after one year shown as dots, according to the legend, in **Figure 46**. The line numbers in the figure are counted from the bottom of the finite element grid. The figure again shows the ability of the model to simulate the movement of the ground water.

In the final evaluation of this preliminary numerical model, the observed movement of the piezometric heads for seven nodes were compared against the simulated values. These comparisons are shown in **Table 12**.

**Table 12:** The movement of the piezometric level as observed at a few boreholes compared to the simulated values in a one-year period.

Borehole / Node		Piezometric head changes	
Borehole no.	Nodal no.	Observed	Simulated
ES277	176	-0.5	-0.13
ES280	189	0.90	1.65
ES308	206	0.09	-1.27
ES299	214	1.31	0.84
ES339	220	0.20	-3.37
ES298	232	0.40	0.92
ES296	245	-1.29	0.37

Although the simulated movements of nodes 176, 189, 214 and 232 are in accordance with the observed values, it is evident from the other nodes that some more refinements are needed for the model to be calibrated.

#### 4.5 The impact of afforestation on the aquifer: A hypothetical case study

The ability of the numerical model to simulate the behavior of the regional Zululand aquifer was furnished in the preceding discussion. However, the limitations of the model, for example the scarcity of geohydrological data and the resulting large elements, restrict its use in forecasting the movement of ground water on a detailed scale. It was therefore decided to apply the model on a hypothetical case study to demonstrate the abilities of the numerical model.

The effect of plantations on the ground water level and, via the ground water, on the lakes, has been the subject of numerous studies in the past (Lindley and Scott, 1987). It was therefore decided to use the numerical model with various, but feasible combinations of rainfall and water yield to demonstrate the effect of afforestation around Lake Sibayi. The region selected coincides with 28 elements on the finite element grid, and can be seen in **Figure 41**, marked around Lake Sibayi. The water level at the lake was kept constant at 20m for all the simulations.

The volume of water consumed by trees varies at large, partially because of differences in species, but also because of differences in the climate in which the plantation reside. Catchment studies (Lindley and Scott, 1987), and also present investigations at forest research centres, indicate an increase in evapotranspiration from grasslands to forests in the order of 200mm to 2000mm annually. The effect of normal rainfall and variations of these evapotranspiration rates were therefore used in the numerical model to show their potential effect on Lake Sibayi.

The cases investigated, were recharge by rainfall of 150 mm per year, combined with evaporation rates, measured per unit area per annum, of 0 mm, 200 mm, 1 000 mm, 1 500 mm and 2 000 mm. The effect of one of these scenarios, that of 150 mm recharge and 2 000mm evapotranspiration, on the ground water levels, is shown in **Figure 47**.

The effect of the high water usage of the plantation on the ground water levels in the vicinity of the lake, can be seen by comparing **Figure 47** with **Figure 45**. Although the differences in the contours are restricted to the area where the plantation was specified, the simulation was done for one year only, and the effect of the plantation on the ground water levels will increase with time.

However, it is difficult to evaluate the effect of the different evapotranspiration rates on the large scale contour map. Two sections were therefore drawn through the lake, one parallel to the coastline and the other perpendicular to the coastline, marked AA' and BB' respectively on **Figure 43**. The simulated ground water levels for the five different evaporation rates, that is 0, 200, 1 000, 1 500 and 2 000 mm per annum, per unit area are compared in **Figures 48 and 49**.

The section perpendicular to the coastline, presented in **Figure 48**, shows a large natural gradient towards Lake Sibayi and the sea. However, this gradient decreases with an increase in the evaporation rate. This means less ground water will flow towards the lake, resulting in an eventual lowering of the water level in Lake Sibayi. **Figure 49** depicts the section parallel to the coast. Under normal conditions, that is with no evapotranspiration, ground water flows from both sides into the Lake. However, all the other cases shows a gradient out of Lake Sibayi, in a southerly direction.



The two sections show that an evapotranspiration rate of 1 000 mm per annum already causes a severe lowering in the ground water level around Lake Sibayi. The larger evapotranspiration figures, which can also be interpreted by being periods of continuous lower annual precipitation, only exaggerates these conditions.

The effect of the evapotranspiration can also be seen by comparing the direction of flow around the lake. In **Figure 50**, the direction of the flow of ground water around the lake and through the simulation area can be seen under normal conditions, that is of rainfall only. A mass balance of flow to and from Lake Sibayi, calculated with the simulation computer program, shows an equilibrium situation.

The extreme case of 150mm recharge, but 2 000mm evapotranspiration, or an effective discharge of 1 850mm per unit area, per year, can be seen in **Figure 51**. The flow vectors are drawn mostly away from the Lake. In this case, the mass balance shows a net outflow of  $8 \times 10^3 \text{ m}^3/\text{d}$  from Lake Sibayi. Therefore, Lake Sibayi will provide water to the plantation, resulting in a severe lowering of the water level in the lake.

#### 4.6 Conclusions

A numerical model for the Zululand aquifer was developed which could at least, on a regional scale, be used to make some predictions on the availability and movement of ground water in the aquifer. However, before detailed evaluations with the model can be undertaken, it has to be calibrated with and verified against a comprehensive set of geohydrological data for the region. This should include transmissivity and storativity values and ground water levels measured over a two- to three-year period, from a representative set of boreholes over the region.

The possible danger of over-utilization of the ground water by large commercial forests, especially during periods of drought, was outlined in a hypothetical case study. The ability of the ground water to act as a water reservoir is well-known and also illustrated in the hypothetical study. However, as with any ground water resource, it has a limited capacity, and should be managed as such.

## CHAPTER 5

### WATER BALANCE CALCULATIONS AND UTILIZATION OF THE GROUND WATER RESOURCES

---

Following the recharge estimates calculated from the chloride balance in **Chapter 3** above, and combining it with the water level contour data presented in **Chapter 4**, it is possible to derive a first estimate of a water balance for the northern part (surface area approximately 330 km<sup>2</sup>) of the study area. For this purpose that area of the coastal plain between the Mocambique border and the northern limit of Lake St. Lucia was chosen.

Using the available data, a water balance can be derived in two ways. Firstly by using the recharge estimates and secondly, using the ground water flow equation.

#### 5.1 Recharge driven water balance

In **Chapter 3** the recharge rate as a percentage of the mean annual precipitation and the distance from the coast was estimated. This ranges from 19% at the coast to 5% in the interior (**Table 10, Chapter 3**). The decrease of MAP with distance from the coast has been obtained from the MAP maps produced by Dent et al (1989). The rainfall onto this part of the Zululand coastal plain has been calculated to be  $3.3 \times 10^8$  m<sup>3</sup>/year. By integrating the MAP maps with the percentage recharge distribution an average figure for recharge (11%) and rainfall (900mm) over this area could be obtained. This results in an annual nett recharge to the coastal plain aquifer of about  $3.28 \times 10^8$  m<sup>3</sup>/y. If it is accepted that this total volume exits the coastal plain as seepage along the coast, a figure of  $3.28 \times 10^5$  m<sup>3</sup>/ y/km of coastline results.

#### 5.2 Flow equation derived water balance

A comprehensive set of permeability determinations of the sediments of the Coastal Plain is not available. Permeability values have been determined by Australian Groundwater Consultants (1975), Worthington (1978), Simmonds (1990) and Davies Lynn and Partners (1992). The most comprehensive set of permeabilities was derived for the EIA study the Eastern Shores area of Lake St. Lucia. Geologically the coastal dune cordon divided stratigraphically into "Cover sands", "Older aeolian sands", "Interlayered deposits" and Port Durnford Formation resting on a floor of Cretaceous age siltstones. Permeabilities determined for these different sequences are:

Cover sands	15.6 m/d
Older aeolian sands	0.87 m/d
Port Durnford Formation	4.3 m/d

By using the water level contour map (**Figure 44**) an average gradient towards the coast of 1:250 can be derived. Taking into account the relative thicknesses of the different geological formations, an average permeability of 5m/d is a realistic figure. This value compares favourably with that cited by Pitman and Hutchinson (1975). Worthington (1978) established an average permeability of 2,5m/d through pumping tests in the Richards Bay area. For an average aquifer thickness of 50m above the impermeable Cretaceous floor, a total flow from the northern part of the coastal plain aquifer towards the sea is calculated to be  $4.4 \times 10^7 \text{ m}^3/\text{y}$  or  $3.7 \times 10^5 \text{ m}^3/\text{y}/\text{km}$  of coastline. Although there is a fair agreement between the flow volumes derived with the two techniques, these values must be seen as a first approximation as the parameters used for the calculations are average values.

### 5.3 Preferential flow paths to the sea

There are selected areas where the ground water flow towards the sea is considerably more. One known area is the outflow from lake Sibayi. The geophysical results have revealed the presence of a deep erosion channel east of Lake Sibayi. Although untested by drilling, this erosional channel is believed to be filled with approximately 120-140m of Holocene age sediments with a permeability probably of the same order as that of the Cover sands at St. Lucia. Based on the difference in head between Lake Sibayi and the sea (approximately 20m) and assuming permeability values derived from pumping tests at Richards Bay, Pitman Hutchinson (1975) calculated that the seepage from the lake towards the sea to be between  $1 \times 10^5 \text{ m}^3/\text{y}$  and  $4 \times 10^5 \text{ m}^3/\text{y}$  per kilometre of the coast. However, these figures were based on the elevation of the impermeable floor being at -25m below mean sea level. The geophysical derived depth of the impermeable floor is on average -100m below mean sea level and the width of the palaeo-channel approximately 20 km. Using these figures and the same permeability values as Pitman and Hutchinson, the outflow is calculated to be between  $1.1 \times 10^8 \text{ m}^3/\text{y}/\text{km}$  and  $4.4 \times 10^8 \text{ m}^3/\text{y}/\text{km}$ . This is equivalent to  $5.4 \times 10^6 \text{ m}^3/\text{y}/\text{km}$  to  $2.2 \times 10^7 \text{ m}^3/\text{y}/\text{km}$  of coast. These figures should be compared to the volume of the lake calculated to be  $9.81 \times 10^8 \text{ m}^3$  (Ramsey, 1990). The ratio between the annual seepage from the lake volume in the lake, indicates a turnaround time of between approximately 2½ and 10 years. This estimate is consistent with the stable isotope data which indicated that the  $\delta^{18}\text{O}$  and chloride concentrations of lake water show almost no seasonal changes. This constant feature is an indication that the water remains in the lake for a number of years (See **Chapter 4**)

At least one more known occurrence of a similar type palaeo-channel is known to occur along the coast of northern Zululand. During drilling to establish the geological succession of the Eastern Shores area as part of the Environmental Impact Assessment study of mining on the Eastern Shores, a palaeo-channel south of Mission Rocks was discovered. The floor of this channel is believed to be at about -80 m below sea level. There are, however, no fresh water seepages occurring along this section of the coastline.

#### 5.4 Utilization of ground water resource

Currently substantial amounts of ground water are only abstracted in two areas. These are in the flood plain of the Mhlatuze where ground water is used for irrigating the sugar cane field and in the vicinity of the Richard Bay Minerals mining operation.

The latter is mainly used as an emergency supply in times of drought. Depending on the pumping costs involved and the permits issued by DWA&F&F for abstraction from Lake Mzingazi and Nhlabane, this ground water abstraction scheme may become a permanent source of water. No information is, however, available on the volume of water pumped from this well field or the yield from the individual wells.

As the main aquifers are the Uloa and Port Durnford Formations, the exact distribution of these formations need to be known. Due to the regional nature of the study, it is possible to identify accurately individual wellfield development areas. Based on all available geohydrological information, a classification of low, medium and high ground water potential was devised. Factors that influence the classification of an area, thickness of sediments above the Cretaceous, depth to water level, quality of water, expected development of Uloa and Port Durnford Formation in an area and the proximity (lateral) of outcrops of Cretaceous siltstones. These areas are marked on **Figure 52**. This map must however be treated only as a rough approximation of potential development areas and before any development of ground water resources is planned, further study and exploration drilling and borehole testing will be necessary.

## CHAPTER 6

### CONCLUSIONS AND RECOMMENDATIONS

---

#### 6.1 Conclusions

The objectives for the project as stated in the contract conditions, and listed in the introduction to this report, have been met, with the exception of all the exploration drilling and test pumping originally envisaged. This was due to the build up of political unrest in the area which made the area unsafe for the drilling and test pumping crews.

The earlier statement that the Zululand Coastal Plain Aquifer can be regarded as one of the largest alluvial aquifers in South Africa has been confirmed by the additional information collected during this investigation. Although the investigation has also led to a better understanding of the aquifer system, several aspects warrant more study. In this regard the interaction between vegetation, whether it be natural or commercial (forestry and agriculture for example), and the ground water regime needs to be assessed thoroughly before any large scale development of the ground water resource is envisaged.

There exists a fine balance between the ecology of the region and the ground water regime. Any future development plans for the region, whether development for tourism, rural settlements, agriculture, mining or afforestation have to take into account the delicate balance of the ecosystem.. Ground water plays a crucial role in this ecosystem and any change in the ground water conditions may influence the ecosystem negatively.

Some specific conclusions emanating from this study are listed below:

- The thickness of the aquifers stratigraphically above the Cretaceous age sediments, was mapped over the entire coastal plain using geophysical techniques calibrated against a limited amount of borehole information.
- The electrical resistivity sounding technique used to determine the depth to the top of the Cretaceous age formations is more appropriate than the electromagnetic techniques to determine the thickness of the different units in the geological succession.
- Depth penetration by EM techniques is restricted due to the decrease in resistivity with depth of the different geological units and the very conductive nature of the sedimentary succession.
- Interpretation of DC soundings is complicated also because of the continuous decrease of the resistivity with depth.
- Resolution of individual geological units with geophysical methods proved not always to be successful. The depth to the top of the Cretaceous formations can, however, be determined with a large degree of confidence.

- Borehole geophysical measurements also failed to clearly identify different geological horizons.
- Gravity surveys were not able to detect palaeo-channels subsequently filled with younger sediments.
- Two palaeo-channels were detected through which increased seepage towards the sea can occur. One of these is situated opposite Lake Sibayi and the other one is near Mission Rocks opposite Lake St Lucia.
- A water level contour map was constructed for the entire coastal plain using measured water levels and applying statistical techniques to infer elevations in areas where data points were sparse.
- A ground water divide, roughly parallel to the coastline, could clearly be identified from this map.
- From the available water level information, three different water level scenarios in the vicinity of the coastal dune cordon could be identified. These are at Lake Sibayi, Eastern Shores of Lake St Lucia, and at Richards Bay.
- A regional mathematical simulation model was designed to simulate steady state conditions. This model was used to determine ground water flow directions and velocities over the entire coastal plain.
- It was further used to simulate the effect of an afforested area around Lake Sibayi to determine the effect on lake and ground water levels. This model indicates that if evapotranspiration by the plantations exceeds 1 000 mm/ha/a, water levels in the lake may already be affected. A number of assumptions have, however, been made during this simulation. These figures should therefore be regarded as provisional.
- A rainfall-recharge relationship was established which varies with distance from the coast. Recharge as a percentage of MAP varies from 18 % at the coast to 5 % at a distance of 50 km inland.
- The rainfall-recharge relationship was used as input to the mathematical simulation exercise.
- The Cl concentration in rainfall decreases rapidly from the coast to the inland.
- Ground water quality over the entire coastal plain is generally of good quality. There are, however, regional differences in the chemical character.
- A "fingerprinting" technique was developed successfully to correlate the water chemistry with the geological horizon from which it originates.
- Stable isotopes were used to great advantage to distinguish between seepage from lakes and ground water. Stable isotopes also confirmed a considerable residence time for water in the larger lakes like Sibayi and Bhangazi.
- No seasonal isotopic variation was recognized in rainwater. Isotope analyses could also not be used to trace the movement of ground water due to insignificant variations observed
- Carbon-14 analyses indicated that the ground water recharge is mostly post-1960. This is in accordance with the high through-flow of water through the aquifer deduced from recharge estimates and modelling.

- Isotope analyses confirmed that the fresh water occurrence along the coast opposite Lake Sibayi originates from the lake.
- Sea-water intrusion into the aquifer is unlikely to occur due to an effective above sea level piezometric head along the coastal dune cordon.
- The aquifer is highly vulnerable to surface sources of pollution.

## 6.2 Recommendations

In view of the ecologically sensitive nature of the area and the dominating role that ground water plays in maintaining the balance, a number of important recommendations are made. These include that:

- the water level monitoring program should be maintained;
- the interaction between the ground water and the vegetation in the area be investigated in detail and that a research program to address this aspect be compiled as soon as possible;
- this research program should include input from ecologists, the Department of Water Affairs and Forestry, the commercial forestry sector, nature conservation officials, tourism authorities and regional planners;
- further work is required to quantify the effect of afforestation on the ground water conditions in more detail;
- the mathematical simulation model should be refined and updated once more data becomes available;
- the pollution vulnerability of the aquifer should be brought to the attention of the planners.

## LIST OF REFERENCES

---

- ALLANSON, B R (1979). Lake Sibayi. W Junk, The Hague, 364p.
- ARCHIBALD, C G M and MULLER M S (1987). Physical and chemical characteristics of bulk precipitation in the Richards Bay area. SA J of Sci, **83**, 700-704.
- AUSTRALIAN GROUNDWATER CONSULTANTS (PTY) LTD (1975). Richards Bay Groundwater Investigations - Richards Bay Heavy Minerals Project. Confidential Report.
- BOTHA J F, VERWEY J P, BUYS, J, TREDoux G, MOODIE J W and HODGKISS M (1990). Modelling Groundwater Contamination in the Atlantis aquifer. WRC Report No 175/1/90, Water Research Commission, Pretoria.
- BREDENKAMP, D B (1980). Kwantitatiewe ramings van grondwateraanvulling met behulp van eenvoudige hidrologiese modelle. Ground water 1980 Symposium, 7-9 July, Pretoria.
- BREDENKAMP, D B (1985). Estimation of ground water recharge in dolomitic aquifers. Abstract, Ground Water '85 Symposium, Pretoria, 98-107.
- BREDENKAMP, D B (1993). Recharge estimation based on chloride profiles. Dept. of Water Affairs and Forestry, Pretoria, Report GH 3804 (Draft copy), 22p.
- BREDENKAMP, D B, BOTHA, L J, VAN TONDER, G J and VAN RENSBURG, H J (1995). Manual on quantitative estimation of recharge and aquifer storativity based on practical hydro-logical methods. Water Research Commission Report TT 73/95.
- BUYS J, BOTHA J F and MESSERSCHMIDT, H J (1992). Triangular irregular meshes and their application in the graphical representation of geohydrological data. WRC Report No 271/2/92, Water Research Commission, Pretoria.
- COASTAL AND ENVIRONMENTAL SERVICES (1992). Specialist Reports. In: Environmental Impact Assessment, Eastern Shores of Lake St Lucia, Kingsa/Tojan Lease. Area. Volume 1, Part 1, Grahamstown, pp 1-20.
- COETSEE, VdA (1991). Bepaling van gesteente hidrouliese en geoëlektriese eienskappe. CSIR Internal Report No EMA-I 9113.
- COOPER, M R and MCCARTHY, M J (1988). The stratigraphy of the Uloa Formation. Abstracts Geocongress '88, Geol. Soc. S. Afr., Durban.



- DAVIES, LYNN AND PARTNERS. (1992) Landform geomorphology and geology. In: Environmental Impact Assessment, Eastern Shores of Lake St. Lucia, Kingsa/Tojan Lease Area, Vol. I, Part 1, Specialist Reports. Coastal and Environmental Services, Grahamstown, SR2., 21-62.
- DINGLE, R V, SIESSER, W G and NEWTON, A R (1983). Mesozoic and Tertiary geology of Southern Africa. Rotterdam. Balkema.
- DU PREEZ, J W and WOLMARANS, L G (1986). S. Afr. Geol. Surv. Map Explanation Sheet 2632 (Kosi Bay). Government Printer, Pretoria.
- EDMUNDS, W M, DARLING, W G and KINNIBURGH, D G (1990). Solute profiling techniques for recharge estimation in semi-arid and arid terrain. In: D N Lerner, A S Issar, I Simmers (ed)., Groundwater Recharge, Verlag Heinz Hesse, Hannover, Germany.
- ERIKSSON, E and KHUNAKASEM, V (1969). Chloride concentrations in groundwater. Recharge rate and rate of deposition of chloride in the Israel coastal plain. J of Hydrology, 7, 178-197.
- FOCKEMA, P D (1986). The heavy mineral deposits of Richards Bay, 2301-2307. In: Anhaeusser, C.R. and Maske, S., (eds.), Mineral Deposits of Southern Africa, Vol. 2, 2335pp.
- FRANKEL, J J (1960). Late Mesozoic and Cenozoic events in Natal, South Africa. Trans. N.Y. Acad. Sc., Ser. II, Vol. 22, No. 8, 565-577.
- FRANKEL, J J (1966). Basal rocks of the Tertiary at Uloa, Zululand, South Africa. Geol. Mag., 103, 214-230.
- GAT, J R and GONFIANTINI (1981). Stable isotope hydrology. Tech. Report 210, IAEA, Vienna, pp 337.
- GIESKE, A S M (1992). Dynamics of groundwater recharge. PhD Thesis, Free Univ. Amsterdam, 289p.
- HASSANIZADEH, S M and CARRERA, J (1992). Editorial. Advances in Water Research, 15, 1-3.
- HOBDAV, D K and ORME, A R (1974). The Port Durnford Formation. A major barrier lagoon complex along the Zululand coast. Trans. Geol. Soc. S. Afr. 77, 141-149.
- HOBDAV, D K and JACKSON, M P A (1979). Transgressive shorezone sedimentation and depositional deformation in the Pleistocene of Zululand, South Africa. Journ. Sediment. Petrol. 49, 145-158.

- HINGSTON, F J and GAILITIS, V (1976). The geographic variation of salt precipitated over western Australia. *Australian J. Soil Res*, 14, 319-335.
- HUTCHISON, I P G and PITMAN, W V (1973). Climatology and Hydrology of the St Lucia Lake System. Hydrological Research Unit, Report 1/73, University of the Witwatersrand, Johannesburg.
- JUNGE, C E and WERBY, R T (1958). The concentration of chloride, sodium, potassium, calcium and sulphate in rain water over the United States. *J Meteorol*, 15, 417-425.
- KELBE, B and RAWLINS, B K (1992). Hydrology. In: Environmental Impact Assessment, Eastern Shores of Lake St. Lucia, Kingsa/Tojan Lease Area, Vol. I, Part 1, Specialist Reports. Coastal and Environmental Services, Grahamstown, SR3, 63-124.
- KENNEDY, W J, and KLINGER, H C (1975). Cretaceous faunas from Zululand and Natal, South Africa. Introduction. Stratigraphy. *Brit. Mus. (Nat. Hist.) Bull. Geol.* No 25.
- KRUGER, G P and MEYER, R (1988). A sedimentological model for the northern Zululand Coastal Plain. Abstracts Geocongress '88, Geol. Soc. S. Afr., Durban, 423-425.
- KRUGER, G P (1986). An investigation into the feasibility of rice cultivation on the Ngwavuma Coastal Plain, northern Natal. A report on the results of a hydrogeological and geomorphological Survey. IDC Confidential Internal Report, 42 pp.
- LINDLEY, A J and SCOTT, D F (1987). The impact of pine plantations on the ground-water resources of the Eastern Shores of Lake St Lucia. SAFRI Report No. JFRC 87/01.
- MAMANE, Y (1987). Chemistry of precipitation in Israel. *Science of the Total Environment*, 61, 1-13.
- MAUD, R R (1961). A preliminary review of the structure of coastal Natal. *Trans. Geol. Soc. S. Afr.*, 64, 247-256.
- MAUD, R R and ORR, W N (1975). Aspects of post-Karoo geology in the Richards Bay area. *Trans. Geol. Soc. S. Afr.*, 78, 101-109.
- MCCARTHY, M J (1988). Some observations on the occurrence of "Berea-type" Red Sand along the Natal coast. Abstracts Geocongress '88, Geol. Soc. of S. Afr., Durban. 403b-d.
- MCCARTHY, M J (1992). Unpublished notes prepared on Geological Excursion in the Durban area, 31p.

- MCMILLAN, I K (1987). The genus *Ammonia* Brunnich, 1772 (Foraminiferida) and its potential for elucidating the latest Cainozoic stratigraphy of South Africa. *S. Afr. J. Sc.* 83, 32-42.
- MEYER, R and DE BEER, J H (1981). A geophysical study of the Cape Flats aquifer. *Trans. Geol. Soc. S. Afr.*, 84, 107-114.
- MEYER R, DE BEER J H and BLUME, J (1982). A geophysical-geohydrological study of an area around Lake Sibayi, northern Zululand. Confidential CSIR Report Kon/Gf/81/1.
- MEYER, R, DUVENHAGE, A W A, BLUME, J, VALLENDUUK, J W and HUYSEN, R M J (1983). Report on a geophysical and geohydrological investigation of the ground water potential between Lambert's Bay and Graafwater and the coastal region between Lambert's Bay and Elands Bay. Confidential CSIR Report No. Kon/Gf/79/1.
- MEYER, R, HUYSEN, R M J, COETSEE, VdA and AUCAMP, J J (1987). A geoelectrical survey of an area between Lake Sibayi and Lake Kosi, Northern Zululand. CSIR Confidential Report C-FIS 129.
- MEYER, R and KRUGER, G P (1987). Geophysical and geohydrological investigations along the Zululand coastal plain. Abstract, Hydrological Sciences Symposium Proceedings: Volume I, Rhodes University, Grahamstown, South Africa, 299-311.
- MEYER, R, COETSEE, VdA en TALMA, A S (1989). Tussentydse verslag, WNK-projek K5/221 Geohidrologiese ondersoek en evaluasie van die Zoelandse kusakwifer. WNNR Vertroulike Verslag nr. EMA-C 8928.
- MEYER, R, DUVENHAGE A W A and AUCAMP, J J (1989). Final report on the geoelectrical investigation of an area around Port Durnford on the Zululand coastal plain. Confidential report No. EMA-C 88115.
- MEYER, R, MCCARTHY, M J and EGLINGTON, B M (1993). Further investigation of the geology and geohydrology of the dune cordon on the eastern shores of Lake St Lucia. Report No. EMAP-C-93032.
- MURGATROYD, A L (1983). Spatial variations in precipitation chemistry over Natal, South Africa. *SA J Sci*, 79, 408-410.
- ORME, A R (1973). Barrier and lagoon systems along the Zululand coast, South Africa. In: D.R.Coates (Ed.) *Coastal Geomorphology*. New York: N.Y. State Univ. Press., 181--217.
- ORR, W N and CHAPMAN, J R (1974). Danian (Palaeocene) marine rocks at Richards Bay, South Africa. *S. Afr. J. Sci.* 70, 247-249.

- PITMAN, W V and HUTCHINSON, I P G (1975). A preliminary hydrological study of Lake Sibaya. Report 4/75. Hydrol. Res. Unit, Univ. of the Witwatersrand, Johannesburg, pp35.
- RAWLINS B K (1991). A geohydrological assessment of the behaviour and response of the Zululand Coastal Plain to both environmental influences and human activity. Unpublished MSc thesis, University of Zululand.
- RAWLINS, B K and KELBE, B E (1990). A geohydrological study of the behaviour and response of the Zululand Coastal Plain to both environmental influence and human activity. Annual Report. University of Zululand.
- ROZANSKI, K, ARAGUAS, L A and GONFIANTINI, R (1992). Relation between long-term trends of oxygen-18 isotopic composition of precipitation and climate. *Science*, **258**, 981-985.
- SIMMONDS, A L E (1990). Investigations into possible saline intrusion at lake Mzingazi, Richard Bay. Department of Water Affairs and Forestry, Directorate geohydrology, Report No. GH 3711.
- STAPLETON, R P (1975). Planktonic foraminifera and calcareous nannofossils at the Cretaceous-Tertiary contact in Zululand. *Palaeont. afr.* 18, 53-69.
- STAPLETON, R P (1977) Planctonic foraminifera and the age of the Uloa Pecten Bed. *Geol. Surv. S. Afr. Bull.*, 60, 11-15.
- TINLEY, K L (1985). Coastal dunes of South Africa. *S. Afr. Nat. Sci. Programme Report No.* 109.
- VAN TONDER, G J, BOTHA, J F, and MULLER, J (1986). The problem of sea water intrusion near Lake Mzingazi at Riochards Bay. *Water S.A.*, 12(2), 83-88.
- VAN WYK, W L (1963). Groundwater studies in northern Natal, Zululand and surrounding areas. *S. Afr. Geol. Surv. Mem. No.* 52.
- VAN ZIJL, J S V (1971). Results of an electrical sounding profile, Eastern Shores area, St Lucia. Confidential NPRL, CSIR Report, Pretoria.
- VOGEL, J C and VAN URK, H (1975). Isotopic investigation of Lake St Lucia. Internal NPRL, CSIR Report, Pretoria.
- WOLMARANS, L G and DU PREEZ, J W (1986). *S. Afr. Geol. Surv. Map Explanation Sheet* 271/232 (St. Lucia).

WORTHINGTON, P F (1978). Groundwater conditions in the Zululand coastal plain around Richards Bay. CSIR Report, FIS 182, 209pp.

WRIGHT, C I and MASON, T R (1990). The sedimentation of Lake Sibaya, North KwaZulu. Unpublished Joint Geological Survey - University of Natal Report No. 1990-0147, 25pp.

## FIGURES

## **APPENDIX A**

### **GEOCHEMICAL CLASSIFICATION OF ZULULAND GROUND WATER**

**APPENDIX B**  
**GROUND WATER RECHARGE CALCULATIONS**



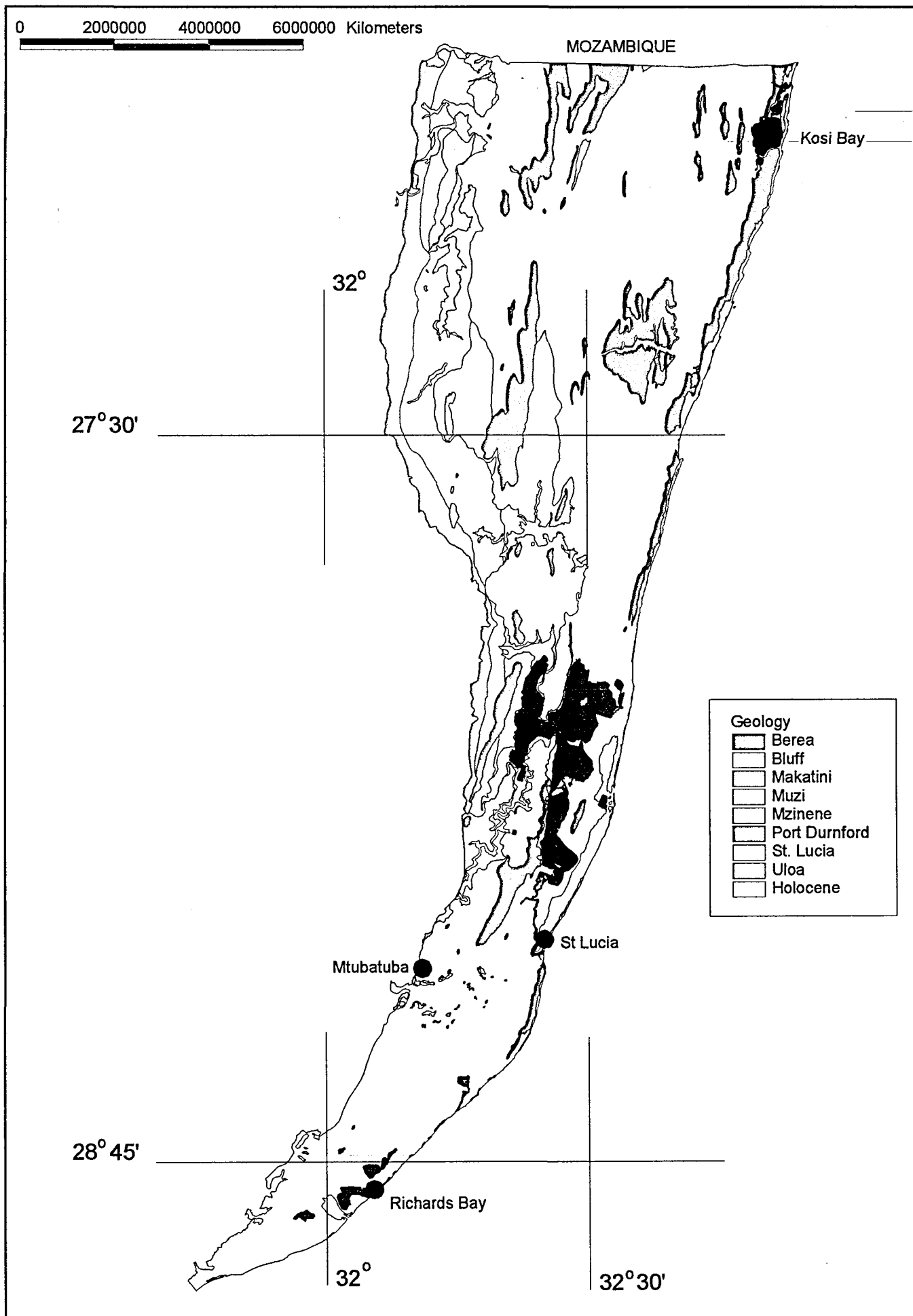


Figure 1. Geological map of the Zululand Coastal area.

Verslag 221/1/01

200 afskrifte.

B.No. 11968.

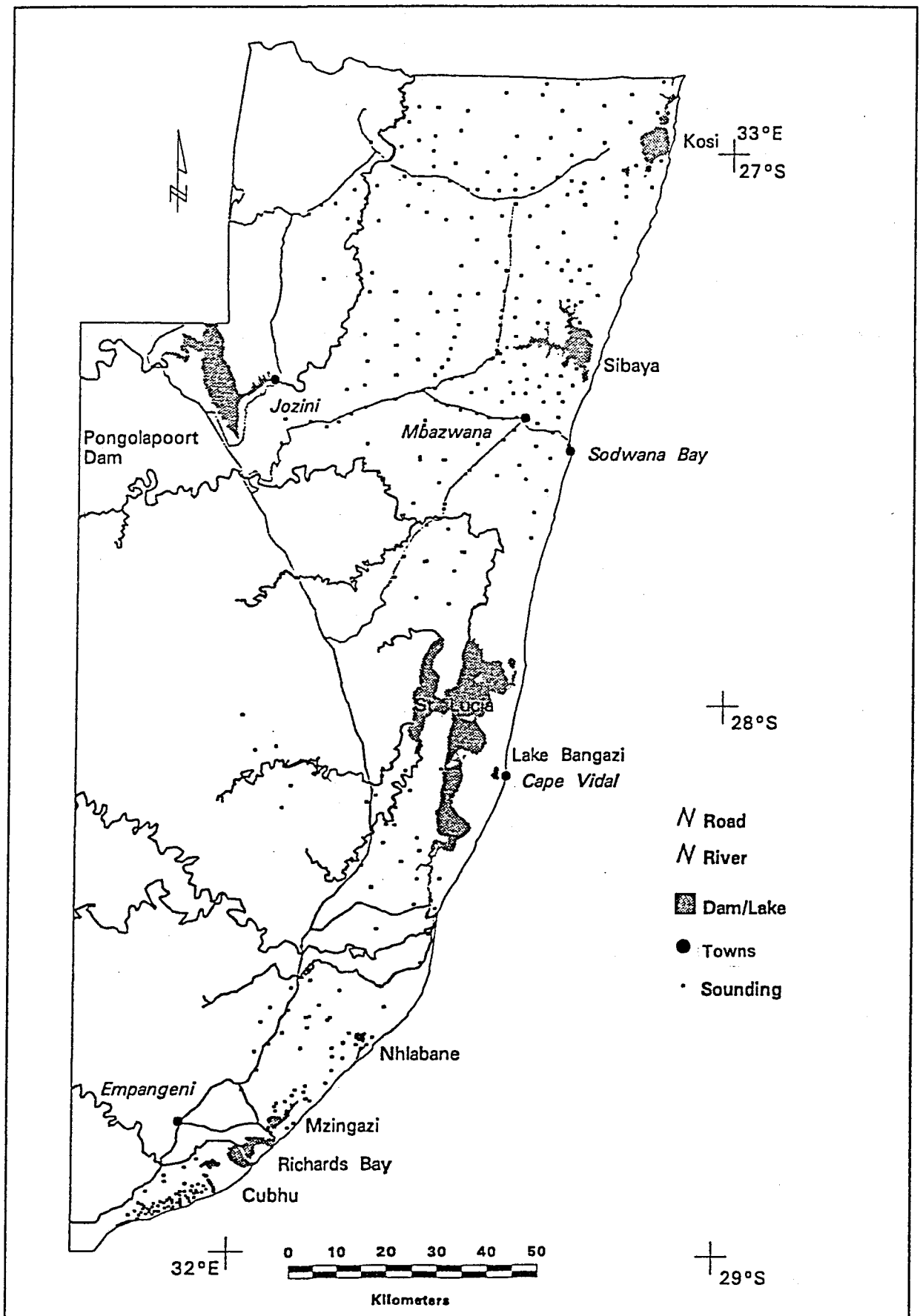


Figure 2: Resistivity sounding locations.

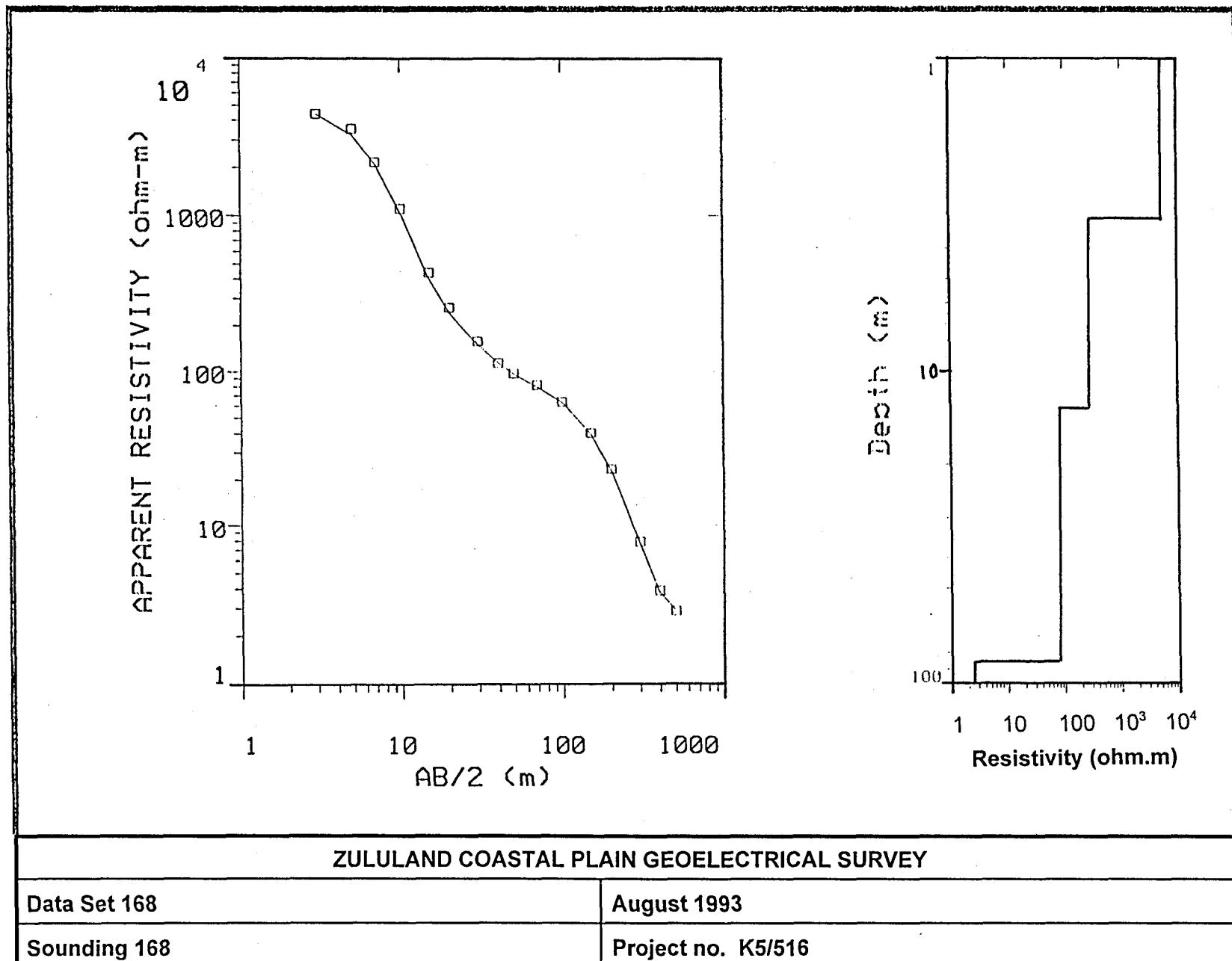
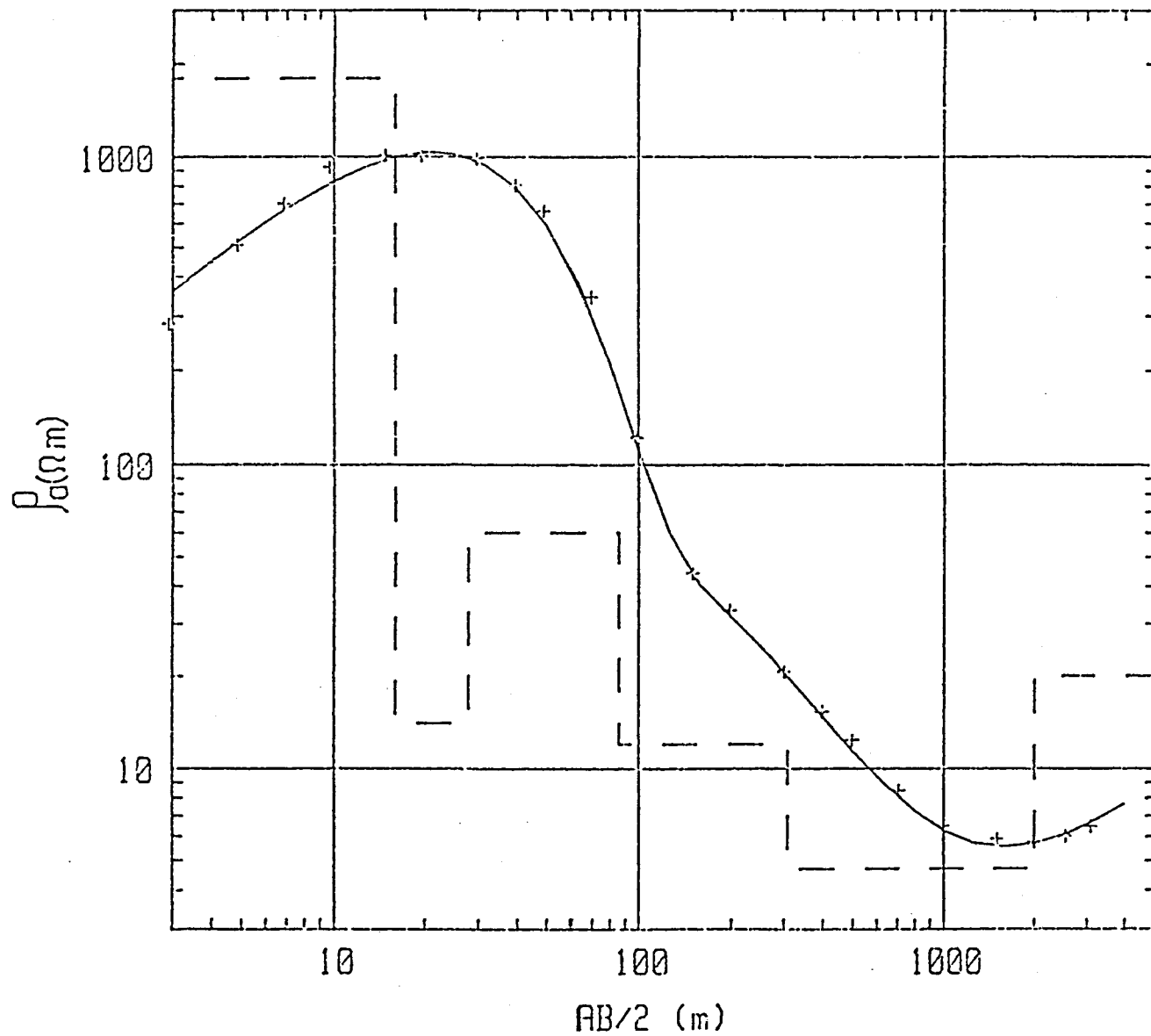


Figure 3: A typical direct current (DC) resistivity sounding curve and interpretation.

ES 85



**Figure 4:** Sounding curve and model for resistivity sounding ES 85.

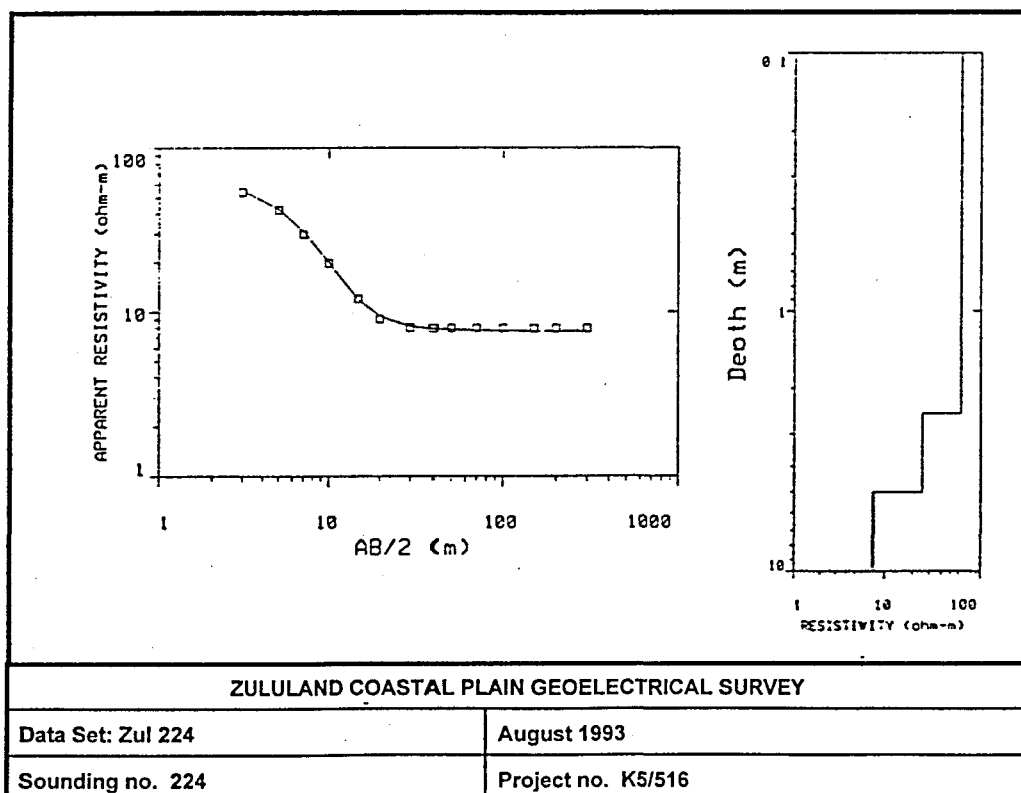
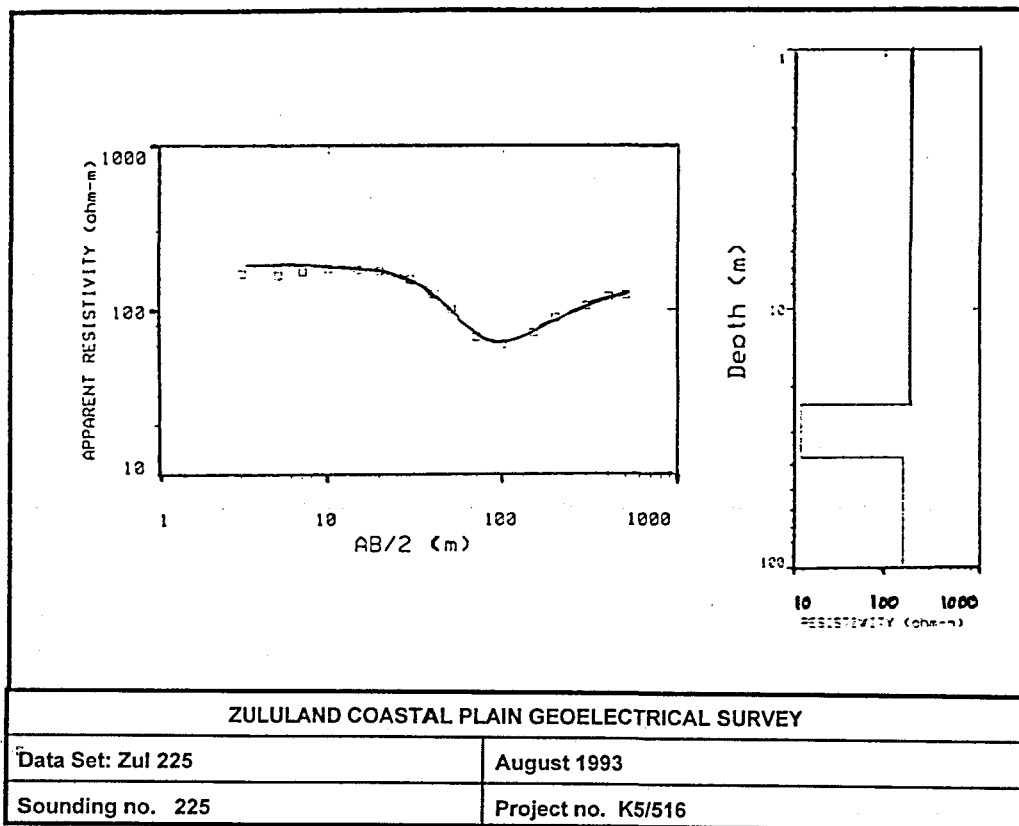
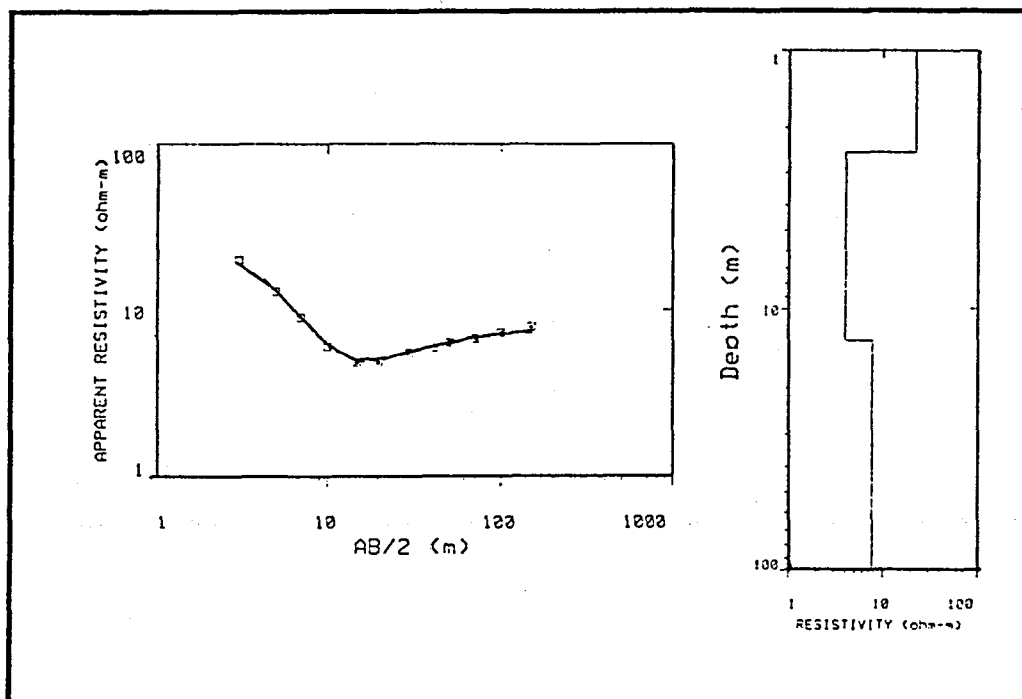
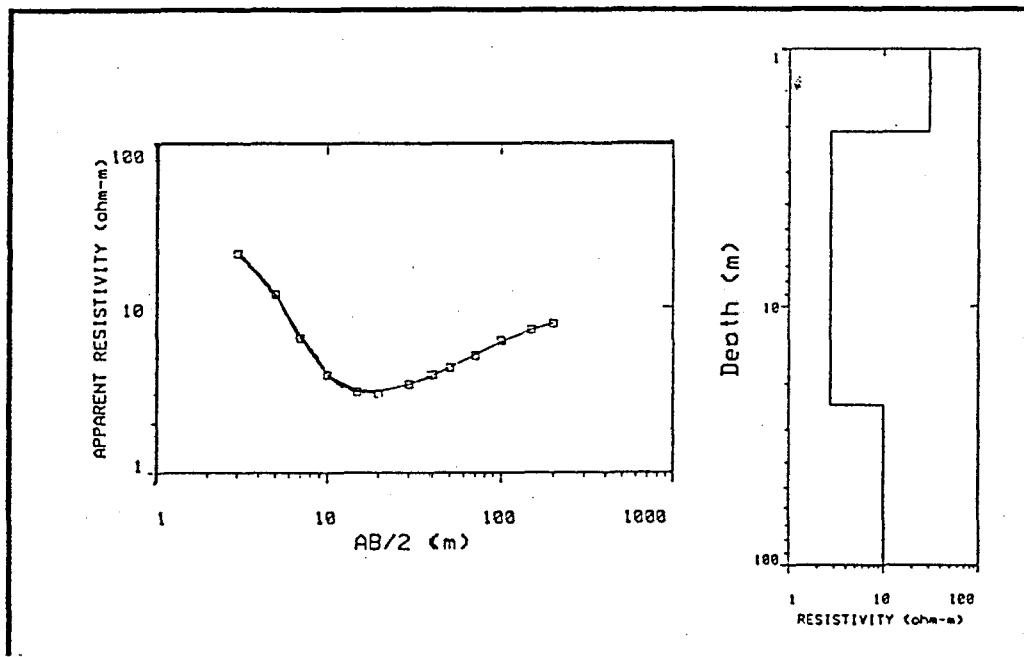


Figure 5: DC sounding curve and interpretations for ES 235 (Lebombo Group) and ES 224 Makatini Formation).



ZULULAND COASTAL PLAIN GEOELECTRICAL SURVEY	
Data Set: Zul 180	August 1993
Sounding no. 180	Project no. K5/516



ZULULAND COASTAL PLAIN GEOELECTRICAL SURVEY	
Data Set: Zul 155	August 1993
Sounding no. 155	Project no. K5/516

Figure 6: DC sounding curve and interpretations for ES 180 (Mzineni Formation) and ES 155 (St Lucia Formation).

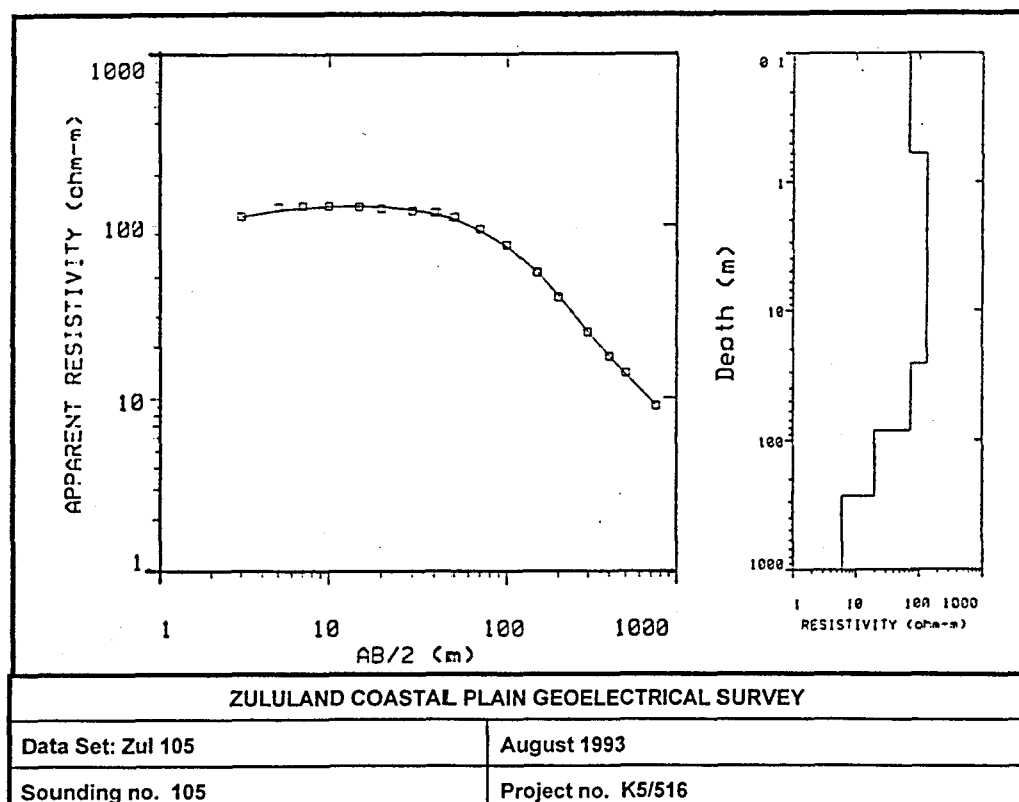
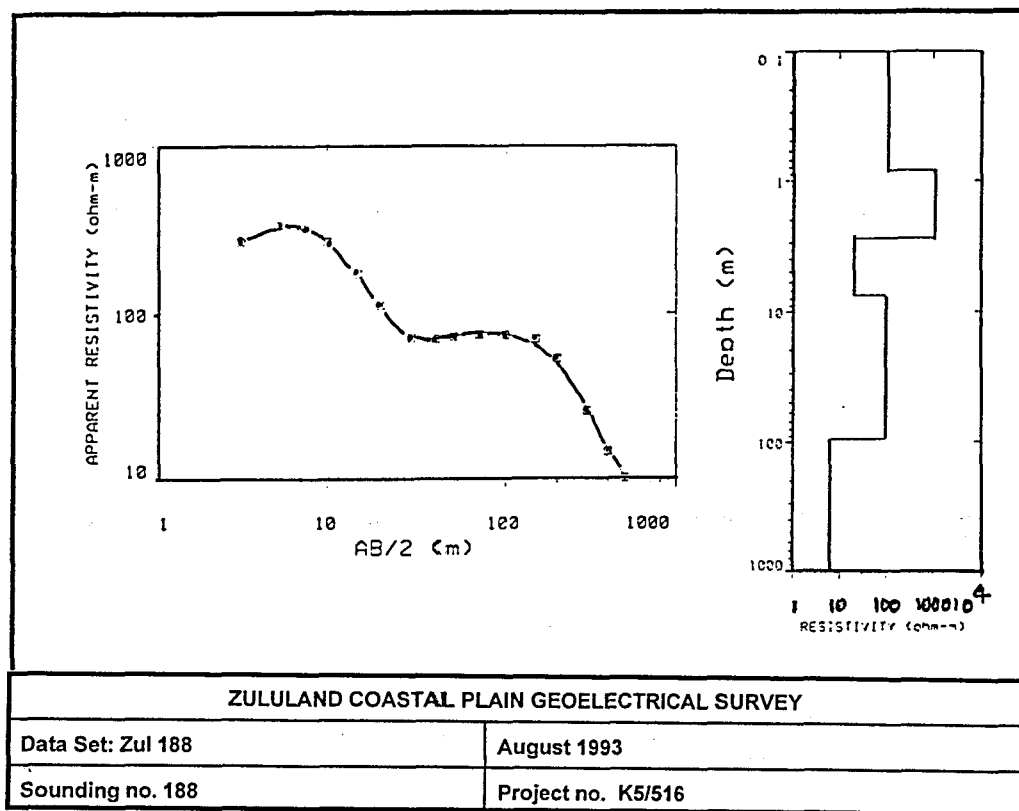


**Figure 7:** DC sounding curve and interpretations for ES 188 (Uloa Formation) and ES 105 (Port Durnford Formation).



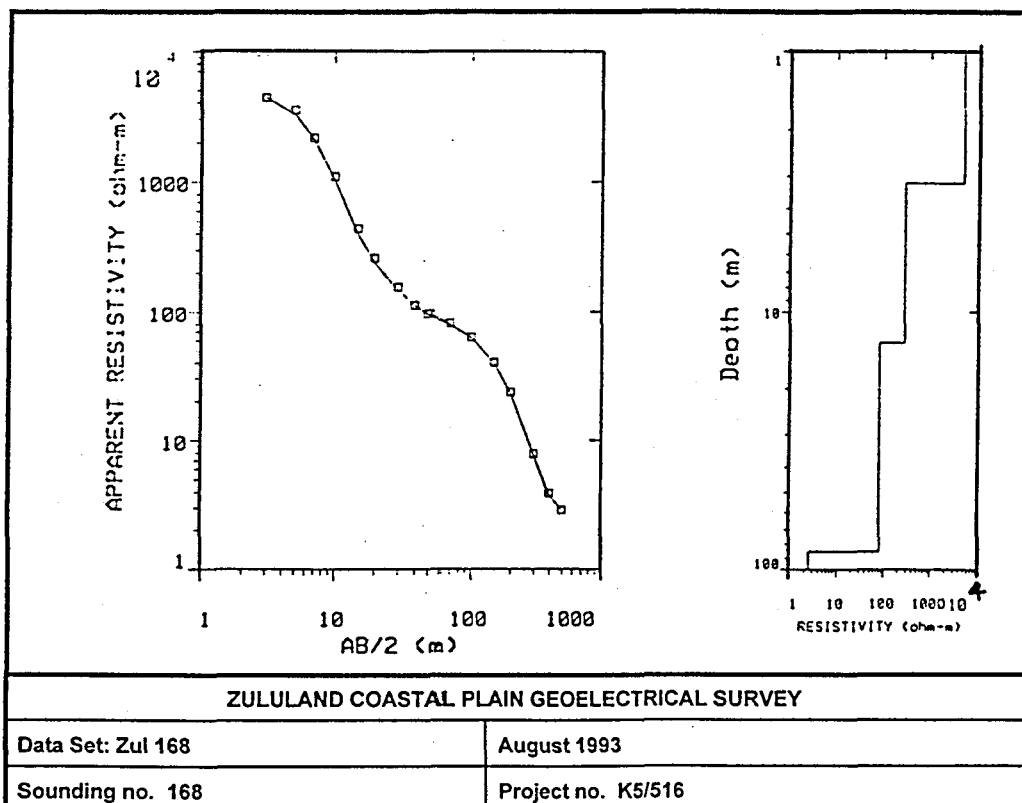
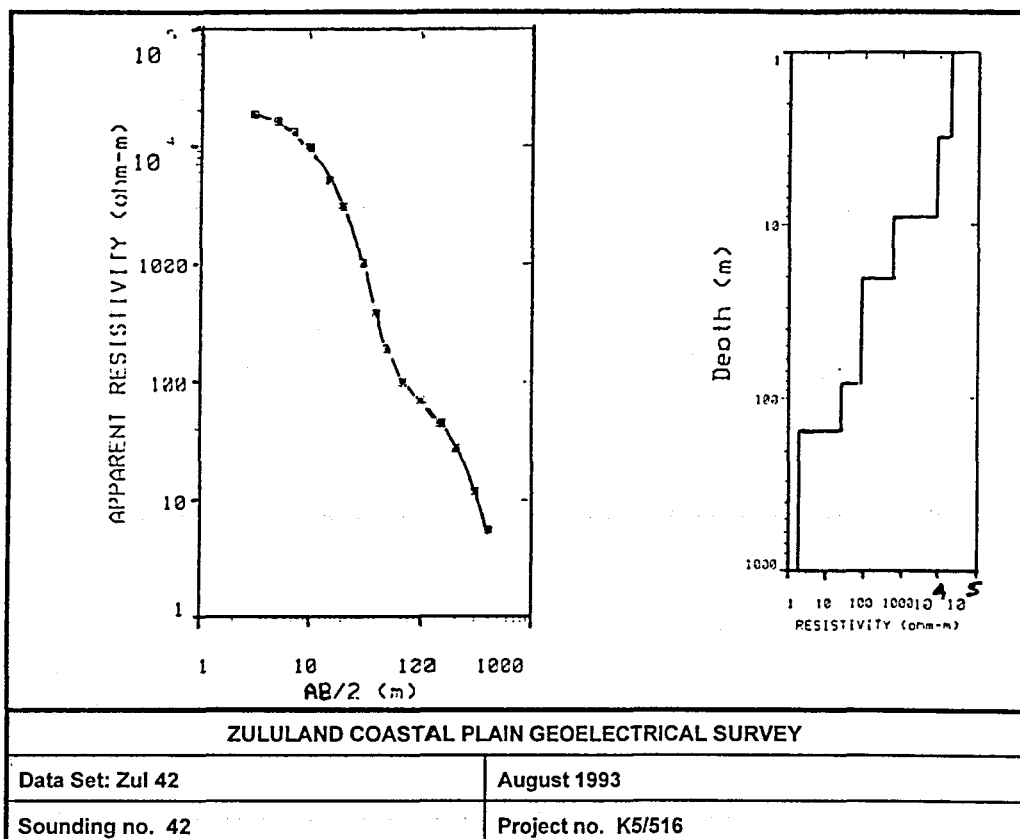
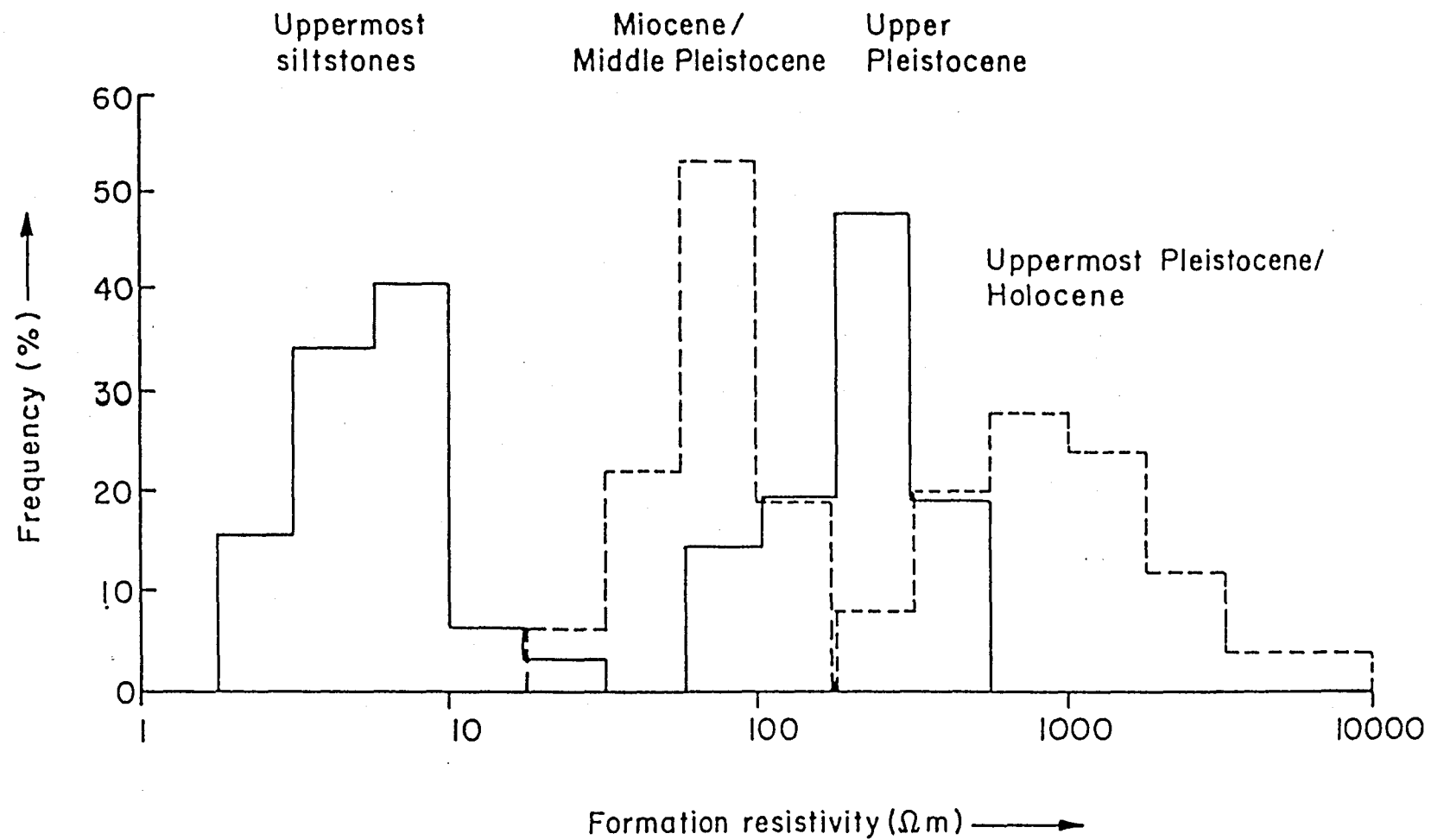
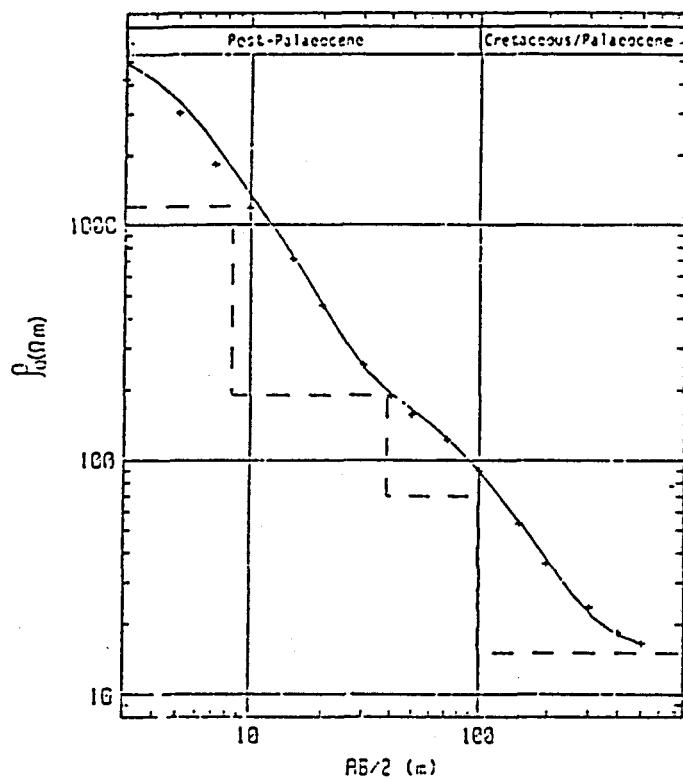


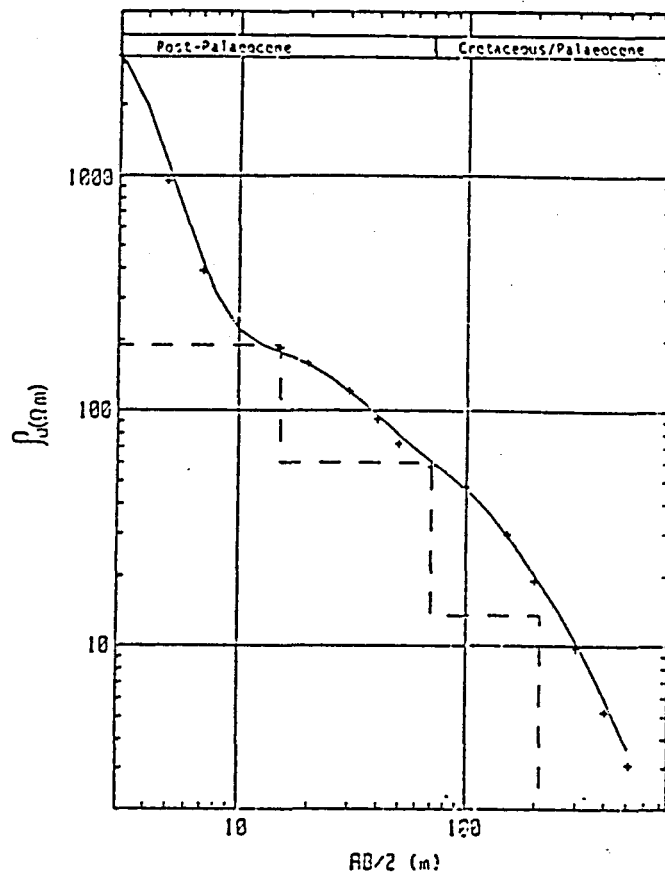
Figure 8: DC sounding curve and interpretations for ES 42 (Berea-type Red Sand) and ES 168 (Holocene sands).



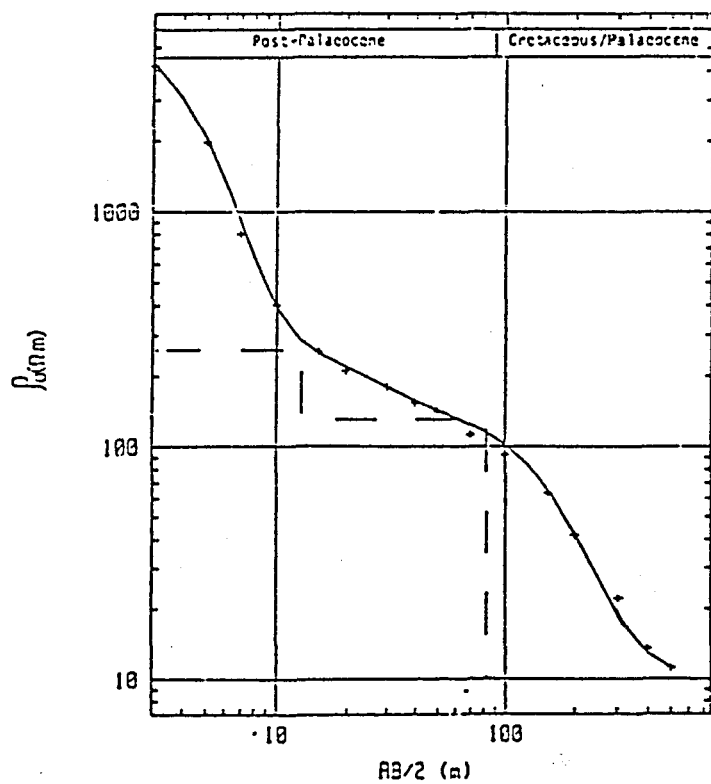
**Figure 9:** Histogram of surface measured formation resistivities based on calibration soundings (Worthington, 1979).



Sounding curve and model for ES 1 measured at Soekor borehole ZF 1/72



Sounding curve and model for ES 2 measured at Soekor borehole ZG 1/72



Sounding curve and model for ES 4 measured at Soekor borehole ZE 1/71

Figure 10: Sounding curves and models for ES 1, ES 2 and ES 4.

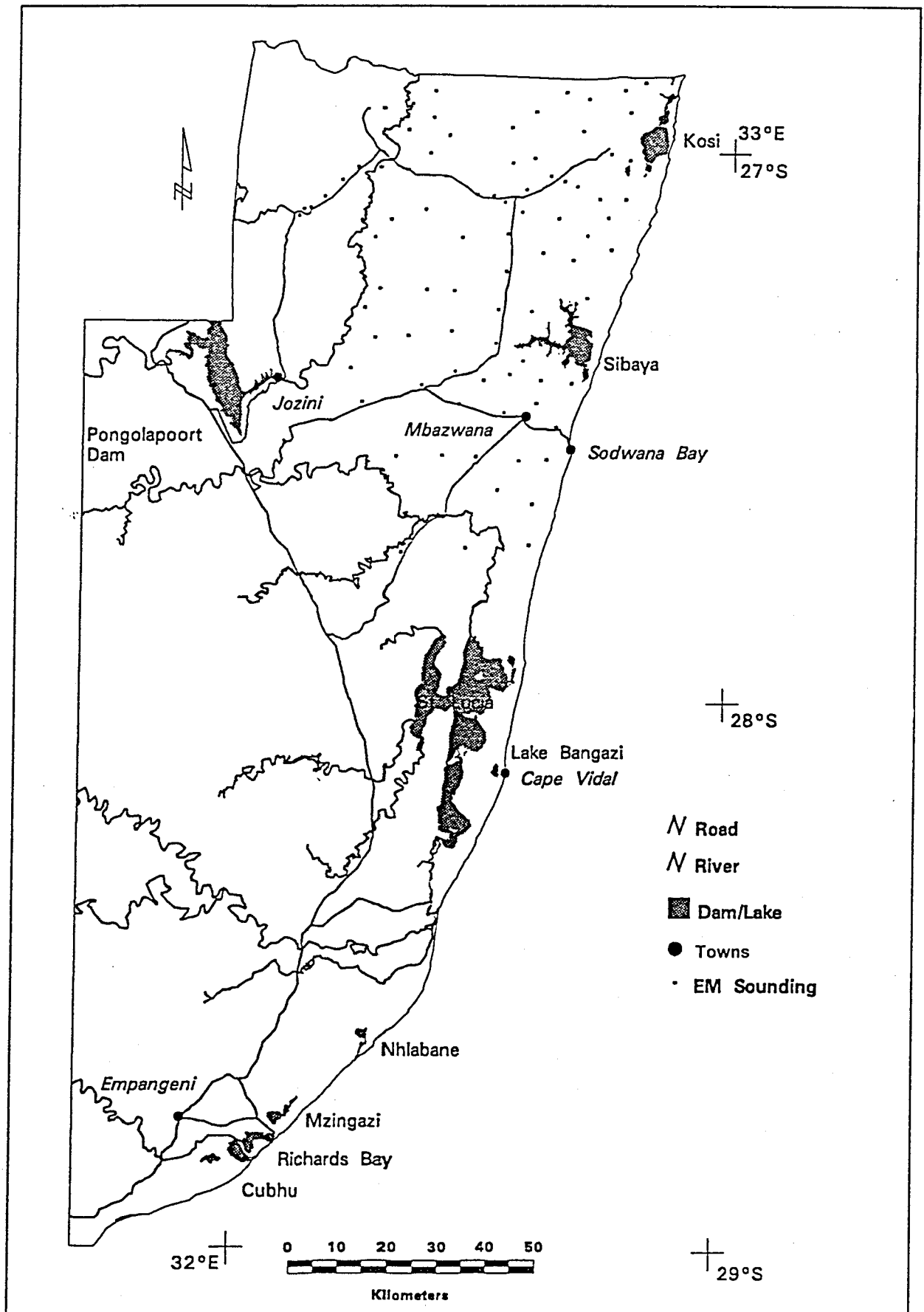


Figure 11: Electromagnetic sounding (EM-37) Sounding locations.

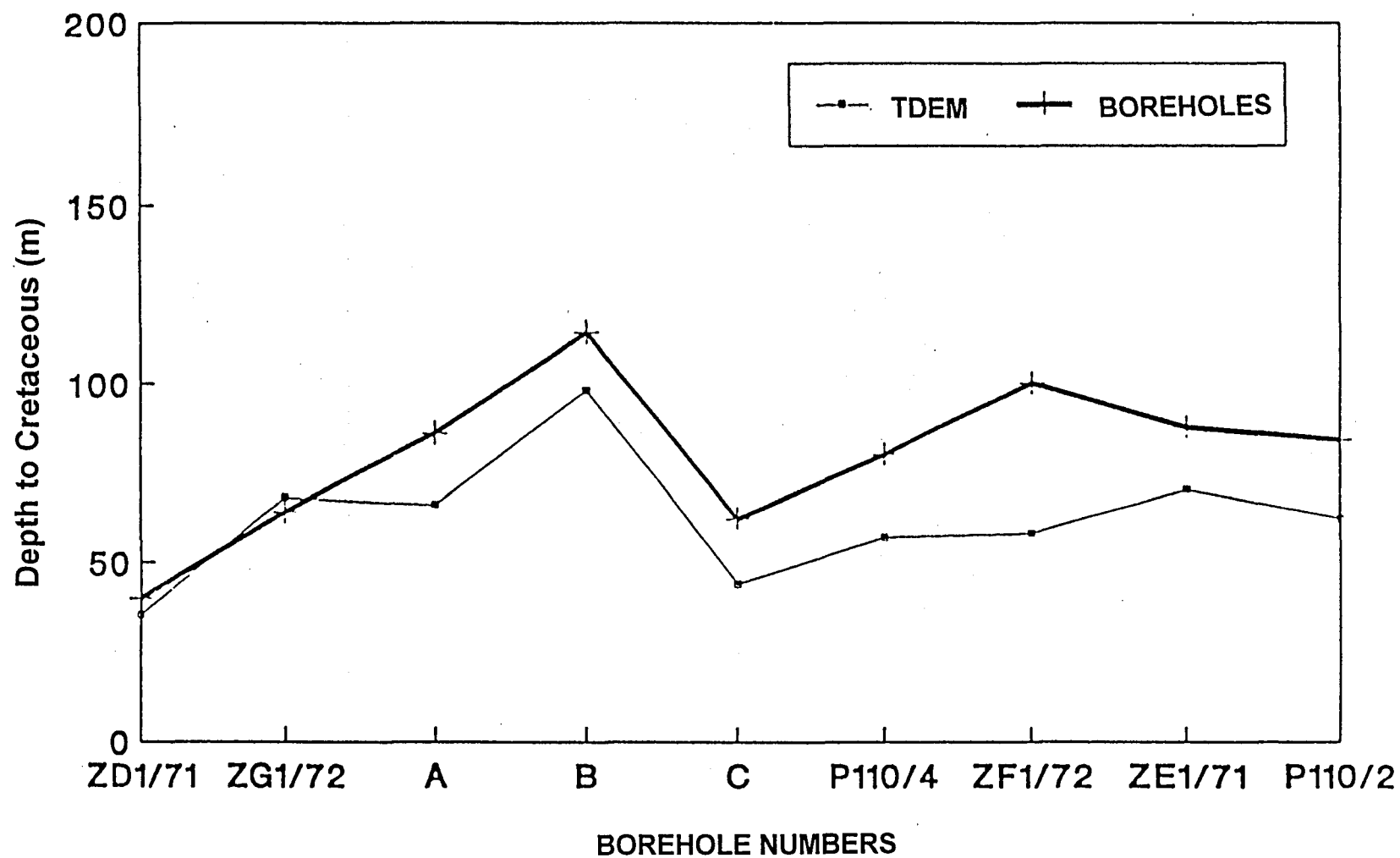


Figure 12: Comparison between the results of time domain electromagnetic sounding interpretations (TDEM) and drilling results.

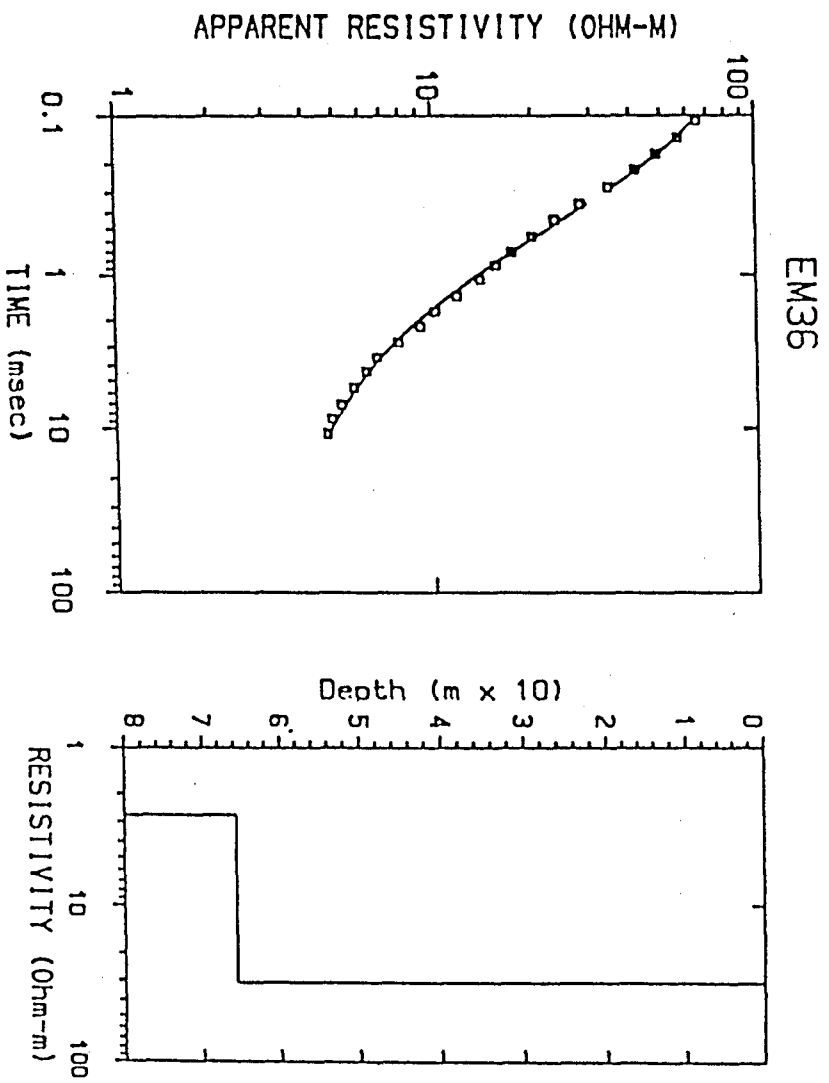
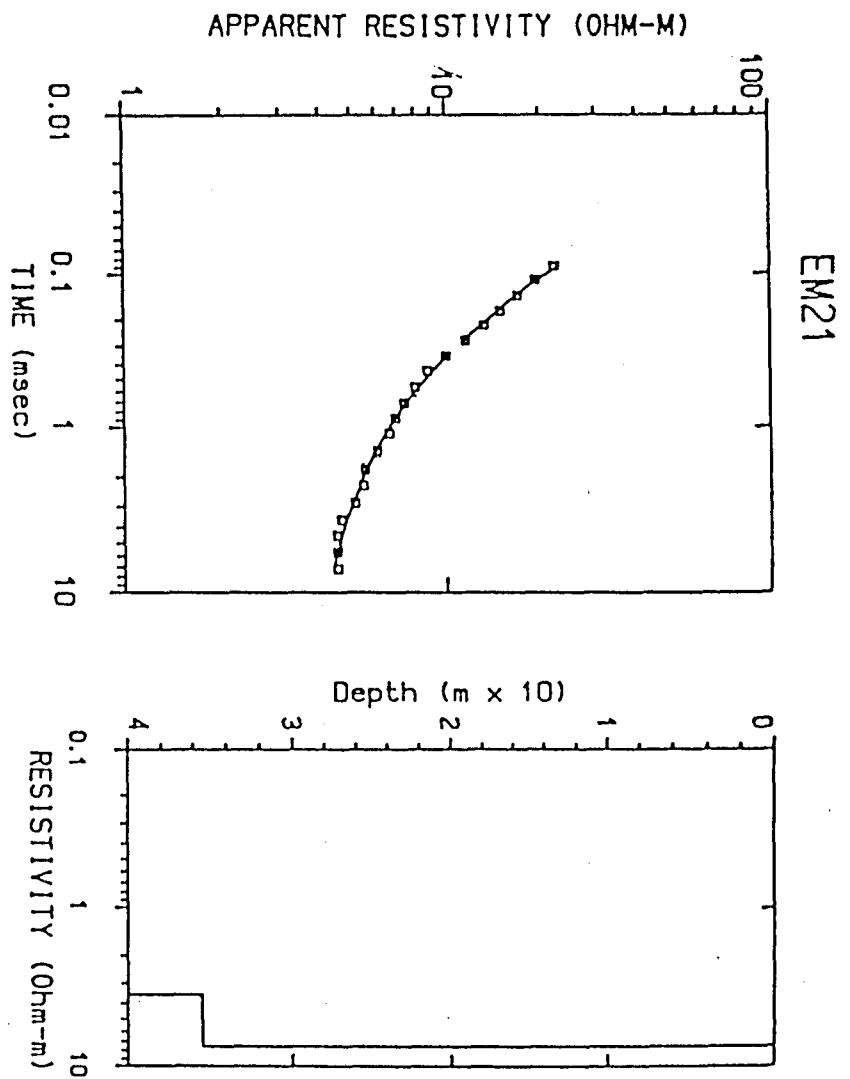


Figure 13: Transient electromagnetic sounding curves and models for soundings EM 21 and EM 36.

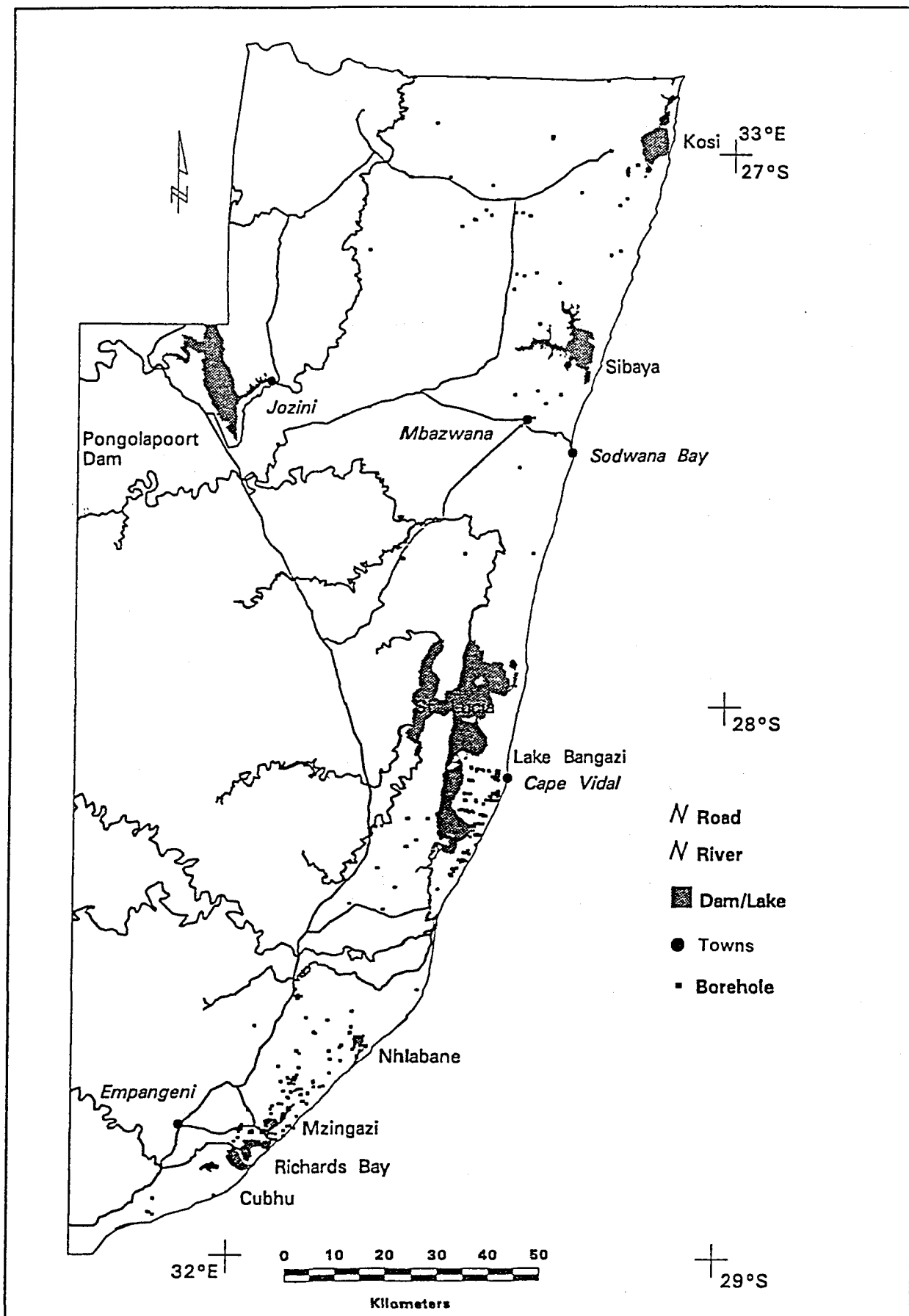


Figure 14: Borehole positions on the Zululand Coastal Plain.

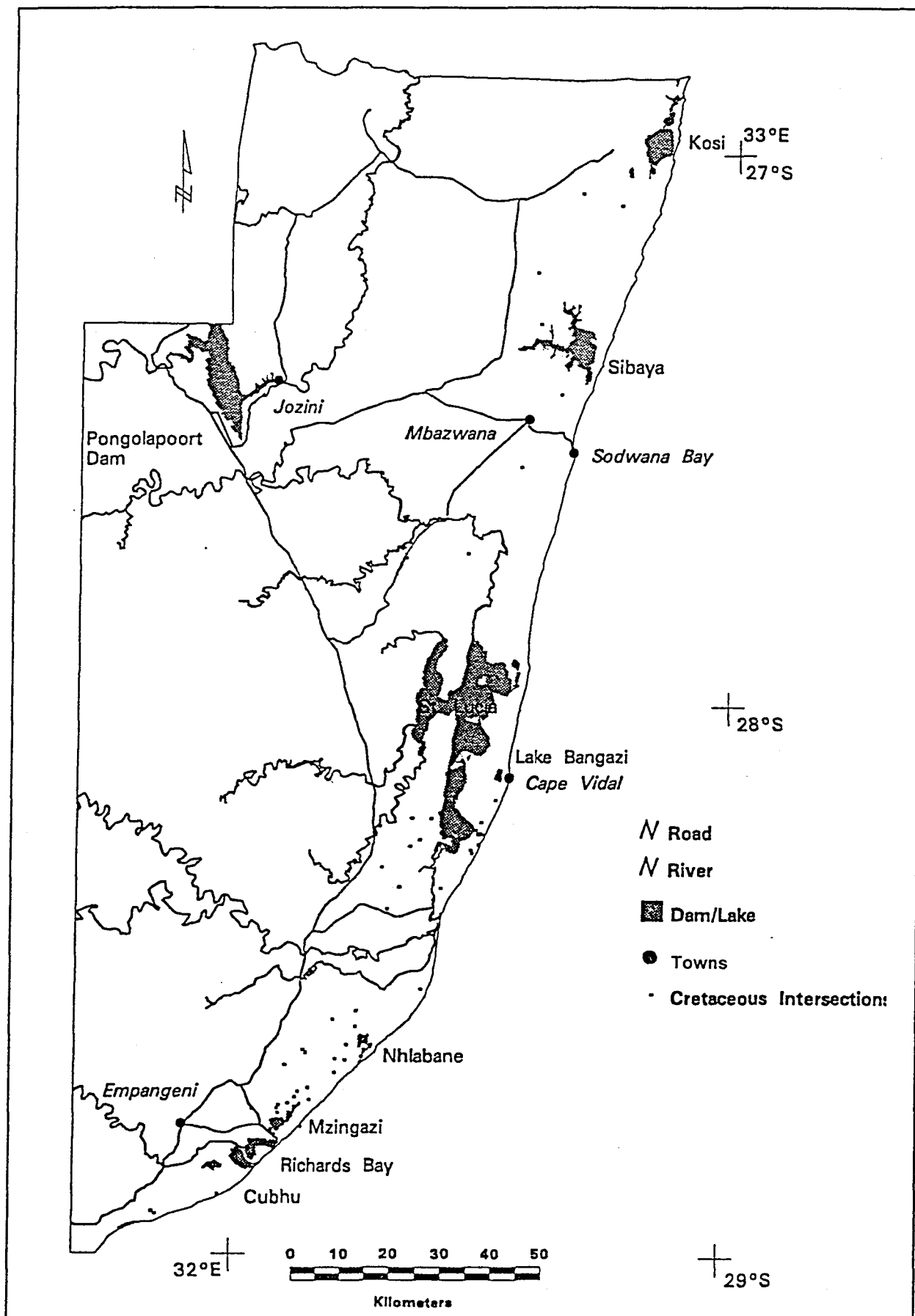


Figure 15: Boreholes where Cretaceous age rocks were intersected.



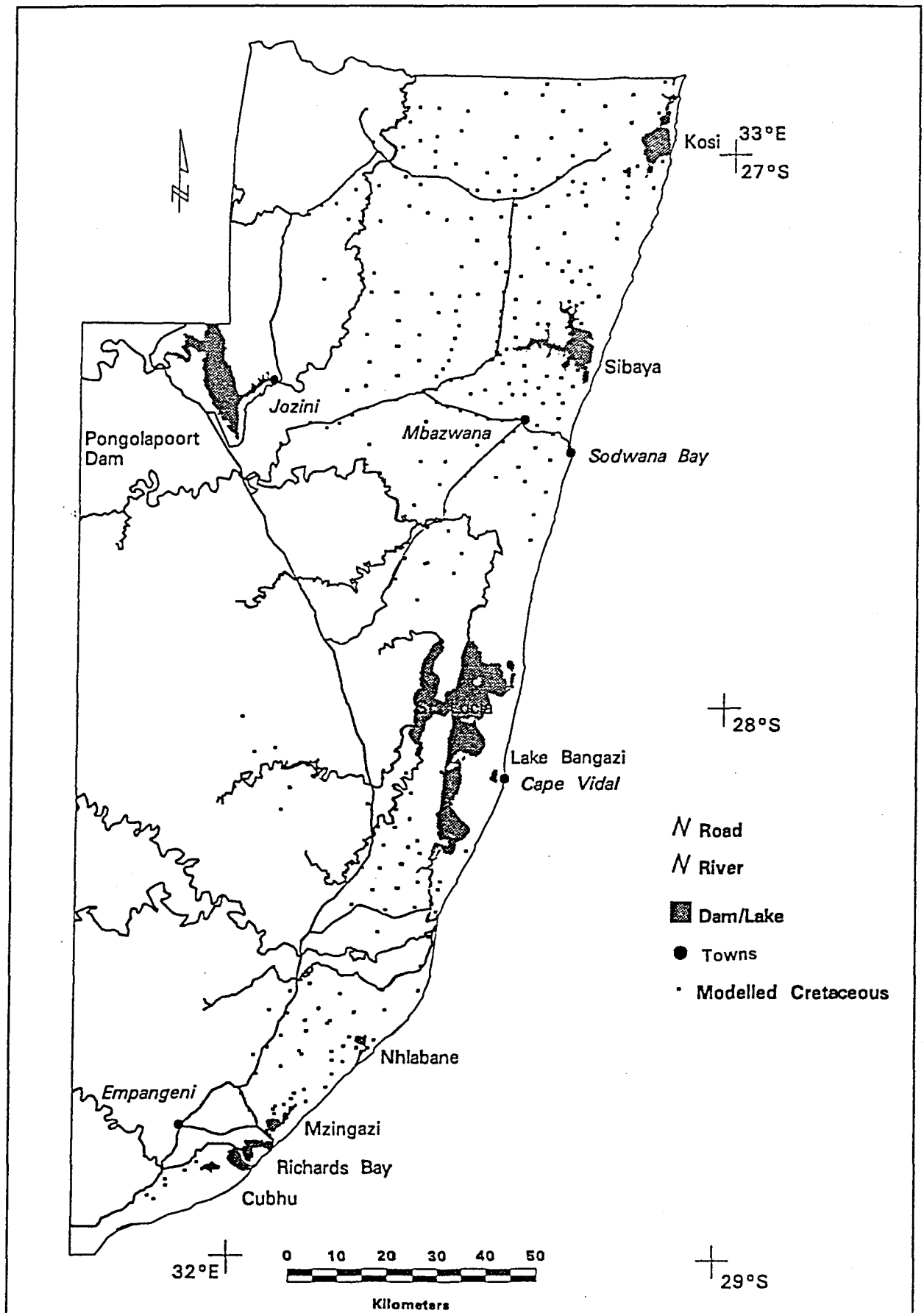


Figure 16: Positions of modeled depths to Cretaceous.

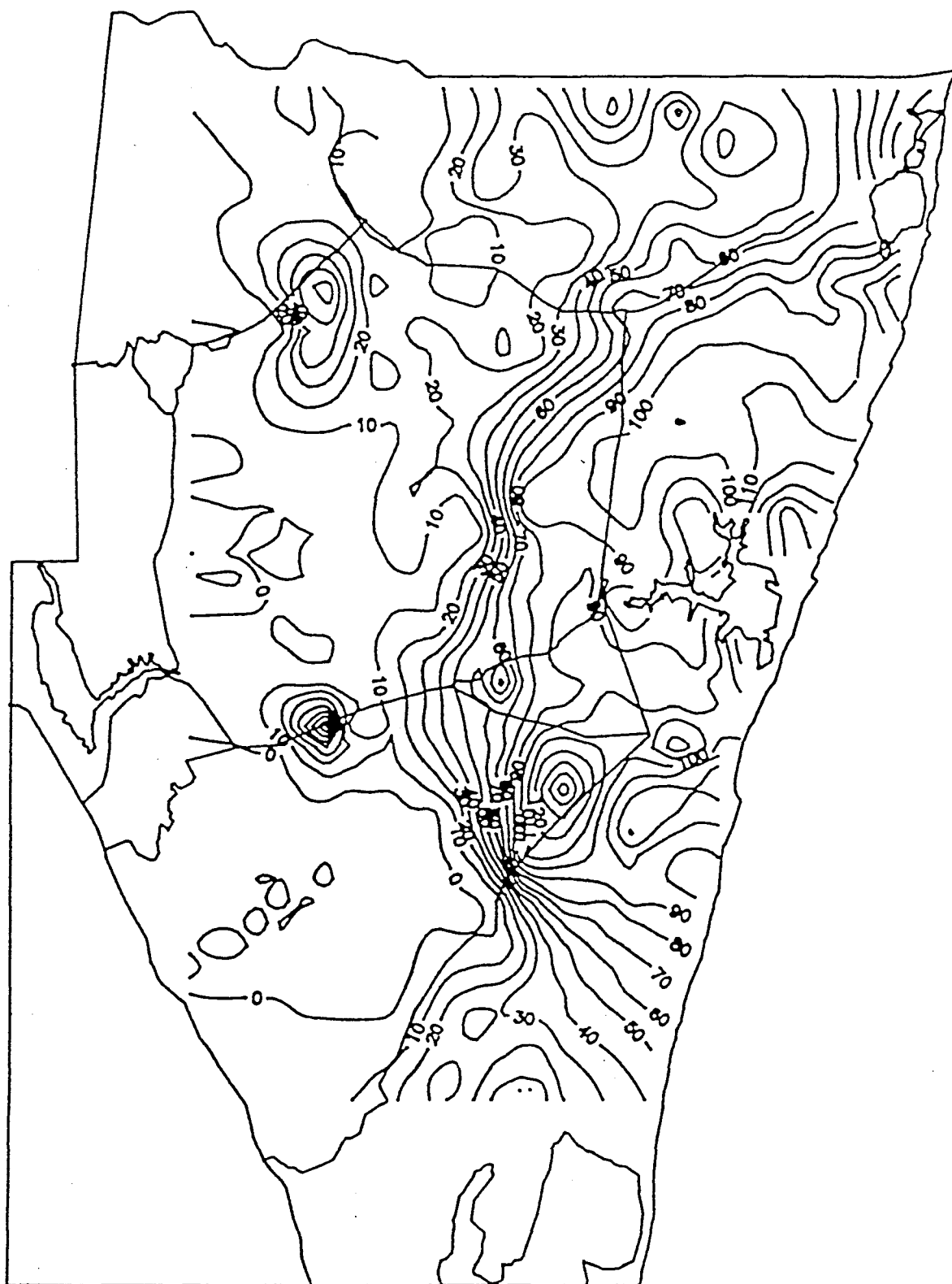


Figure 17: Post Cretaceous sediment thickness north of Lake St Lucia.

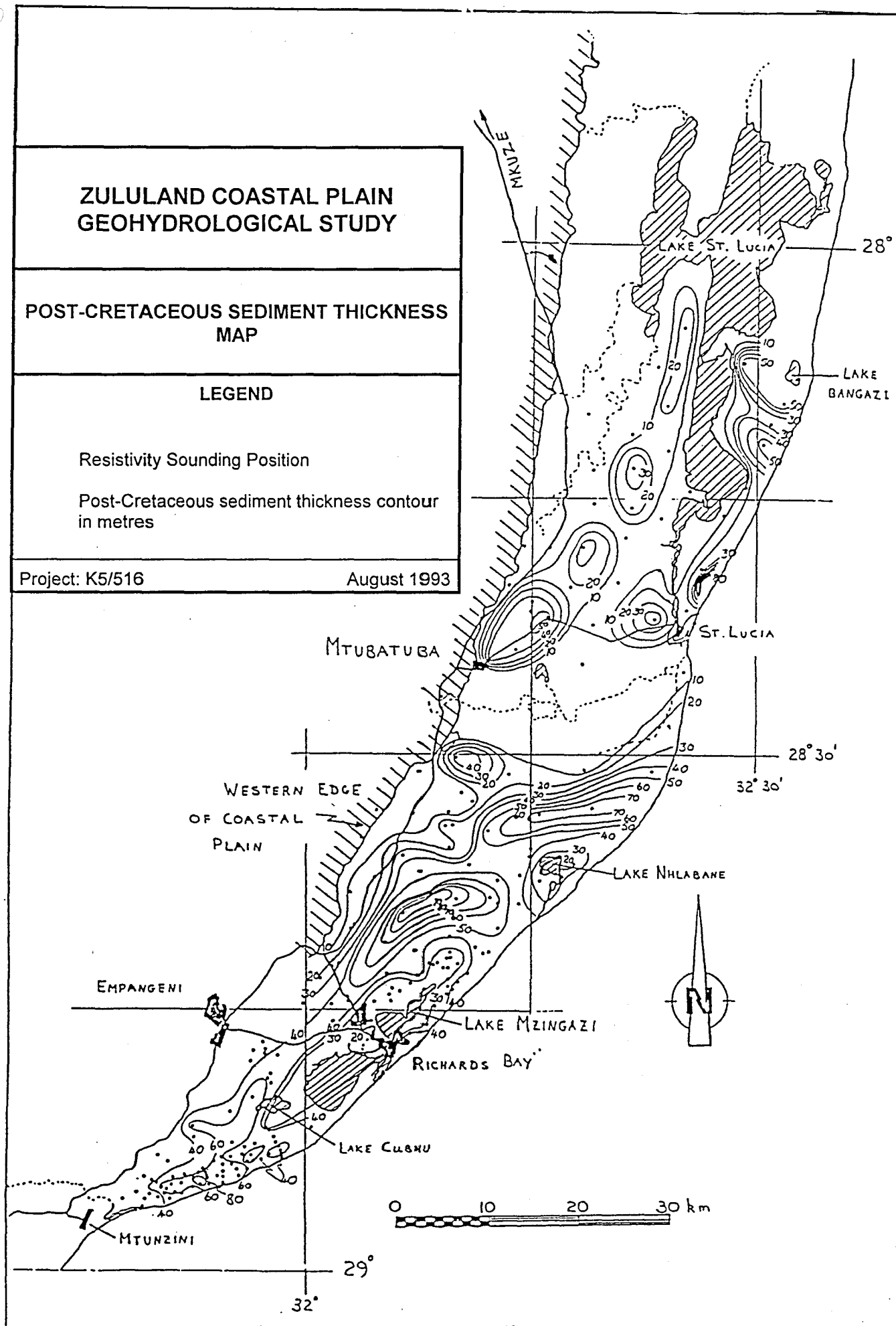


Figure 18: Post-Cretaceous sediment thickness on the Zululand Coastal Plain south of

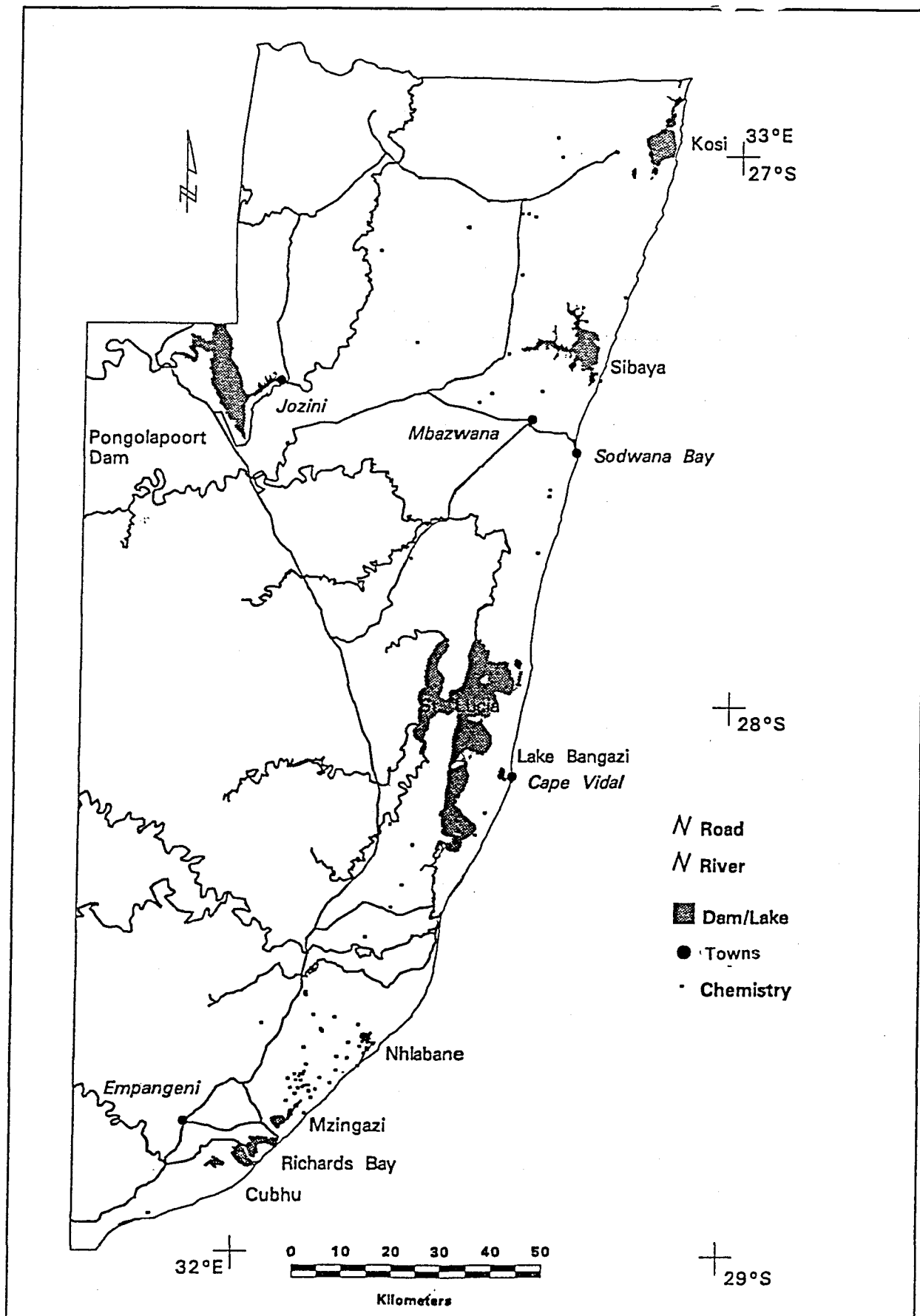
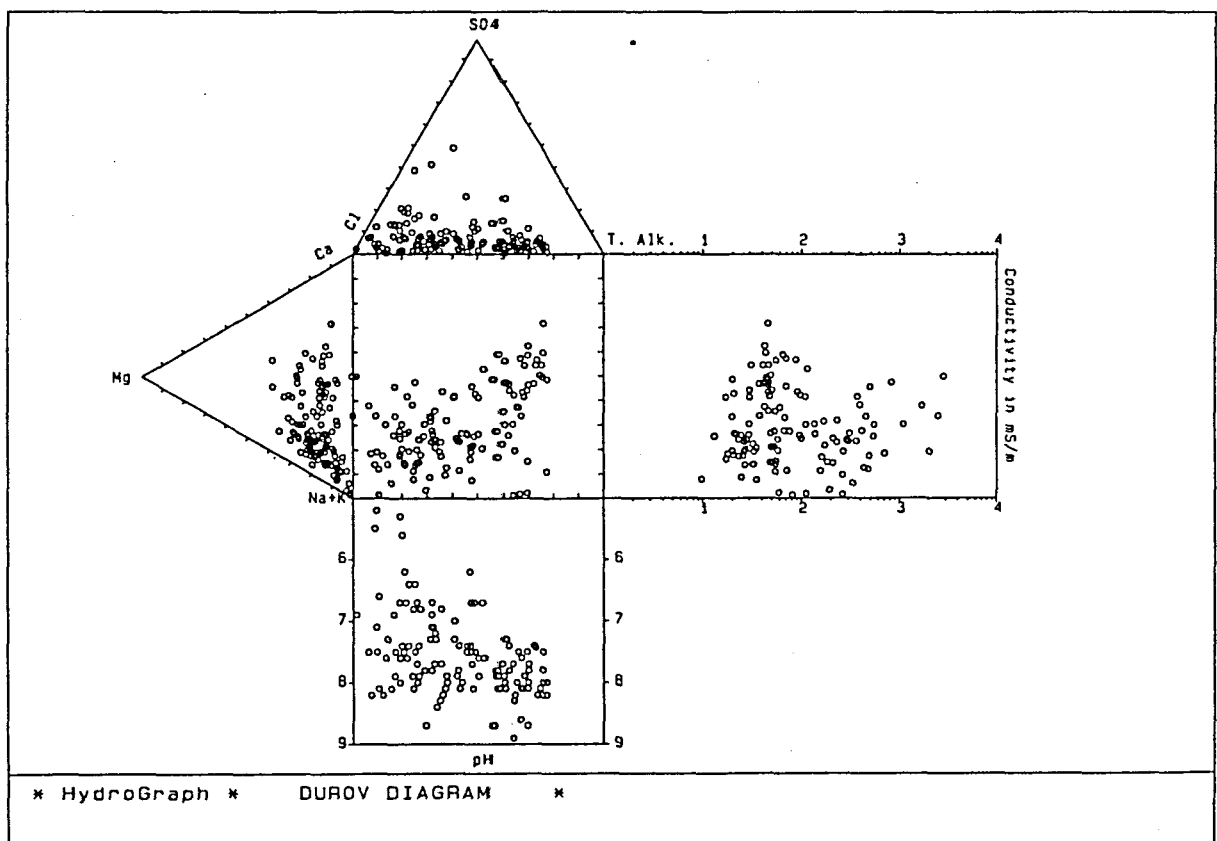
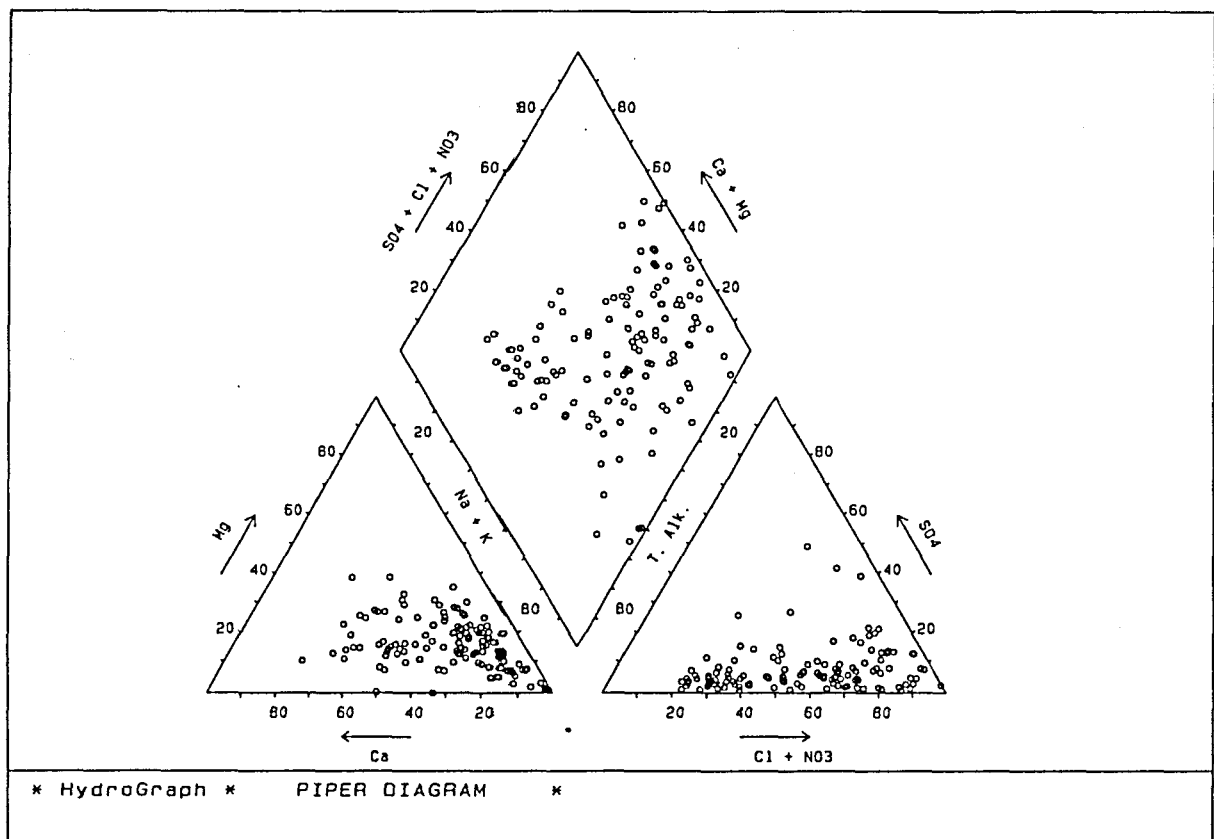
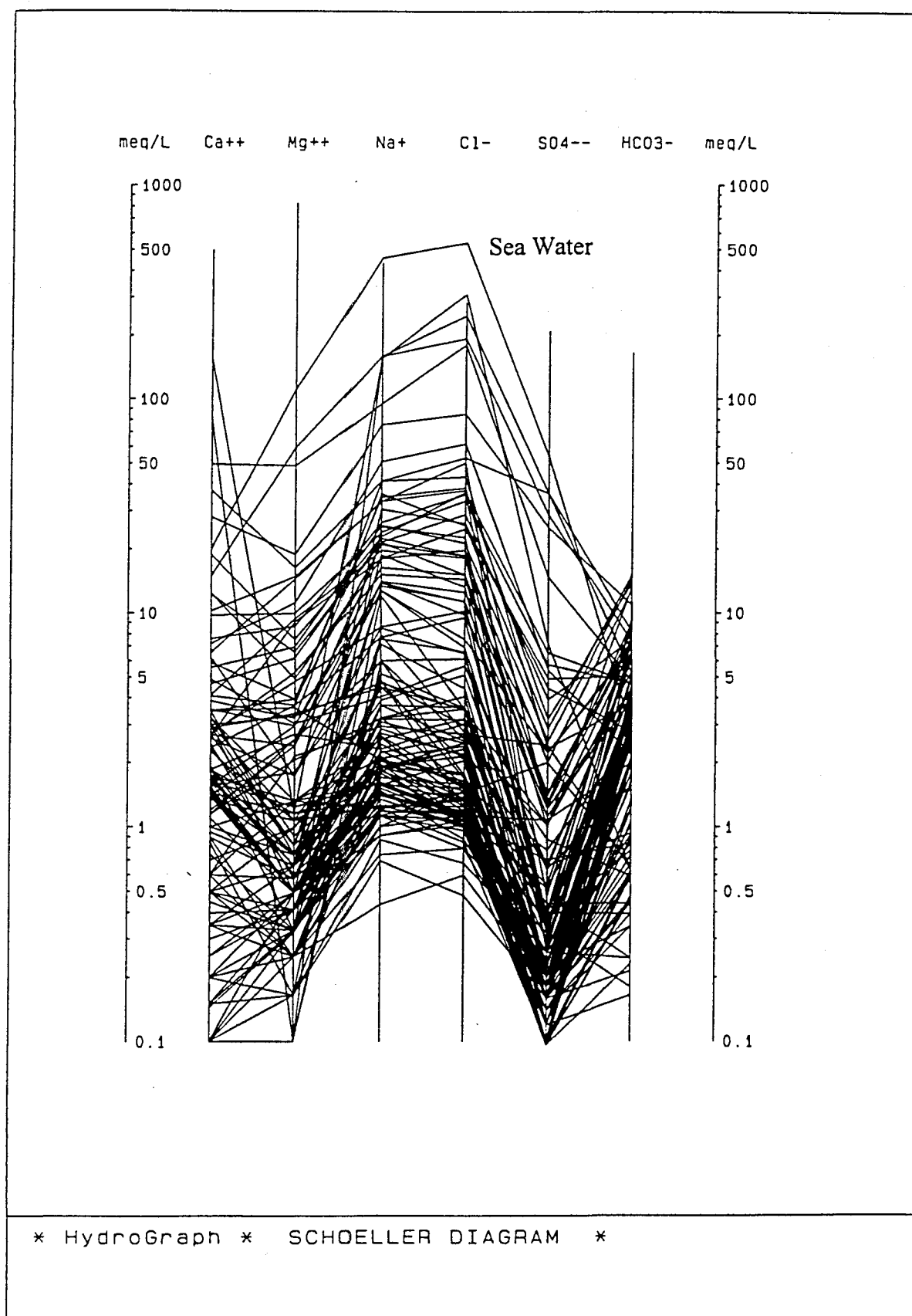


Figure 19: Boreholes sampled for water chemistry.



**Figure 20a:** Results of chemical analyses of all water samples entered into the Hydrocom database. Data are represented as Piper and Durov diagrams.



**Figure 20b:** Results of chemical analyses of all water samples entered into the Hydrocom database. Data are represented on a Schoeller diagram.

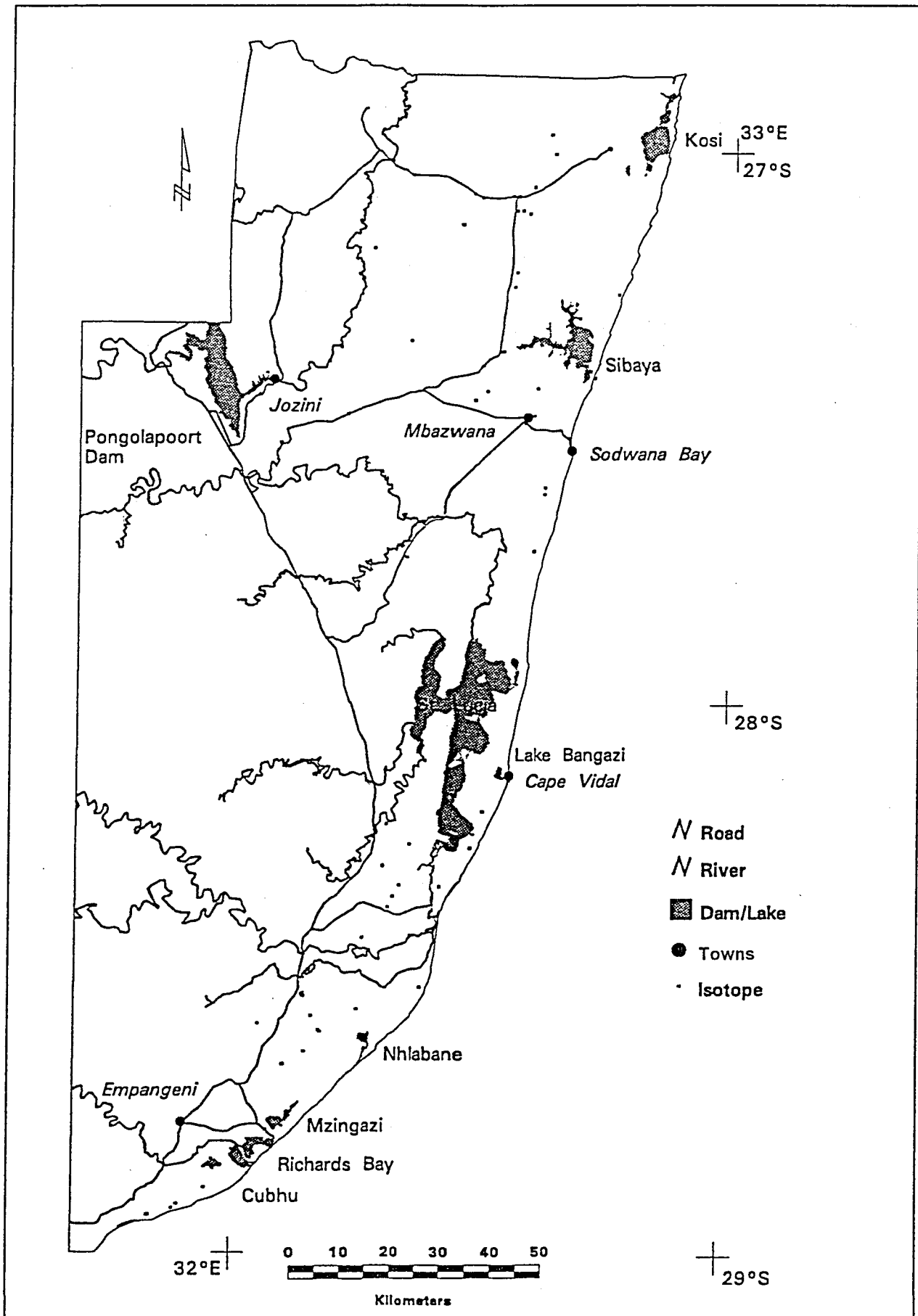
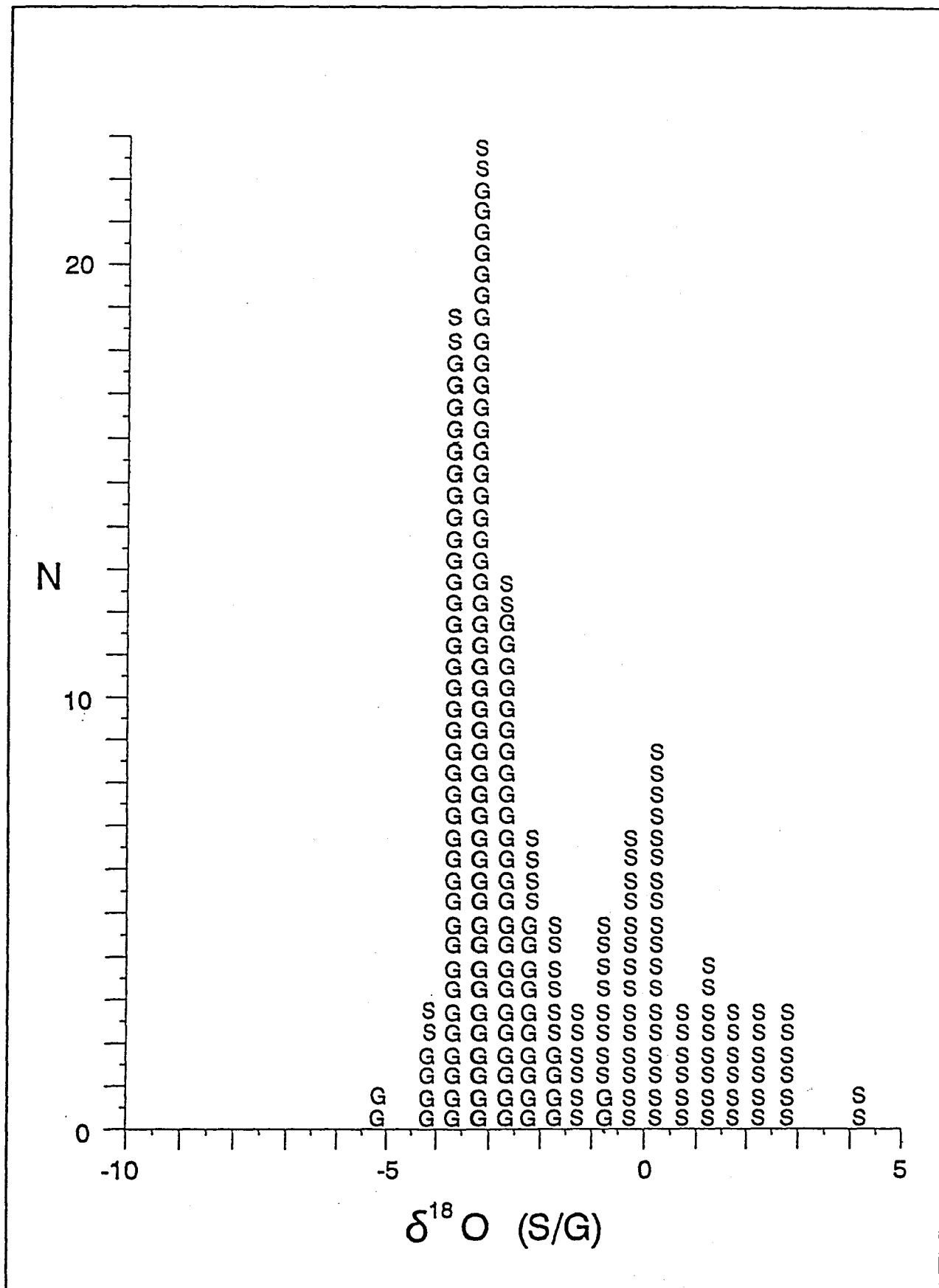
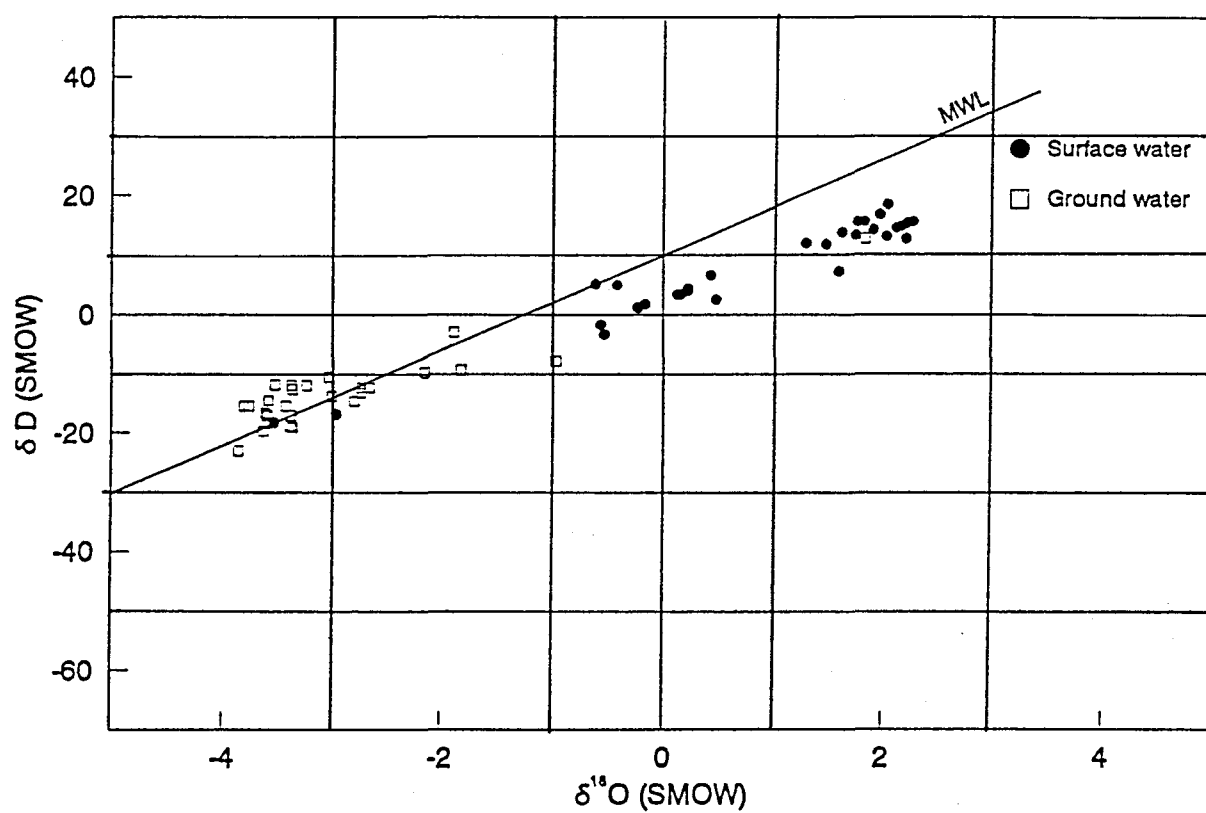


Figure 21: Ground water sampling positions for isotope analyses.



**Figure 22:** Distribution of  $\delta^{18}\text{O}$  levels on ground water and surface water in the study area. Surface waters show the effect of isotope enrichment due to evaporation.





**Figure 23:** Relation between  $^{18}\text{O}$  and deuterium in ground water and surface water. Ground water falls on the Meteoric Water Line (MWL) following a general pattern. Deviations from the MWL by surface water are due to evaporation enrichment.

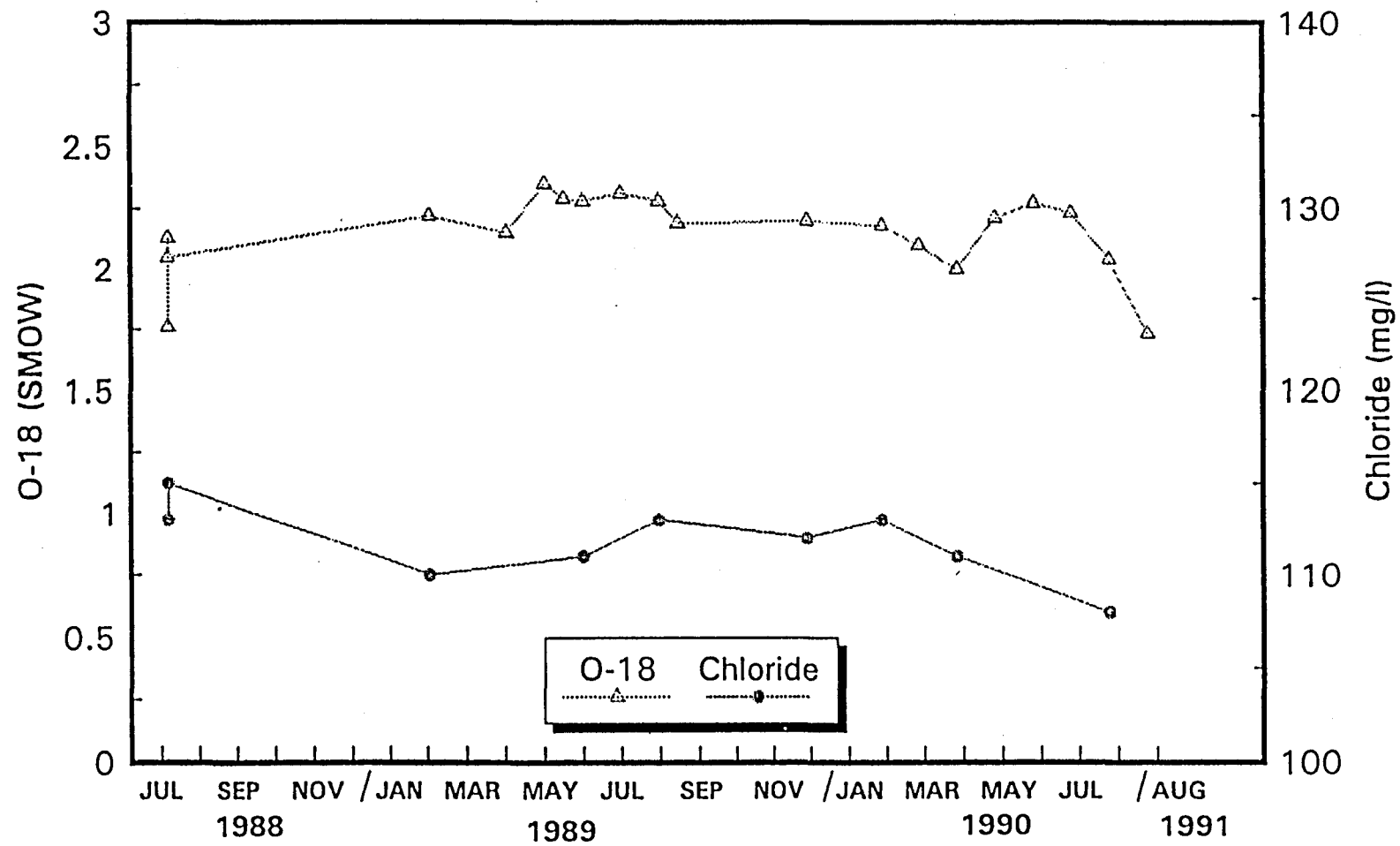


**Figure 24:** Time series of chloride (Cl) and  $^{18}\text{O}$  in Lake Sibayi. The overall constancy of both parameters indicates that the annual (rain/ground) water inflow is small compared with the lake volume.

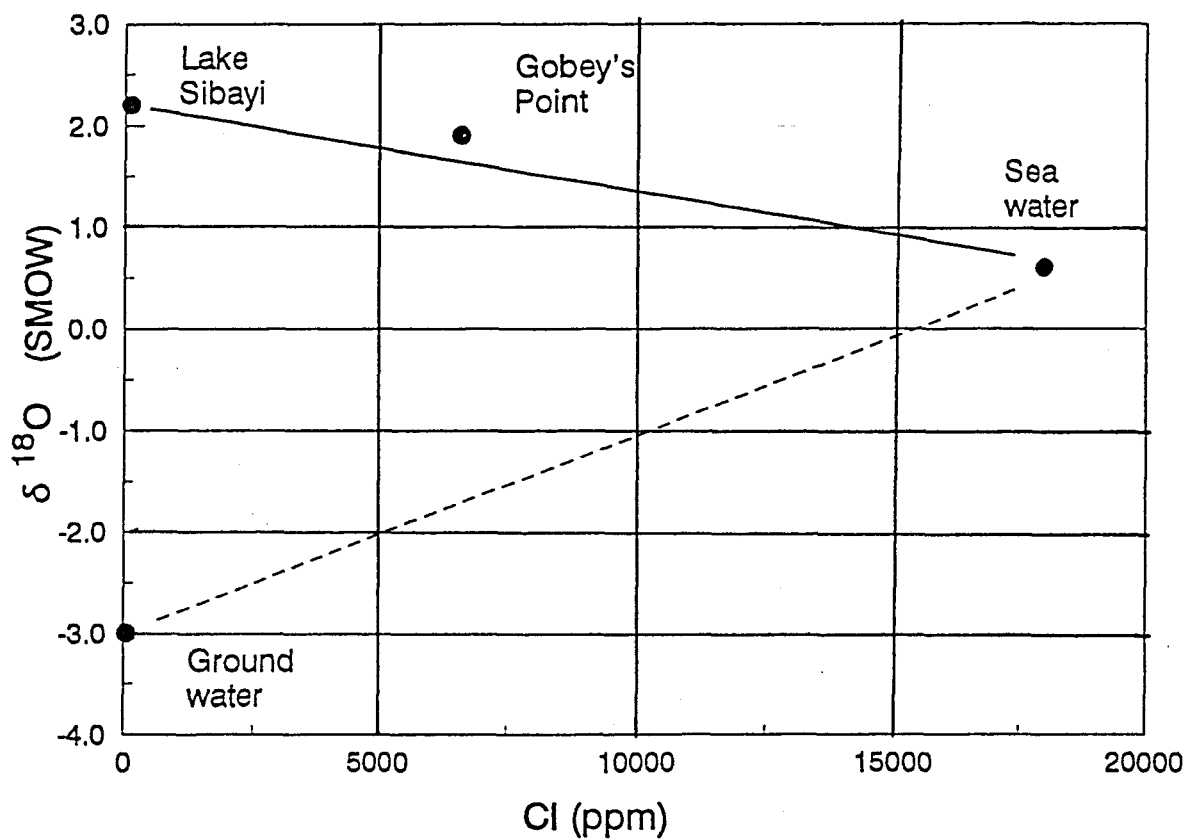


**Figure 25:**  $^{18}\text{O}$  and chloride relation for the Gobey's Point seepage and the waters likely to be its sources.

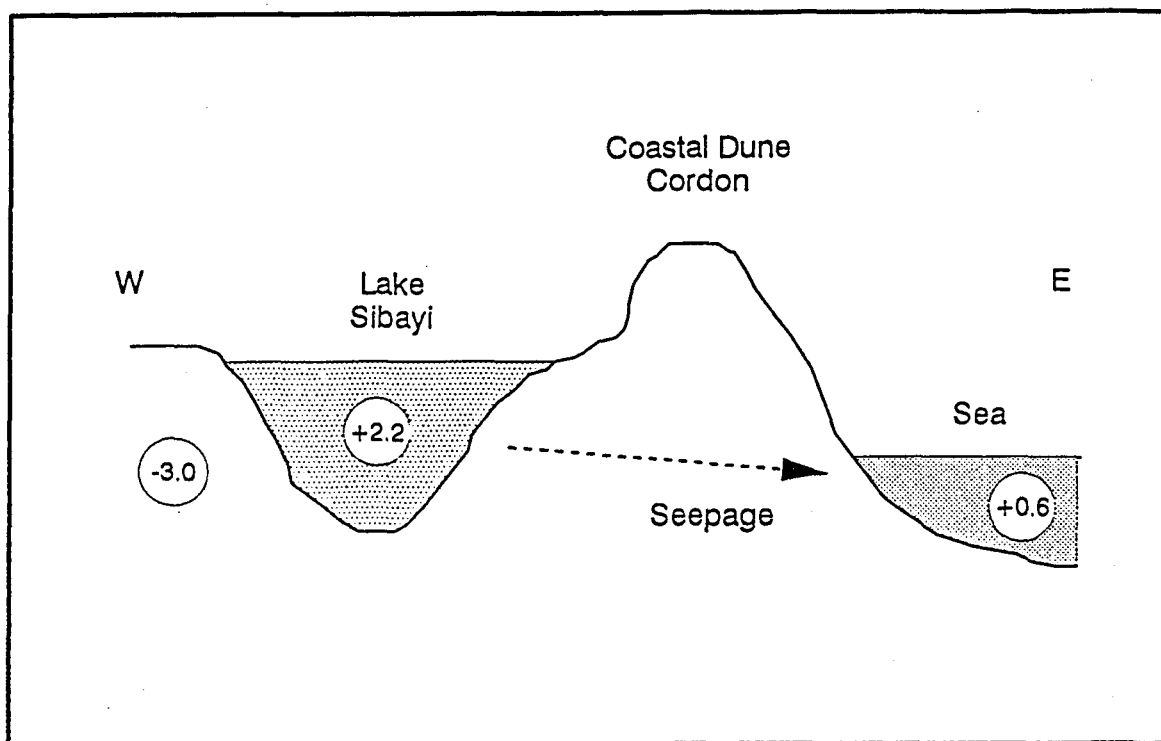


**Figure 26:** Schematic cross-section through the coastal dune between Lake Sibayi and the sea.

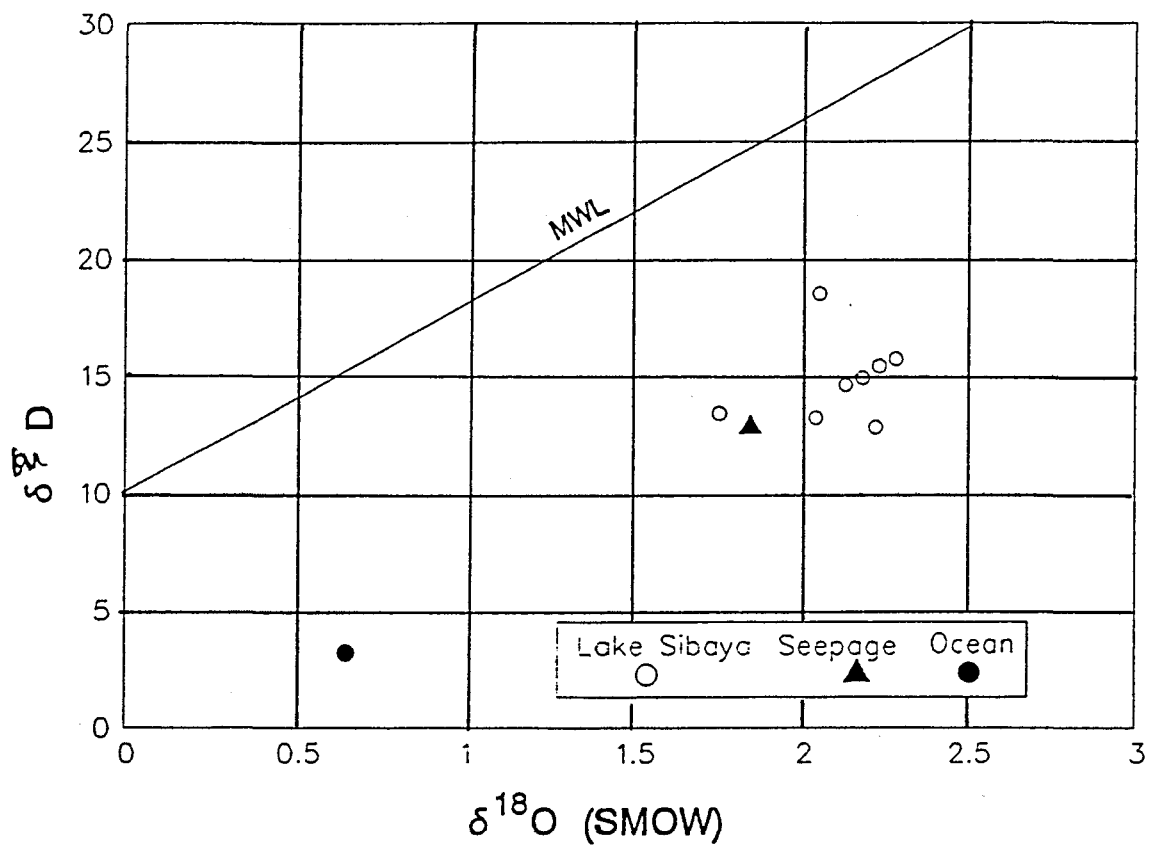


**Figure 27:**  $^{18}\text{O}$  and deuterium relation for Gobey's Point seepage and its likely sources. The seepage is also located directly on the mixing line between lake and sea water and distinctly different from the MWL representing rain and ground water.

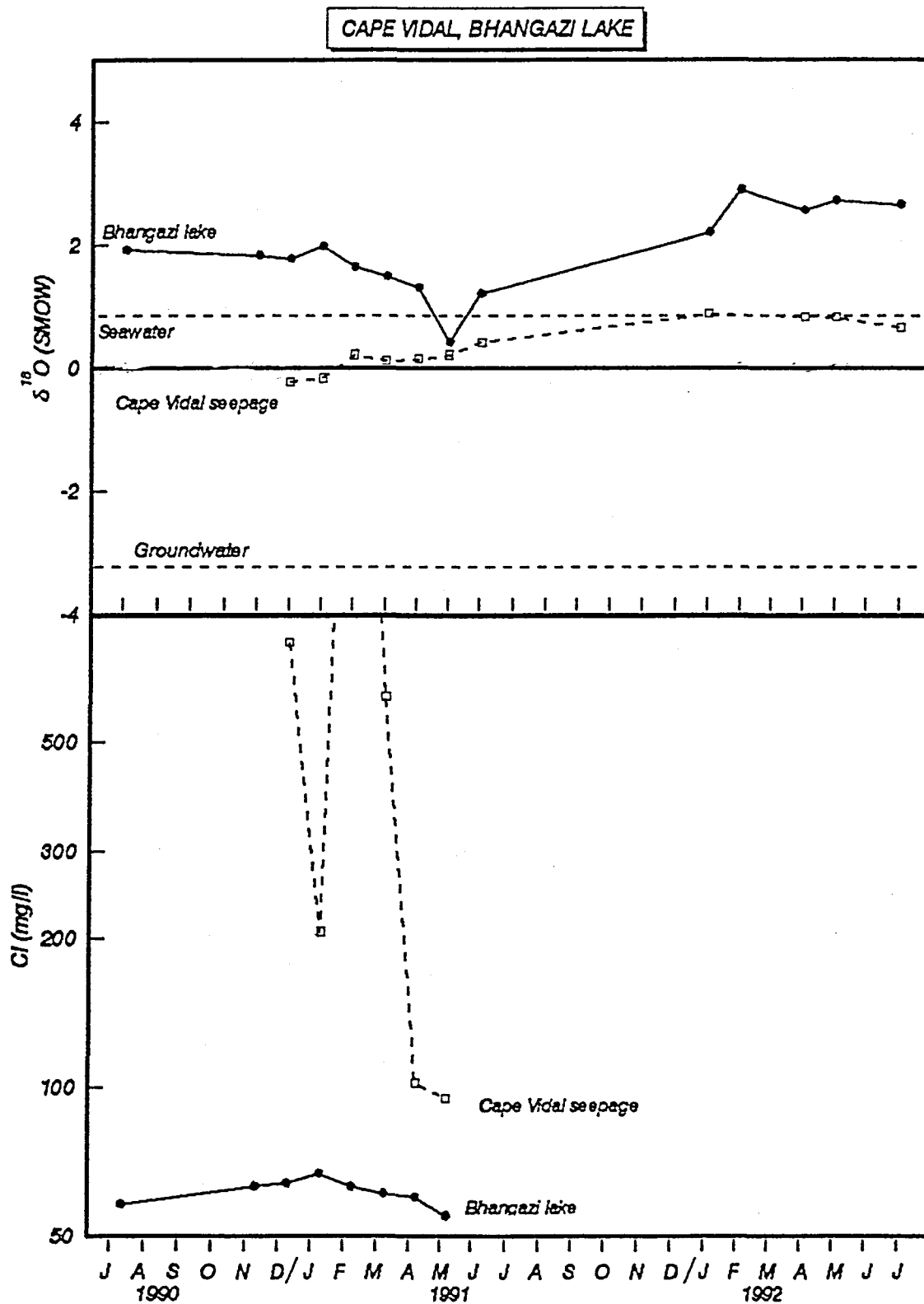


Figure 28:  $^{18}\text{O}$  and chloride time series of Lake Bhangazi and the Cape Vidal seepage water. The average  $^{18}\text{O}$  content of ground water is shown for comparison.

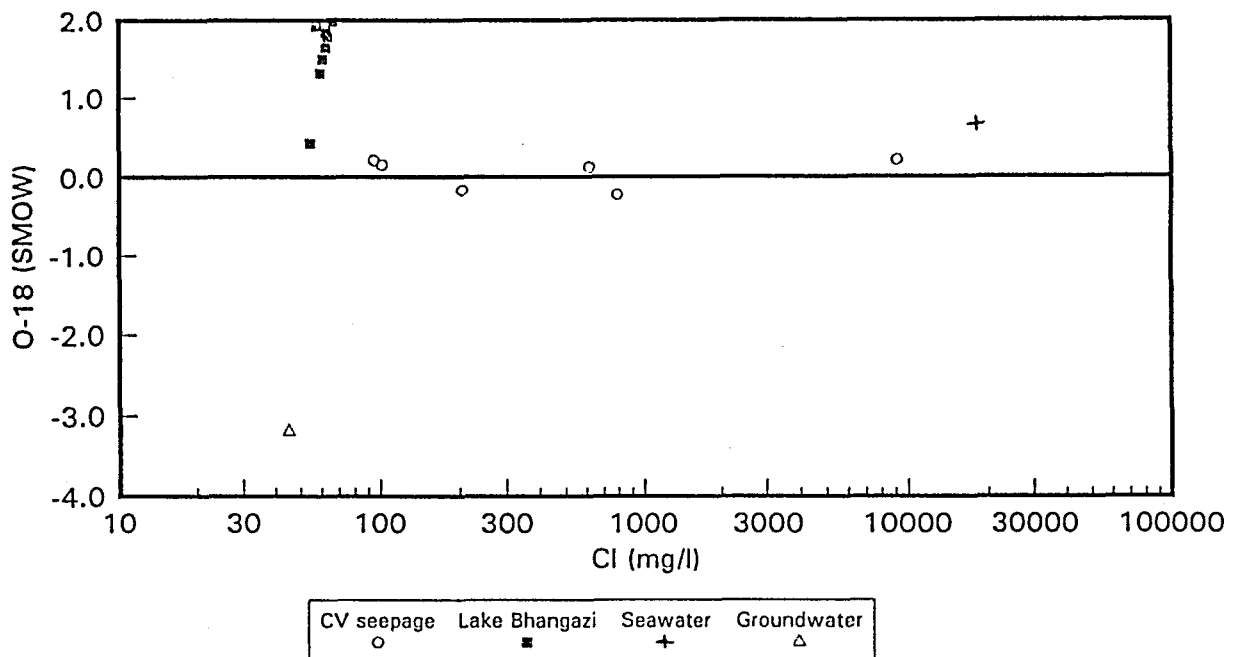
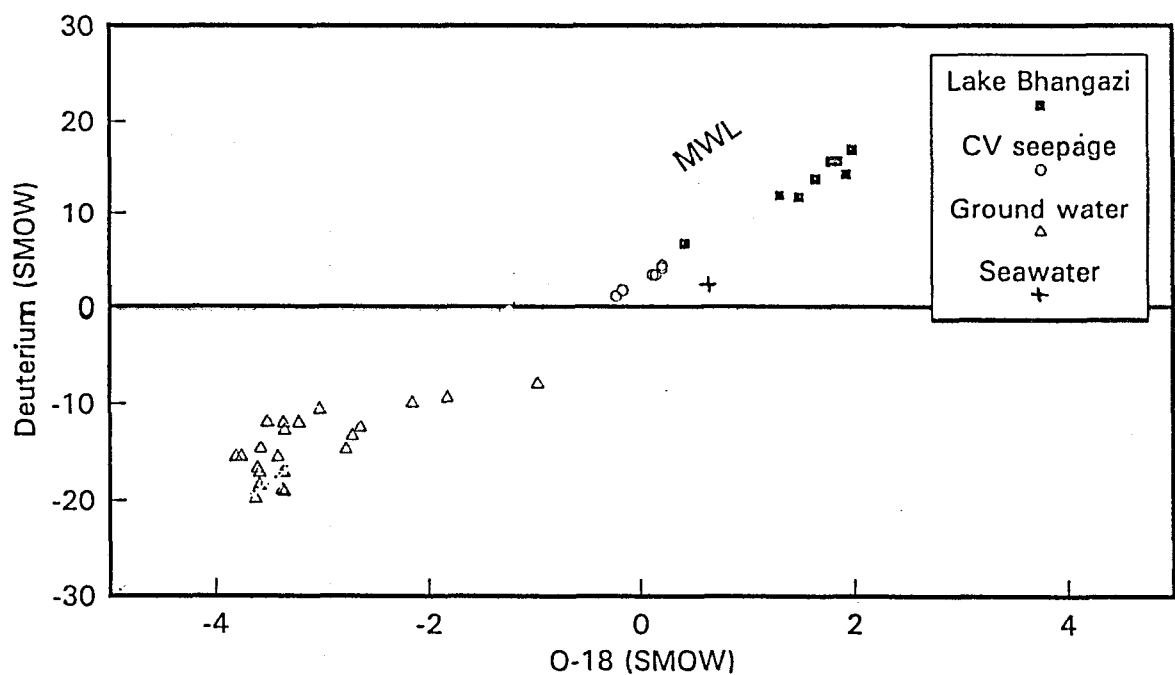


Figure 29: Comparison of  $\delta^{18}\text{O}$  and Cl in the Cape Vidal/Bhangazi system. Average values for ground water in the area are taken from Bredenkamp (1993). Cape Vidal seepage can be seen to be a mixture between Lake Bhangazi water and ground water with occasional sea water contributions. Note the logarithmic scale.



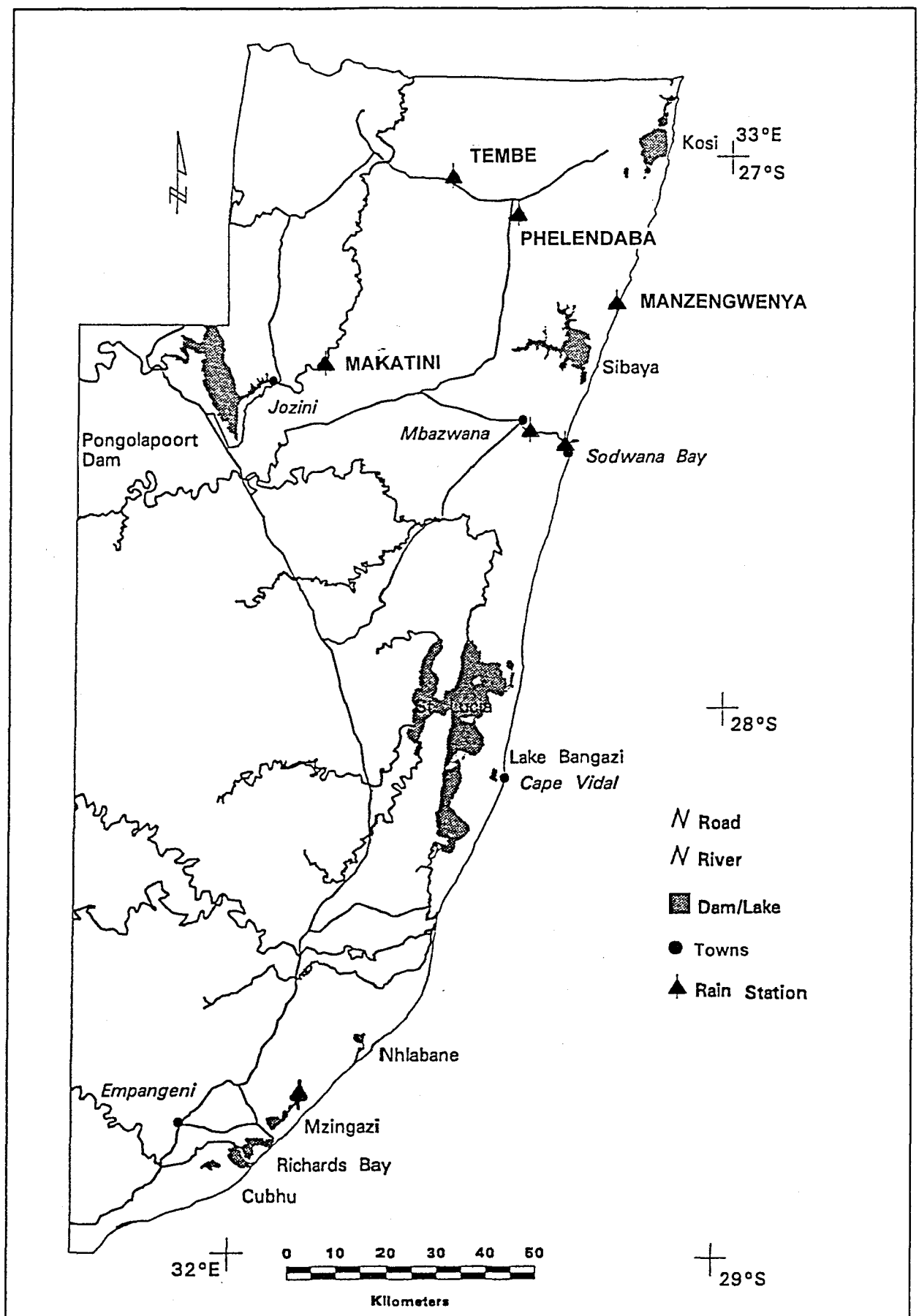


Figure 31: Rainfall monitoring stations used for this study.

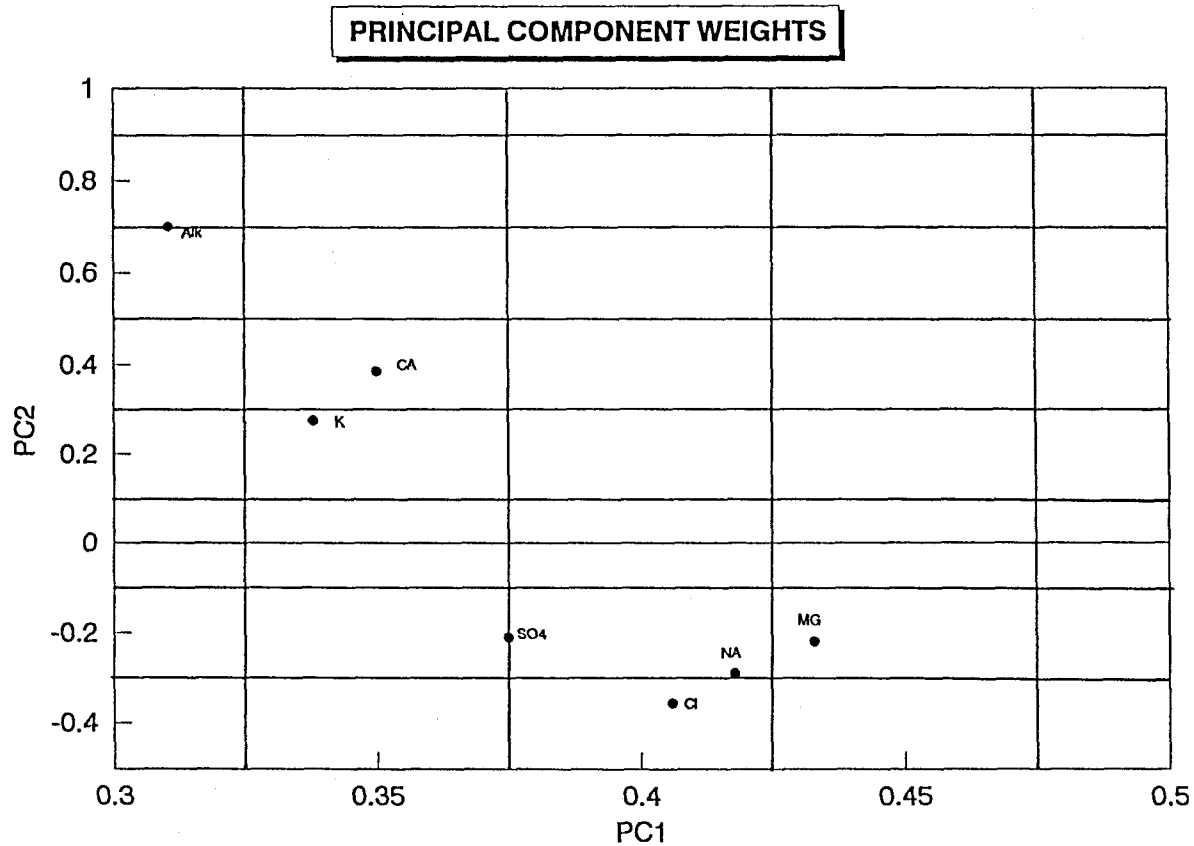


Figure 32: Results of principle component analysis of the rainfall chemistry data. The weights of the various ions contributing to the first two principle components are shown.

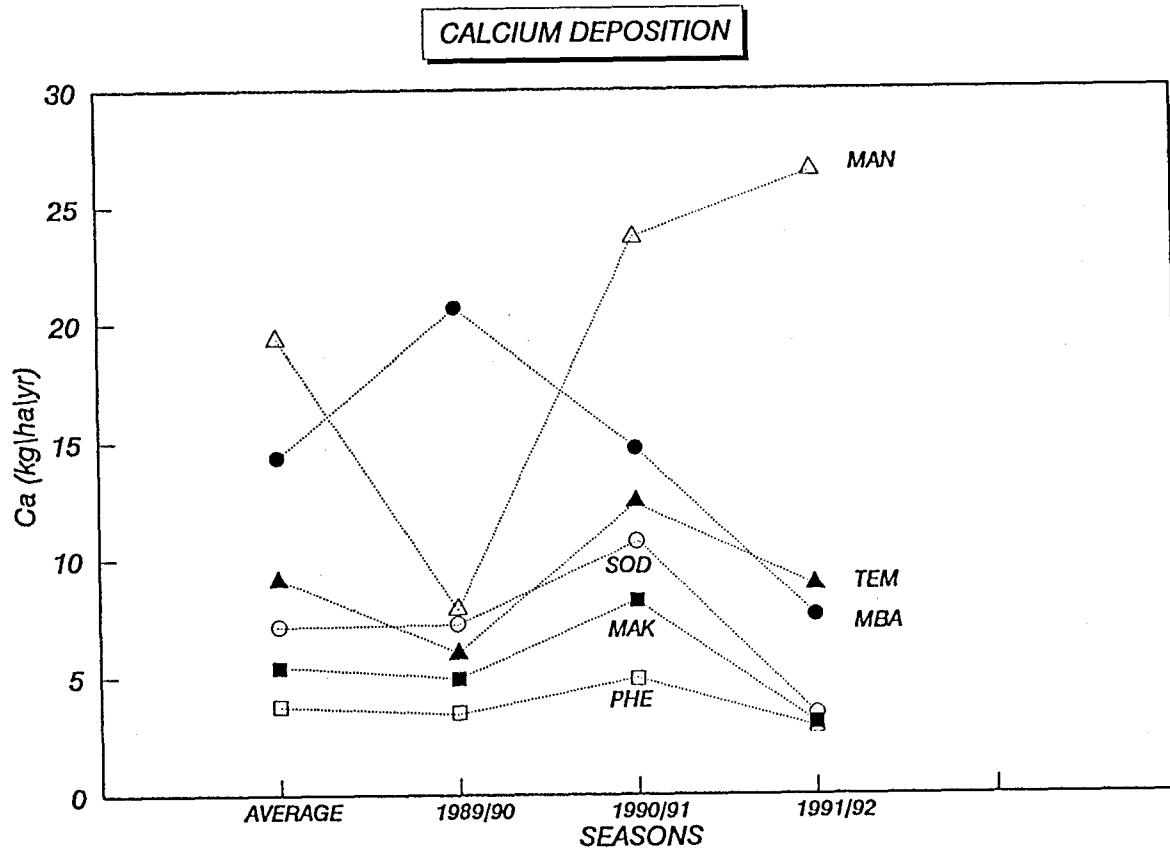


Figure 33: Annual calcium deposition rates for the three sampling years.



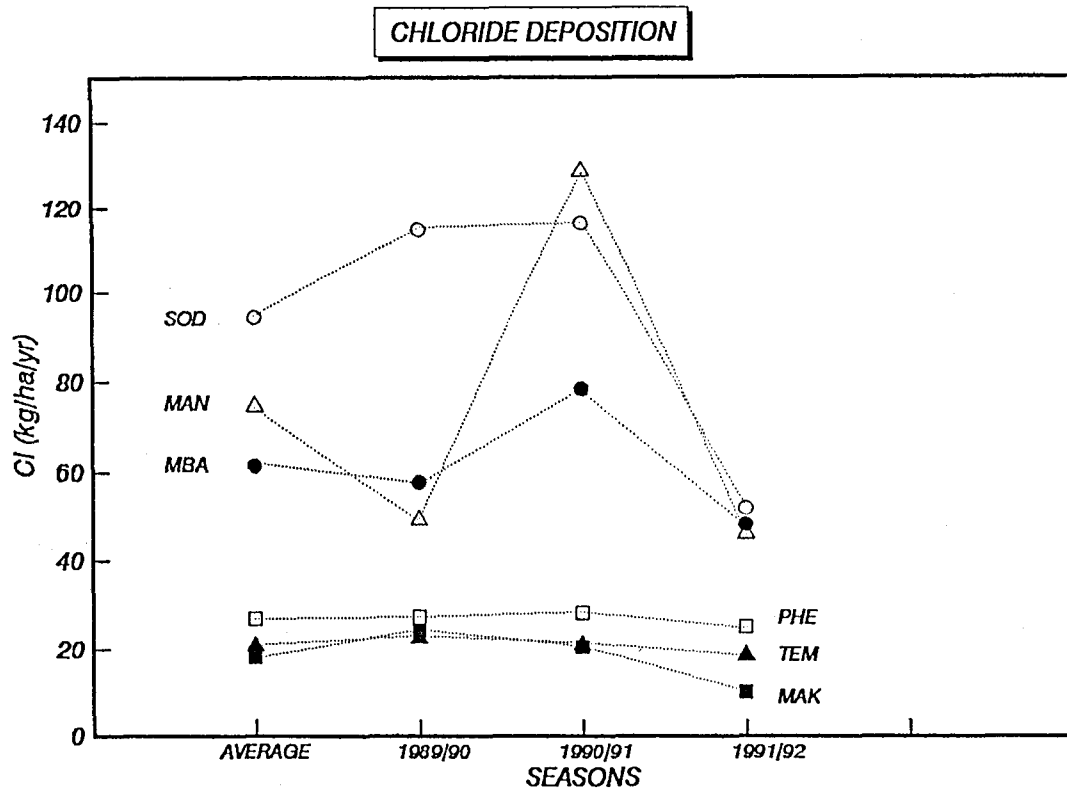


Figure 34: Annual chloride deposition rates for the three sampling years. The coastal stations (SOD, MBA, MAN) show more annual variations than do the inland stations.

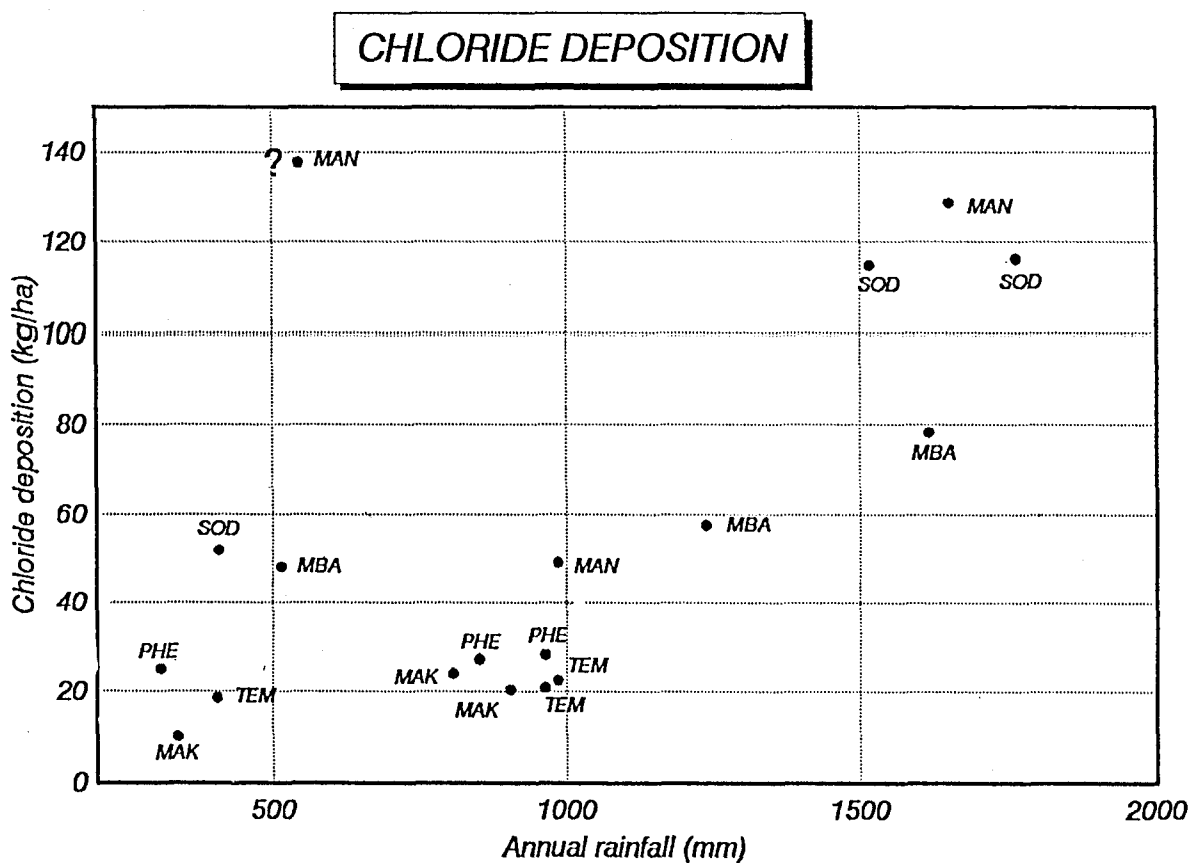


Figure 35: Relation between annual chloride deposition (for each of the three years) and the rainfall of that year.

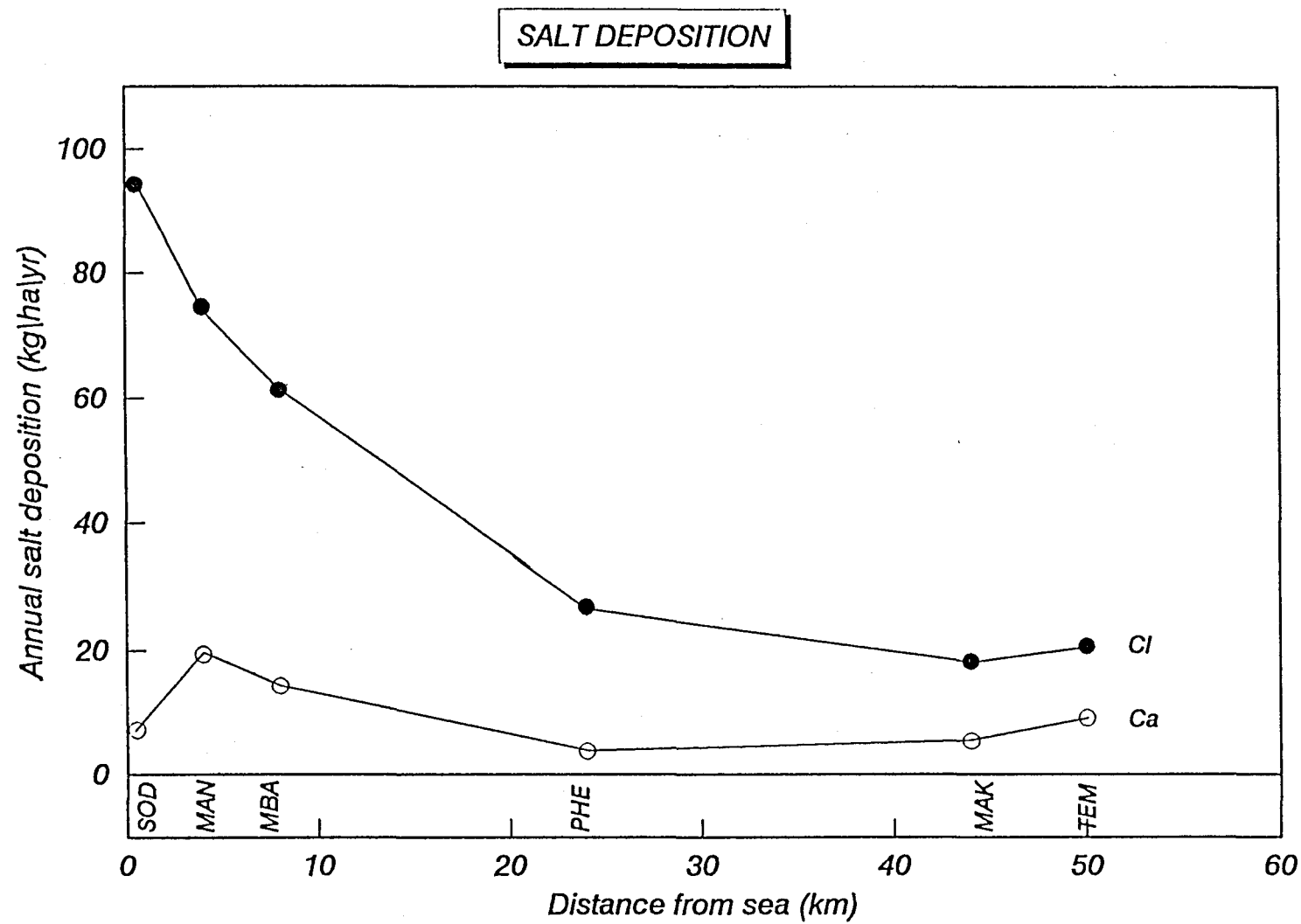


Figure 36: Average (three years) chloride and calcium deposition with distance inland.

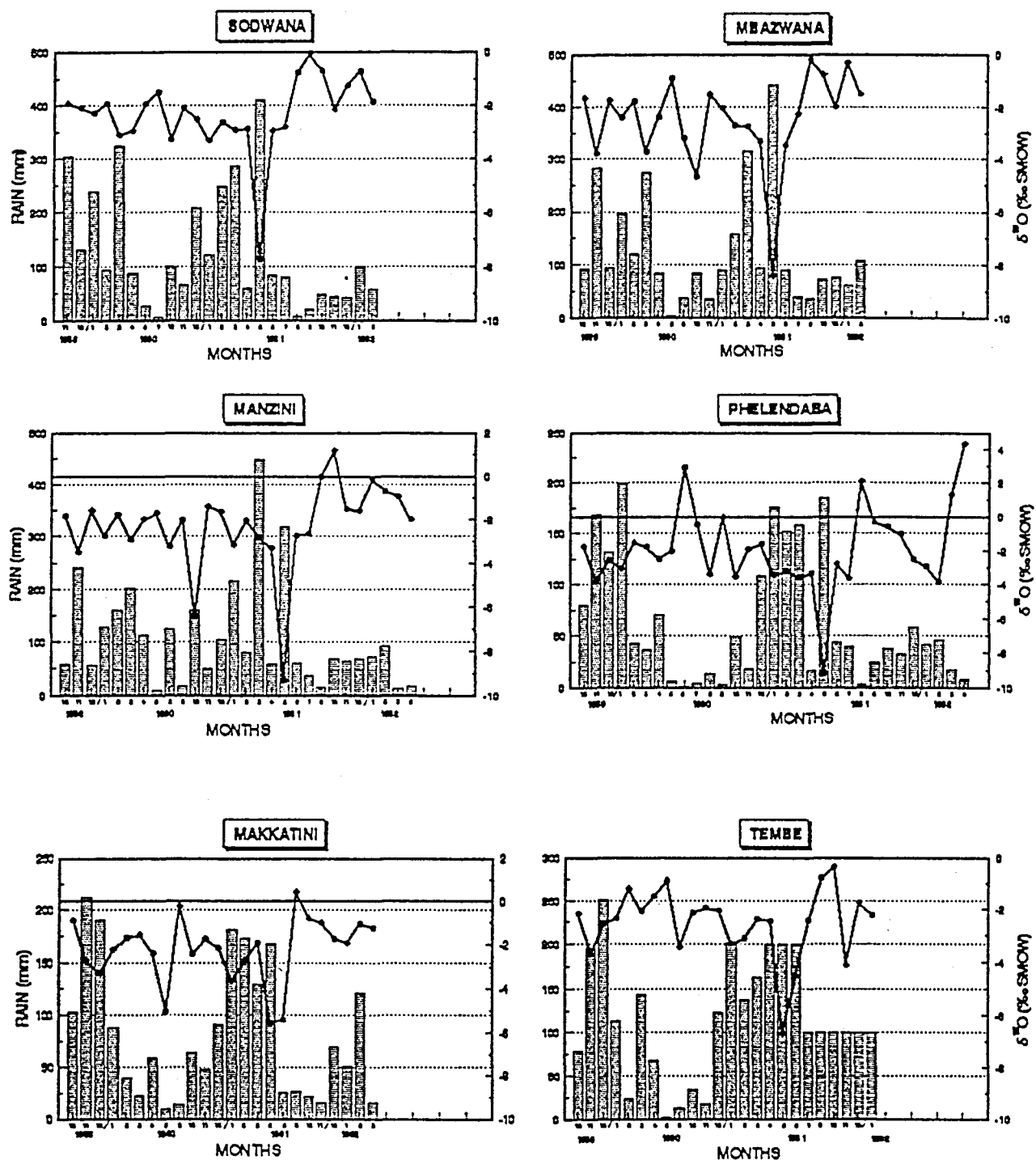


Figure 37: Seasonal pattern of rainfall and its  $^{18}\text{O}$  content for the six rainfall stations (October 1989 to January 1992).

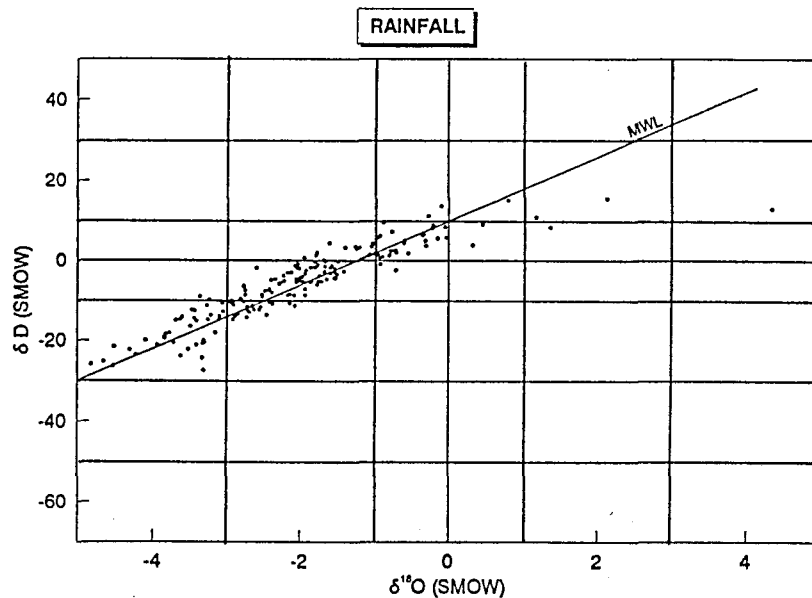


Figure 38:  $^{18}\text{O}$  deuterium relation for rainfall. Most are located on the MWL ( $\delta\text{D} = 8\delta^{18}\text{O} + 10$ ) which holds worldwide (Gat and Giofanti, 1981).

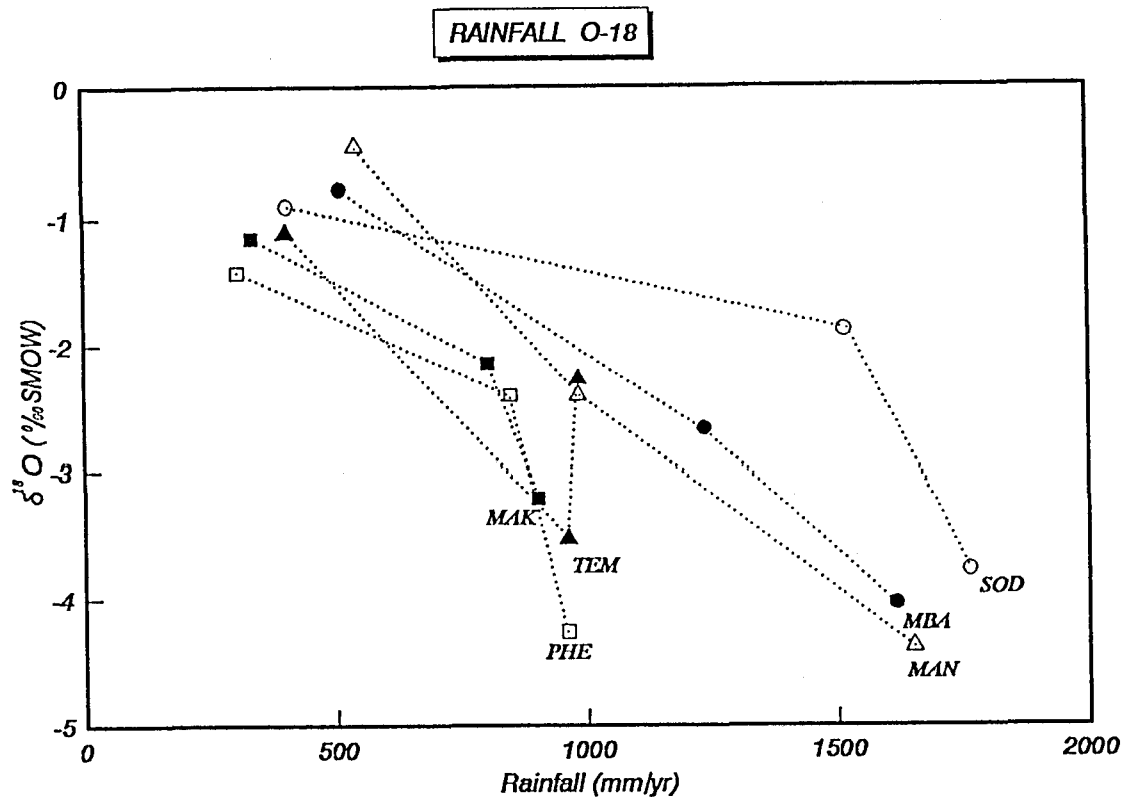
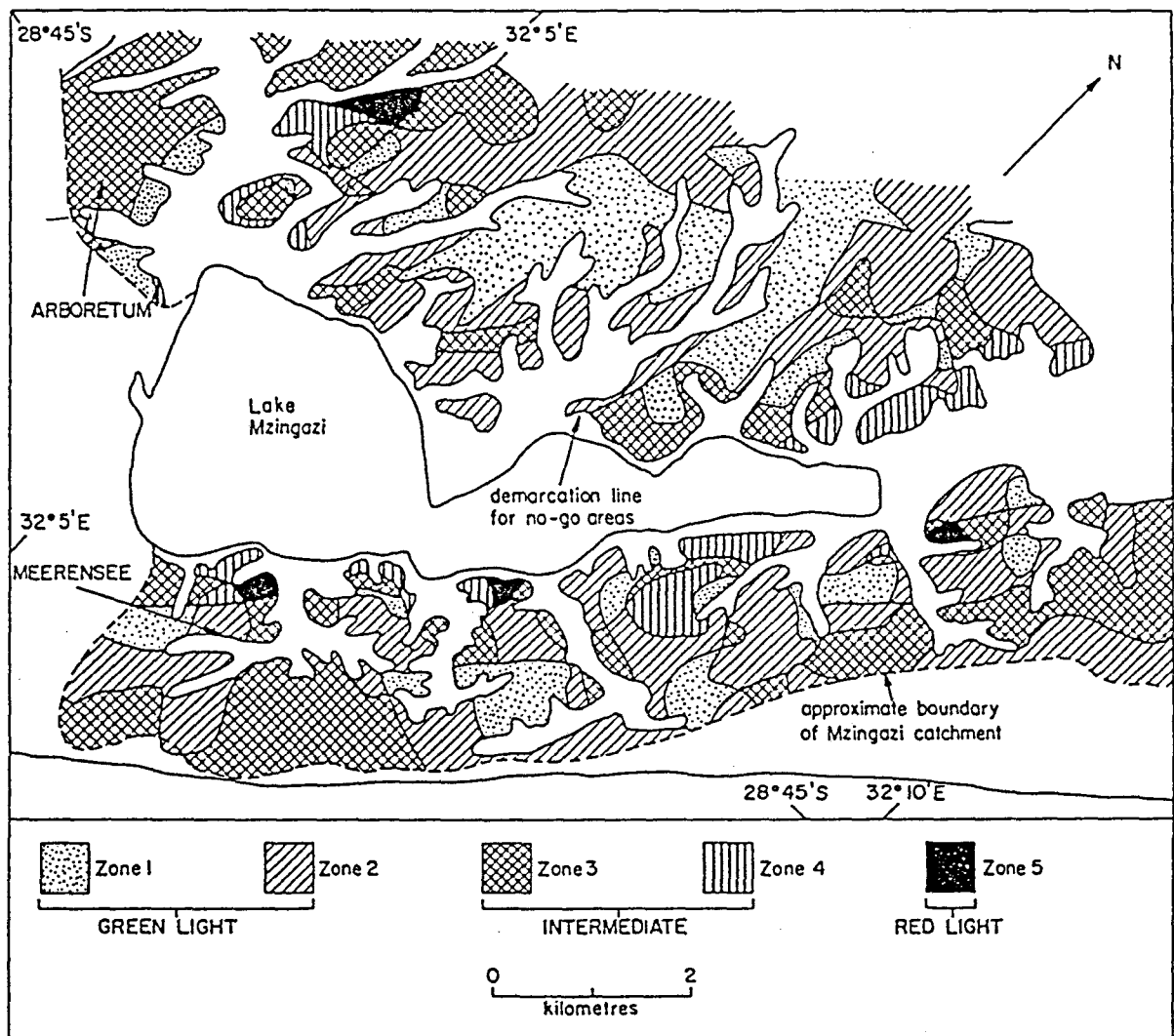
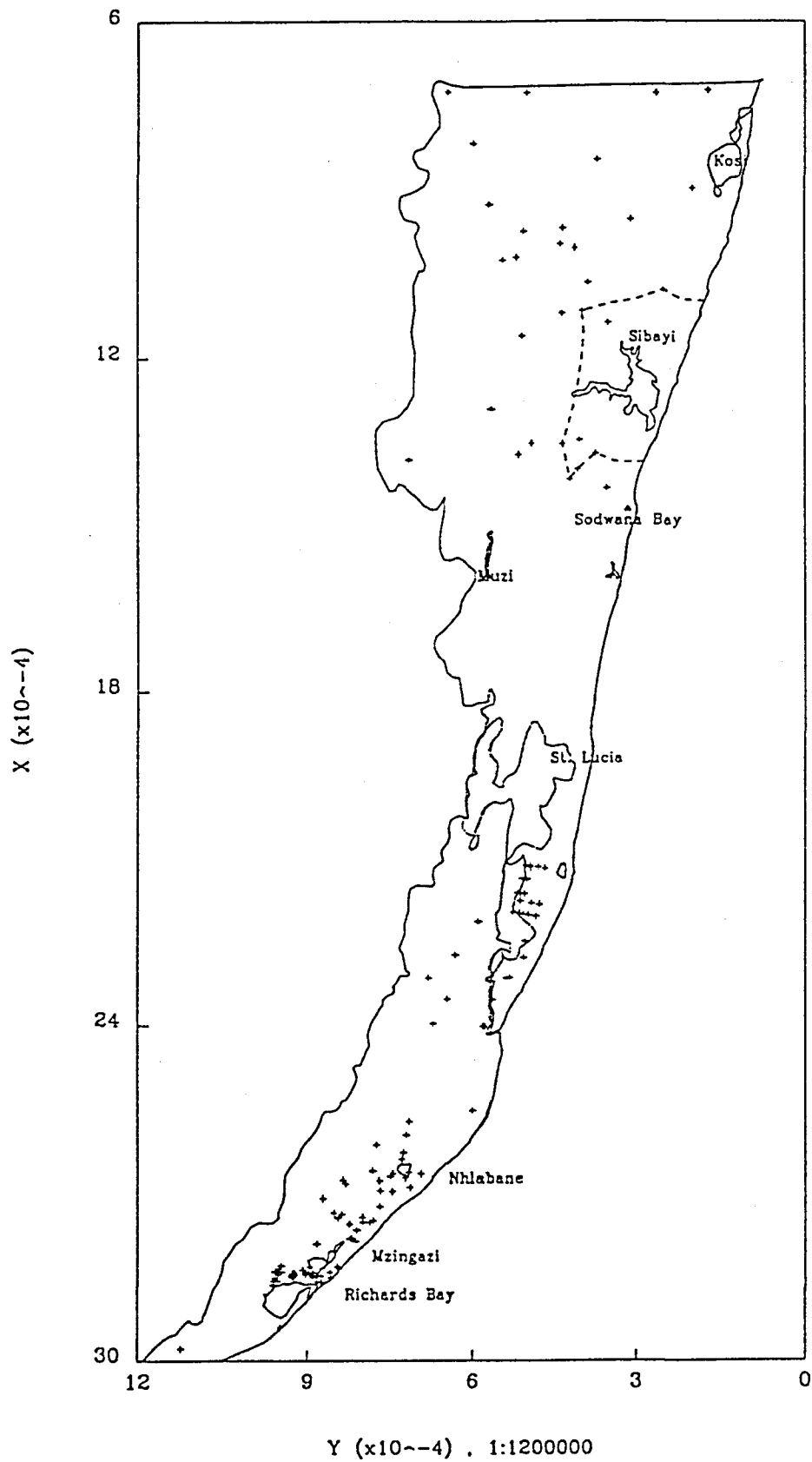


Figure 39: Relation between weighted annual  $^{18}\text{O}$  content in rain and the total rainfall for that year. Note the large difference (especially for the coastal stations SOD, MAN, MBA) and the driest year (1991/92).



**Figure 40:** Pollution vulnerability map for the fresh waters of the inner catchment of Lake Mzingazi (Worthington, 1978).



**Figure 41:** The borders of the Zululand aquifer, as well as the positions of the lakes and boreholes used in this study, are shown. The hypothetical afforestation around Lake Sibayi is also shown.

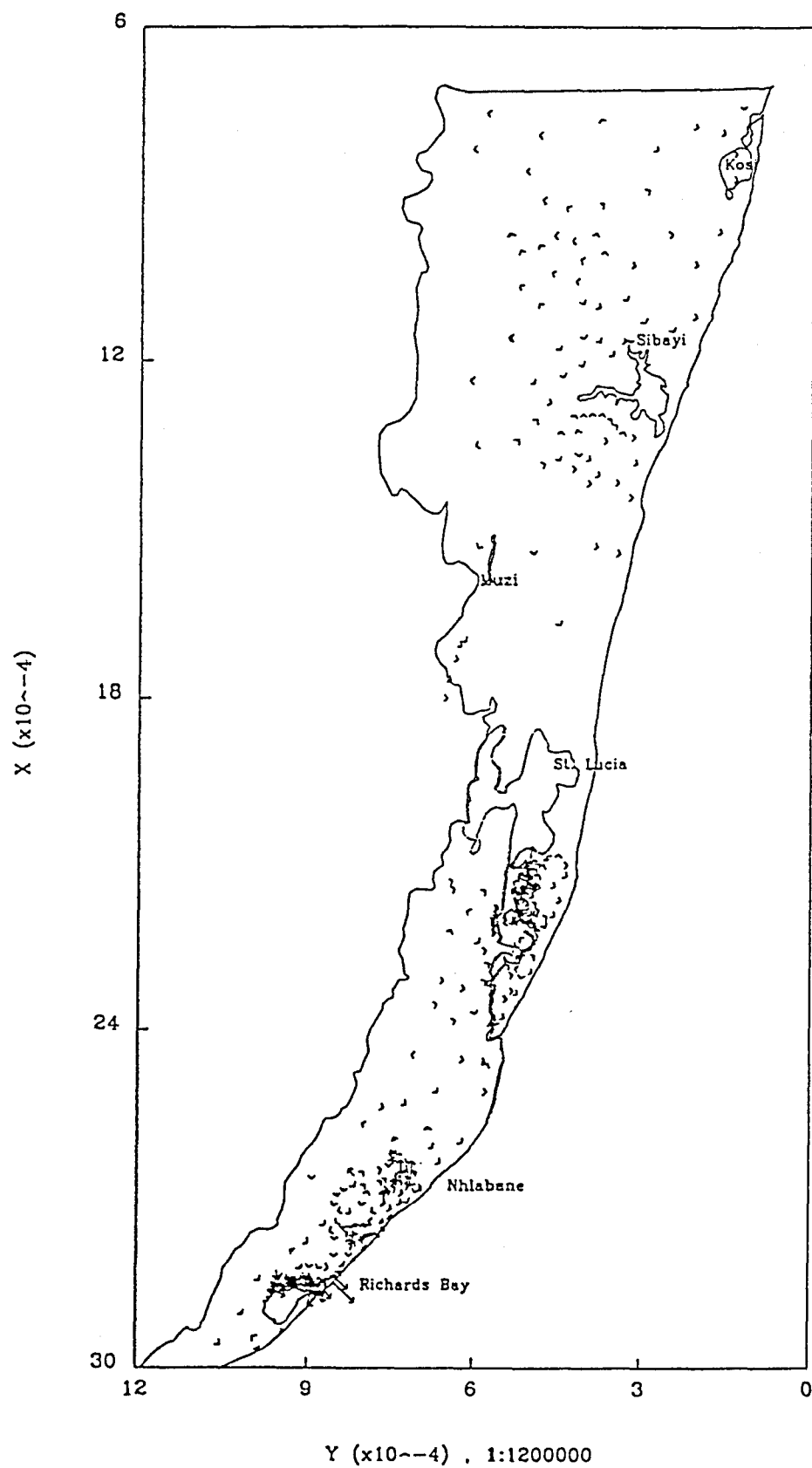


**Figure 42:** The ground water velocities in the Zululand aquifer, as computed from the 140 boreholes.

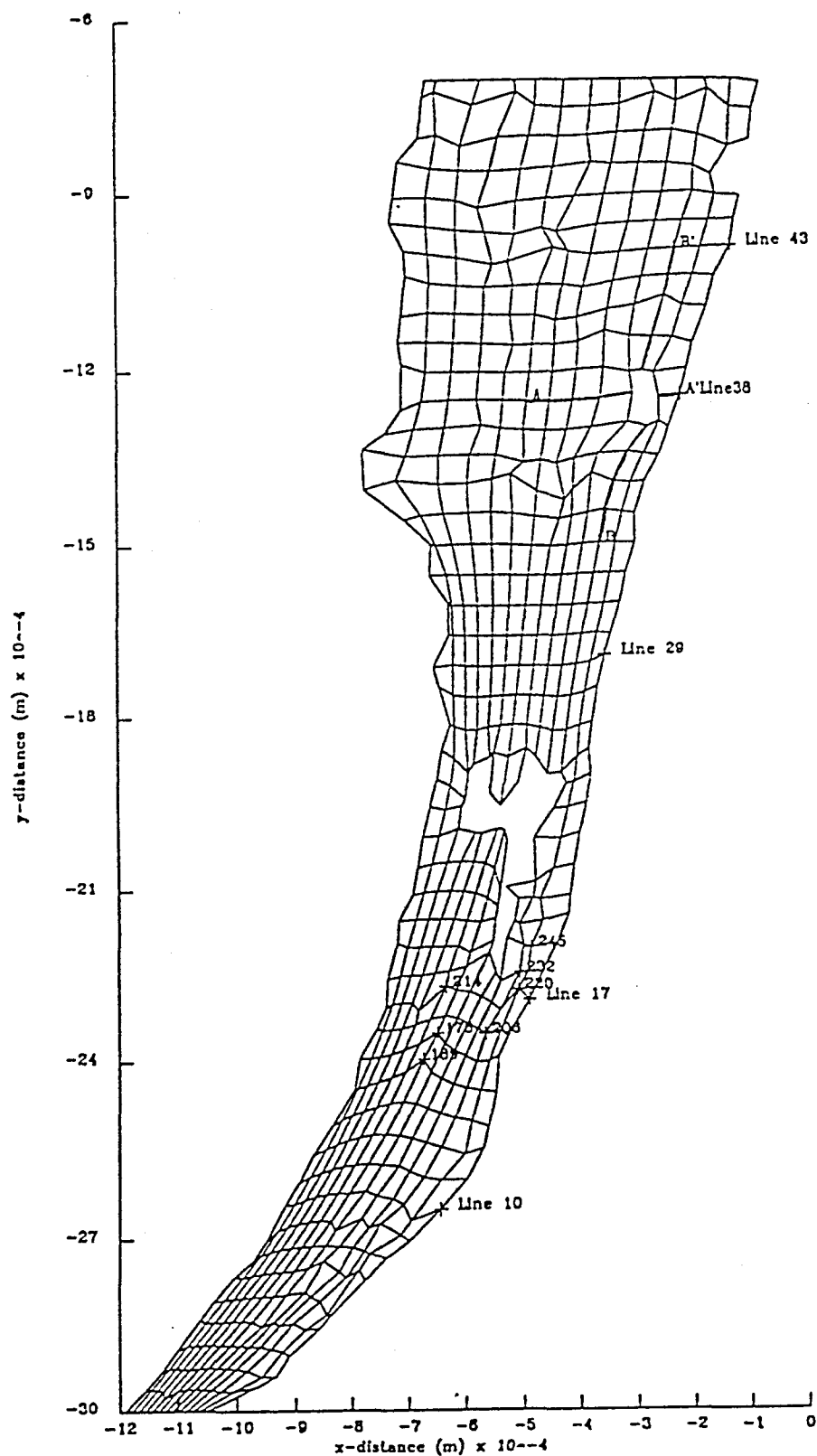


**Figure 43:** The finite element grid drawn over the Zululand aquifer. The grid excludes the three lakes, Lake St Lucia, Lake Sibayi and Lake Kosi.



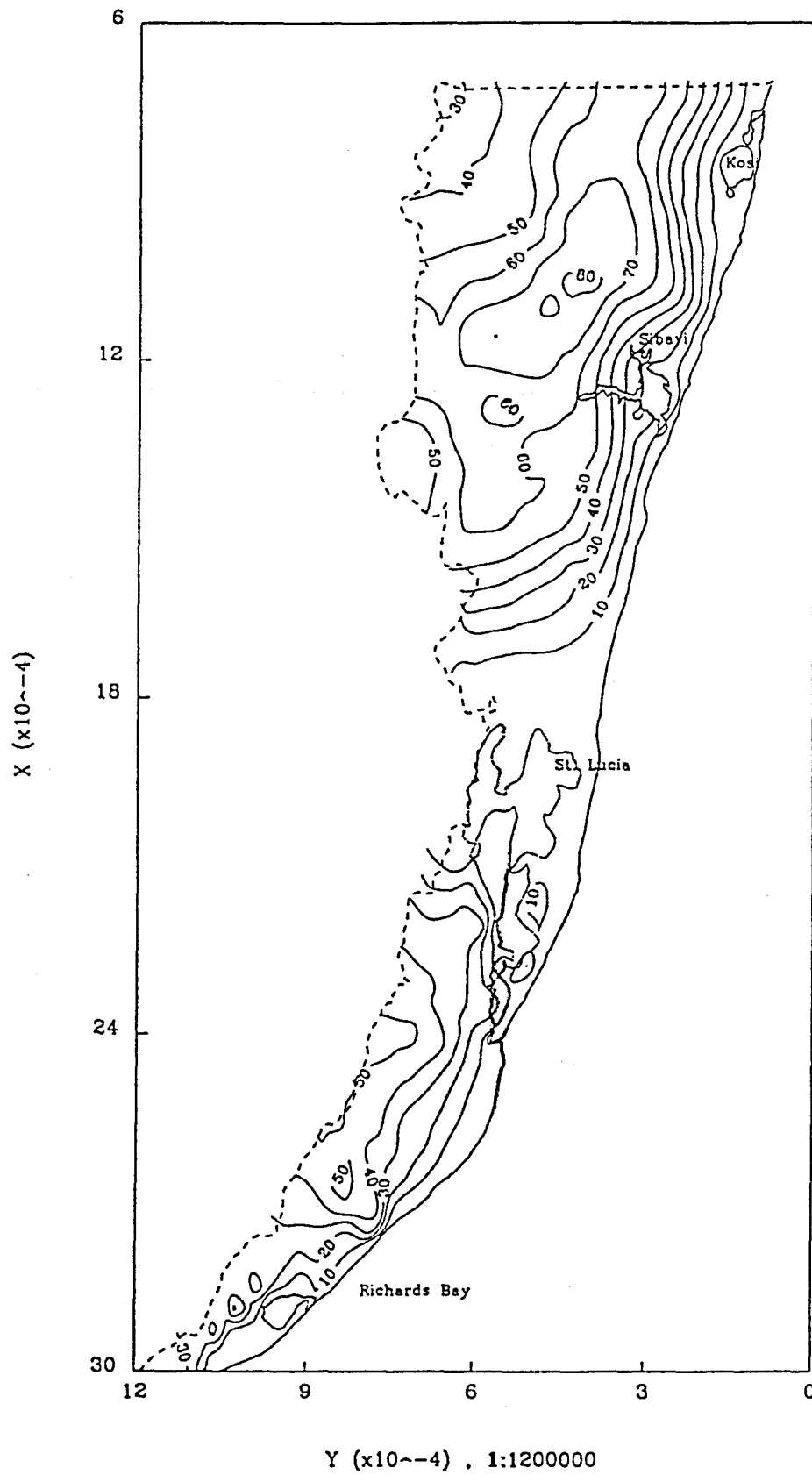


**Figure 44:** The piezometric heads from the 140 boreholes were interpreted to all the nodes of the finite element grid, resulting in head contours as shown.

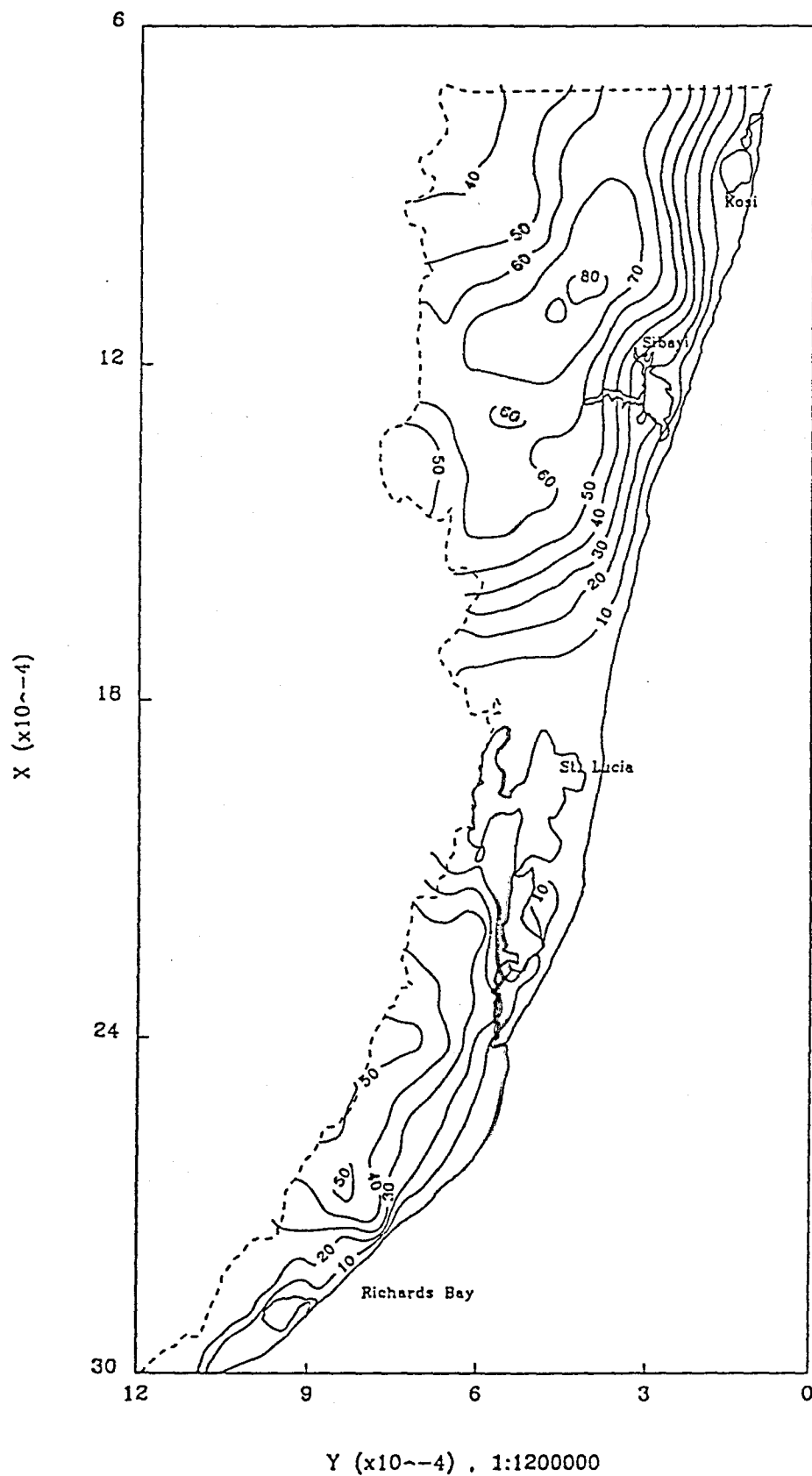


**Figure 45:** Contours from the simulated piezometric heads for the Zululand aquifer after a simulation period of one year.

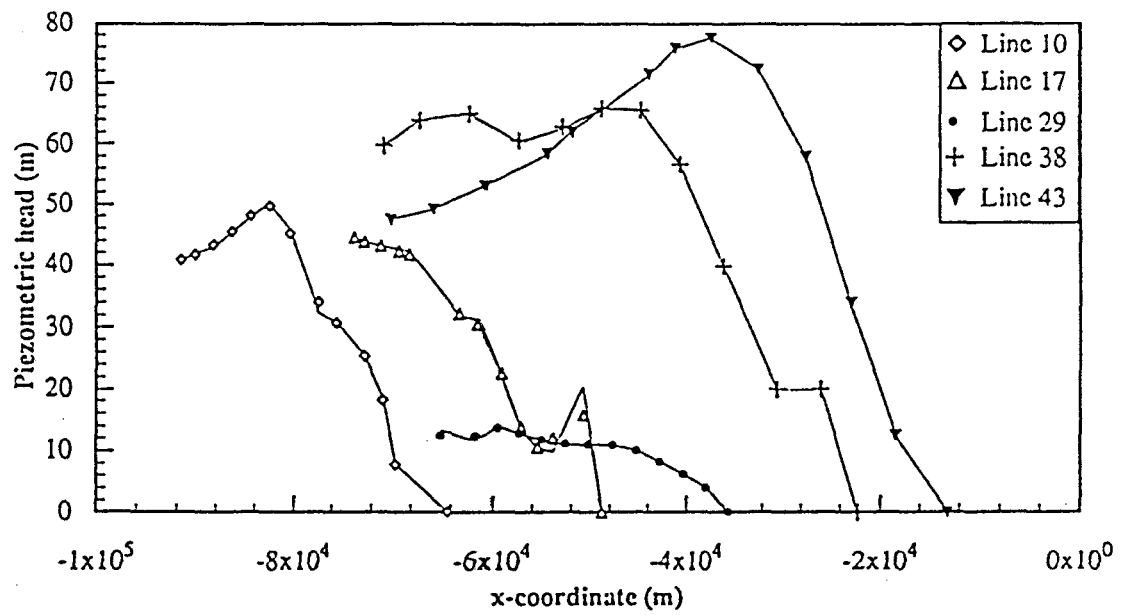


**Figure 46:** A comparison of the initial (solid lines) and simulated (dots) piezometric heads of the numerical model, taken at a few sections parallel to the x-axis. The line numbers are according to the finite element model of Figure 47, counted from the bottom of the grid.

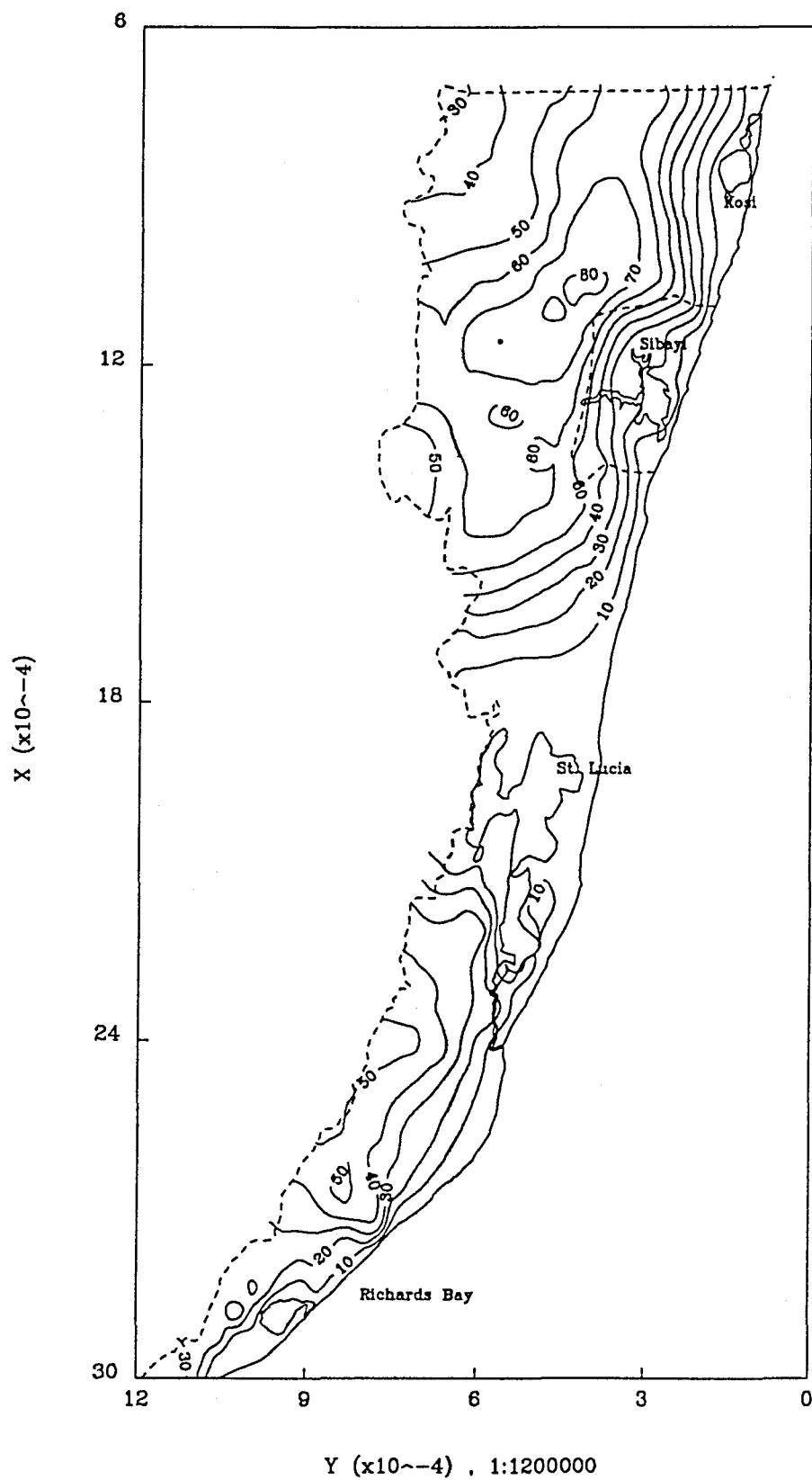


**Figure 47:** Contours of the water levels, simulated for one year, with hypothetical; recharge and evaporation figures of 150 mm/year and 200 mm/year respectively. Contours passing through the lakes are due to the coarse finite element grid used.

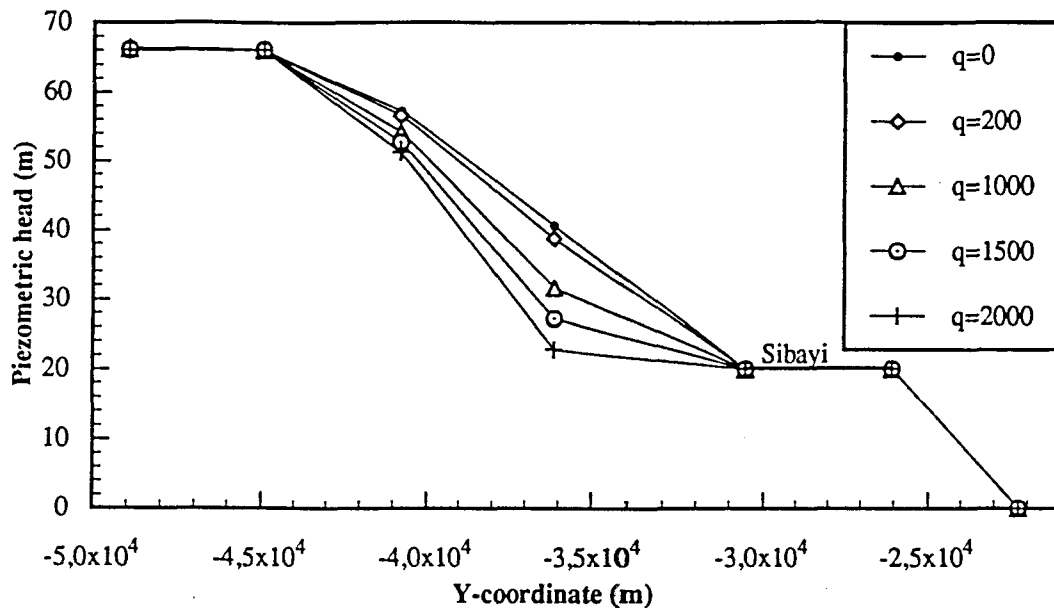


**Figure 48:** Section AA' through Lake Sibayi, perpendicular to the coast, showing the effect of a variation in evapotranspiration values. The evapotranspiration specified for the cases was 0, 200, 1 000, 2 000 and 4 000 mm per annum, per unit area.

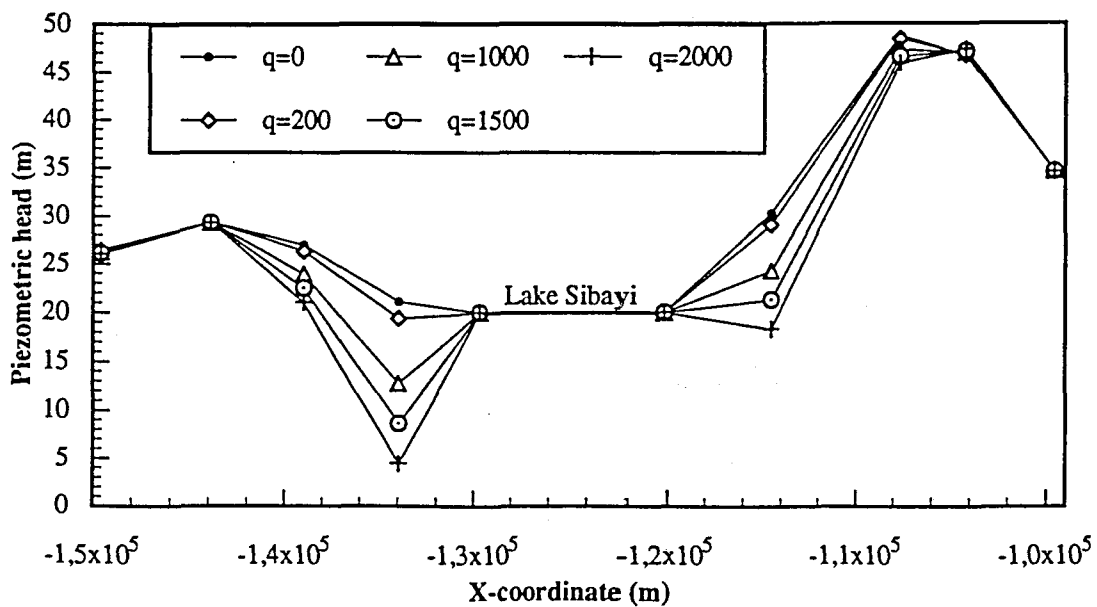


**Figure 49:** Section BB' through Lake Sibayi, parallel to the coast, showing the effect of a variation in evapotranspiration values. The evapotranspiration specified for the cases was 0, 200, 1 000, 2 000 and 4 000 mm per annum, per unit area.

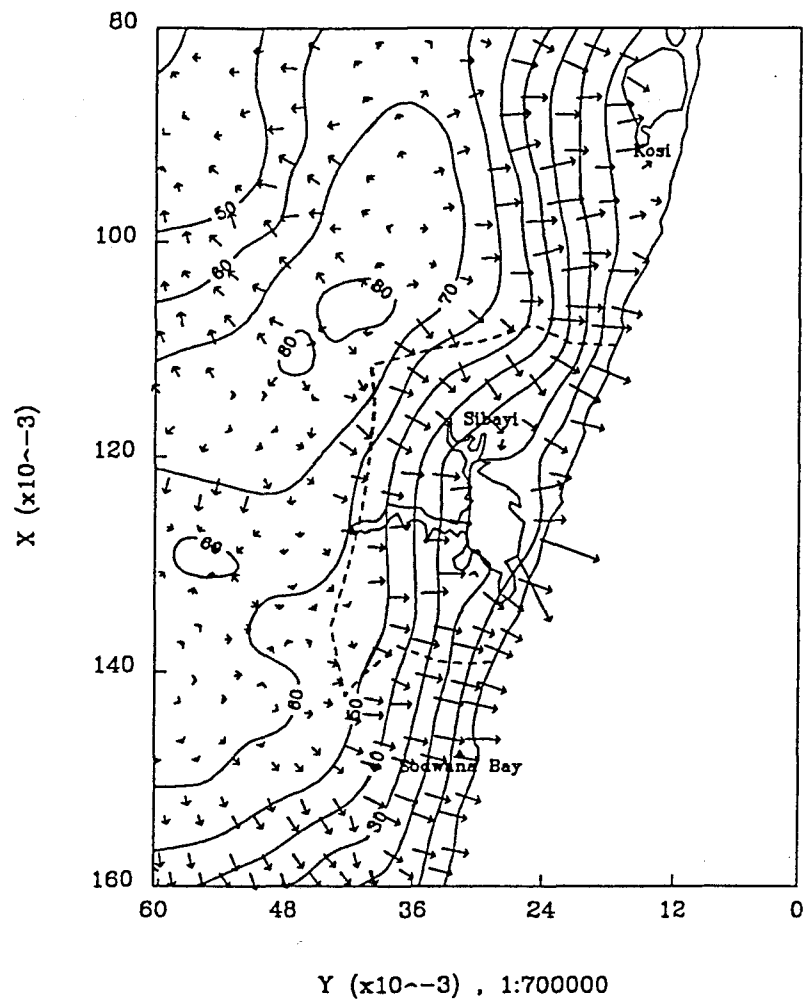


**Figure 50:** The direction of flow of ground water around Lake Sibayi and through the simulation area under normal conditions of 150 mm recharge per year.

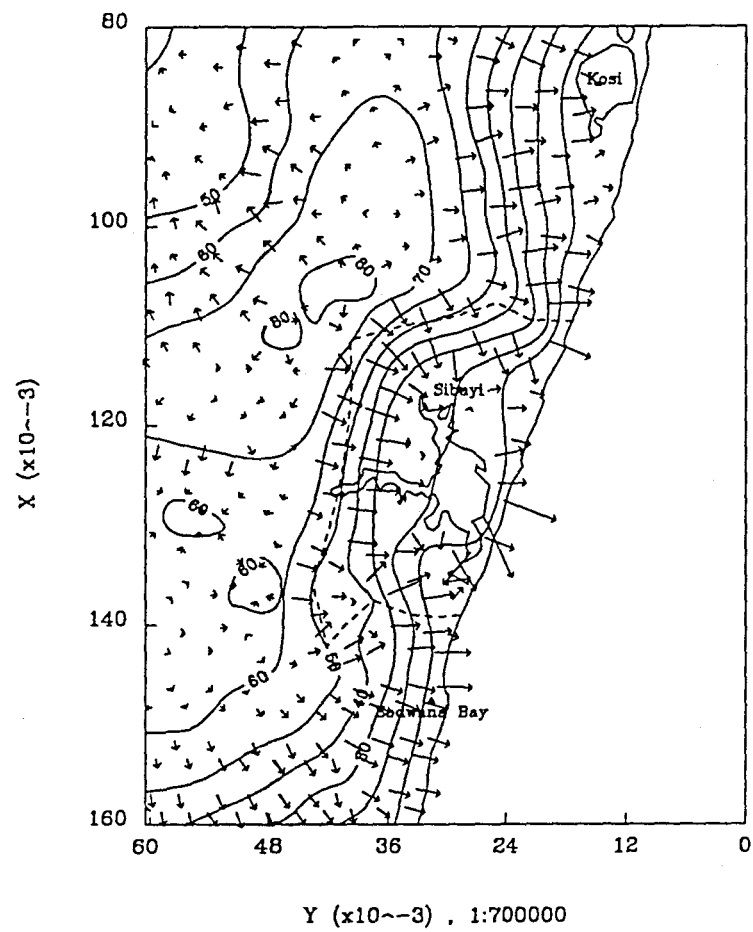


**Figure 51:** The direction of flow of ground water around Lake Sibayi and through the simulation area under extreme conditions of an effective discharge of 2 500 mm per year.

# Aquifer Potential

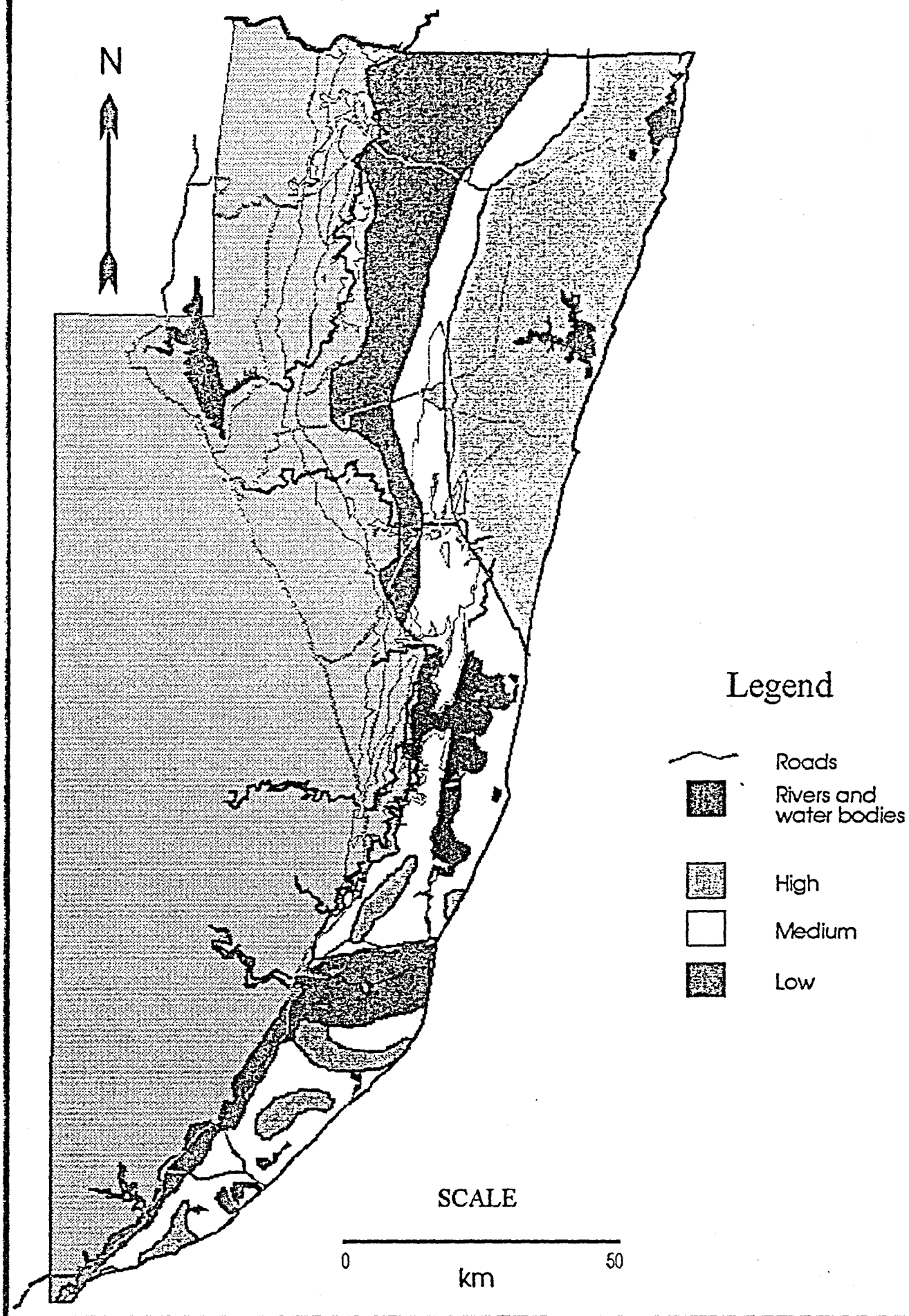


**Figure 52:** Map indicating the aquifer potential in different parts of the Zululand Coastal Plain.



## **APPENDIX A**

### **GEOCHEMICAL CLASSIFICATION OF ZULULAND GROUND WATER**

**Table A1: Lithological units from which water samples were collected.**

Geological formation or position in stratigraphic column	Lithological description	No of samples
Upper Port Durnford	Sandstone	7
Lower Port Durnford	Argillaceous sandstone	2
Lignite band	Lignite	3
Upper Miocene Unit	Sandstone	3
Uloa Formation	Calcarenite	12
St Lucia	Mudstone	4

This method makes provision for the use of a small data set (i.e. relatively high uncertainties) in order to classify any unknown unpolluted ground water sample to either have originated from a specific lithological unit or to be a mixture of waters from different lithological units. The method entails making use of the 'fingerprint' table to determine strata of high probable origin following which a consideration of specific chemical ratios would yield the most probable of the high probability cases.

A description of the data reduction and development of the 'fingerprint' table is given below. The application is then explained using some analyses selected from the available Zululand water chemistry data base. The origin of the water sample so determined is then compared with that of the geological borehole description and the depth from which the sample was taken.

### **A.3 SORTING AND DATA REDUCTION**

All available analyses of water samples collected from specific geological units were sorted according to geological origin. The chemical analyses in both mg/ℓ and meq/ℓ, depth from which sample was taken as well as the ratios of concentration of all elements to each other (in meq/ℓ) for each stratigraphic unit and means of these parameters have been compiled. The mean values of the chemical parameters and a summary of the Element/TDS ratios values for each geological unit are listed in **Table A.2**. The mass % ratio of all elements with respect to the total dissolved solids were also calculated.

### **A.4 GRAPHICAL AND STATISTICAL MANIPULATION**

Schoeller diagrams were drawn for each of the boreholes with depth data. Note that these Schoeller diagrams are essentially similar to the 'fingerprinting' technique to be discussed, yet are a much simplified version of this technique. These diagrams also have elemental concentrations in meq/ℓ and the slope of any line between two adjacent elements represents the ratio between them. Its application is limited, however, since

only a limited number of elements are represented, since direct relations are shown only between adjacent elements, and since only a limited number of analyses can be portrayed without cluttering. Yet these diagrams still show the typical chemical fingerprint of a specific layer, even though nothing is shown about the variation of any parameter about its mean.

Complete statistics including mean, variance, standard deviation and percentiles were further performed for the following:

- a) All physical and chemical parameters for each layer separately.
- b) All ratios of elements to other elements for each layer separately.
- c) All ratios of elements to TDS for each stratum separately.

Tables II and III present the means and standard deviations for each of these parameters for comparison purposes.

## A.5 EXAMPLE TO ILLUSTRATE THE APPLICATION OF THE METHOD

### A.5.1 Setting up the 'Fingerprint' table

To set up the 'fingerprint' table, the statistical distribution of parameters as defined by the mean and standard deviation, are used. This is illustrated by the following example:

From **Table A.2** the values of Ca/TDS means and standard deviations were used to produce the distribution graph in **Figure A1**. From the graph 'good' resolution can be seen between samples A, B, D, and samples E, C with F covering the whole range. Consider the ranges where  $\text{Ca/TDS} \geq 10\%$ ,  $\geq 20\%$ ,  $\leq 10\%$ . An analysis of unknown origin with

- 1)  $\text{Ca/TDS} \geq 10\%$  can belong to C, E, F or A, maybe even B, but definitely not D.
- 2)  $\text{Ca/TDS} \geq 20\%$  can belong to C and F maybe even E, but not A, B, or D.
- 3)  $\text{Ca/TDS} \leq 10\%$  can belong to either A, B, D, F but not E or C.

(1) and (2) are examples of maximum fingerprinting with (3) being a minimum fingerprint. This means that an unknown analysis with  $\text{Ca/TDS} \geq 20\%$  has a much higher probability to belong to groups C and F than to A, B, D.

This example forms the basis of the method presented here. If sufficient information is available it should be possible to distinguish and designate any unknown analysis to a specific origin.

Two questions that may come to mind at this stage are:

- Are the mean and standard deviation good indicators for such a small sample?
- What is the resolution of the method (i.e. how well can be distinguished between water resident in different geological units)?

The answer to these questions is to consider as many ratios as possible and to carefully consider the data at hand before making any deductions.

#### A.5.2 Use of the 'fingerprint' table

To illustrate how the origin of an unknown water sample is determined from the 'fingerprint' table, first determine all the possible ratios (in meq/l) and then test these by means of the fingerprint table (**Table A3**). As an example, a water sample from the Richards Bay area is taken (sample number 2832CA00033, from Zululand Hydrocom data base).

From the Fingerprint Test Table (**Table A5**)

- $\text{Ca/TDS} = 6,82 \%$
- $\text{Mg/TDS} = 3,71 \%$
- $\text{Na/TDS} = 19,62 \%$

Using the fingerprint table (**Table A3**) the sample is grouped in the following classes:

- $\text{Ca/TDS}$  not larger than 10%
- $\text{Mg/TDS}$  larger than 3,5% but not 5%
- $\text{Na/TDS} \geq 15\%$  but not larger than 20%

From these three ratios the following deductions are made:

- $\text{Mg/TDS} \geq 3,5\%$  implies that the sample may belong to A, B, D, or E.
- $\text{Na/TDS} \geq 15\%$  implies that the sample was most likely derived from A, B, D, E, or F.
- The method is not directly reversible and the  $\text{Ca/TDS}$  ratio is of no use here.

This process of testing is now applied to all the parameters as set out in the fingerprint table. The total score for each lithological unit is the number of times that the given data set satisfied the testing parameters.

*(Note: Elements not denoted as a ratio to another element on the table should be read as element/TDS in %)*

For this sample the scores were:

A = 26	D = 14
B = 20	E = 14
C = 11	F = 13

It is clear that the probability of the sample being A (Upper Port Durnford Formation) is quite good, yet for the case when more than one stratum has very high probability (i.e. when its score  $\geq$  average score), a more detailed look at the probability strata needs to be taken.

This phenomenon can be caused by two factors - mixture of waters (should especially be suspected if two adjacent strata are concerned) or the two statistical distribution chemistries are too close to be properly resolved. The two most probable strata can now be tested by looking at specific ratios where these two layers have minimum distribution overlap.

In the case of the example, the Na/TDS ratio distribution is shown in **Figure A2**. It should be clear that the sample originated from A, yet the more the ratios that can be used to distinguish between the layers the better. If no clear distinction can be made between two layers of high probability one would need to look at other information such as borehole depth screen position and geological borehole descriptions in order to determine whether the sample is a mixture of waters from two strata or just a lack of resolution feature. Thus by using the method described, the example could be assigned to a specific layer; in this case the Upper Port Durnford Formation.

## **A.6 MORE EXAMPLES OF IDENTIFYING ORIGIN WITH 'FINGERPRINT' TECHNIQUES**

Additional samples obtained during the pump testing of boreholes recently drilled around Lake Mzingazi by the Department of Water Affairs (Table V), were also subjected to this fingerprint analysis technique. The results are discussed below.

As noted in the text the method followed may, and possibly will, yield more than one probable origin. The examples given below are all of known origin and the testing was done to ensure the efficiency of the method and also to give an idea of the resolution of the method. The samples were treated as unknowns and only after testing were the results compared to the actual origin.

### **A.6.1 Example 1: Water sample 2832CB0004 from Zululand Hydrocom data base**

Only B, E, and F were considered.

B was discounted due to low Ca/TDS and low  $\text{HCO}_3/\text{TDS}$ .

E rejected due to low Cl/TDS and K/TDS.

Conclude source to be F, which is correct.

A.6.2 Example 2: Water sample 2832CA00038 from Zululand Hydrocom data base

Consider only C and E.

E discounted due to generally lower Si/TDS and higher Na/TDS.

Conclude source to be C, which is correct.

A.6.3 Example 3: Water sample 2832CA00033 from Zululand Hydrocom data base

Consider A and B. No good separation could be made between these two layers; the sample is in fact from A yet it must be kept in mind that layer B (Lignite layer) is not a true aquifer and that water denoted as B probably consists of 'A' water with leaching products from B.

Therefore these two layers will be considered as being the same for the rest of the examples.

A.6.4 Example 4: Water sample 2832CA00032 from Zululand Hydrocom data base

Consider A, B, and D.

A and B were rejected due to their low Ca/TDS and high Si/TDS.

C and E difficult to separate yet Na/TDS and  $\text{SO}_4/\text{TDS}$  point towards E.

Conclude the source to be E, which is correct.

A.6.5 Example 5: Water sample 2832CA00030 from Zululand Hydrocom data base

Consider A, B, and F.

F discounted due to its Na/TDS, K/TDS, and  $\text{HCO}_3$  being too high.

A and B indistinguishable.

The sample is actually from B.

A.6.6 Example 6: Water sample 2832CA00015 from Zululand Hydrocom data base

Consider A, B, and D.

Both high Si/TDS and very high  $\text{NO}_3/\text{TDS}$  point towards D.

Conclude source to be D, which is correct.

1076

A.6.7 Example 7: Water sample 39422

Consider A, B, and E.

Low Si/TDS and high Ca/TDS of sample discounts A and B whilst high Cl/TDS discounts C.

Conclude source to be E, which is correct.

A.6.8 Example 8: Water sample 39421

Consider A, B, and E.

A and B rejected as above, and C on account of high Si/TDS.

Concluded source to be E. In this case the sample was a mixture of waters from 9 m Uloa (E) and 2 m St Lucia (F). The major component was identified as the source yet the F fingerprint could not be seen. This may be due to either poor resolution or lack of contribution from F. (*Note that thicknesses quoted only signify the length of the screen in each stratum.*)

A.6.9 Example 9: Water sample 39254

Consider A, B, and E.

No distinction could be made using Ca/TDS and Si/TDS yet both HCO<sub>3</sub>/TDS and Cl/TDS point towards A.

Conclude A to be source. In this case the sample from 6 m Port Durnford (A) and 2 m St Lucia (F). Again only the major component could be identified.

A.6.10 Example 10 Water sample 39250

Consider A, B, and F.

Ca/TDS point to A, B, E, and F.

Si/TDS points to E and F.

Mg/TDS points to F.

Na/TDS points to A, B, E, and F.

K/TDS points to A, B, and E.

HCO<sub>3</sub>/TDS points to A.

Cl/TDS points to A and F.

No proper distinction could be made and the sample was concluded to be a mixture of A, E, and F. The sample was reported to have come from a borehole in which 10 m of Port Durnford (A), 9 m of Uloa (E), and 7 m of St Lucia (F) was intersected. This indicates that a mixture with no dominant species cannot readily be identified as representing a particular geological horizon.

## A.8 CONCLUSIONS

A qualitative method for the determination of the probable origin of water of any specific chemistry based on quantitative statistical studies on a small data set was developed with special reference to the Zululand aquifer. For the Zululand data presented it was found that the fingerprint table set up gave good first approximations which could then be narrowed down by considering specific parameters.

From the examples it follows that when in high probabilities, clear distinctions could be made between the more arenaceous units of the Upper Port Durnford, the lignite layer, and the Miocene sand and the argillaceous Lower Port Durnford, Uloa Calcarenite and St Lucia Mudstone, by only considering Ca/TDS, Si/TDS, and  $\text{HCO}_3/\text{TDS}$  ratio.

Difficulty was encountered in separating Lower Port Durnford from Uloa Calcarenite due to the small difference in chemistry between their waters, yet Na/TDS, Si/TDS,  $\text{SO}_4/\text{TDS}$ , and  $\text{NO}_3/\text{TDS}$  may show a separation for these strata.

The Upper Port Durnford was indistinguishable from the lignite layer yet this could have been expected since the lignite layer is not an aquifer in the true sense of the word and the sample denoted as such is probably Upper Port Durnford water deriving chemical constituents from the lignite band.

Most of the samples tested indicated a single layer of the aquifer as the main source of the water except in the case of sample 39250 where the origin was indistinguishable due to approximately equal contributions to the sample from three aquifer horizons. It can be seen that all the contributing strata show high probability, yet separate ratios pointed to all the possible strata and no clear deduction, else than it being a mixture, could be drawn.

The method discussed was thus used with relative success in predicting the aquifer layer where any ground water sample could have originated. In Figures A3, A4, and A5 the hydrochemical character of water samples from the different geological units within the Zululand aquifer are given.



TABLE A.1

Zululand Groundwater Chemistry  
Means of Physical and Chemical Parameters

Stratigraphic position	pH	EC mS/m	TDS mg/l	Ca mg/l	Mg mg/l	Na mg/l	K mg/l	Si mg/l	HCO <sub>3</sub> mg/l	SO <sub>4</sub> mg/l	Cl mg/l	NO <sub>3</sub> mg/l
Pleistocene Upper Pt Durnford	6.70	20.67	136.00	13.26	4.10	26.44	2.93	16.56	41.99	13.21	46.54	4.55
Lignite	6.53	31.10	238.67	16.37	13.33	32.60	11.47	11.73	116.30	22.17	51.60	3.86
Pleistocene Lower Pt Durnford	7.55	39.00	271.00	54.85	7.15	22.75	6.70	25.25	187.75	8.25	44.00	0.44
Miocene sand (Uloa)	6.27	19.83	136.67	6.73	4.80	29.60	5.80	29.00	55.53	17.60	42.60	19.59
Miocene Calcarenite (Uloa)	7.30	45.88	317.25	50.61	10.52	45.03	7.82	15.32	217.07	24.68	57.89	3.34
Cretaceous mudstone (St.Lucia)	7.65	39.13	267.00	36.43	3.33	76.13	26.05	12.70	195.35	25.88	77.98	3.07

TABLE A.2

Zululand Chemistry  
Ratio(Element/TDS)

Stratigraphic position		Ca	Mg	Na	K	Si	HCO <sub>3</sub>	SO <sub>4</sub>	Cl	NO <sub>3</sub>
Pleistocene Upper Pt Durnford	Mean	8.13	3.28	20.86	2.30	11.24	27.73	11.07	37.20	4.24
	St.Dev.	7.11	1.05	5.35	1.21	6.09	15.03	7.96	11.38	5.05
Lignite	Mean	7.16	4.17	14.45	5.83	6.24	42.45	9.70	24.21	1.85
	St.Dev.	2.96	4.39	2.42	6.91	4.34	27.08	5.39	8.52	0.69
Pleistocene Lower Pt Durnford	Mean	20.56	2.66	8.35	2.58	9.54	70.43	3.12	16.28	0.17
	St.Dev.	4.43	0.30	0.73	1.41	3.20	16.26	1.09	0.52	0.02
Miocene sand (Uloa)	Mean	4.68	3.42	21.90	4.25	22.41	40.32	13.11	32.32	14.62
	St.Dev.	3.12	0.79	1.97	0.35	9.35	8.86	1.81	8.87	4.74
Miocene Calcarenite (Uloa)	Mean	16.05	3.29	14.34	2.57	4.83	68.83	7.70	18.37	1.08
	St.Dev.	4.09	1.02	4.52	1.86	1.61	12.39	4.49	4.52	0.90
Cretaceous mudstone (St.Lucia)	Mean	15.37	1.38	27.66	11.46	5.24	78.17	9.97	29.46	0.97
	St.Dev.	10.82	0.77	8.27	10.84	3.19	28.18	2.18	3.33	1.36

TABLE A.3

Zululand Groundwater Chemistry  
Ratio Comparison File

STRATIGRAPHY		Ca/Mg meq/meq	Ca/Na meq/meq	Ca/K meq/meq	Ca/Si meq/meq	Ca/HCO3 meq/meq	Ca/SO4 meq/meq	Ca/Cl meq/meq	Ca/NO3 meq/meq	Ca/F meq/meq	Mg/Na meq/meq	Mg/K meq/meq	Mg/Si meq/meq	Mg/HCO3 meq/meq	Mg/SO4 meq/meq	Mg/Cl meq/meq	Mg/NO3 meq/meq	Mg/F meq/meq	Na/K meq/meq	Na/Si meq/meq	Na/HCO3 meq/meq
A = Pleistocene Upper Pt Durnford (Aren.)	Mean	2.06	0.55	8.88	0.29	0.90	3.86	0.52	50.22	126.00	0.30	5.14	0.23	0.84	2.17	0.26	12.61	32.00	17.80	0.76	2.87
	St.Dev.	2.51	0.57	8.89	0.22	0.62	4.18	0.56	82.15	114.55	0.04	2.29	0.16	0.53	2.60	0.06	13.18	4.24	8.61	0.43	1.94
B = Lignite	Mean	1.06	0.58	6.94	0.78	0.66	2.32	0.58	13.27	"	0.63	10.40	1.37	0.46	2.24	0.73	18.17	"	10.42	1.24	1.47
	St.Dev.	1.33	0.23	5.97	0.82	0.34	1.69	0.29	7.36	"	0.75	15.62	2.18	0.23	2.50	0.96	25.26	"	8.52	1.18	1.37
C = Pleistocene Lower Pt Durnford (Argil.)	Mean	4.65	2.86	17.34	0.77	0.89	15.84	2.23	273.50	273.50	0.61	3.82	0.17	0.20	3.45	0.48	59.00	59.00	6.68	0.29	0.33
	St.Dev.	0.46	0.86	6.00	0.10	0.01	2.03	0.42	20.51	20.51	0.13	1.67	0.04	0.02	0.78	0.04	1.51	1.41	4.11	0.12	0.11
D = Miocene sand + silt (Uloa)	Mean	0.83	0.25	2.19	0.09	0.33	0.87	0.28	1.27	33.33	0.30	2.55	0.10	0.44	1.06	0.33	1.30	39.33	8.68	0.32	1.49
	St.Dev.	0.54	0.18	1.65	0.08	0.15	0.59	0.21	1.31	25.11	0.08	0.55	0.04	0.16	0.37	0.15	0.57	15.18	0.63	0.09	0.38
E = Miocene Calcarenite (Uloa)	Mean	3.30	1.53	16.36	1.27	0.70	20.93	1.71	70.40	223.00	0.49	6.45	0.41	0.25	6.16	0.54	23.44	101.00	14.23	0.98	0.58
	St.Dev.	1.43	0.97	7.25	0.51	0.08	43.79	0.81	89.03	70.70	0.27	4.75	0.14	0.11	13.94	0.16	28.49	21.41	10.94	0.33	0.24
F = Cretaceous mudstone (St. Lucia)	Mean	6.29	0.81	3.29	1.12	0.56	3.62	0.93	13.50	59.84	0.11	0.49	0.17	0.09	0.53	0.14	2.64	11.50	6.50	2.12	1.08
	St.Dev.	1.48	0.77	2.71	0.81	0.29	2.53	0.67	11.17	34.17	0.09	0.28	0.09	0.03	0.27	0.08	2.21	6.36	4.33	1.50	0.61

		Na/SO4 meq/meq	Na/Cl meq/meq	Na/NO3 meq/meq	Na/F meq/meq	K/Si meq/meq	K/HCO3 meq/meq	K/SO4 meq/meq	K/Cl meq/meq	K/NO3 meq/meq	K/F meq/meq	Si/HCO3 meq/meq	Si/SO4 meq/meq	Si/Cl meq/meq	Si/NO3 meq/meq	Si/F meq/meq	HCO3/SO4 meq/meq	HCO3/Cl meq/meq	HCO3/NO3 meq/meq	HCO3/F meq/meq	SO4/Cl meq/meq	SO4/NO3 meq/meq	SO4/F meq/meq	Cl/NO3 meq/meq	Cl/F meq/meq	TDS/EC meq/meq	SPR
A	Mean	6.83	0.09	46.17	129.50	0.05	0.16	0.48	0.06	3.19	6.00	4.37	11.40	2.02	151.45	248.00	4.43	0.57	45.83	77.00	0.21	9.29	36.00	49.50	151.50	6.49	1.85
	St.Dev.	7.08	0.12	51.63	4.95	0.04	0.10	0.52	0.03	3.68	2.83	2.97	10.51	2.23	243.57	114.55	4.74	0.58	70.14	76.37	0.11	8.88	19.80	55.34	7.78	0.92	0.49
B	Mean	3.63	0.97	22.61	"	0.15	0.55	0.59	0.18	4.35	"	2.54	4.70	1.16	25.75	"	4.67	1.31	31.43	"	0.30	7.21	"	22.94	"	7.72	1.71
	St.Dev.	1.68	0.23	7.90	"	0.10	0.86	0.44	0.19	4.64	"	3.05	3.73	0.60	12.79	"	3.53	1.24	33.40	"	0.12	3.50	"	3.54	"	0.89	0.56
C	Mean	5.91	0.80	99.00	99.00	0.05	0.06	0.95	0.14	17.00	17.00	1.16	20.55	2.96	359.50	359.50	17.80	2.52	308.00	308.00	0.15	17.50	17.50	124.00	124.00	6.95	0.77
	St.Dev.	2.49	0.09	22.63	22.63	0.01	0.02	0.21	0.07	7.07	7.07	0.13	0.07	0.91	71.42	71.42	1.98	0.52	28.28	28.28	0.05	3.54	3.54	14.14	14.14	0.98	0.20
D	Mean	3.52	1.08	4.35	129.00	0.03	0.17	0.41	0.12	0.50	15.00	5.09	11.49	3.43	13.79	413.33	2.45	0.76	3.25	91.00	0.31	1.26	36.67	4.12	120.33	6.85	2.26
	St.Dev.	0.33	0.20	1.44	16.70	0.01	0.05	0.07	0.04	0.16	3.00	2.56	3.39	0.59	3.90	81.59	0.59	0.26	2.07	30.45	0.04	0.50	3.51	1.44	7.02	0.47	0.41
E	Mean	8.24	1.20	37.42	197.80	0.10	0.06	1.14	0.13	4.35	12.00	0.63	20.78	1.38	63.72	230.40	27.19	2.39	93.76	317.60	0.30	8.48	57.20	37.55	171.80	6.93	1.54
	St.Dev.	10.81	0.24	21.77	80.96	0.08	0.04	2.06	0.08	4.62	5.00	0.21	53.50	0.52	111.75	90.30	53.82	1.06	105.92	51.27	0.16	6.92	35.33	37.44	31.22	0.47	0.56
F	Mean	6.01	1.45	62.30	310.50	0.36	0.21	1.29	0.34	6.07	31.00	0.56	3.50	0.88	18.27	126.00	6.16	1.54	37.34	208.00	0.25	8.60	37.00	36.34	165.00	6.79	3.92
	St.Dev.	2.45	0.45	44.27	218.50	0.13	0.12	0.91	0.28	4.15	22.63	0.17	1.55	0.45	5.57	125.87	1.60	0.48	21.87	169.71	0.03	7.35	19.80	29.23	99.00	1.39	2.68

- 1)  $\text{Ca} \geq 10\%$   
 $\text{Ca} \geq 20\%$
- 2)  $\text{Mg} \geq 3.5\%$   
 $\text{Mg} \geq 5\%$
- 3)  $\text{Na} \geq 15\%$   
 $\text{Na} \geq 20\%$   
 $\text{Na} \geq 25\%$
- 4)  $\text{K} \geq 5\%$   
 $\text{K} \geq 15\%$
- 5)  $\text{Si} \geq 10\%$   
 $\text{Si} \geq 15\%$
- 6)  $\text{HCO}_3 \geq 50\%$   
 $\text{HCO}_3 \geq 70\%$
- 7)  $\text{SO}_4 \geq 10\%$
- 8)  $\text{Cl} \geq 20-30\%$   
 $\text{Cl} \geq 35\%$
- 9)  $\text{NO}_3 \geq 3\%$   
 $\text{NO}_3 \geq 10\%$
- 10)  $\text{Ca}:\text{Mg} \geq 4.5$
- 11)  $\text{Ca}:\text{Na} \geq 2$
- 12)  $\text{Ca}:\text{K} \geq 20$
- 13)  $\text{Ca}:\text{Si} \geq 1$
- 14)  $\text{Ca}:\text{HCO}_3 \geq 0.5$   
 $\text{Ca}:\text{HCO}_3 \geq 1.0$
- 15)  $\text{Ca}:\text{SO}_4 \geq 10$
- 16)  $\text{Ca}:\text{Cl} \geq 1$   
 $\text{Ca}:\text{Cl} \geq 2$
- 17)  $\text{Mg}:\text{Na} \geq 0.5$
- 18)  $\text{Mg}:\text{K} \geq 5$   
 $\text{Mg}:\text{K} \geq 10$
- 19)  $\text{Mg}:\text{Si} \geq 0.5$
- 20)  $\text{Mg}:\text{HCO}_3 \geq 0.5$   
 $\text{Mg}:\text{HCO}_3 \geq 1$
- 21)  $\text{Mg}:\text{SO}_4 \geq 2$
- 22)  $\text{Mg}:\text{Cl} \geq 0.8$
- 23)  $\text{Na}:\text{K} \geq 15$
- 24)  $\text{Na}:\text{Si} \geq 1$
- 25)  $\text{Na}:\text{HCO}_3 \geq 1$   
 $\text{Na}:\text{HCO}_3 \geq 2$
- 26)  $\text{Na}:\text{SO}_4 \geq 6$
- 27)  $\text{Na}:\text{SO}_4 \geq 10$
- 28)  $\text{K}:\text{Si} \geq 0.1$   
 $\text{K}:\text{Si} \geq 0.35$
- 29)  $\text{K}:\text{HCO}_3 \geq 0.2$   
 $\text{K}:\text{HCO}_3 \geq 0.4$
- 30)  $\text{K}:\text{SO}_4 \geq 1$
- 31)  $\text{K}:\text{Cl} \geq 0.3$
- 32)  $\text{Si}:\text{HCO}_3 \geq 2$
- 33)  $\text{Si}:\text{SO}_4 \geq 10$   
 $\text{Si}:\text{SO}_4 \geq 20$
- 34)  $\text{Si}:\text{Cl} \geq 3$
- 35)  $\text{HCO}_3:\text{SO}_4 \geq 10$
- 36)  $\text{HCO}_3:\text{Cl} \geq 2.5$
- 37)  $\text{SO}_4:\text{Cl} \geq 0.25$   
 $\text{SO}_4:\text{Cl} \geq 0.4$

[illegible]

- 1)  $\text{Ca} \leq 10\%$
- 2)  $\text{Mg} \leq 2\%$
- 3)  $\text{Na} \leq 8\%$   
 $\text{Na} \leq 14\%$
- 4)  $\text{K} \leq 3\%$
- 5)  $\text{Si} \leq 4\%$
- 6)  $\text{HCO}_3 \leq 30\%$
- 7)  $\text{SO}_4 \leq 2.5\%$   
 $\text{SO}_4 \leq 3.5\%$
- 8)  $\text{Cl} \leq 20\%$
- 9)  $\text{NO}_3 \leq 0.5\%$
- 10)  $\text{Ca}:\text{Mg} \leq 1.5$
- 11)  $\text{Ca}:\text{Na} \leq 0.4$
- 12)  $\text{Ca}:\text{K} \leq 8$
- 13)  $\text{Ca}:\text{Si} \leq 0.45$
- 14)  $\text{Ca}:\text{HCO}_3 \leq 0.4$
- 15)  $\text{Ca}:\text{SO}_4 \leq 1.5$
- 16)  $\text{Ca}:\text{Cl} \leq 0.5$
- 17)  $\text{Mg}:\text{Na} \leq 0.2$   
 $\text{Mg}:\text{Na} \leq 0.4$
- 18)  $\text{Mg}:\text{K} \leq 1$   
 $\text{Mg}:\text{K} \leq 2$
- 19)  $\text{Mg}:\text{Si} \leq 0.15$
- 20)  $\text{Mg}:\text{HCO}_3 \leq 0.1$
- 21)  $\text{Mg}:\text{SO}_4 \leq 0.5$   
 $\text{Mg}:\text{SO}_4 \leq 1$
- 22)  $\text{Mg}:\text{Cl} \leq 0.3$
- 23)  $\text{Na}:\text{K} \leq 5$
- 24)  $\text{Na}:\text{Si} \leq 0.5$
- 25)  $\text{Na}:\text{HCO}_3 \leq 0.6$
- 26)  $\text{Na}:\text{SO}_4 \leq 3$
- 27)  $\text{Na}:\text{Cl} \leq 0.8$
- 28)  $\text{K}:\text{Si} \leq 0.05$
- 29)  $\text{K}:\text{HCO}_3 \leq 0.05$   
 $\text{K}:\text{HCO}_3 \leq 0.1$
- 30)  $\text{K}:\text{SO}_4 \leq 0.3$
- 31)  $\text{K}:\text{Cl} \leq 0.05$
- 32)  $\text{Si}:\text{HCO}_3 \leq 0.9$
- 33)  $\text{Si}:\text{SO}_4 \leq 3$
- 34)  $\text{Si}:\text{Cl} \leq 1.5$
- 35)  $\text{HCO}_3:\text{SO}_4 \leq 2$
- 36)  $\text{HCO}_3:\text{Cl} \leq 1$
- 37)  $\text{SO}_4:\text{Cl} \leq 0.1$   
 $\text{SO}_4:\text{Cl} \leq 0.2$

[illegible]

A = Upper Port Durnford  
B = Lignite Layer  
C = Lower Port Durnford  
D = Miocene Sand  
E = Uloa Calcarenite  
F = Cretaceous Mud St. Lucia

TABLE A.5

Site-ID	Lds	Ca	Mg	Na	K	Si	HCO3	SO4	Cl	NO3	Na/K	Na/Si	Na/HCO3	Na/SO4	Na/Cl	K/Si	K/HCO3	K/SO4	K/Cl	Si/HCO3	Si/SO4	STRATIGRAPHY	
																						mg/l	mg/l
(i)	20320R00033	132.00	9.00	4.90	25.90	3.00	5.70	39.00	2.50	50.00	6.20	0.00										0.45	0.04 Pleistocene Upper Pt Durnford (Pren.)
(ii)	20320R00030	150.00	15.50	3.00	23.70	4.00	11.60	60.30	9.00	40.50	9.54	0.00										0.98	0.17 Lignite
(iii)	20320R00036	291.00	51.90	7.80	26.40	4.70	21.70	175.60	7.00	47.40	0.44	0.10										2.15	0.11 Pleistocene Lower Pt Durnford (Hgl.)
(iv)	20320R00015	154.00	6.50	6.50	33.00	7.00	20.20	52.00	17.00	40.00	26.56	0.10										0.75	0.33 Miocene sand + silt (Uloa)
(v)	20320R00032	500.00	76.20	19.20	67.00	6.50	27.20	322.10	48.00	92.00	2.21	0.00										2.04	0.39 Miocene Calcaremite (Uloa)
(vi)	20320R00004	246.00	63.10	4.60	39.90	17.00	9.70	207.30	22.00	65.50	0.05	0.09										1.84	0.25 Cretaceous mudstone (St. Lucia)
(vii)	39421	519.00	74.60	8.10	57.20	4.63	15.80	274.60	13.50	85.90	0.05	0.09										1.86	0.12 Uloa (7a) + St. Lucia (2a)
(viii)	39422	423.00	51.30	9.90	58.70	3.14	8.28	177.30	5.40	117.20	0.10	0.18										0.88	0.03 Uloa (2a)
(ix)	39250	526.00	47.60	6.80	114.70	9.00	8.16	86.80	39.90	220.80	0.00	0.23										0.23	0.13 Pt Durnford(10a)+Uloa(9a)+St. Lucia(7a)
(x)	39254	172.00	12.80	5.60	29.50	1.38	6.96	67.80	2.00	52.80	0.10	0.19										0.74	0.03 Pt Durnford (6a) + St. Lucia (2a)

Sample	Ca	Mg	Na	K	Si	HCO3	SO4	Cl	NO3	Na/K	Na/Si	Na/HCO3	Na/SO4	Na/Cl	K/Si	K/HCO3	K/SO4	K/Cl	Si/HCO3	Si/SO4	
(i)	20320R00033	6.02	3.71	19.62	2.27	4.32	29.55	1.89	37.88	4.70	14.12	1.40	1.77	22.60	0.80	0.10	0.13	1.60	0.06	1.27	16.20
(ii)	20320R00030	10.33	2.00	15.80	2.67	7.73	45.53	6.00	27.00	2.36	10.30	0.62	0.92	5.42	0.90	0.06	0.09	0.53	0.09	1.47	8.68
(iii)	20320R00036	17.42	2.45	8.86	1.58	7.28	58.93	2.35	15.91	0.15	9.58	0.37	0.40	7.67	0.86	0.04	0.04	0.80	0.09	1.07	20.60
(iv)	20320R00015	3.57	4.22	21.43	4.55	18.31	33.77	11.56	25.97	17.25	8.00	0.36	1.69	3.89	1.27	0.04	0.21	0.49	0.16	4.73	10.86
(v)	20320R00032	15.24	3.84	13.40	1.30	5.44	64.42	9.60	18.40	0.44	17.12	0.75	0.55	2.91	1.12	0.04	0.03	0.17	0.07	0.73	3.87
(vi)	20320R00004	25.65	1.87	16.22	6.91	3.94	84.27	8.94	26.63	0.00	4.05	1.26	0.51	3.78	0.94	0.31	0.13	0.93	0.23	0.41	3.00
(vii)	39421	14.37	1.56	11.02	0.89	3.04	52.91	2.60	16.55	0.01	20.75	1.11	0.55	8.89	1.03	0.05	0.03	0.43	0.05	0.50	8.04
(viii)	39422	12.13	2.34	13.88	0.74	1.96	41.91	1.28	27.71	0.02	31.87	2.16	0.88	23.18	0.77	0.07	0.03	0.73	0.02	0.41	10.73
(ix)	39250	9.05	1.29	21.81	1.71	1.55	16.50	7.59	41.98	0.00	21.70	4.30	3.51	5.01	0.80	0.20	0.16	0.28	0.04	0.82	1.40
(x)	39254	7.44	3.26	17.15	0.80	4.05	39.42	1.16	30.70	0.06	32.00	1.29	1.15	32.00	0.86	0.04	0.04	1.00	0.03	0.89	24.75

Si/Cl	HCO3/SO4	Ca/Mg	Ca/Na	Ca/K	Ca/Si	Ca/HCO3	Ca/SO4	Ca/Cl	Mg/Na	Mg/K	Mg/Si	Mg/HCO3	Mg/SO4	Hg/Cl
0.57	12.80	1.13	0.40	5.69	0.56	0.70	9.00	0.32	0.35	5.00	0.49	0.63	8.00	0.28
1.45	5.89	3.08	0.75	7.70	0.47	0.69	4.05	0.68	0.24	2.50	0.15	0.22	1.32	0.22
2.31	19.20	4.32	2.25	21.58	0.84	0.90	17.27	1.93	0.52	5.00	0.19	0.21	4.00	0.45
3.56	2.30	0.51	0.19	1.50	0.07	0.32	0.73	0.24	0.37	2.94	0.13	0.62	1.43	0.47
1.49	5.28	2.41	1.31	22.35	0.98	0.72	3.80	1.47	0.54	9.29	0.41	0.30	1.58	0.61
0.75	7.39	8.29	1.81	7.33	2.28	0.93	6.85	1.70	0.22	0.88	0.29	0.11	0.83	0.21
0.93	16.07	5.55	1.49	31.00	1.65	0.83	13.29	1.54	0.27	5.58	0.30	0.15	2.39	0.28
0.36	26.45	3.16	1.00	32.00	2.17	0.88	23.27	0.77	0.32	10.13	0.69	0.28	7.36	0.24
0.19	1.71	4.25	0.48	10.35	2.05	1.68	2.87	0.38	0.11	2.43	0.48	0.39	0.67	0.09
0.66	27.75	1.39	0.50	16.00	0.65	0.58	16.00	0.43	0.36	11.50	0.46	0.41	11.50	0.31

## B. GROUND WATER RECHARGE CALCULATIONS

---

If the salt (chloride) concentration in precipitation water (rain water) is given by  $C_p$  (in mg/l) and the precipitation amount is  $P_m$  (mm/month), then the salt deposition rate  $S_m$  is:

$$S_m = (C_p P_m) / 100 \quad [\text{kg/ha/month}]$$

or

$$S_m = (C_p P_m) / 10 \quad [\text{g/m}^2/\text{month}]$$

Summing and averaging the salt deposition rates yields an annual average salt deposition rate  $S_a$  (kg/ha/year). If  $C_w$  is the salt concentration in ground water, then the recharge will be:

$$R = (S_a / C_p) \times 100 \quad (\text{mm/year})$$

and the percentage recharge will be

$$\% \text{ recharge} = R / P_a$$

*Note:*  $100 \text{ mg/m}^2 = 0.1 \text{ g/m}^2 = 1 \text{ kg/ha}$